

**LOS ALAMOS SCIENTIFIC LABORATORY**  
**of the**  
**University of California**  
LOS ALAMOS • NEW MEXICO

**Biological and Medical Research Group (H-4)**  
**of the Health Division -- Annual Report**  
**July 1964 Through June 1965**

IS-4 REPORT SECTION

**REPRODUCTION**  
**COPY**

FILE BARCODE



00131474

1045931

UNITED STATES  
ATOMIC ENERGY COMMISSION  
CONTRACT W-7405-ENG. 36

**LANL**

## LEGAL NOTICE

This report was prepared as an account of Government sponsored work. Neither the United States, nor the Commission, nor any person acting on behalf of the Commission:

A. Makes any warranty or representation, expressed or implied, with respect to the accuracy, completeness, or usefulness of the information contained in this report, or that the use of any information, apparatus, method, or process disclosed in this report may not infringe privately owned rights; or

B. Assumes any liabilities with respect to the use of, or for damages resulting from the use of any information, apparatus, method, or process disclosed in this report.

As used in the above, "person acting on behalf of the Commission" includes any employee or contractor of the Commission, or employee of such contractor, to the extent that such employee or contractor of the Commission, or employee of such contractor prepares, disseminates, or provides access to, any information pursuant to his employment or contract with the Commission, or his employment with such contractor.

All LA...MS reports are informal documents, usually prepared for a special purpose and primarily prepared for use within the Laboratory rather than for general distribution. This report has not been edited, reviewed, or verified for accuracy. All LA...MS reports express the views of the authors as of the time they were written and do not necessarily reflect the opinions of the Los Alamos Scientific Laboratory or the final opinion of the authors on the subject.

Printed in USA. Price \$6.00. Available from the Clearinghouse for Federal Scientific and Technical Information, National Bureau of Standards, United States Department of Commerce, Springfield, Virginia



**LOS ALAMOS SCIENTIFIC LABORATORY**  
**of the**  
**University of California**  
**LOS ALAMOS • NEW MEXICO**

Report written: July 1965

Report distributed: December 20, 1965

**Biological and Medical Research Group (H-4)**  
**of the Health Division -- Annual Report**  
**July 1964 Through June 1965**

Group Leader, W. H. Langham  
Division Leader, T. L. Shipman

## CONTENTS

	Page
CHAPTER 1 - INTRODUCTION	15
CHAPTER 2 - MAMMALIAN METABOLISM SECTION	21
1. Distribution of Manganese-54 in Rats	21
J. E. Furchner, G. A. Drake, and C. R. Richmond	
2. Enhancement of Cesium-137 Excretion by Rats Given Ferric Ferrocyanide Chronically	25
C. R. Richmond, D. E. Bunde, J. S. Findlay, and J. E. London	
3. Oxygen Consumption and the Retention of Cesium-137 in Mice	28
J. E. Furchner, G. A. Drake, and C. R. Richmond	
4. Effect of Conditioning to Temperature Stress on the Excretion of Cesium by Mice	33
J. E. Furchner, G. A. Drake, and C. R. Richmond	
5. Cesium-137 Content of New Mexico Control Subjects: Current Data and a Ten-Year Recapitulation	36
C. R. Richmond, J. E. London, and J. S. Findlay	



6.	Correction of Metabolic Data for Changes in Fallout Cesium-137	41
	C. R. Richmond, J. S. Findlay, and J. E. London	
7.	Support Activities of the LASL Whole-Body Counting Facility	48
	C. R. Richmond, J. E. London, and J. S. Findlay	
	Abstracts of Mammalian Metabolism Section Publications and Manuscripts Submitted	54
1.	Application of Regression Analysis to the Power Function	54
	P. C. McWilliams, J. E. Furchner, and C. R. Richmond	
2.	Effects of Environmental Temperature on Retention of Chronically Administered Cesium-137	54
	J. E. Furchner, C. R. Richmond, and G. A. Drake	
3.	Metabolic Kinetics	54
	C. R. Richmond and J. E. Furchner	
4.	Comparative Metabolism of Radionuclides in Mammals. III. Retention of Manganese- 54 by Four Mammalian Species	55
	J. E. Furchner, C. R. Richmond, and G. A. Drake	
	CHAPTER 3 - MAMMALIAN RADIOBIOLOGY SECTION	56
1.	Genetic Effects of X Irradiation to Consecutive Generations of Male Mice	56
	J. F. Spalding, M. R. Brooks, and R. F. Archuleta	

Genetic Effects. I. Comparative Breeding Characteristics of Offspring of the 25th Generation	57
Genetic Effects. II. Radiation Resistance, LD <sub>50</sub> , and Continuous Exposure (4 to 5 rads/hr) Studies in Mice from 30 Generations of X-Irradiated Sires	59
Genetic Effects. III. A Spontaneous Mutation for a Recurring Hairless Condition	63
Genetic Effects. IV. Hemoglobin Molecular Characteristics of Mice Exposed to 32 Consecutive Generations of X Irradiation	64
J. C. Hensley, R. O. Eikelberry, and C. N. Roberts	
Genetic Effects. V. Comparative Hematology and Clinical Blood Chemistry of Mice of the F <sub>32</sub> Generation	69
J. C. Hensley, C. F. Bidwell, and A. M. Martinez	
2. Effective Residual Dose Studies with Mice	75
J. F. Spalding	
3. Effect of Single Acute and Second Gamma-Ray Exposures on Erythropoiesis in the Mouse	79
J. F. Spalding, N. J. Basmann, O. S. Johnson, and R. F. Archuleta	
4. Phencyclidine Hydrochloride as a General Anesthetic for Laboratory Primates	85
J. C. Hensley	
5. Comparative Extraction Techniques for Mandibular and Maxillary Canine Teeth (Cuspids): Dentitious and Gingival Morphology of Macaca Mulatta and Macaca Speciosa	90
R. I. Howes, Jr., and J. C. Hensley	

**Abstracts of Mammalian Radiobiology Section Publications  
and Manuscripts Submitted** 99

1. Dose Rate Effect on Survival of Mice during Continuous (23-24 hr/day) Gamma Ray Exposures 99  
J. F. Spalding, T. T. Trujillo, and P. McWilliams
2. Radiation Lethality and Circadian Rhythmicity in Mice 99  
J. F. Spalding and P. McWilliams
3. Dose Rate Effects on Lethality of Mice Exposed to Fission Neutrons 99  
J. F. Spalding, J. A. Sayeg, and O. S. Johnson
4. Observations on Lifespan, Radioresistance, and Productivity in Offspring from 5 to 25 Generations of X-Irradiated Male Mice 100  
J. F. Spalding, M. Brooks, and P. McWilliams
5. A Study on the Effective Residual Dose Concept of Exposure to Ionizing Radiation 100  
J. F. Spalding, P. McWilliams, J. Basmann, and W. H. Langham
6. Acute Radiosensitivity as a Function of Age in Mice 100  
J. F. Spalding, O. S. Johnson, and R. F. Archuleta
7. Reduction in Life Expectancy as a Measure of Radiation-Induced Genetic Damage in Mice 101  
J. F. Spalding and M. R. Brooks

8. Changes in a Mouse Population Resulting from  
a Single Dose of X-Irradiation of Each Male  
Progenitor for as Many as 31 Generations 101

R. R. J. Chaffee, J. C. Hensley, E. A.  
Hyatt, and W. H. Langham

CHAPTER 4 - BIOPHYSICS SECTION 102

1. Erythrocyte Volume Distributions during  
Recovery from Bone Marrow Arrest 102

M. A. Van Dilla, N. J. Basmann, J. M.  
Hardin, and J. F. Spalding

2. Flow of Particles through a Coulter Aperture:  
Hydrodynamic Considerations 107

F. H. Harlow and M. A. Van Dilla

3. An Electronic Particle Separator with  
Potential Biological Application 114

M. J. Fulwyler

4. In Vivo Measurement of Plutonium-239 Lung  
Burdens in Humans 119

P. N. Dean and J. H. Larkins

Abstracts of Biophysics Section Publications and  
Manuscripts Submitted 124

1. Half-Life of Cesium-132 124

P. N. Dean and C. R. Richmond

2. Detection of an Interstellar Flux of Gamma-  
Rays 124

A. E. Metzger, E. C. Anderson, M. A.  
Van Dilla, and J. R. Arnold

3. On the Retention of Cesium-137 in People 124

M. A. Van Dilla

4. **Experimental Technique for High Precision Calibration of Whole-Body Counters: Application to a 4π Liquid Scintillator and a Large Sodium Iodide (Tl) Crystal Spectrometer** 125  
P. N. Dean
5. **Erythrocyte Size Distributions following Radiation-Induced Bone Marrow Arrest** 125  
M. A. Van Dilla, J. M. Hardin, N. J. Basmann, and J. F. Spalding
6. **Radioactive Contamination of Contemporary Lead** 126  
R. I. Weller, E. C. Anderson, and J. L. Barker
7. **Radiation Biology and Space Environmental Parameters in Manned Spacecraft Design and Operations** 126  
W. H. Langham, P. M. Brooks, and D. Grahn, eds.
8. **Automatic Data Acquisition, Reduction and Analysis** 127  
P. N. Dean and C. R. Richmond
9. **Some Biological Aspects of Radioactive Microspheres** 128  
W. H. Langham, C. R. Richmond, J. C. Hensley, P. N. Dean, and M. A. Van Dilla
10. **Computer Reduction of Metabolic Data Obtained from Scintillation Counters** 128  
P. N. Dean
11. **Electronic Separation of Biological Cells by Volume** 129  
M. J. Fulwyler

<b>CHAPTER 5 - CELLULAR RADIOBIOLOGY SECTION</b>	<b>130</b>
1. Time of Synthesis of RNA and Protein Species Essential to Division in Four Cell Lines	130
R. A. Tobey, D. F. Petersen, and E. C. Anderson	
2. RNA Synthesis in Cultured Mammalian Cells during Thymidine Inhibition of DNA Synthesis and during Synchronous Growth following Release	134
A. G. Saponara and M. D. Enger	
3. The Energy Metabolism of Cultured Mammalian Cells. I. The Incorporation of Orthophos- phate	142
C. T. Gregg	
4. The Energy Metabolism of Cultured Mammalian Cells. II. Nature of the Phospholipid Fraction	148
C. T. Gregg	
5. The Energy Metabolism of Cultured Mammalian Cells. III. Respiratory Properties of Chinese Hamster Ovary Cells	153
W. D. Currie and C. T. Gregg	
6. Isolation of Nuclei from Chinese Hamster Ovary and Mouse Lymphoma L-5178Y Cells in Tissue Culture	158
E. A. Hyatt	
7. Synthesis of Nucleic Acids by Nuclei from Chinese Hamster Ovary and Mouse Lymphoma (L-5178Y) Cells	162
E. A. Hyatt	

8. Concentrations of Metallic Elements at Various Times in the Life Cycle of Cultured Mammalian Cells 166

R. R. J. Chaffee, D. F. Petersen, and C. Metz

9. Mechanism of Infection of Escherichia Coli by Phage  $\lambda$ -Deoxyribonucleic Acid 169

B. J. Barnhart

Abstracts of Cellular Radiobiology Section Publications and Manuscripts Submitted 171

1. Culture and Slide Preparation of Leukocytes from Blood of Macaca 171

P. C. Sanders and G. L. Humason

2. Life Cycle Analysis of Mammalian Cells. II. Cells from the Chinese Hamster Ovary Grown in Suspension Culture 171

T. T. Puck, P. C. Sanders, and D. F. Petersen

3. A Digitized Comparator for Karyotype Analysis 171

P. M. LaBauve, R. J. LaBauve, and D. F. Petersen

4. Quantity Production of Synchronized Mammalian Cells in Suspension Culture 171

D. F. Petersen and E. C. Anderson

5. Synchronized Mammalian Cells: An Experimental Test of a Model for Synchrony Decay 172

E. C. Anderson and D. F. Petersen

6. RNA Synthesis in Synchronously-Dividing Chinese Hamster Ovary Cells 172

A. G. Saponara, M. D. Enger, and W. H. Langham

7.   **Timing of Synthesis of m-RNA and Protein  
Essential for Cell Division** 172  
  
           R. A. Tobey, D. F. Petersen, and E. C.  
           Anderson
  
8.   **Mengovirus Replication. III. Virus Reproduc-  
tion in Chinese Hamster Ovary Cells** 173  
  
           R. A. Tobey and E. W. Campbell
  
9.   **Mengovirus Replication. IV. Inhibition of  
Chinese Hamster Ovary Cell Division as a  
Result of Infection with Mengovirus** 173  
  
           R. A. Tobey, D. F. Petersen, and E. C.  
           Anderson
  
10.   **Inhibition of the Respiration of Cultured  
Mammalian Cells by Oligomycin** 173  
  
           W. D. Currie and C. T. Gregg
  
11.   **Neutron Activation of Sulfur in Hair; Applica-  
tion in a Nuclear Accident Dosimetry Study** 174  
  
           D. F. Petersen and W. H. Langham
  
12.   **Incorporation of [<sup>3</sup>H]Uridine and [Me-<sup>14</sup>C]-  
Methionine into Chinese Hamster Cell RNA** 174  
  
           A. G. Saponara and M. D. Enger
  
13.   **Temperature Effects on Mitotic Rate and Cell  
Volume of Cells from Hibernators vs Cells  
from Non-Hibernating Species and of Polyoma-  
Transformed Cells vs Non-Transformed Controls** 175  
  
           R. R. J. Chaffee, E. C. Anderson, and  
           D. F. Petersen
  
14.   **Sialic Acid of Mammalian Cell Lines** 175  
  
           P. M. Kraemer



15.	Polyriboadenylate Synthesis by Nuclei from Developing Sea Urchin Embryos	176
	E. A. Hyatt	
16.	Rapid Estimation of Fast Neutron Doses following Radiation Exposure in Criticality Accidents: The $^{32}\text{S}(\text{n},\text{p})^{32}\text{P}$ Reaction in Body Hair	176
	D. F. Petersen	
CHAPTER 6 - MOLECULAR RADIOBIOLOGY SECTION		178
1.	Enzymatic Synthesis of Polydeoxyribonucleotides 5'-Terminated with Chemically Synthesized Oligodeoxyribonucleotides	178
	F. N. Hayes and V. E. Mitchell	
2.	The Chemical Synthesis of Oligodeoxyribonucleotides	187
	D. L. Williams, D. E. Hoard, V. N. Kerr, E. Hansbury, E. H. Lilly, and D. G. Ott	
3.	Chemical Synthesis of Oligodeoxyribonucleotides: Protective Groups for 5'-Phosphate	196
	D. L. Williams	
4.	Chemical Studies on Nucleotide Polymerization	201
	A. Murray	
5.	Synthesis of 2'-Deoxy-5'-Nucleotide $\text{P}^1, \text{P}^2$ -Pyrophosphates	211
	A. W. Schwartz and V. N. Kerr	
6.	Oligonucleotide Chromatography	215
	A. Murray	

7. **Sephadex Chromatography of Nucleic Acid Derivatives** 225  
G. T. Fritz and F. N. Hayes
8. **Computer Analysis of Multicomponent Ultraviolet Spectra** 229  
G. T. Fritz
9. **Studies on the Ribonucleotide Polymerases** 237  
D. A. Smith, R. L. Ratliff, and T. T. Trujillo
10. **Purification of Polydeoxyribonucleotide Polymerases from Calf Thymus** 241  
R. L. Ratliff and T. T. Trujillo
11. **High Resolution Disc Electrophoresis of Histones. I. An Improved Method** 244  
G. R. Shepherd, L. R. Gurley, and B. J. Noland
12. **High Resolution Disc Electrophoresis of Histones. II. A Survey of Histones from Various Laboratories** 248  
L. R. Gurley, G. R. Shepherd, and B. J. Noland
13. **A Procedure for Automatic Amino Acid Analysis on the Nanomolar Level** 258  
G. R. Shepherd, C. N. Roberts, and R. D. Hiebert

**Abstracts of Molecular Radiobiology Section Publications and Manuscripts Submitted** 263

1. **The Reaction of 5'-Thymidylic Acid with the Condensation Product of Phosphorus Pentoxide and Ethyl Ether** 263  
F. N. Hayes and E. Hansbury

2. Effect of the Phosphorylation State of Thymidine Derivatives on Sephadex  $K_d$  Values 263  
F. N. Hayes, E. Hansbury, and V. E. Mitchell
3. BODPRO II: Analysis of T<sub>4</sub>-Bacteriophage Ultracentrifugal Boundaries 263  
G. R. Shepherd, B. J. Noland, and P. N. Dean
4. Conversion of Mono- and Oligodeoxyribonucleotides to 5'-Triphosphates 264  
D. E. Hoard and D. G. Ott
5. ARCHPRO: A Computer Program for the Computation of Molecular Weights by the Archibald Method 264  
G. R. Shepherd, P. N. Dean, and B. J. Noland
6. A Fluorescence Assay Suitable for Histone Solutions 264  
G. R. Shepherd and B. J. Noland
7. Liquid Scintillators. XIII. Steric Inhibition of Resonance in Liquid Scintillators 265  
R. L. Taber, G. H. Daub, F. N. Hayes, and D. G. Ott
8. Quench Monitoring and Efficiency Calibration through External Standardization 265  
F. N. Hayes

## CHAPTER 1

### INTRODUCTION

#### (a) Program Orientation

The biological and medical research program is divided roughly into two general categories: fundamental and programmatic or applied investigations. The former, which now represents about 65 percent of the group's effort, is directed toward studies of biological phenomena at the molecular- and cellular-levels; the latter is concerned largely with somatic and genetic effects of radiation, from both internal and external sources, on animals. These activities, although further subdivided on the basis of the general disciplines concerned, often involve considerable collaboration where the nature of the problem requires a multidisciplinary approach.

The increased emphasis during the past few years on molecular- and cellular-level studies instigated many new projects which are now producing interesting results. Expansion of this program has essentially leveled off, although a few key staff and technical positions remain to be filled. Additional laboratory and office space in the Health Research Laboratory will be realized during the coming year through transfer of the Industrial Hygiene and Field Studies Groups to their new facilities.

Somatic Effects of Radiation.--The Effective Residual Dose (ERD) concept of radiation injury is being studied through tests of mathematical models describing various biological reparable and irreparable injury conditions. Potential external and internal hazards from radioactive materials

associated with space applications of nuclear power systems are being investigated theoretically and experimentally. Interspecies comparative metabolic studies of radionuclides are continuing to provide needed data. Development, calibration, and use of external counting methods for the assessment of radioelement burdens in animals and man continue.

**Radiation Genetics.**--Studies of cumulative genetic effects in the progeny of successive generations of irradiated mice are now in the seventh year. After more than 35 generations of irradiation, differences in the progeny of the experimental and control lines are not particularly striking. Further analysis is required, but it is contemplated that termination of these studies will be started after the fortieth generation. Microbial and biochemical genetics efforts will be increased.

**Molecular- and Cellular-Level Studies.**--The molecular biology activity involves a very favorable consolidation of organic chemistry, biochemistry, and enzymology. Through combinations of chemical and enzymatic syntheses, model systems are available for detailed studies of biological information transfer reactions and the associated polymerase enzymes. The structure of histones and their possible function in this process are being investigated. Cellular biology activities are primarily concerned with establishing the temporal sequence of cellular processes in relation to specific portions of the life cycle. Extensive use is made of synchronized mammalian cells grown in suspension culture. Investigation of the mechanism of certain radiation effects will be started during the coming year. Studies of extracellular materials and cell surface phenomena will be somewhat increased. Electronic cell sizing, counting, and separating systems are being devised and improved in support of both the fundamental and programmatic biology programs, as well as automatic systems for continuous monitoring of the growth of tissue cultures.

(b) Terminations

The following terminations occurred during the present report period:

Miss R. L. DePriest, data analyst, Biophysics Section.

Mrs. R. E. Hine, research assistant, Molecular Radiobiology Section.

Mrs. G. E. Oakley, research assistant, Mammalian Radiobiology Section.

Mr. D. G. Valdez, technician, Mammalian Radiobiology Section.

Mr. A. R. Vigil, electronics technician, Biophysics Section.

(c) Leave of Absence

Dr. Irene U. Boone, staff member, Cellular Radiobiology Section, is continuing her second year's leave of absence to practice medicine in the Los Alamos Medical Center. It is anticipated that she will return to the group in September 1965.

(d) New Staff Members

Benjamin J. Barnhart (staff member, Cellular Radiobiology Section), Sc.D. in Biochemistry, [REDACTED]  
[REDACTED]

R. R. J. Chaffee (staff member, Cellular Radiobiology Section), Ph.D. in Cellular Physiology; [REDACTED]  
[REDACTED]

M. Duane Enger (staff member, Cellular Radiobiology Section), Ph.D. in Biochemistry, [REDACTED]

Lawrence R. Gurley (staff member, Molecular Radiobiology Section), Ph.D. in Biochemistry, [REDACTED]

Paul M. Kraemer (staff member, Cellular Radiobiology Section), Ph.D. in Microbiology, [REDACTED]  
[REDACTED] Dr. P.H. in Virology, [REDACTED]  
[REDACTED]

(e) Acceptance of Offer of Employment

Charles H. Blomquist (staff member, Cellular Radiobiology Section), Ph.D. in Biochemistry, [REDACTED]  
[REDACTED] will join the group in August 1965.

(f) Postdoctoral Research Appointments

Under the recently initiated postdoctoral program of the Laboratory, William D. Currie (Ph.D. in Biochemistry, [REDACTED]) joined the Cellular Radiobiology Section, and Alan W. Schwartz (Ph.D. in Biochemistry, [REDACTED]) joined the Molecular Radiobiology Section.

(g) Organization

The following chart indicates the major divisions of effort within the group.

## GROUP H-4

BIOMEDICAL RESEARCH

W. H. Langham, Ph.D., Leader  
 D. G. Ott, Ph.D., Alt. Group Leader  
 O. S. Johnson, B.S., Administrative Deputy  
 E. M. Sullivan, Group Secretary

MAMMALIAN METABOLISM

C. R. Richmond, Ph.D.,  
 Leader

Staff Member

J. E. Furchner, Ph.D.

Research Assistants

G. A. Drake, B.S.  
 J. S. Findlay, B.S.  
 J. E. London, B.S.

Technical Staff

S. Cordova  
 R. Martinez

\* Casual employee.

MAMMALIAN RADIOBIOLOGY

J. F. Spalding, Ph.D.,  
 Leader

Staff Member

J. C. Hensley, D.V.M.

Research Assistants

M. R. Brooks, B.Ch.E.  
 C. F. Bidwell, M.S.

Technical Staff

R. C. Adams  
 F. Archuleta  
 R. F. Archuleta  
 J. E. Atencio  
 N. J. Basmann  
 A. M. Martinez, B.S.  
 L. Ortiz  
 A. Trujillo  
 F. Valdez  
 J. G. Valdez  
 E. A. Vigil

BIOPHYSICS

M. A. Van Dilla, Ph.D.,  
 Leader

Staff Members

P. N. Dean, M.A.  
 M. J. Fulwyler, B.S.  
 J. H. Larkins, B.S.\*  
 J. D. Perrings

Research Assistant

J. M. Hardin, M.S.

Electronics Technician

L. J. Carr



CELLULAR RADIOBIOLOGY

D. F. Petersen, Ph.D.,  
Leader

Staff Members

E. C. Anderson, Ph.D.  
B. J. Barnhart, Ph.D.  
I. U. Boone, M.D. \*\*  
R. R. J. Chaffee, Ph.D.  
M. D. Enger, Ph.D.  
C. T. Gregg, Ph.D.  
E. A. Hyatt, Ph.D.  
P. M. Kraemer, Ph.D.  
A. G. Saponara, Ph.D.  
R. A. Tobey, Ph.D.

Research Assistants

E. Campbell, B.S.  
S. Carpenter, B.A.  
S. H. Cox, B.A.  
P. M. LaBauve, B.A.  
P. C. Sanders, M.S.  
F. Sapir, M.S.

Technical Staff

V. M. Gibbs, B.S.  
J. L. Hanners

\*\* Leave of absence.

MOLECULAR RADIOBIOLOGY

F. N. Hayes, Ph.D.  
Leader

Staff Members

L. R. Gurley, Ph.D.  
D. E. Hoard, Ph.D.  
V. N. Kerr, M.A.  
A. Murray, M.S.  
R. L. Ratliff, Ph.D.  
G. R. Shepherd, Ph.D.  
D. A. Smith, Ph.D.  
T. T. Trujillo, B.S.  
D. L. Williams, M.S.

Research Assistants

G. T. Fritz, B.S.  
E. Hansbury, M.A.  
E. H. Lilly, B.S.  
B. J. Noland, B.A.  
C. N. Roberts, B.A.

Technical Staff

V. E. Mitchell

POSTDOCTORAL APPOINTEES

W. D. Currie, Ph.D.  
A. W. Schwartz, Ph.D.

## CHAPTER 2

### MAMMALIAN METABOLISM SECTION

DISTRIBUTION OF MANGANESE-54 IN RATS (J. E. Furchner, G. A. Drake, and C. R. Richmond)

#### INTRODUCTION

The distribution of manganese in rats was measured as part of the programmatic investigation of the retention and distribution of a number of gamma-emitting isotopes. A literature survey (1) reports bone and liver as the tissues with highest manganese concentrations. Cotzias (2) found high concentrations in mitochondria and in tissues whose cells are rich in mitochondria.

#### METHODS

Forty-four white male Sprague-Dawley rats about 3 months old, weighing ~ 325 g, were injected intraperitoneally with 0.5  $\mu$ Ci of manganese-54 as the chloride. They were assayed for whole-body activity within 0.5 hour of injection and again on the day of sacrifice. The following tissues were removed for manganese-54 activity determinations: entire gut and its contents, pelt, lungs, heart, liver, muscle, bone, brain, kidneys, and testes. In addition, a blood sample was assayed as was the carcass (whole body minus pelt and viscera) and the remains (mesentery, mesenteric fat, and blood). The rats were sacrificed in groups of 4.

## RESULTS AND DISCUSSION

The results are presented as percent of injected dose per g of tissue. Figures 1 and 2 are plots of the concentration in the various tissues as a function of time. In Fig. 1 is included a plot of the whole-body retention function determined from a group of 6 rats injected intraperitoneally with manganese-54, along with the average whole-body activity for each group. The concentration changes in the various tissues seem to follow approximately the whole-body retention. The liver and gut appear to lose the isotope more quickly, while bone and brain appear to lose it more slowly than the whole body and other tissues.

The concentration in the brain appears to undergo a build-up to an ill-defined maximum, perhaps indicating a blood-brain barrier to the isotope. The manganese appears to be fairly evenly divided in the soft tissues. The high concentration in bone agrees with the findings of Fore and Morton (1), but the high concentration in brain is not in agreement with these or other (2) authors. Tissue distribution after chronic exposure to constant levels of manganese-54 will be determined.

## REFERENCES

- (1) H. Fore and R. A. Morton, Biochem. J. 51, 600 (1952).
- (2) L. S. Maynard and G. C. Cotzias, J. Biol. Chem. 214, 489 (1955).

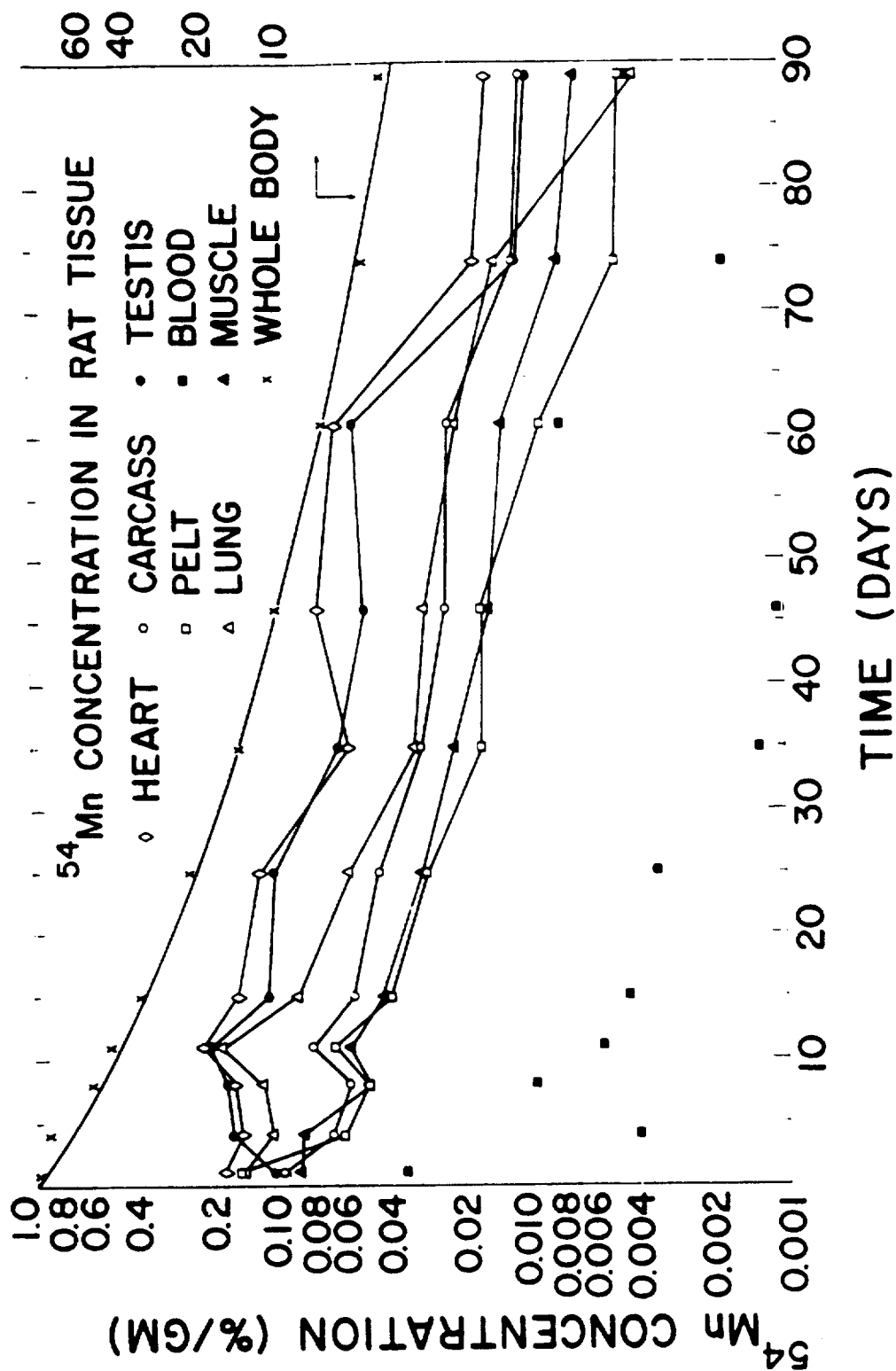


Fig. 1. Tissue concentration of manganese-54 as a function of time after administration. Each data point is an average value from 4 rats. The whole-body retention function (upper, smooth curve) is from data of 6 rats given a single intraperitoneal dose of manganese-54.

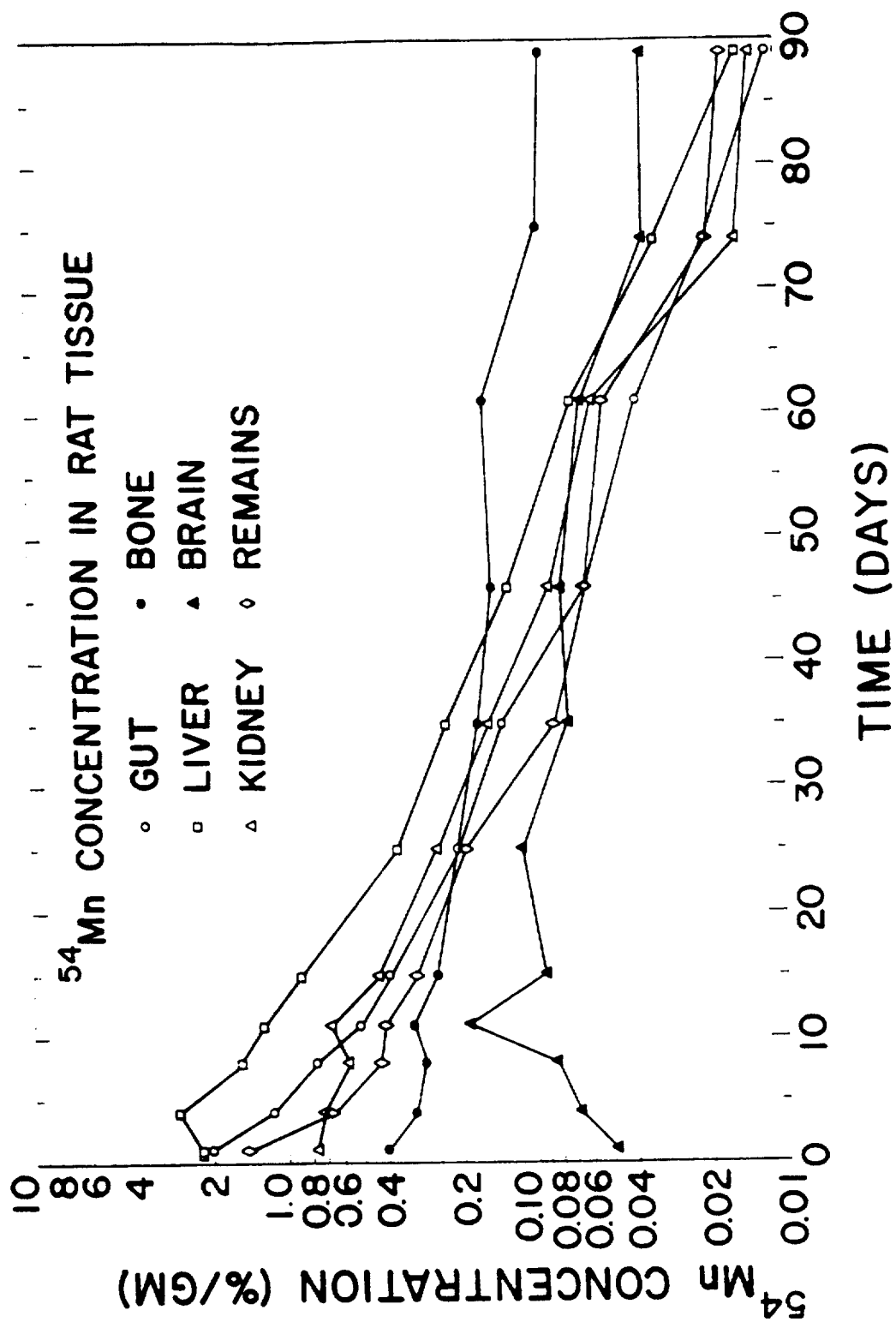


Fig. 2. Tissue concentration of manganese-54 as a function of time after administration.

**ENHANCEMENT OF CESIUM-137 EXCRETION BY RATS GIVEN FERRIC FERROCYANIDE CHRONICALLY (C. R. Richmond, D. E. Bunde,\* J. S. Findlay, and J. E. London)**

**INTRODUCTION**

Nigrovic (1) recently reported a significant increase in cesium-137 excretion by rats given ferric ferrocyanide,  $\{\text{Fe}[\text{Fe}(\text{CN})_6]_3\}$ , by gastric gavage. Lack of toxic side effect, even at high dosages, led him to suggest this compound as a therapeutic agent in cases of accidental incorporation of radiocesium. The action of the compound is by interrupting the enteral cycling of cesium-137. This report summarizes work currently in progress in which ferric ferrocyanide is chronically administered to rats at several concentrations.

**METHODS AND RESULTS**

Twenty-four male Sprague-Dawley rats were used. All were kept in individual stainless steel metabolism cages to allow quantitative separation of urine and feces. Each rat was fed ground lab chow and was allowed to drink water ad libitum from a calibrated watering device. After several weeks acclimatization to these cages, each animal was injected intravenously (lateral tail vein) while under Nembutal anesthesia with  $\sim 1 \mu\text{Ci}$  carrier-free cesium-137 as the chloride. About 30 minutes later and at subsequent times, each rat was measured in a  $4\pi$  geometry liquid scintillation counter (2). After the initial measurement, three groups of 6 rats each were given ferric ferrocyanide (FFC) as a drinking solution in place of tap water. Although FFC is insoluble in water, no settling occurred even at the highest concentration of 2.5 g FFC per liter. Concentrations of 0.25 and 0.025 g FFC per liter were also used. The remaining control group was allowed to drink tap water. No changes in fluid intake or food consumption have been noted to date (6 weeks). Body weight changes are comparable for each group.

Figure 1 shows the retention patterns for each group. No difference is seen between the control group and the lowest FFC concentration. Marked changes are seen for the intermediate and highest FFC concentrations as compared with the

---

\* Associated Rocky Mountain Universities visiting Assistant Professor of Zoology from Idaho State University.

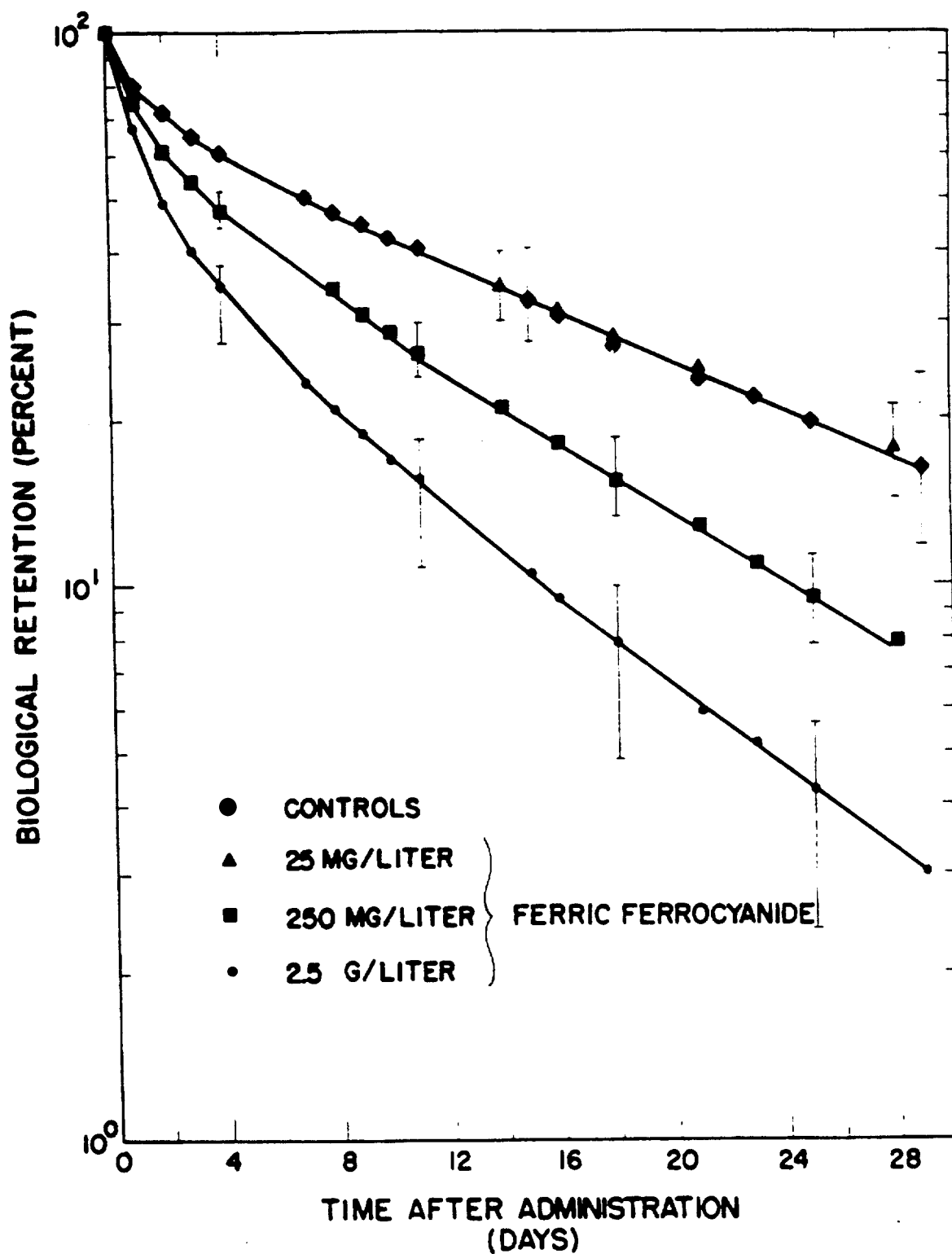


Fig. 1. Whole-body biological retention of rats given different concentrations of ferric ferrocyanide.

controls. At 10 days following injection the average cesium-137 burden in the highest FFC concentration group is only 40 percent of the control value. At 29 days the cesium-137 burden of the control group is ~6 times higher than that of the highest FFC concentration group. Vertical bars shown in Fig. 1 are ranges (not statistical errors).

## DISCUSSION

Ferric ferrocyanide appears to be a non-toxic, insoluble dye that may be useful as a therapeutic agent for cesium-137 contamination. Its effect is primarily, if not solely, one of binding  $\text{Cs}^+$  ions in the lumen of the gut and hence preventing absorption and subsequent recycling of the ion. As a result, more  $\text{Cs}^+$  ions are lost via the feces than in normal animals. The effect on other group I ions (e.g.,  $\text{Na}^+$  and  $\text{K}^+$ ) and on group II ions is of current interest, as preliminary results indicate enhanced urinary excretion of  $\text{Na}^+$ ,  $\text{K}^+$ , and  $\text{Ca}^{++}$  during FFC treatment at high concentrations. Tracer studies are in progress using sodium-22 and barium-133, and urinary sodium-23 concentrations will be measured by neutron activation analysis. As yet we have no explanation for increased urinary levels of  $\text{Na}^+$ ,  $\text{K}^+$ , and  $\text{Ca}^{++}$  in FFC-treated animals. One might also speculate on the meaning of the rate constants which control excretion in the treated groups as less or no enteral recycling of the tracer takes place; therefore, observed turnover rates may be more representative of real turnover rates for each  $\text{Cs}^+$  reservoir. Specific ion binding may prove to be a helpful tool in the study of metabolic kinetics.

## REFERENCES

- (1) V. Nigrovic, Intern. J. Radiation Biol. 7, 307 (1963).
- (2) C. R. Richmond, J. E. London, J. S. Findlay, and J. E. Furchner, Los Alamos Scientific Laboratory Report LA-3132-MS (1964), p. 76.



# **OXYGEN CONSUMPTION AND THE RETENTION OF CESIUM-137 IN MICE** (J. E. Furchner, G. A. Drake, and C. R. Richmond)

## **INTRODUCTION**

A relation between body weight and whole-body retention in small mammals has been used for estimating retention parameters in man. This practice is based on the assumption that the well-known parabolic relation between body weight and such metabolic indices as  $O_2$  consumption or caloric output may be, in some degree, applicable to the gross metabolism of various radioactive contaminants administered to the various species. If it is true that the decreasing metabolic rate accompanying increasing body weight in mammals is also manifest in the decreasing excretion rates of radionuclides such as cesium-137, iodine-131, zinc-65, manganese-54, etc., then altering the metabolic rates should also alter the excretion rates; this has been found to be true in a qualitative sense (1). Further supporting evidence is given by the following experiment.

## **METHODS**

Radiocesium was administered intraperitoneally to 3 groups, each consisting of 8 female RF mice 60 days old and weighing ~25 g. The activity in each mouse was determined in a 4 $\pi$  geometry scintillation detector immediately after administration and at intervals thereafter for about 1 month. During the course of the experiment, the mice were maintained in individual cages where they had free access to water and food. One group was maintained at 35°C (high-temperature animals), one at 7°C (low-temperature animals), and one at 22°C (control animals). At various times during the experiment the oxygen consumption was measured with a commercial spirometer which necessitated the removal of the high- and low-temperature animals from their test environments to room temperature for oxygen consumption measurements.

## **RESULTS**

The percent whole-body effective retention for each of the 3 groups is shown in Fig. 1. The smooth curves are plots of

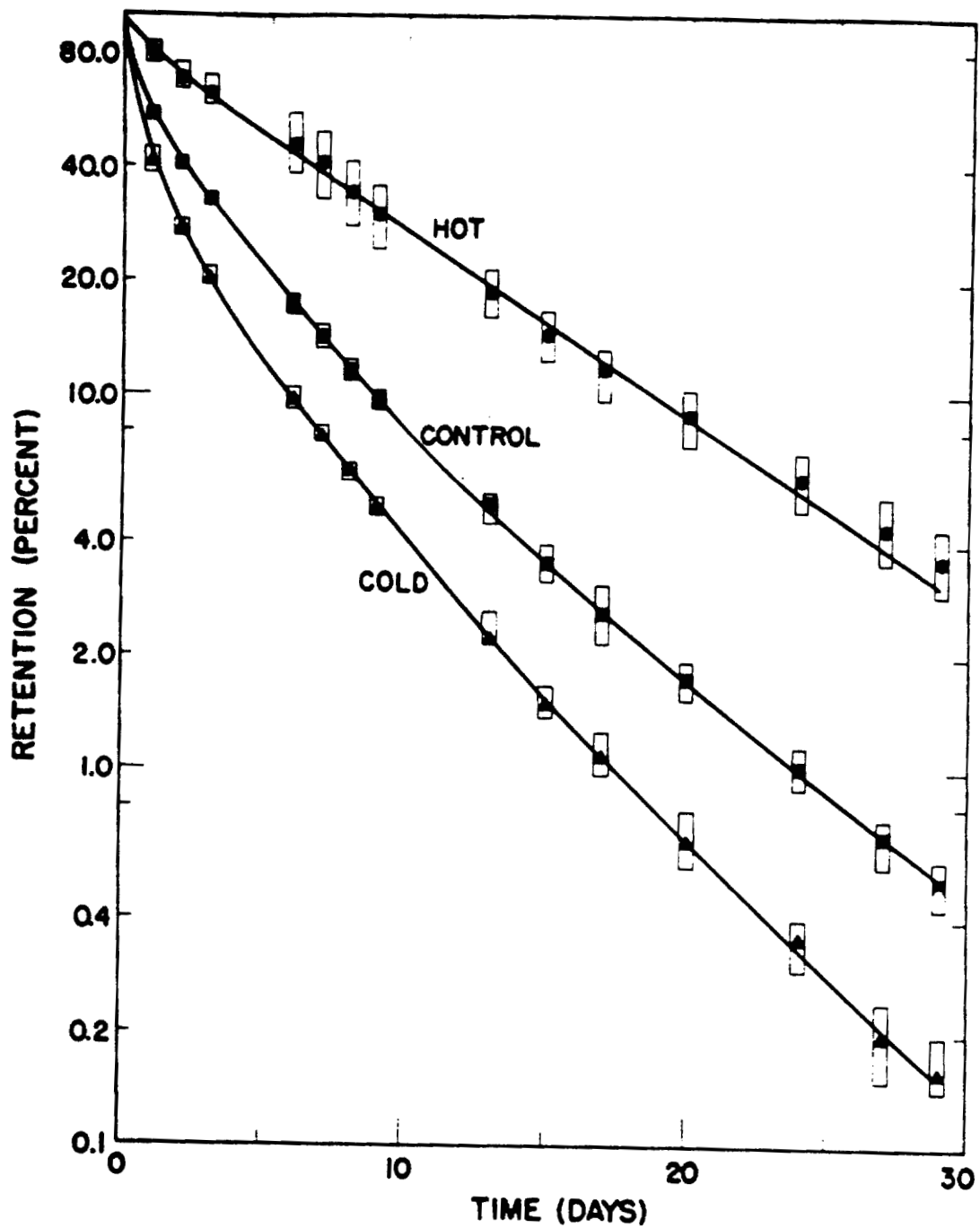


Fig. 1. The effect of temperature on the retention of cesium-137 in mice. The smooth curves are plots of the best-fit retention function. The closed data points are average retention values. The vertical bars indicate the range of values at each point.

the retention functions, and the vertical rectangles indicate the range of values at each measuring time. Clearly, excretion is enhanced by low temperatures.

In Fig. 2 the oxygen consumption per g of body weight converted into percent of the control values is plotted as a function of time. The deviation from the control value seems clear after 2 weeks for the low-temperature animals and 10 days for the high-temperature animals.

### DISCUSSION

The abnormal temperatures had an immediate effect on retention of cesium-137, but had a questionable effect on oxygen consumption before 2 weeks exposure. However, before and during the oxygen consumption measurements the test animals were at the control temperature and the early absence of effect is attributed to this factor. That is, cesium was excreted for 23.5 hr/day at stress temperatures, whereas oxygen consumption was measured at room temperatures. The later changes in oxygen consumption are attributed to "conditioning" (2) of the metabolic rates to abnormal temperatures. If this interpretation is valid, then cesium excretion and oxygen consumption are only loosely coupled rather than united in a cause-effect relationship. The parabolic relation between body weight and metabolic rate is of the form:

$$R = aB^k,$$

where R is the metabolic rate, B is body weight, and a and k are constants. The value of the constant k, calculated from the basal metabolic rates of many animals by Brody (3), is 0.73. Data relating the integral of the retention function for cesium-137 in 5 mammalian species to their body weight give a value of ~0.5 for k (4). The difference in the values for k suggests that basal metabolic rates do not directly mediate the cesium excretion rates.

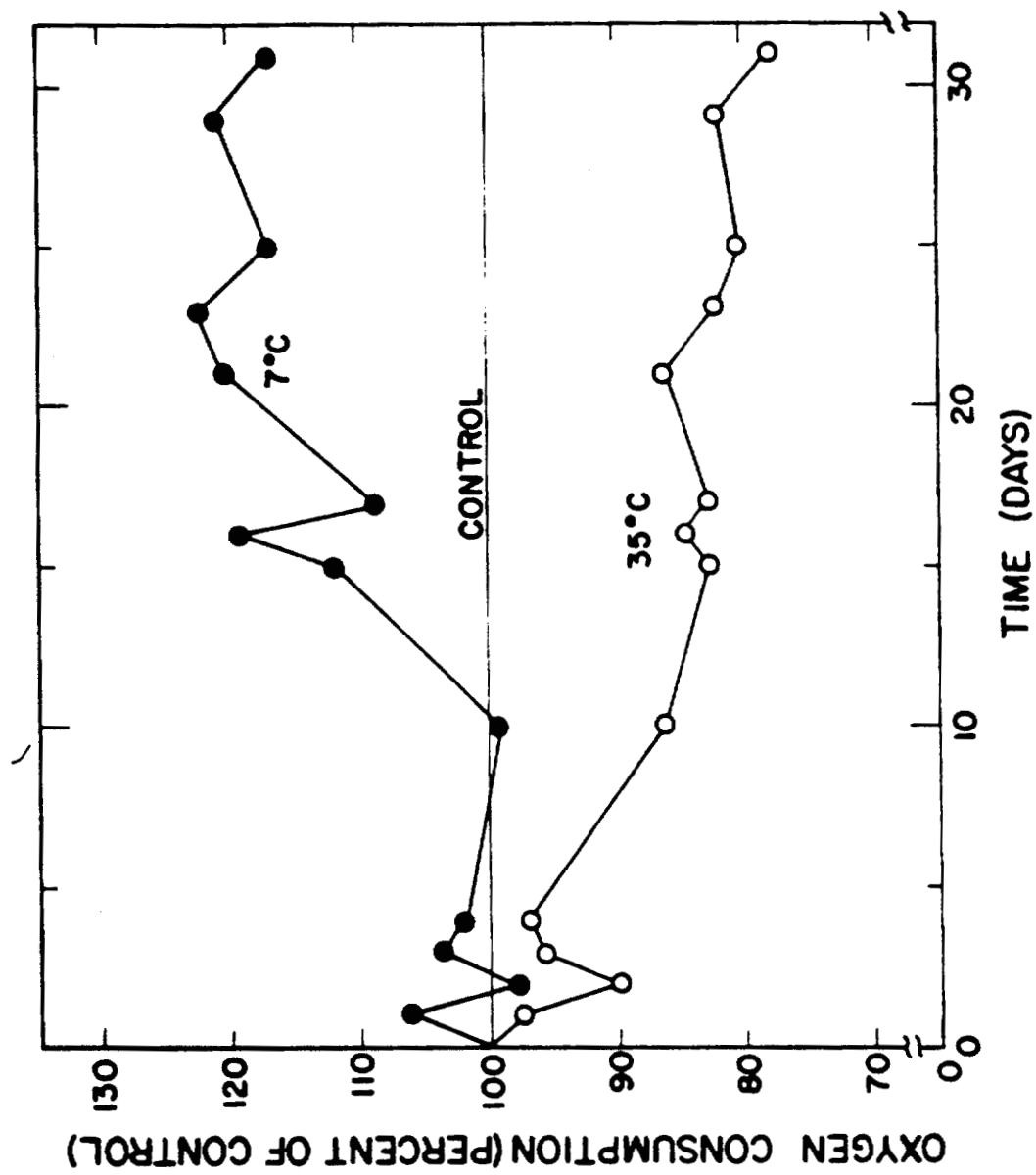


Fig. 2. The effect of temperature on oxygen consumption. Small differences early in the experiment are not significant ( $p > 0.05$ ) but are at the end [ $p < 0.05$  (A.O.V.)].

#### REFERENCES

- (1) J. E. Furchner and C. R. Richmond, J. Appl. Physiol. 18, 786 (1963).
- (2) J. S. Hart, Brit. Med. Bull. 17, 19 (1961).
- (3) S. Brody, Bioenergetics and Growth, Reinhold Publishing Corp., New York (1945), p. 370.
- (4) C. R. Richmond, J. E. Furchner, and W. H. Langham, Los Alamos Scientific Laboratory Report LAMS-2627 (1961), p. 175.

**EFFECT OF CONDITIONING TO TEMPERATURE STRESS ON THE EXCRETION OF CESIUM BY MICE (J. E. Furchner, G. A. Drake, and C. R. Richmond)**

**INTRODUCTION**

Mice maintained at abnormal temperatures excrete cesium at rates different from the cesium excretion rate in mice maintained at normal temperatures. If such alterations in excretion rates are the result of superficial responses to temperature stress, such as increased or decreased food and water intake, then mice which have been exposed to a temperature stress should show a normal excretion pattern when the stress is removed. If the alterations in excretion rates result from a profound metabolic response such as a change in enzyme patterns, then abnormal excretion rates should persist for a while after the removal of the temperature stress.

**METHODS**

Three groups of mice, each consisting of 8 RF females, were maintained at 35°, 22°, and 7°C for 58 days. During this time each animal was in a single cage and had access to water and commercial food ad libitum. At the end of 58 days, each animal was injected intraperitoneally with 0.6  $\mu$ Ci of cesium-137 as the chloride. Each group was maintained in a common cage. Whole-body cesium-137 activity was measured periodically. Determinations of urinary and fecal activities were also made.

**RESULTS**

Figure 1 shows a plot of the retention function fit to the whole-body retention data by computer analysis (smooth curves). The vertical bars represent the range of the data points. The early portion of the retention data from the animals exposed to low temperatures is omitted for the sake of clarity. It seems clear that the terminal portions of the curve are almost parallel, and the half-times for these components of the retention functions for the high-, normal-, and low-temperature animals are 6.1, 6.5, and 6.3 days, respectively. It seems clear then that the small differences are due to early differences in excretion rates.

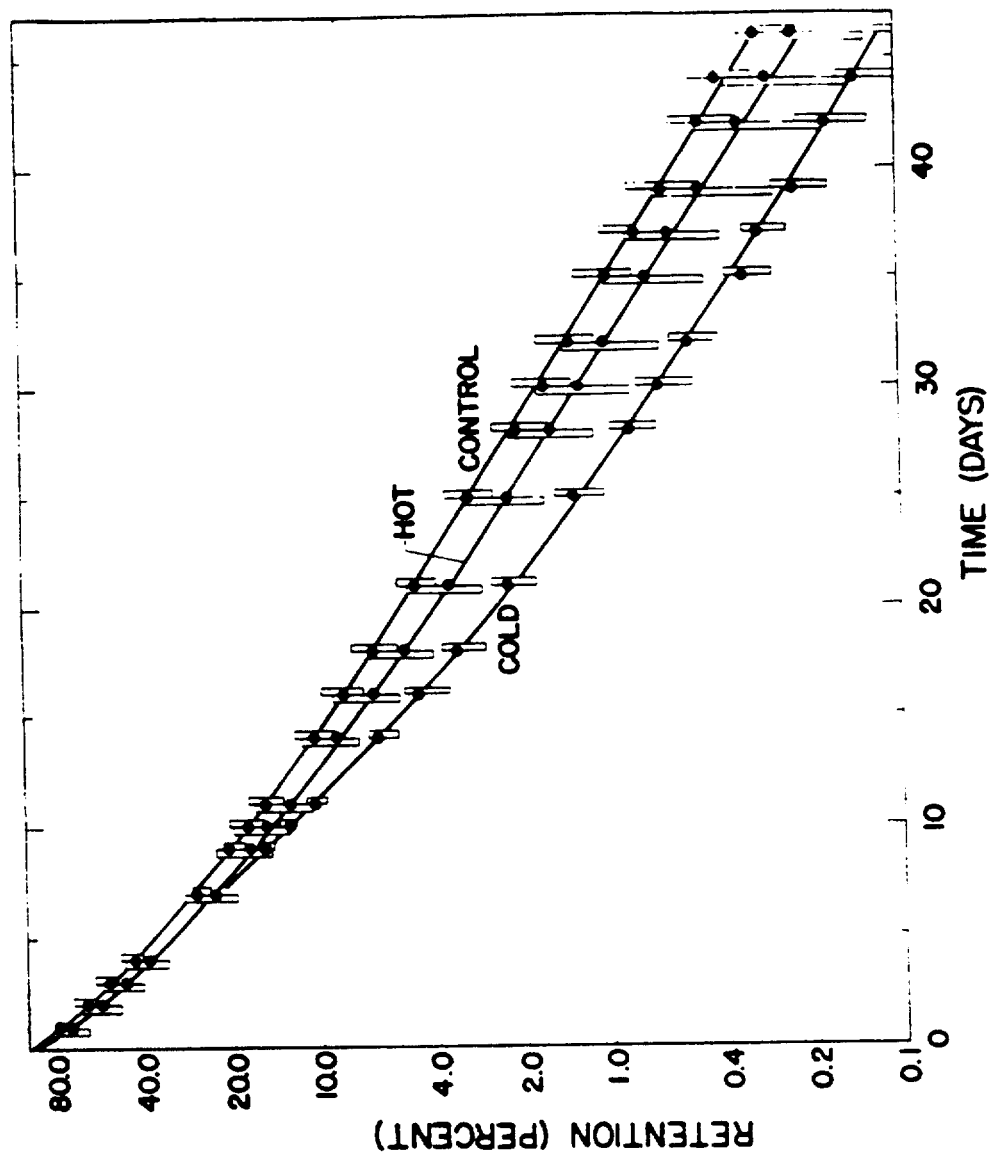


Fig. 1. Cesium-137 excretion in mice after 2 months exposure to 37°C (hot), 7°C (cold), and 22°C (control). The smooth curves are plots of the retention functions fit to the data by computer analysis. The vertical bars show the range of the data points for each group. The data points show average values for the group.

The urinary-to-fecal ratios for cesium-137 during the first few days after removal from adverse temperatures were 9.7, 7.8, and 5.2 for the high-, normal-, and low-temperature animals, respectively, whereas at the end of the experiment these ratios were 8.7, 8.1, and 8.7 in the same order.

## DISCUSSION

The change in the excretion rate of cesium-137 imposed on mice by high temperatures apparently is eliminated by a return to normal temperatures. The change imposed by cold stress persists for a week or more after removal of the temperature stress. Thus, the increased energy expenditure associated with prolonged cold stress demands a change in enzyme patterns (1), while the response to heat stress seems more superficial. The decreased fecal excretion in the high-temperature animals is attributed to the decreased food intake, and the converse is assumed to be true for the low-temperature animals. The effect of temperature stress on cesium-137 excretion is not a simple cause-effect relation with basal metabolism or oxygen consumption but is mediated by a complex of responses, of which oxygen consumption is but a facet.

## REFERENCE

- (1) F. Depocas, Brit. Med. Bull. 17, 25 (1961).



**CESIUM-137 CONTENT OF NEW MEXICO CONTROL SUBJECTS: CURRENT DATA AND A TEN-YEAR RECAPITULATION (C. R. Richmond, J. E. London, and J. S. Findlay)**

**INTRODUCTION**

At the request of the U. S. Atomic Energy Commission's Division of Biology and Medicine in 1962, this Laboratory began systematic measurements on the secular changes in whole-body cesium-137 burdens. Previously, from 1956 until 1962, similar measurements were made on normal New Mexico subjects. Information has been obtained on cesium-137 burdens in a control population for almost an entire decade. This report contains data obtained from June 1964 to July 1965 and presents a recapitulation of data obtained during the last decade in this Laboratory.

**METHODS AND RESULTS**

Whole-body activity measurements were made in nearly 4 $\pi$  steradian geometry liquid scintillation detectors. HUMCO I was used prior to April 1962, and since that date HUMCO II has been in operation. One group of subjects is measured weekly and another monthly. On the average, 31 people from the monthly control group of 35 subjects were measured each month during the past year. Each subject is measured for 200 sec; no showers are required but disposable paper suits are worn. Statistical error (standard error of the mean) for body potassium is roughly  $\pm 3$  g, or about 2 percent of the body potassium content for an average adult male. For cesium-137, the corresponding statistical error is about  $\pm 5$  pCi cesium-137 per g potassium. All counting data are processed by electronic computer.

Table 1 lists average cesium-137 concentrations in weekly and monthly control groups for 13 months beginning with June 1964. The peak reached in July 1964 represents the highest value yet. Previously, a high of  $\sim 70$  pCi per g potassium was reached early in 1960. One standard deviation ( $\sigma_x$ ) is given for each mean value. This statistical error is the quotient of  $\sigma_1/\sqrt{n}$ , where  $\sigma_1$  is the standard deviation for a single measurement and  $n$  is the number of measurements. In every case, the average for the weekly group is higher

TABLE 1. CESIUM-137 BODY BURDENS OF NEW MEXICO SUBJECTS

Month	No. of Subjects	Average Cs-137 (pCi/g K)*	No. of Measurements	Average Cs-137 (pCi/g K)*
<u>1964</u>				
June	33	113.87 $\pm$ 4.52	23	129.03 $\pm$ 8.15
July	31	119.38 $\pm$ 5.22	33	139.30 $\pm$ 10.97
August	30	117.11 $\pm$ 5.23	29	132.41 $\pm$ 5.82
September	27	111.81 $\pm$ 4.93	28	137.13 $\pm$ 6.98
October	34	114.42 $\pm$ 4.24	37	120.16 $\pm$ 6.23
November	34	112.25 $\pm$ 4.59	34	117.80 $\pm$ 6.47
December	22	109.82 $\pm$ 5.46	39	116.39 $\pm$ 6.05
<u>1965</u>				
January	35	104.65 $\pm$ 4.39	38	110.88 $\pm$ 5.93
February	33	104.19 $\pm$ 4.21	39	108.32 $\pm$ 5.52
March	35	100.74 $\pm$ 4.36	49	106.01 $\pm$ 4.31
April	33	96.40 $\pm$ 4.66	39	107.55 $\pm$ 5.11
May	27	93.42 $\pm$ 4.96	40	100.32 $\pm$ 4.73
June	31	93.58 $\pm$ 4.44	50	96.80 $\pm$ 3.83

\* Mean  $\pm$   $\sigma_{\bar{x}}$ .

than that for the monthly group. However, if one tests the difference between the means (students t test) for each group for significance, only the September values differ importantly. The reason for this high but apparently real value for weekly controls is not known.

Figure 1 shows average cesium-137 concentrations for the monthly control group compared with values obtained by Cohn et al. (1) on 10 control subjects at the Brookhaven National Laboratory. Agreement between fall 1962 and mid-1963 is excellent. Peak concentrations in July 1964 were also noted by Cohn. The reason for the large discrepancies observed at the 1962 low and during the 1964 peak is not known. Vertical error-band around each mean is  $\sigma_{\bar{x}}$ . Figure 2 shows temporal changes in New Mexico control subjects for a period of 10 years. Quarterly averages obtained from the monthly control group are plotted. Statistical error, shown by vertical bars, is  $\sigma_{\bar{x}}$ . Atmospheric weapons tests since 1960 are indicated along the abscissa. Increases in cesium-137 concentrations as a result of two atmospheric tests during 1964 and 1965 are not anticipated.

#### DISCUSSION

Peak cesium-137 body burdens of  $\sim 120$  pCi per g potassium resulting from fallout were reached in July 1964 in New Mexico control subjects; the cesium-137 burden for a normal adult male was about 20 nCi. Peak concentrations were observed at the same time in Long Island, New York, but at the considerably higher level of 150 to 160 pCi per g potassium. If no additional atmospheric testing occurs cesium-137 burdens will probably fall to 70 pCi per g potassium, the previous early 1961 peak, by late spring 1966. Continued measurements will afford an opportunity to observe the rate of decrease in cesium-137 burdens in this control population.

#### REFERENCE

- (1) S. H. Cohn, E. A. Gusmano, and R. A. Love, Nature 205, 537 (1965).

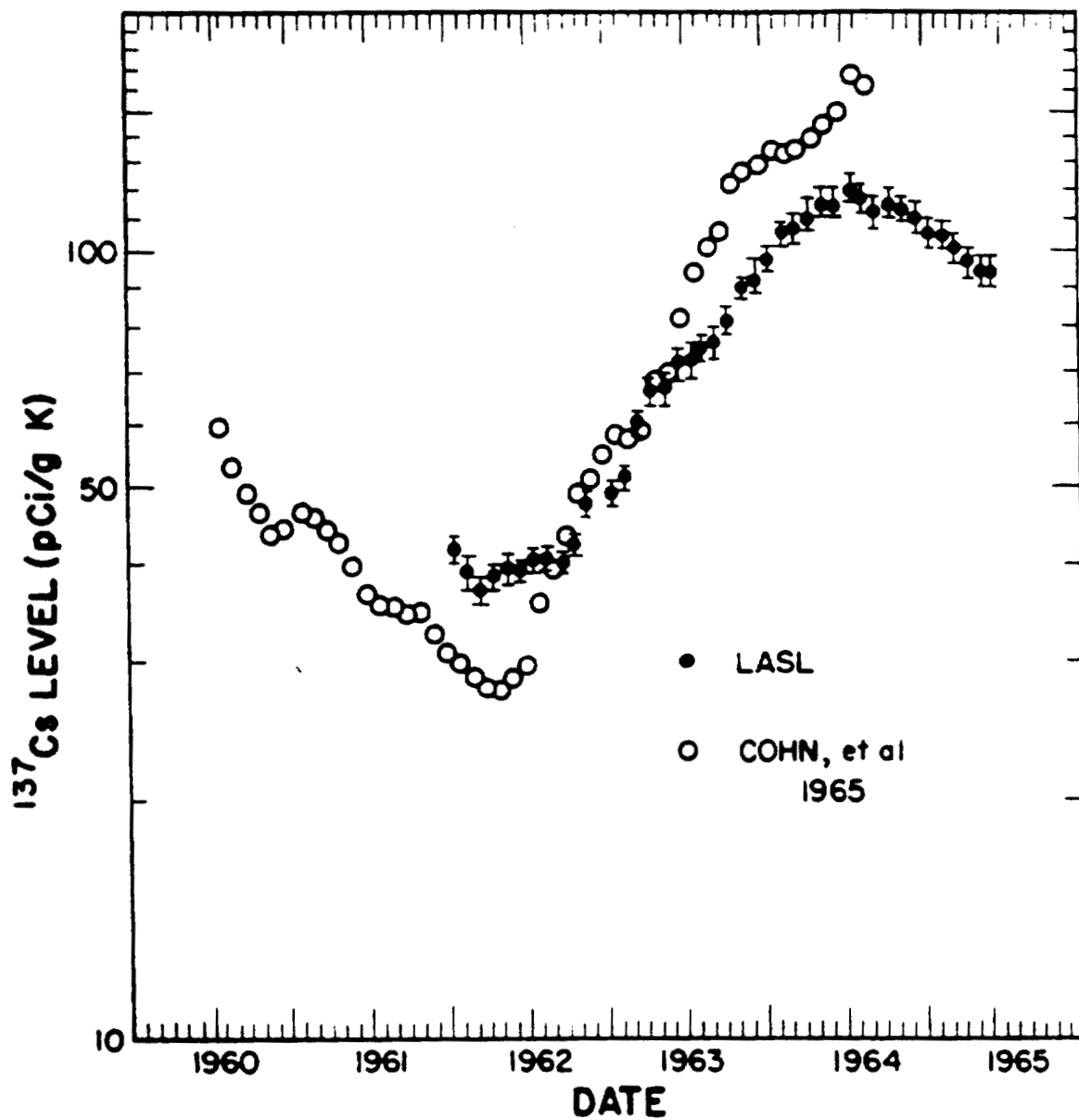


Fig. 1. Cesium-137 concentration in control populations from New Mexico and New York. The statistical error is one standard deviation for the indicated mean.

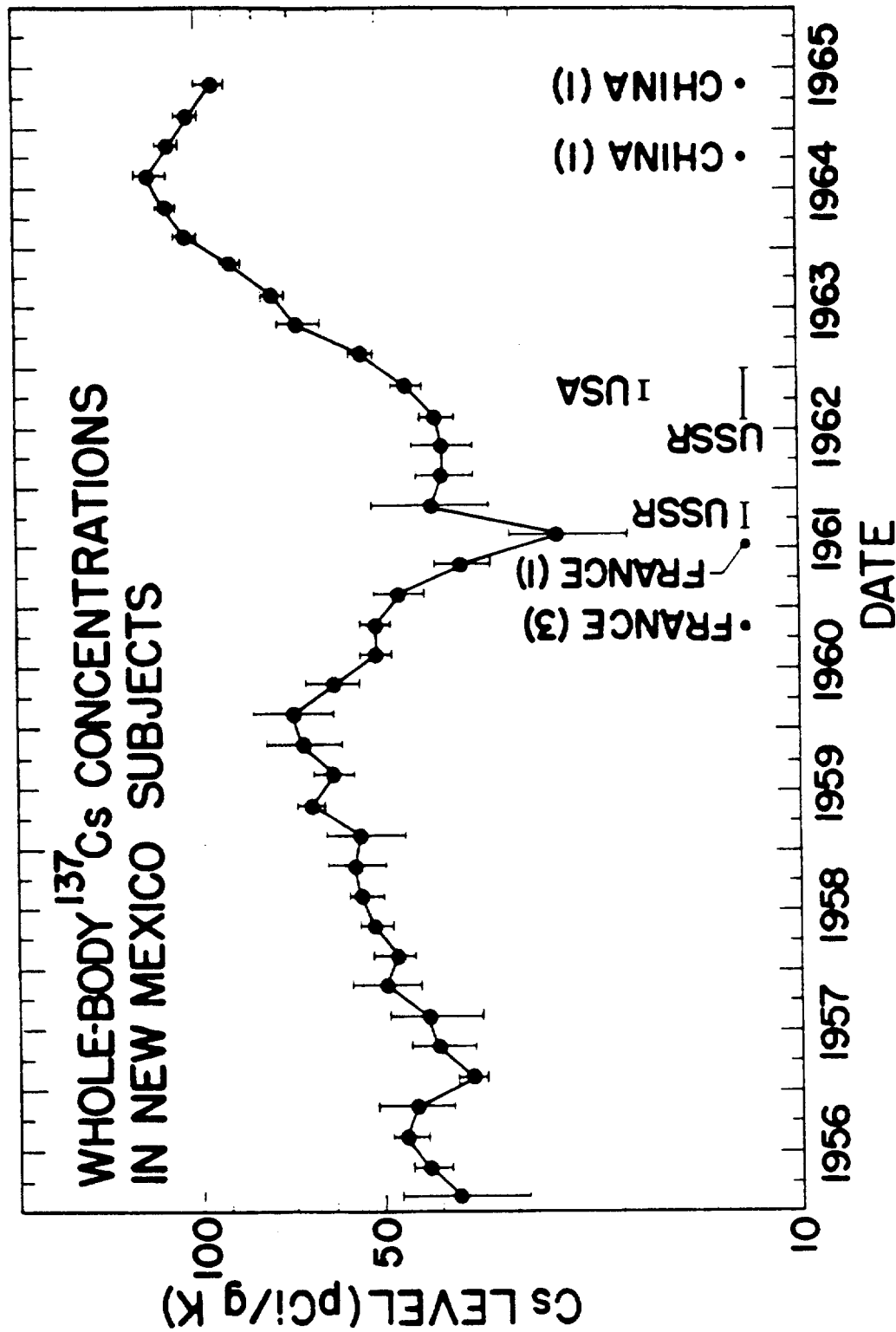


Fig. 2. Cesium-137 concentrations in New Mexico control subjects over a 10-year period. The statistical error is one standard deviation for the indicated mean.


# **CORRECTION OF METABOLIC DATA FOR CHANGES IN FALLOUT CESIUM-137 (C. R. Richmond, J. S. Findlay, and J. E. London)**

## **INTRODUCTION**

Temporal changes in the amount of fission product radionuclides within the body must be accounted for during the time-course of low-level tracer experiments. Usually the amounts of activity in the energy regions of interest are measured in the experimental subject prior to radionuclide administration. The resultant values are then subtracted from the activity in the subject at each subsequent measurement. Unfortunately, in many instances the subject's "pre-experimental" background will vary as a complex function of season, fallout rate, and environmental concentrations. This report shows one such correction for cesium-137 changes encountered during a low-level tracer experiment in several human subjects.

## **METHODS AND RESULTS**

All whole-body radioactivity measurements were made in HUM-CO II, a large-volume,  $4\pi$  liquid scintillation counter, using 200-sec counting times. Statistical error (standard error of the mean) is about + 5 pCi cesium-137 per g of body potassium. Because a normal male adult weighing 70 kg contains about 150 g of potassium, the gross cesium-137 error of about + 0.75 nCi is small compared with recent cesium-137 body burdens of 20 nCi.

In August 1963, a low-level tracer experiment was started in 3 male subjects. Three hundred nCi cesium-137 were given each subject; body cesium-137 fallout burdens at that time were about 11 nCi for an average 70-kg male. During the following 10 months cesium-137 fallout levels in a group of 35 control subjects increased by some 70 percent. One subject (HMCs-) showed a gross body burden of 88 nCi cesium-137 about 10 months after administration. Subtraction of the "pre-experimental" cesium-137 fallout activity indicated a net burden of 77 nCi remaining from the administered cesium-137. However, if the "pre-experimental" activity had increased by 70 percent, the net burden remaining 10 months after administration would be 69 nCi. Thus, an error approximating 10 percent might be experienced by not correcting

data for increased cesium-137 fallout burdens. More importantly, this error would increase with time so long as the cesium-137 fallout burden also increased with time.

Although cesium-137 fallout burdens in people vary with time, the increase for 10 months following August 12, 1963, appeared to be quite constant, and data for several control subjects were fitted to a linear function by an iterative least-squares method programmed for an IBM 7094 computer. Figure 1 shows such a computer fit for one control subject. Over the 10 months, the cesium-137 level increased from 14.3 nCi to ~21.5 nCi, or by roughly 67 percent. Table 1 gives the intercept and slope constants obtained for several control subjects. An average slope constant of 0.023 was found.

TABLE 1. INTERCEPT AND SLOPE VALUES FOR LINEAR REGRESSION FUNCTIONS DESCRIBING INCREASE IN BODY CESIUM-137 FROM FALLOUT\*

Subject	Intercept (nCi cesium-137)	Slope
●	14.3	0.0231
●	11.5	0.0244
●	8.9	0.0211
$\bar{x}$	11.6	0.0229

\*For 330 days following August 12, 1963.

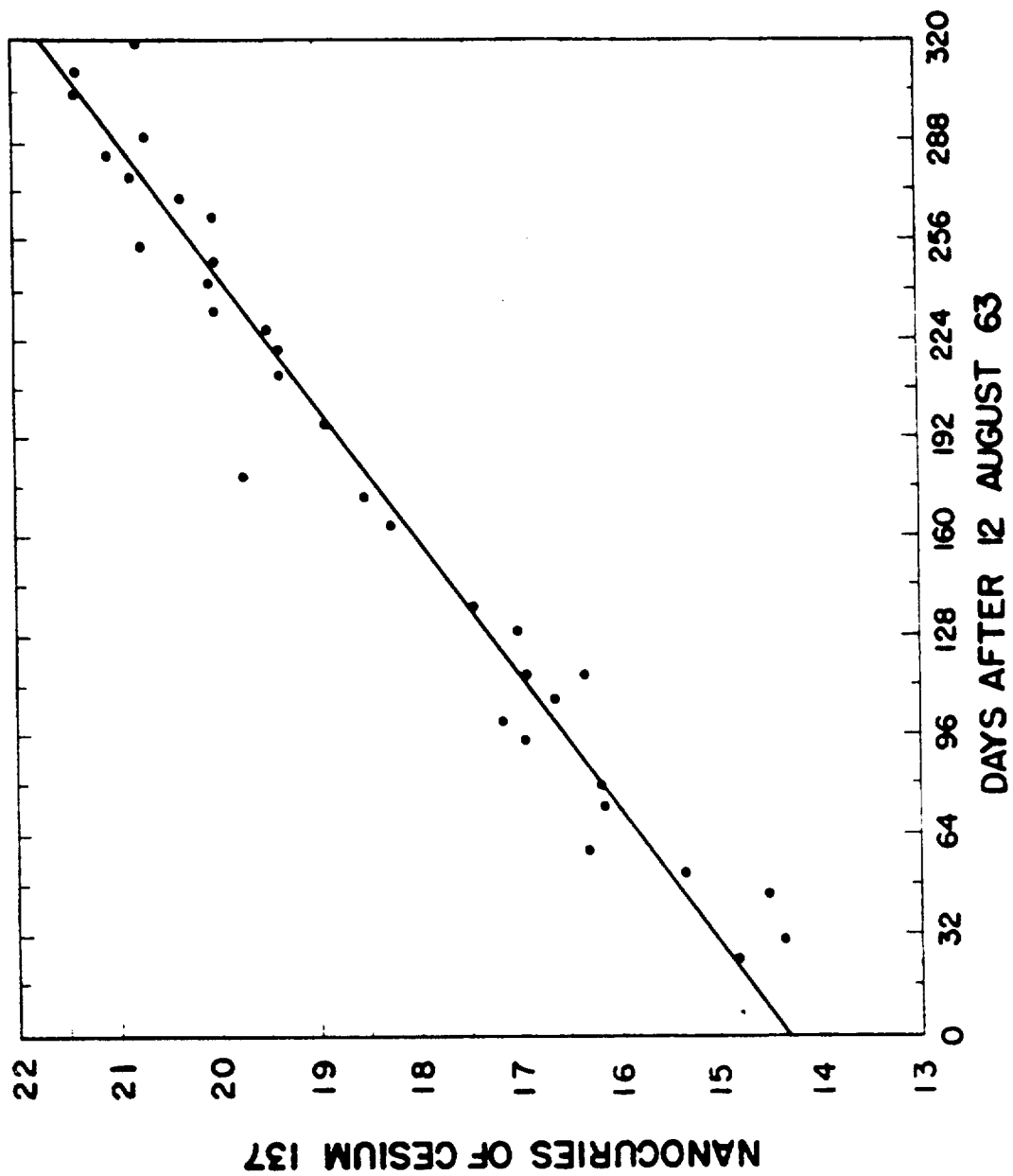


Fig. 1. Increase in fallout cesium-137 for 320 days following August 12, 1963, in a weekly control subject.



Corrections for each subject in the tracer study were made by subtracting a variable amount of "fallout" cesium-137 at each measuring time. This amount (y) was calculated from a linear regression equation,

$$y = a + b x,$$

in which a is the subject's "pre-experimental" cesium-137 burden; b is 0.023, the average obtained from the 3 control subjects; and x is days after time zero (August 12, 1963).

Figure 2 shows the whole-body cesium-137 retention data for subject HMCs-~~10~~. After 200 days most observed retention values fall above the exponential regression line. Figure 3 shows the corrected data points and best-fit regression line for HMCs-~~10~~. As an example, the last data point changes downward from 77 to 69 nCi after applying the correction. Table 2 compares various parameters for data given in Figs. 2 and 3. After using the correction factor, the biological half-life ( $T_b$ ) value decreased from 161 to 154 days, or by about 5 percent. The smaller weighted variance obtained after correcting the data indicates a better fit to the regression line. Changes on the order of 5 percent were observed for 2 other subjects.

## DISCUSSION

Analysis of low-level tracer experiments may be complicated by small but variable amounts of radionuclides from fallout. This report gives an example of a correction based on data obtained from control subjects. As tracer experiments become more sophisticated and environmental concentrations of radiocontaminants increase, this problem becomes more important. Control animals (dogs, monkeys, and humans) are now counted on a routine schedule in the detectors used for metabolic studies on these species. If necessary, data can be corrected for changes observed in the control populations.





TABLE 2. COMPARISON OF CESIUM-137 RETENTION BY HMCs-  
BEFORE AND AFTER CORRECTIONS FOR INCREASED FALL-  
OUT CESIUM-137

	Non-Corrected	Corrected
Number of Points	61	61
Time Span (days)	0-330	0-330
Biological Half-Life (days)	161	154
Intercept (nCi)	308.2	309.7
Area* (nCi · days)	233	222
Iterations**	6	6
Weighted Variance	9.9	5.9

$$* \text{Area} = \int_0^{\infty} R_t dt.$$

\*\* Required for convergence in fitting procedure.

**SUPPORT ACTIVITIES OF THE LASL WHOLE-BODY COUNTING FACILITY**  
(C. R. Richmond, J. E. London, and J. S. Findlay)

**INTRODUCTION**

In addition to routine programmed metabolic studies, the Los Alamos whole-body counting facility is used in support of activities carried on by other parts of the Laboratory and by researchers from other installations. This report enumerates some of these activities.

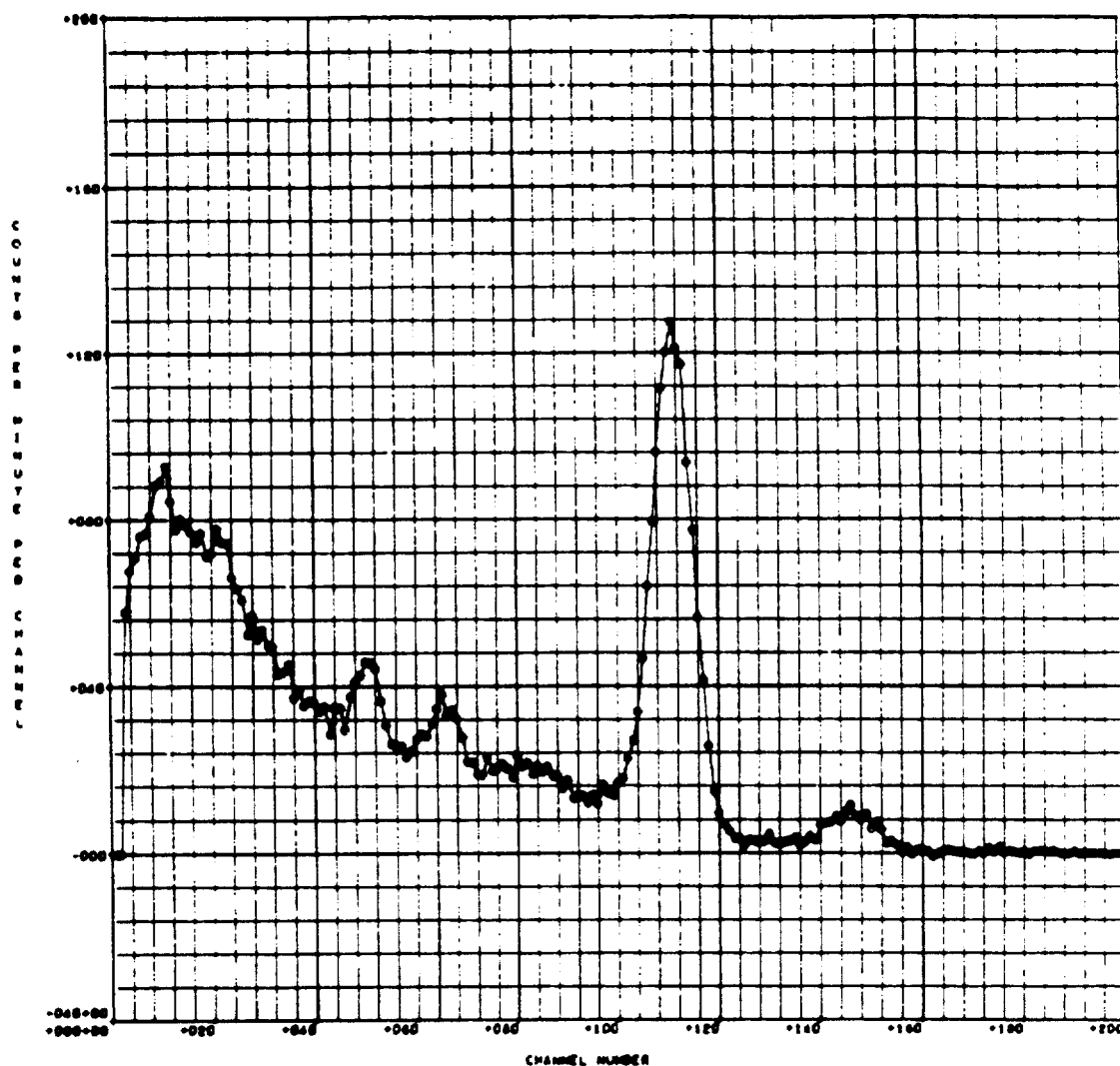
**METHODS AND RESULTS**

Approximately 200 people were measured in the whole-body counters during the past year as part of several support-type projects. Table 1 gives a general breakdown of the numbers and categories involved. Figure 1 shows the gamma-ray spectrum obtained from one LASL employee who was contaminated with zinc-65 while working at another laboratory. The photopeaks at 0.66 and 1.46 Mev correspond to normally occurring cesium-137 and potassium-40. In addition to the main zinc-65 photopeak at 1.12 Mev, a small peak due to annihilation of the positron is apparent at 0.51 Mev. By comparing areas under the zinc-65 and potassium-40 photopeaks and estimating the subject's potassium-40 burden from other subjects of similar body build, zinc-65 burden is estimated to be about 0.25  $\mu$ Ci. The subject is being measured periodically. This amount is about 1/240th of the q value reported by the International Commission for Radiation Protection for zinc-65.

Figure 2 shows the spectrum obtained for a Laboratory employee referred to us by the LASL Health Physics Group. In addition to photopeaks corresponding to cesium-137 and potassium-40, other structure is noted at  $\sim$  0.48, 0.75, and 1.60 Mev. The peak at 0.75 corresponds to several gamma rays (0.72 to 0.76 Mev) from the zirconium-95/niobium-95 combination. Peaks at  $\sim$  0.48 and 1.60 Mev are from the barium-140/lanthanum-140 combination. These nuclides are fission products arising from operations conducted where the subject worked as a radiological monitor. Similar spectra were obtained for several other subjects. For comparison, Fig. 3 shows the spectrum obtained from a normal non-contaminated (except for fallout cesium-137) subject. Note the absence of structure

TABLE 1. SUPPORT ACTIVITIES OF THE LOS ALAMOS WHOLE-BODY COUNTING FACILITY

Project No.	Category	Laboratory	Number of People
1	Applied Health Physics	Los Alamos Scientific Laboratory	24
2	Aerospace Pilots	Lovelace Foundation	30
3	Muscular Dystrophy	Lovelace Foundation	19
4	Athletes and Physical Education Majors	Lovelace Foundation and University of New Mexico	61
5	Large Counter Calibration	Kirtland Air Force Base Robert A. Taft Sanitary Engineering Center	28
6	Miscellaneous	Laboratory Visitors	3
			30



SUBJECT ( ) STANDARD CRYSTAL POSITION 2MEV/200 CHANNELS DATE 2/ 5/65  
 SERIAL NUMBER 11 100 MINUS 19 104 100104 BACKGROUND SCP 2 MEV/200 CHANNELS

Fig. 1. Gamma-ray spectrum obtained from subject contaminated internally with zinc-65. Abscissa is equivalent to  $\sim 2$  Mev. Photopeaks in channels 51 and 111 represent zinc-65. Cesium-137 and potassium-40 are shown as peaks in channels 65 and 146, respectively.

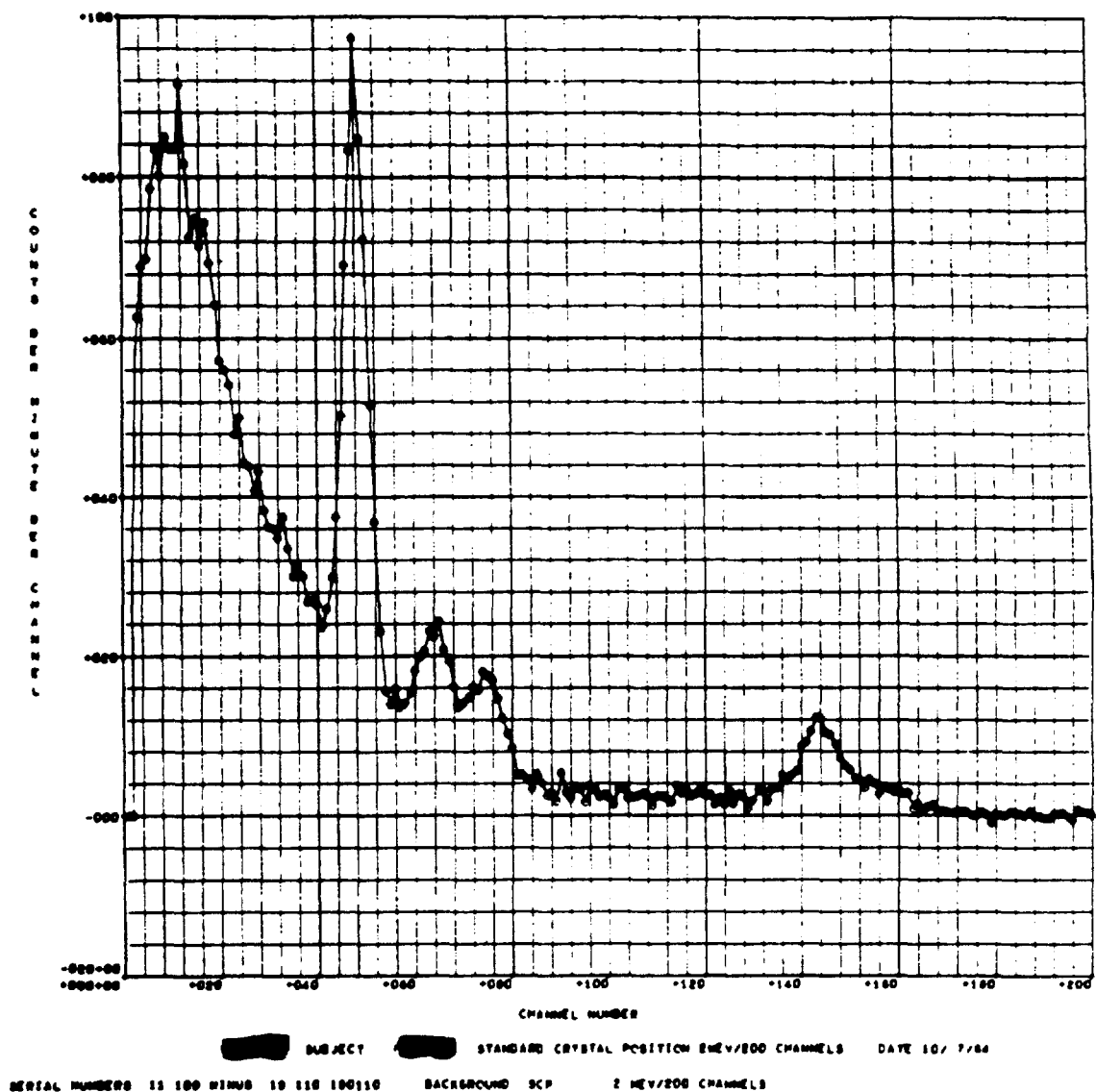


Fig. 2. Gamma-ray spectrum obtained from subject contaminated with several fission product radionuclides. In addition to cesium-137 and potassium-40, photopeaks from barium-140/lanthanum-140 are present in channels 48 and 160. The photopeak in the region of channel 74 corresponds to zirconium-95/niobium-95. Two-hundred channels represent  $\sim 2$  Mev.



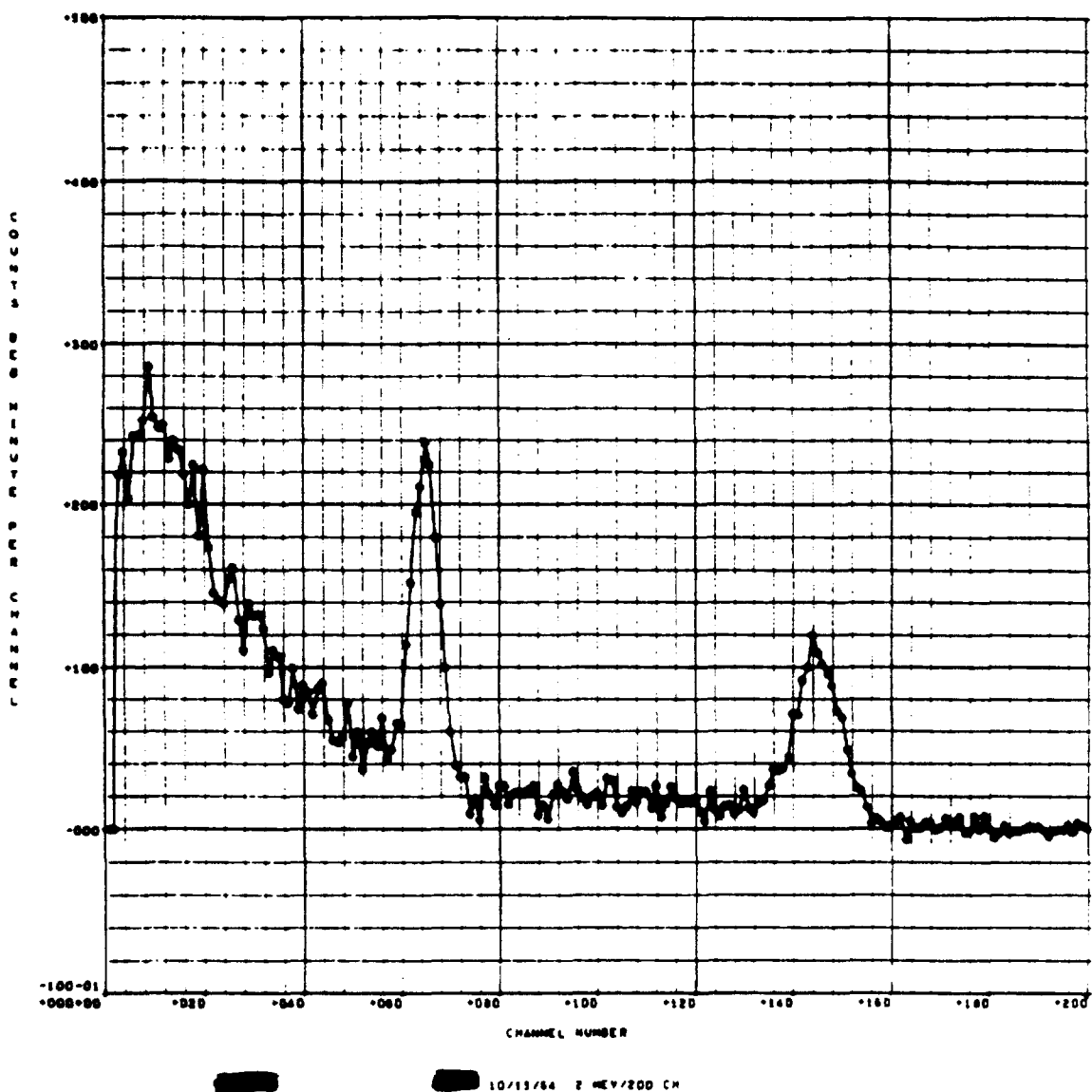


Fig. 3. Gamma-ray spectrum obtained from normal uncontaminated subject. Naturally-occurring potassium-40 is identified as photopeak in channel 144. Fallout cesium-137 corresponds to photopeak in channel 65. Two-hundred channels are equivalent to ~ 2 Mev.

between the cesium-137 and potassium-40 photopeaks. Measurements are routinely made on several subjects from each of several Laboratory sites where internal contamination is a known possibility. Prior to employment termination, measurements are made on employees engaged in certain types of work.

Body cesium-137 and potassium-40 measurements are made in HUMCO II on numerous subjects (Table 1) referred to us by staff members of the Lovelace Foundation in Albuquerque. Body potassium is of interest in muscular dystrophy cases, as potassium levels are indicative, as in normal subjects, of lean body mass. The highest potassium concentration recorded by us to date was for a [REDACTED], and the lowest in a [REDACTED].

Twenty-eight subjects of varying weights and body builds were measured in HUMCO II. Information on body cesium-137 and potassium-40 will be compared with data obtained for the same subjects measured in a 2 $\pi$  counter at the Kirtland Air Force Base in Albuquerque. Several subjects from the Robert A. Taft Sanitary Engineering Center in Cincinnati, Ohio, were measured for similar reasons.

#### DISCUSSION

The whole-body gamma-ray spectrometer is a versatile instrument for detecting small amounts of gamma-emitting radionuclides in man. Its value as an adjunct to applied health physics studies is well established. Identification of small amounts of internally-deposited radionuclides also affords an opportunity to measure secular changes in the body burden. Measurement of normal subjects from outside the Laboratory adds to our knowledge of potassium concentrations in specialized groups. This project will be continued at about the same level during the next year.

## MAMMALIAN METABOLISM SECTION

### PUBLICATIONS AND ABSTRACTS OF MANUSCRIPTS SUBMITTED

APPLICATION OF REGRESSION ANALYSIS TO THE POWER FUNCTION,  
P. C. McWilliams, J. E. Furchner, and C. R. Richmond.  
Health Phys. 10, 817-822 (1964).

Abstracted in Los Alamos Scientific Laboratory Report LA-3132-MS (1964), p. 102.

EFFECTS OF ENVIRONMENTAL TEMPERATURE ON RETENTION OF CHRONICALLY ADMINISTERED CESIUM-137, J. E. Furchner, C. R. Richmond, and G. A. Drake. Health Phys. 11, 623-628 (1965).

Abstracted in Los Alamos Scientific Laboratory Report LA-3132-MS (1964), p. 102.

METABOLIC KINETICS, C. R. Richmond and J. E. Furchner. To be included as a chapter in "The Beagle as an Experimental Dog," A. C. Anderson and F. Carter, eds. (University of California, Davis).

This chapter is devoted to the application of whole-body counting systems (radiation detectors) to the study of gross metabolic kinetics in the beagle. Included is a general description of liquid scintillation detectors and sodium iodide crystal detectors. One section discusses the use of the power function and the exponential function as mathematical models for describing gross metabolic data. Data are included for hydrogen, sodium, potassium, rubidium, and cesium as representative elements from Group I in the period

classification. Beryllium, strontium, barium, and zinc are included as representative Group II elements. A miscellaneous group, including cerium, ruthenium, iodine, silver, niobium, and manganese, is also covered. Although emphasis is on gross whole-body retention of radioactive tracers of these elements, information on gastrointestinal absorption and tissue deposition is included.

COMPARATIVE METABOLISM OF RADIONUCLIDES IN MAMMALS. III.  
RETENTION OF MANGANESE-54 BY FOUR MAMMALIAN SPECIES, J. E.  
Furchner, C. R. Richmond, and G. A. Drake. Health Phys.  
(submitted).

Radiomanganese (Mn-54) was administered to mice and rats by the oral, intravenous, and intraperitoneal routes and to dogs and monkeys by the oral and intravenous routes. Whole-body counting techniques, utilizing 4 $\pi$  liquid scintillation counters, were used to determine whole-body retention parameters. Retention functions consisting of the sum of three or four exponential expressions were adequate descriptions of retention until the body burden was less than 1 percent of the administered dose. The longest effective half-times after intravenous injections were 119, 146, 99, and 68 days for mice, rats, monkeys, and dogs, respectively. Tissue distribution studies in rats showed that, for most tissues, concentration as a function of time roughly paralleled whole-body retention. Both bone and brain were found to have a slower rate of loss than other tissues. Using a parabolic relation between body weights and the integrals of the retention functions, it was estimated that  $7 \times 10^{-3}$   $\mu\text{c/ml}$  was the maximum permissible concentration in water for man. This value is in good agreement with the current ICRP recommended value of  $8 \times 10^{-3}$ .

## CHAPTER 3

### MAMMALIAN RADIOBIOLOGY SECTION

GENETIC EFFECTS OF X IRRADIATION TO CONSECUTIVE GENERATIONS  
OF MALE MICE (J. F. Spalding, M. R. Brooks, and R. F.  
Archuleta)

#### INTRODUCTION

A radiation genetics program to study heritable effects of X-ray exposure to consecutive generations of mice has been continued through the 35th generation. The program was started with one sib pair of RFM strain mice (F<sub>3</sub> from RFM No. 25-5, Oak Ridge). Two lines of mice were started with the mating of this sib pair. An irradiated line (F<sup>X</sup>) has been continued in which all male mice are exposed to 200 rads of X rays at 26 + 2 days of age and caged with their sisters. The second line is an unirradiated control line (F<sup>C</sup>) having the same parental origin and inbreeding. Two additional sub-lines, one from the F<sup>X</sup> line and one from the F<sup>C</sup> line, are also under study. The sub-line (F<sup>XN</sup>) was started from one litter of the F<sup>X</sup> line after 10 generations of X irradiation and has been continued for an additional 25 generations with no additional X-ray exposure in the same manner as the control line. This sub-line was started to test natural selection as a means of eliminating the radiation-induced depression in litter characteristics evidenced after 10 generations of X irradiation. The second sub-line (F<sup>CX</sup>) was started from one litter of the F<sup>C</sup> line after 25 generations of inbreeding. The males in the F<sup>CX</sup> sub-line are exposed to 200 rads of X rays at 26 + 2 days of age in the same manner as is the F<sup>X</sup> line. This sub-line was started to test the possibility of a radiation-induced genetic change in radioresistance which

was discovered in line  $F^X$  after 10 generations of X-ray exposure. For the purpose of this report, progress has been categorized according to specific objective of the program, and the above will serve as an introduction to all objectives reported.

#### GENETIC EFFECTS. I. COMPARATIVE BREEDING CHARACTERISTICS OF OFFSPRING OF THE 25TH GENERATION

Selected breeding characteristics through the 20th generation of this program have been reported (1,2). The following is a tabulation of some of the breeding characteristics of 8 groups of offspring from three of the four lines of mice described in the introduction (namely, lines  $F_{25}^C$ ,  $F_{25}^X$ , and  $F_{25}^{XN}$ ). Sib and non-sib matings were done on  $F_{26}^C$ ,  $F_{26}^X$ , and  $F_{26}^{XN}$ . Reciprocal crosses were also made between  $F_{26}^C$  and  $F_{26}^X$ . Some of the breeding characteristics and litter data from these matings are tabulated in Table 1.

The total number of mice born to the 50 breeding pairs in each group was greater in  $F_{26}^C$  than in  $F_{26}^X$ . The  $F_{26}^{XN}$  group was intermediate, indicating some natural selection against this decrement over the last 15 generations. Sib and non-sib matings within each line were quite similar, showing no advantage for non-sib matings. The decrement in total production was reflected by females rather than with the origin of male mice. In crosses between the irradiated and nonirradiated lines, it was observed that control females produced the same total whether bred to  $F_{26}^C$  males or to  $F_{26}^X$  males. Irradiated line females showed no improvement in total production when bred to  $F_{26}^C$  males. Although the control line weaned more mice than did the irradiated line, the sib-mated controls had the smallest weaned-to-born ratio of any group studied. Control females  $F_{26}^C$  mated to  $F_{26}^X$  males weaned more mice than any group, and the  $F_{26}^{XN}$  sib matings also weaned more mice than did control line matings.

Many of the characteristics listed in Table 1 showed that ancestral X irradiation history of the male had little effect on breeding as influenced by the male, but that any decrement incurred was expressed almost entirely by the female.

It has been the intent of this program to determine whether or not minor mutations (individually not detectable) would accumulate additively to reach significant levels or would reach genetic equilibrium in a relatively short time. It

TABLE 1. BREEDING CHARACTERISTICS OF MICE FROM CONTROL AND X-IRRADIATED ANCESTRY  
(50 BREEDING PAIRS PER LINE)

Characteristic	Control Line (FC)		X-Irradiated Line (FX)		X-Irradiated Sub-Line (FXN)		Line Crosses	
	Sib- Mated	Nonsib- Mated	Sib- Mated	Nonsib- Mated	Sib- Mated	Nonsib- Mated	F <sup>C</sup> Females x F <sup>X</sup> Males	F <sup>C</sup> Females x F <sup>C</sup> Males
Mice Born	1721	1647	1304	1301	1536	1438	1732	1332
Mice Weaned	1177	1153	1027	1056	1291	1230	1342	1172
Weaned to Born (percent)	68	70	79	81	84	86	77	88
Litters Born	267	270	232	223	273	249	288	206
Litters Weaned	197	198	176	177	227	211	219	182
Litter Size (average at birth)	6.45	5.86	5.62	5.83	5.63	5.78	6.01	6.47
Weaning Weight (average g)	10.48	10.71	10.33	10.56	11.32	10.88	10.75	11.23
Litters Cannibalized	114	93	182	147	97	94	95	105
Sterility	0	0	1	3	0	0	2	3

would appear at this time that genetic equilibrium has been reached in this program and that serious concern that minor sublethal mutations are in the long run the most serious threat to the genetic well-being of an irradiated population is open to question. Litter data are being compiled on the 32nd generation in this program at the present time, and terminal studies are being planned for offspring of 40 generations of X-irradiated sires.

#### REFERENCES

- (1) J. F. Spalding and M. R. Brooks, Los Alamos Scientific Laboratory Report LA-3132-MS (1964), p. 109.
- (2) J. F. Spalding, M. Brooks, and P. McWilliams, Genetics 50, 1179 (1964).

GENETIC EFFECTS. II. RADIATION RESISTANCE,  $LD_{50}^{30}$ , AND CONTINUOUS EXPOSURE (4 TO 5 RADS/HR) STUDIES IN MICE FROM 30 GENERATIONS OF X-IRRADIATED SIRES

#### INTRODUCTION

A significant difference in mean survival time during continuous exposure to cobalt-60 gamma rays at 4 to 5 rads/hr between  $F^C$  and  $F^X$  mice has been reported earlier (1-3). The origin of this genetic difference in radioresistance, whether the result of radiation-induced mutations in the  $F^X$  line or due to chance segregation at the start of the experiment, is still not certain. However, the decrement in the  $F^X$  line has persisted at the same level for 20 generations. Studies on these two basic lines ( $F^C$  and  $F^X$ ) are being continued in an effort to better understand the genetic inheritance of this type of radioresistance.

#### METHODS AND RESULTS

##### Acute X-Ray Exposures

Granddaughters, 3 to 4 months of age, from  $F_{30}^C$ ,  $F_{30}^X$ ,  $F_{30}^{XN}$ ,



and  $F_{30}^{CX}$  were used to determine  $LD_{50}^{30}$  values from acute X-ray exposures for each group. The results are shown in Table 2. Resistance to acute X-ray exposures was the same for all 4 groups.

#### Continuous Gamma-Ray Exposures

Granddaughters, 6 weeks + 3 days of age, from  $F_{30}^C$ ,  $F_{30}^X$ ,  $F_{30}^{XN}$ , and  $F_{30}^{CX}$ , and first and second generation mice from reciprocal crosses of the  $F_{30}^C$  and  $F_{30}^X$  lines were used. Mice from all lines and crosses were exposed continuously to cobalt-60 gamma rays at a dose rate of 3.5 rads/hr to determine mean survival time (MST) for each line and line crosses. The results are tabulated in Table 3 and are shown graphically in Fig. 1. Mice from the  $F^C$  control line and its X-irradiated sub-line  $F^{CX}$  had similar MST's and showed greater resistance than did the  $F^X$  irradiated line and its natural selection sub-line  $F^{XN}$ . Reciprocal line crosses produced animals possessing radioresistance somewhat intermediate between the control ( $F^C$ ) and irradiated ( $F^X$ ) lines but higher than would be expected if the resistance factor was controlled at one gene locus.

The genetic difference in resistance to radiation in these lines appears to differ from that reported by other laboratories in different strains of mice in one major respect. The resistance difference to exposure to ionizing radiation in the lines being studied at this Laboratory is limited to continuous exposures and specifically to dose rates of approximately 5 rads/hr. Acute exposures fail to show differences in radioresistance between the two lines ( $F^C$  and  $F^X$ , Table 3), and as the dose rate is lowered below 4 rads/hr the magnitude of difference in radioresistance between the two lines diminishes.

Investigations to date suggest that genetic factors controlling red blood cells and their progenitors are responsible for the differences in radioresistance in these lines. In other strains which show radioresistance differences in acute  $LD_{50}^{30}$  values, different genetic factors are no doubt involved. Further investigations on blood characteristics during continuous exposure are being done at this time.

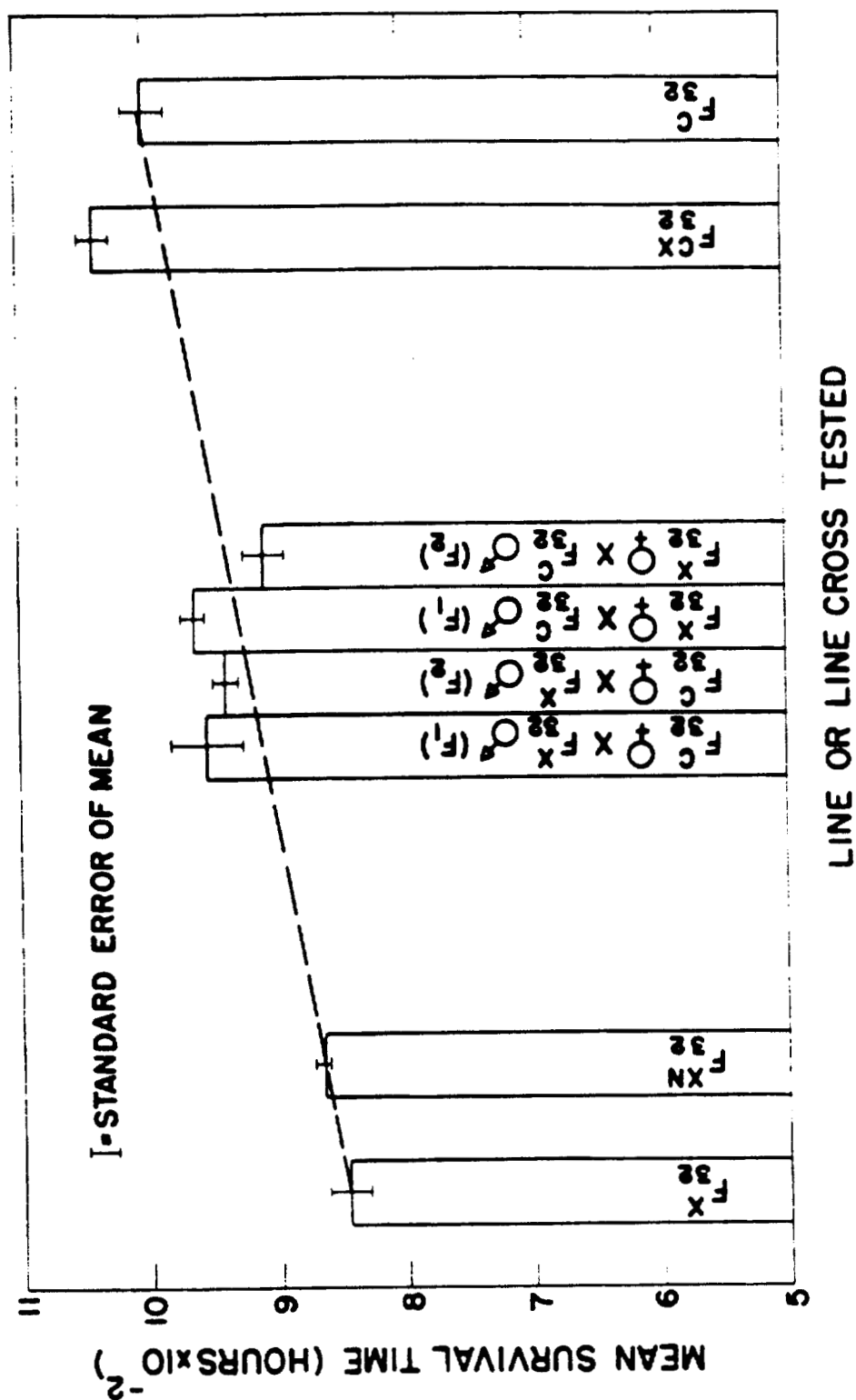


Fig. 1. Mean survival time for each line and line cross of mice exposed continuously to cobalt-60 gamma rays at a dose rate of 3.5 rads/hr.

TABLE 2. LD<sub>50</sub><sup>30</sup> VALUES FOR F<sub>32</sub><sup>C</sup>, F<sub>32</sub><sup>X</sup>, F<sub>32</sub><sup>XN</sup>, AND F<sub>32</sub><sup>CX</sup> MICE

Mouse Line	Number of Mice	LD <sub>50</sub> <sup>30</sup> (rads)*
F <sub>32</sub> <sup>C</sup>	363	638 ± 12.4
F <sub>32</sub> <sup>X</sup>	362	654 ± 12.3
F <sub>32</sub> <sup>XN</sup>	359	659 ± 12.4
F <sub>32</sub> <sup>CX</sup>	361	664 ± 12.4

\* ± Standard Error.

TABLE 3. MEAN AFTER-SURVIVAL TIME (MST) VALUES FOR 32ND GENERATION MICE

Group Studied	Number of Mice	MST (hr)*
F <sub>32</sub> <sup>C</sup>	104	1001 ± 18.3
F <sub>32</sub> <sup>CX</sup>	141	1041 ± 11.9
F <sub>32</sub> <sup>X</sup>	121	846 ± 10.0
F <sub>32</sub> <sup>XN</sup>	169	866 ± 5.2
F <sub>32</sub> <sup>C</sup> Females x F <sub>32</sub> <sup>X</sup> Males		
(F <sub>1</sub> )	105	957 ± 24.5
(F <sub>2</sub> )	134	940 ± 9.2
F <sub>32</sub> <sup>X</sup> Females x F <sub>32</sub> <sup>X</sup> Males		
(F <sub>1</sub> )	88	966 ± 9.6
(F <sub>2</sub> )	125	911 ± 13.5

\* ± Standard Error.

## REFERENCES

- (1) J. F. Spalding, O. S. Johnson, and R. F. Archuleta, Los Alamos Scientific Laboratory Report LA-3132-MS (1964), p. 112.
- (2) J. F. Spalding, T. T. Trujillo, and W. L. LeStourgeon, Radiation Res. 15, 378 (1961).
- (3) J. F. Spalding, M. Brooks, and P. McWilliams, Genetics 50, 1179 (1964).

## GENETIC EFFECTS. III. A SPONTANEOUS MUTATION FOR A RECURRING HAIRLESS CONDITION

An intermittent hairless condition was observed in the offspring from one F<sub>31</sub><sup>C</sup> breeding pair. This condition appeared to be a genetically controlled metabolic deficiency. Offspring which exhibited the condition were maintained and allowed to reproduce until enough mice were available to determine the inheritance of the condition.

## METHODS AND RESULTS

Seven males affected by this hairless condition were mated to 35 RF strain females from our stock colony. The F<sub>1</sub> offspring (over 100) from these matings were normal in appearance. The F<sub>1</sub> offspring were randomly mated, and the number of F<sub>2</sub> mice exhibiting the hairless condition was recorded. A total of 328 F<sub>2</sub> offspring was observed, and the frequency of the hairless condition is shown in Table 4. Contingency table analysis of these data yielded a  $\chi^2$  value of 2.42, which was not significant when compared to the critical value at the 5 percent significance level of 5.412.

The condition for hairlessness is established as a spontaneous mutation at a single gene locus. It is a simple recessive mutant gene and is not influenced by sex.

**TABLE 4. FREQUENCY OF HAIRLESS CONDITION IN F<sub>2</sub> OFFSPRING**

Group	Hairless	Normal	Total
Males	35	136	171
Females	43	114	157
Total	78	250	328

**GENETIC EFFECTS. IV. HEMOGLOBIN MOLECULAR CHARACTERISTICS OF MICE EXPOSED TO 32 CONSECUTIVE GENERATIONS OF X IRRADIATION (J. C. Hensley, R. O. Eikleberry, and C. N. Roberts)**

#### INTRODUCTION

In previous studies on hemoglobin of mice of the F<sub>27</sub> generation (1), electrophoretic studies (Fig. 2) indicated a marked molecular charge difference between the groups tested. Temporal migration patterns of control animals (F<sup>C</sup>) were uniform during elapsed time periods, while deviations in electrophoretic patterns were observed in the irradiated line (F<sup>X</sup>) and irradiated sub-line (F<sup>XN</sup>) animals. Continuing studies were planned at that time in the F<sub>32</sub> generation to determine existent differences, if any, which might be associated with X-ray exposure history.

#### METHODS AND RESULTS

Electrophoretic patterns in the F<sub>32</sub> generation were similar to findings in the F<sub>27</sub> generation. An additional group (F<sup>CX</sup>) was added, this group having had but 5 generations of X-ray exposure. Hematological studies (2) indicated some erythropoietic differences among the lines tested (groups F<sup>C</sup>, F<sup>X</sup>, F<sup>CX</sup>, and F<sup>XN</sup>), and an additional group of RF strain non-irradiated stock mice were used as program controls.

Three blood samples (Fig. 3) per group with 18 to 20 mice were subjected to globin extraction techniques as described



Fig. 2. Typical migration patterns for typical hemoglobins of the control ( $F^C$ ), irradiated ( $F^X$ ), and sub-irradiated ( $F^{XN}$ ) lines of mice of the F32 generation. Each specimen represents cumulative 45-minute periods of migration at pH 8.6.

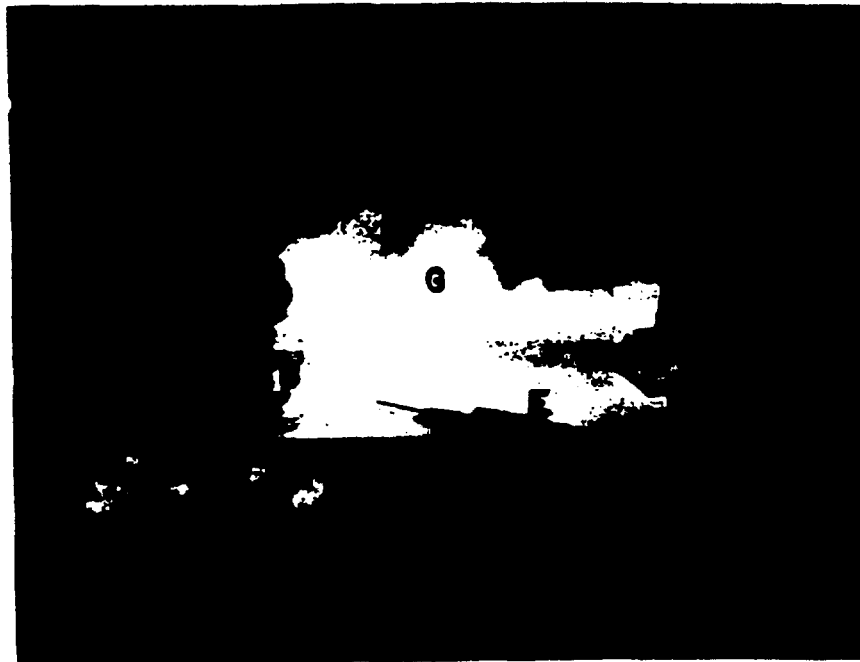


Fig. 3. Exsanguination method as utilized in this study for procurement of large volumes of blood from young mice. The mouthpiece (A) attached to Erlenmeyer flask (B) applies suction to the Pasteur pipette (C), which is used in the orbital bleeding technique (3). The dropping plate (D) is used for heparin sodium draft into (C) from the syringe (E). Samples are collected in the cylinder (F).

by Hill et al. (3) with resultant crystallization of pure globins. Amino acid analysis was accomplished with a Beckman Spinco amino acid analyzer, and the results are shown in Table 5. No significant differences exist, especially as concerns those amino acids which ultimately affect hemoglobin electrophoretic mobility or which affirm reasons for other differences seen to exist among F27 groups from a physiological standpoint. Tryptophan analysis awaits a satisfactory analytical procedure before an adequate comparison can be made.

Previous studies (4) suggested hemoglobin differences among the lines tested. Additional studies are contemplated in later generations, when adequate analytical procedures for tryptophan will be available to facilitate a more complete analysis of the globin fractions. Careful comparison of past results with these mice do not indicate significant differences attributable to radiation alone, and the small differences which do exist could be accounted for by the random variation of the life processes.

#### REFERENCES

- (1) J. C. Hensley and N. C. Brown, Los Alamos Scientific Laboratory Report LA-3132-MS (1964), p. 129.
- (2) J. C. Hensley, C. F. Bidwell, and A. M. Martinez, this report, p. 69.
- (3) R. J. Hill, W. Konigsberg, G. Guidotti, and L. C. Craig, In: Biochemical Preparations (G. B. Brown, ed.), Vol. 10, John Wiley and Sons, Inc., New York (1963), pp. 56-57.
- (4) J. C. Hensley, G. E. Oakley, N. C. Brown, and R. I. Howes, Los Alamos Scientific Laboratory Report LA-3132-MS (1964), p. 109.



TABLE 5. AMINO ACID COMPOSITION IN MOUSE GLOBIN GROUPS\*

Amino Acid	Stock Mice	F <sup>C</sup>	F <sup>X</sup>	F <sup>CX</sup>	F <sup>XN</sup>
Lysine	7.8	8.0	8.3	8.3	8.3
Histadine	6.7	6.8	7.2	6.9	6.8
Arginine	2.2	2.2	2.2	2.3	2.2
Aspartic acid	10.4	10.2	10.2	10.2	10.2
Threonine	4.7	4.5	4.5	4.5	4.4
Serine	7.1	6.4	6.2	6.2	6.0
Glutamic acid	5.0	5.1	5.0	5.0	5.1
Proline	3.7	3.6	3.6	3.7	3.5
Glycine	8.4	8.5	8.5	8.4	8.5
Alanine	14.6	14.6	14.4	14.4	14.5
Half cystine	0.8	0.8	0.4	0.6	0.8
Valine	6.6	7.2	7.5	7.5	7.4
Isoleucine	1.5	1.7	1.8	1.8	1.8
Leucine	12.3	12.5	12.5	12.6	12.6
Tyrosine	2.1	2.0	1.8	1.9	1.9
Phenylalanine	5.1	5.0	5.0	5.0	5.0
Methionine and Methionine sulfoxide	0.9	0.9	0.9	0.8	0.8

\*In average  $\mu$ mole percent.

**GENETIC EFFECTS. V. COMPARATIVE HEMATOLOGY AND CLINICAL BLOOD CHEMISTRY OF MICE OF THE F<sub>32</sub> GENERATION (J. C. Hensley, C. F. Bidwell, and A. M. Martinez)**

It was concluded from previous hematological studies on mice of the F<sub>27</sub> generation that no significant differences existed between groups except for absolute white blood cell values (1). Biochemical parameters then under investigation (O<sub>2</sub> and CO<sub>2</sub>) indicated significant differences between the genetic lines tested (2). It is noteworthy that the irradiated sub-line (F<sup>XN</sup>) had the least oxygen capacity and CO<sub>2</sub> content among the F<sub>27</sub> groups. This finding is consistent as concerns the CO<sub>2</sub> content among the F<sub>32</sub> generations as well; however, the oxygen capacity findings indicate an increase (Fig. 4). The methods utilized in the hematological determinations were the same as those previously described (1).

Table 6 demonstrates the mean hematogram values for the F<sub>32</sub> generation. Except for white blood cell total values, no significant differences are seen to exist.

Table 7 shows absolute white blood cell values for the F<sub>32</sub> generation. A significant difference exists between the stock mice (randomly bred) and the control (F<sup>C</sup>) groups. Contrary to F<sub>27</sub> findings, lymphocyte values for the irradiated line (F<sup>X</sup>) are below other group values. The irradiated sub-line (F<sup>XN</sup>) animals show a significant decrease in total number of segmented neutrophils. The controls and irradiated line show a definite juvenile neutrophilia, adding significance to the total white count (Table 6) in that a deterrent to neutrophil production is obvious, both in the control (F<sup>C</sup>) and in the irradiated (F<sup>X</sup>) groups, according to the juvenile neutrophilia seen in Table 7 for these groups.

Of interest is the fact that the irradiated line and the irradiated sub-line show decidedly severe drops in the absolute lymphocyte counts as compared to the stock mice. Note, however, that the control line (F<sup>C</sup>) is also severely decreased in lymphocytes per mm<sup>3</sup>.

From data derived as hematological blood chemistry (Table 8), one notes that the serum CO<sub>2</sub> content of the irradiated sub-line is decidedly below other values in agreement with F<sub>27</sub>

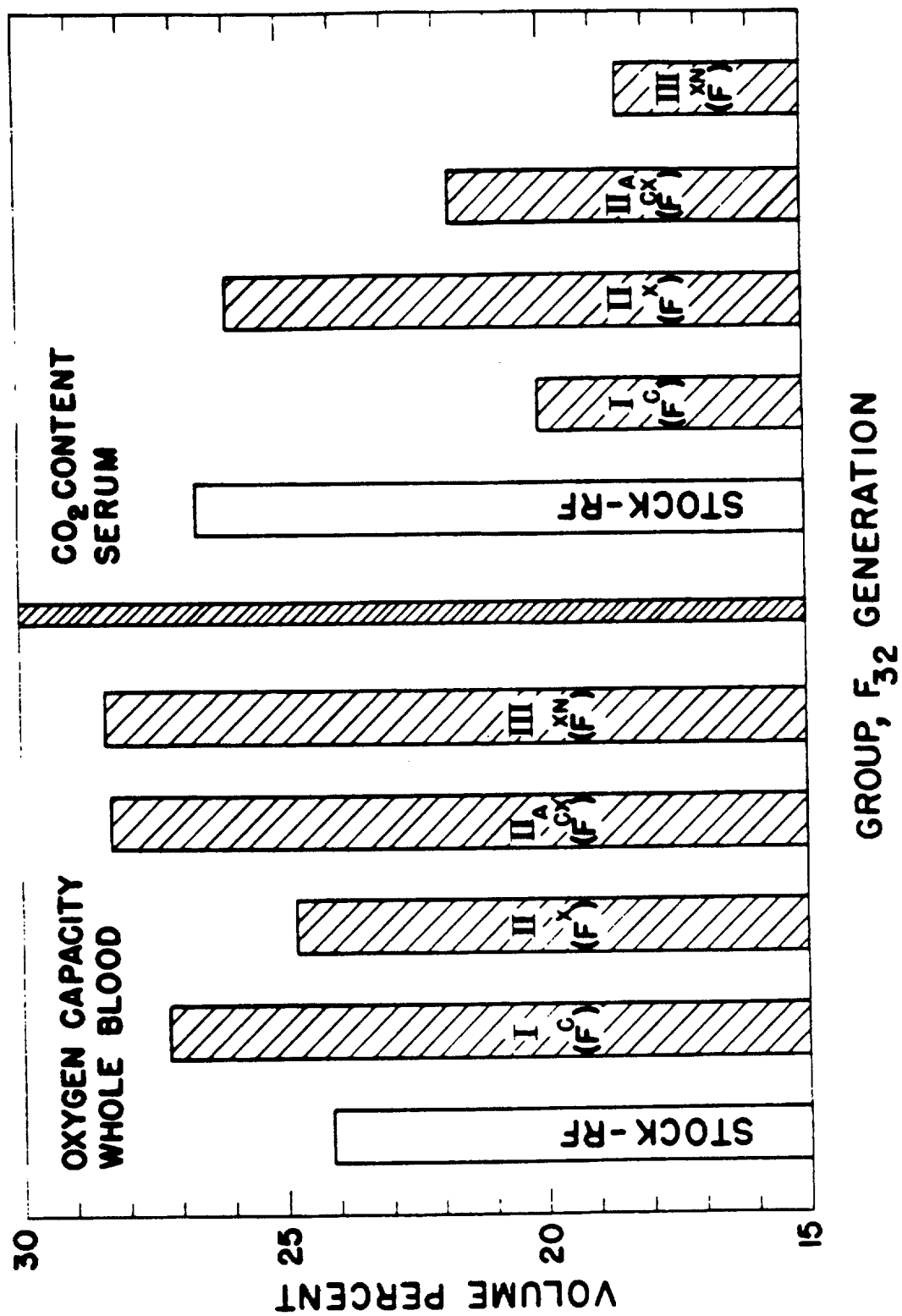


Fig. 4. Mean oxygen capacity and carbon dioxide content of blood samples of the F<sub>32</sub> generation.

TABLE 6. HEMATOGRAM VALUES FOR THE F<sub>32</sub> GENERATION

Genetic Group	Hemoglobin (g/percent)	RBC (10 <sup>6</sup> /mm <sup>3</sup> )	Hematocrit (percent RBC's)	MCV (RBC)	MCH (µg/cell)	MCHC (percent of cell vol.)	Reticulocytes (percent cells per 100 RBC's)	ESR (mm/hr)	WBC (10 <sup>3</sup> /mm <sup>3</sup> )
RF Stock	21.00	10.59	49.87	46.90	19.89	42.15	1.67	1.07	7.73
F <sup>C</sup>	20.46	10.82	52.94	49.43	18.86	38.53	1.86	1.07	10.07
F <sup>X</sup>	20.73	10.58	54.08	51.81	19.66	38.73	1.14	1.00	7.42
F <sup>CX</sup>	19.51	10.68	51.30	48.56	18.55	38.06	1.15	1.00	7.83
F <sup>XN</sup>	21.32	10.81	52.01	48.52	19.90	41.13	2.07	1.33	6.59

TABLE 7. ABSOLUTE DIFFERENTIAL WHITE BLOOD CELL VALUES\* OF MICE OF THE F<sub>32</sub> GENERATION, DERIVED FROM MEAN WBC TOTAL AND DIFFERENTIAL COUNTS

Group	Segmented		Juvenile		Eosinophils	Basophils	Monocytes
	Lymphocytes	Neutrophils	Neutrophils	Neutrophils			
RF Stock	8999	1290	7.28	117.56	0	0	0
F <sup>C</sup>	6067	1335	67.50	22.50	0	0	0
F <sup>X</sup>	5924	1339	22.40	80.00	0	19.40	0
F <sup>CX</sup>	6418	1355	7.00	4.15	0	0	0
F <sup>XN</sup>	5574	955	3.95	39.50	0	8.60	0

\*Thousands/mm<sup>3</sup>.

TABLE 8. MEAN BLOOD CHEMISTRY PARAMETERS FOR F<sub>32</sub> GENERATION MICE

Group	Serum CO <sub>2</sub> Content (volumes percent)	Blood O <sub>2</sub> Capacity (volumes percent)	Glucose Concentration (mg percent)	Serum Sodium (mg percent)	Serum Potassium (mg percent)	
RF Stock	26.57	24.13	120.5	206.5		10.8
F <sup>C</sup>	20.49	27.19	115.2	203.3		13.2
F <sup>X</sup>	26.03	24.77	98.7	203.2		14.2
F <sup>CX</sup>	21.70	28.27	121.6	203.5		11.4
F <sup>XN</sup>	18.46	28.33	108.3	204.5		13.6

the irradiated animals, while the irradiated sub-line is significantly lower than other groups.

Within the accuracy of microchemical determinations, no significant serum sodium changes are evident. All genetic groups except the irradiated sub-line (FCX) show increased serum potassium levels. Examination of this and other physiological data of the experimental and stock groups indicates that most significant differences exist between RF stock and control (FC) lines (2). This suggests that significant differences exist between animals that were randomly bred (RF stock) and selectively sib-bred (other groups).

It may be contended that exposure to ionizing radiation as done in these animals (a) reduced harmful (or lethal) homozygous combinations in irradiated lines to produce animals that are (or appear) physiologically superior to control lines (2); and (b) did actually alter the genetic damage of the initial exposures to produce animals physiologically superior to control group animals. Examination of succeeding generations may confirm or refute the contentions thus formed. It may be that continued selective inbreeding is a more significant detriment to succeeding generations than the radiation exposure of progenitors and that the radiation in this case (from a physiological standpoint) has thus far alleviated otherwise serious effects of continuous inbreeding.

#### REFERENCES

- (1) J. C. Hensley and G. E. Oakley, Los Alamos Scientific Laboratory Report LA-3132-MS (1964), p. 124.
- (2) J. F. Spalding and M. R. Brooks, Los Alamos Scientific Laboratory Report LA-3132-MS (1964), p. 109.

## EFFECTIVE RESIDUAL DOSE STUDIES WITH MICE (J. F. Spalding)

### INTRODUCTION

Report No. 29, "Exposure to Radiation in an Emergency," by the National Committee on Radiation Protection and Measurements, recommends the Effective Residual Dose (ERD) concept of radiation injury and recovery in planning exposure to gamma rays for critical personnel. Although the ERD concept is not a departure from present knowledge of radiation effects on man or animals, its validity has not been tested experimentally. The need is obvious, and pertinent investigations are in progress on mice, monkeys, and dogs.

### METHODS AND RESULTS

Approximately 200 RF strain virgin female mice 90 + 7 days of age are being used in a preliminary study to test the first ERD model. The model and a graphic description of its function are shown in Fig. 1. Assumptions being used with this model are as follows: (a) radiation-induced damage is linear with dose, and recovery is exponential; (b) recovery rate is independent of prior radiation exposure history or size of dose; (c) approximately 5 percent of any gamma-ray exposure is irreparable; and (d) the slow repairable component of radiation-induced injury has a repair half-time ( $RT_{50}$ ) of approximately 7 days. The accuracy of these assumptions is not known, but they are based on the best experimental data available on this strain of mouse.

Mice were randomly divided into 4 groups of approximately 50 mice each. In group I, 100 rads was set as the Maximum Permissible Effective Residual Dose (MP ERD). The MP ERD for group II was 200 rads, and for group III 300 rads. Group IV was a control group. On day zero each group was given a gamma-ray exposure (cobalt-60, 27 rads/hr) equal to its MP ERD (100, 200, or 300 rads). At random time intervals (from 1/2 to 2  $RT_{50}$ 's), an additional gamma-ray exposure was given to each group to return the body burden to its assigned MP ERD. Blood samples were taken prior to each exposure to determine total red blood cell (RBC) count and mean cell volume (MCV) distribution. These data are shown in Fig. 2.

As evidenced in Fig. 2, each challenging dose, regardless of



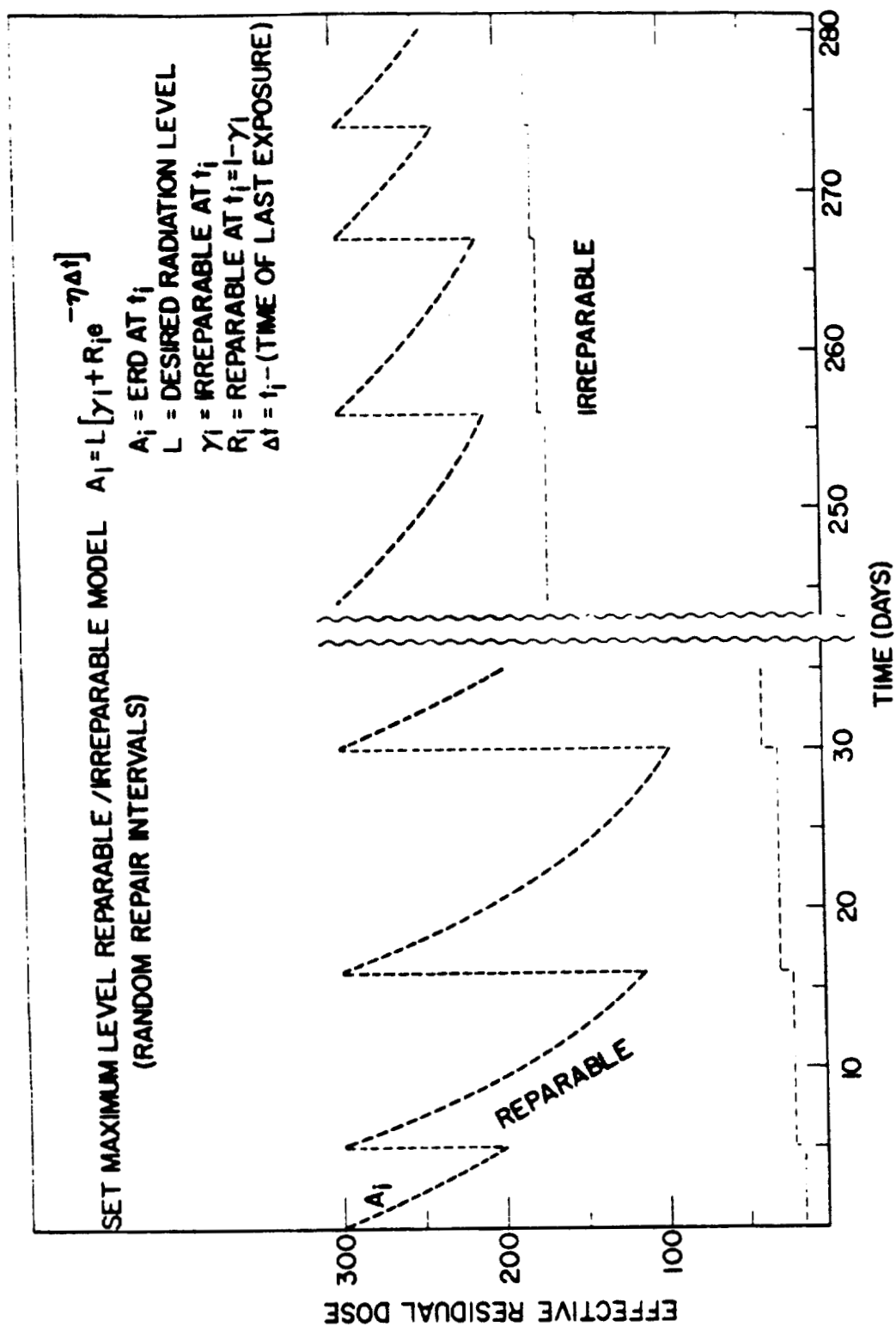


Fig. 1. Graphic description of the Effective Residual Dose model.

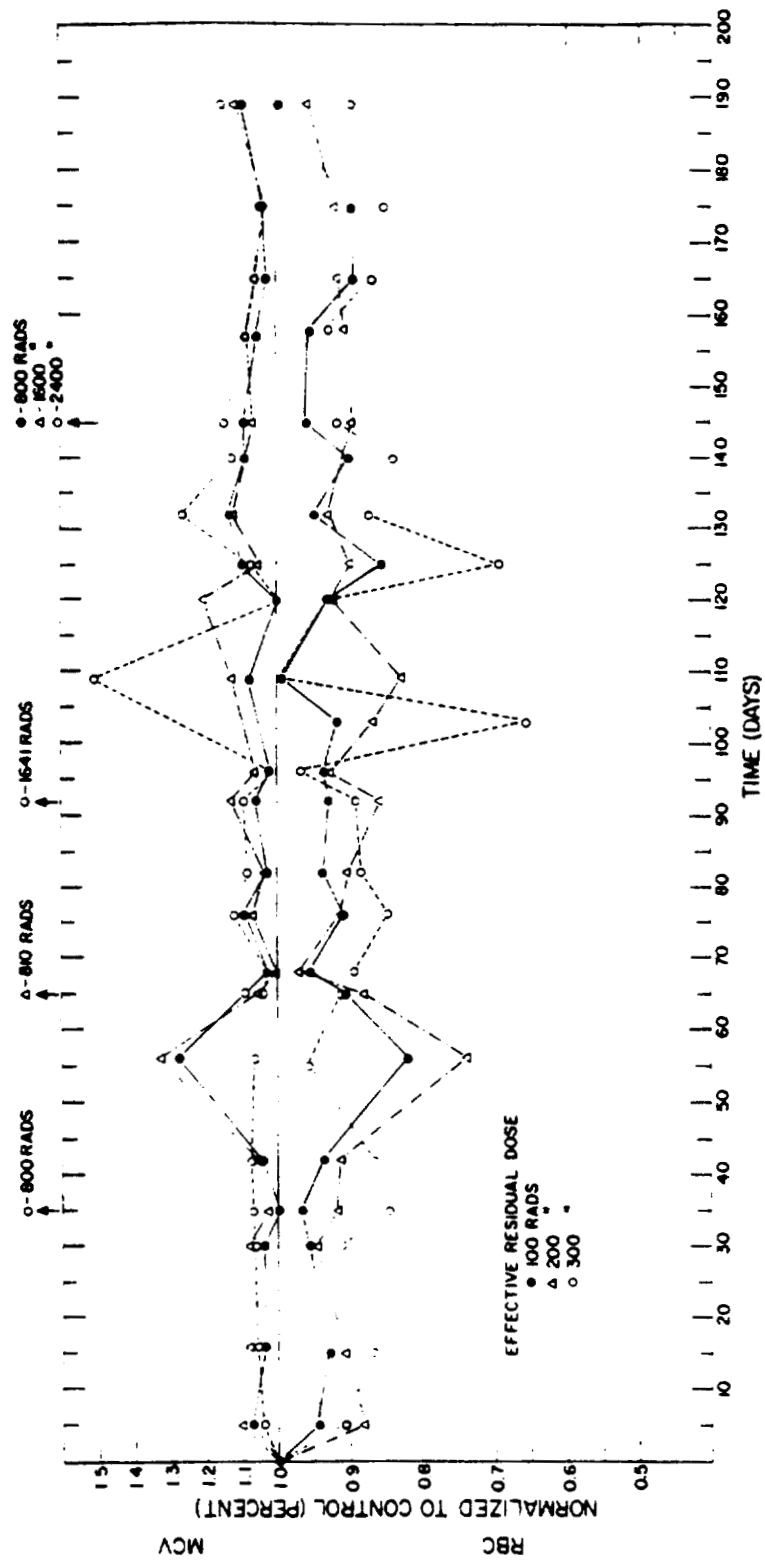


Fig. 2. Total red blood cell (RBC) count and mean cell volume (MCV) distribution with respect to ERD level and accumulated dose.

size, caused a depression in RBC; however, recovery took place rapidly and RBC values dropped to near critical levels only at 2 times during the first 190 days of the experiment. In general, RBC depression was a function of ERD level. There were, however, a few notable exceptions to the generalization. The MCV (top of Fig. 2) is also shown to be quite closely related to RBC and again, in general, the MCV was a function of ERD level with the larger doses producing a more serious challenge to the bone marrow.

Voluntary activity was tested in activity wheels for a 24-hour period after groups I, II, and III had accumulated the equivalent of 1 (800 rads), 2 (1600 rads), and 3 (2400 rads) acute lethal doses. Control animals showed approximately 28 percent more activity in terms of wheel revolutions per 24-hour period than the 3 ERD groups. However, the ERD groups were not different from each other.

Body weights after the accumulation of the equivalent of 1, 2, and 3 lethal doses for ERD groups I, II, and III showed the two lower groups (ERD 100 and ERD 200) to be significantly heavier than the control group; however, the higher group (ERD 300) was no different from control mice.

It is of interest to note that lethality has been greatest in the ERD 200 group and smallest in the group allowed the highest ERD level of 300 rads. At this point in the experiment, groups I, II, and III have accumulated doses of 1150, 2300, and 3450 rads, respectively, and mortality is 38.7, 47.9, and 34.0 percent in the same order. The cause of death in early lethality was attributed to thymic tumors, and apparently the ERD 300 level provided a therapeutic treatment which may account for the lower death rate in this higher group.

The Effective Residual Dose method of programming gamma-ray exposure shows considerable promise in mice. More extensive studies are being done with mice, and additional investigations are in progress with dogs and monkeys.

**EFFECT OF SINGLE ACUTE AND SECOND GAMMA-RAY EXPOSURES ON  
ERYTHROPOIESIS IN THE MOUSE (J. F. Spalding, N. J. Basmann,  
O. S. Johnson, and R. F. Archuleta)**

**INTRODUCTION**

Experimental animals appear to recover quite rapidly from X- or gamma-ray exposures below the lethal dose. One of the critical organs affected by exposure to ionizing radiation is the bone marrow, which also seems to recover rapidly from single acute or protracted exposure to gamma or X rays.

The completeness of bone marrow recovery in experimental animals has not been established and, although recovery in terms of total red blood cell counts per unit volume approaches normal, a smaller than normal number of stem cells dividing more rapidly may account for this apparent recovery. Tubiana et al. (1), using 400 to 600 rads of X irradiation to lower the immunological defenses for kidney grafts, were surprised to find that second 100-rad exposures 2 to 3-1/2 months later produced severe and long lasting bone marrow aplasia. Tubiana attributed this to residual hematopoietic tissue damage from the first exposure and warned of the hazards of extrapolating experimental results from animals to man.

Investigations are being done to study the residual irreparable damage (if any) to erythropoiesis from whole-body gamma-ray exposures.

**METHODS AND RESULTS**

Two hundred and fifty RF strain virgin female mice 4 months + 2 weeks of age were randomized and separated into 5 groups of 50 mice each. On day zero groups I through IV were given single acute (approximately 6 rads/min) gamma-ray exposures of 200, 400, 600, and 800 rads, respectively. Group V was a non-irradiated control group. Starting on day 4 (4 days post exposure), blood samples were taken at frequent intervals through day 90, and the total red blood cell (RBC) count and cell size distribution were obtained for each group. The RBC for each dose group was normalized to control values and plotted against time post exposure. On day 90 groups I through IV were again given single acute gamma-ray exposures; however,

the group doses were reversed so that groups I through IV received 800, 600, 400, and 200 rads, respectively. Following these exposures (day zero<sub>2</sub>), all 4 groups had received a total exposure of 1000 rads in two acute fractions separated by 90 days of repair. Starting on the 4th day post exposure (day 4<sub>2</sub>), blood samples were taken on the same time schedule as was done following the first exposure. An irreparable lesion in bone marrow stem cells as a result of the first exposure would be expected to cause a more severe depression in RBC following the second exposure. The preliminary results of this investigation are shown in Figs. 1, 2, and 3.

Figure 1 shows that RBC depression to day 18 was quite closely related to total dose. At 18 days and from 37 days on, RBC values were not consistent with dose, since overcompensation in higher doses seemed to be more prevalent than in the lower dose range. The effect was more erratic for second exposures, as shown in Fig. 2. However, the greatest depression in RBC was related to total dose of the second exposure, and "control normalized" values were not depressed below first exposure values. Recovery to near normal RBC's followed similar time-course recovery patterns. Figure 3 is a plot of the ratios of "control normalized" RBC values from first exposures to "control normalized" RBC values from second exposures. In general, RBC values were depressed slightly more from second than from first exposures; however, as shown in Fig. 3, there were a number of notable exceptions.

Doses from the two acute fractions in each group totaled 1000 rads. It is of some interest to note lethality, since the total dose was the same for all groups. Total lethality 52 days after the second exposure was 10, 16, 8, 18, and 2 percent, respectively, for groups I through V. These values have not been tested; however, if a difference in irradiated groups does exist, the group with the greatest first exposure and smallest second exposure (group IV, 800 rads and 200 rads) would show the greatest lethality. Lethality from the first exposure was responsible for this difference. Second exposure lethality appeared to be the same for all groups.

The results of this investigation show no residual bone marrow damage in mice such as was apparently observed by Tubiana in human subjects.

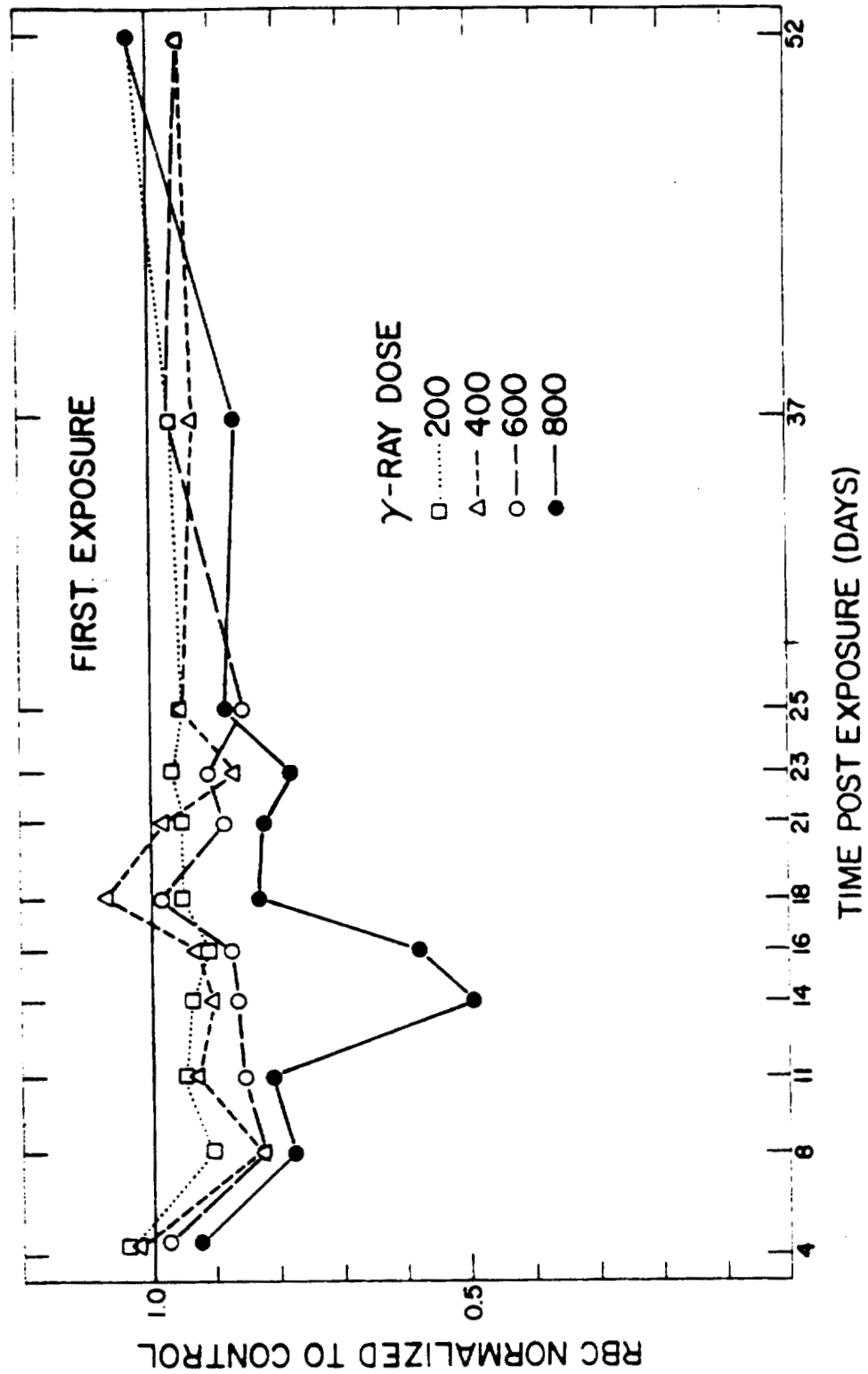


Fig. 1. Red blood cell count (normalized to control) following single acute gamma-ray exposures.

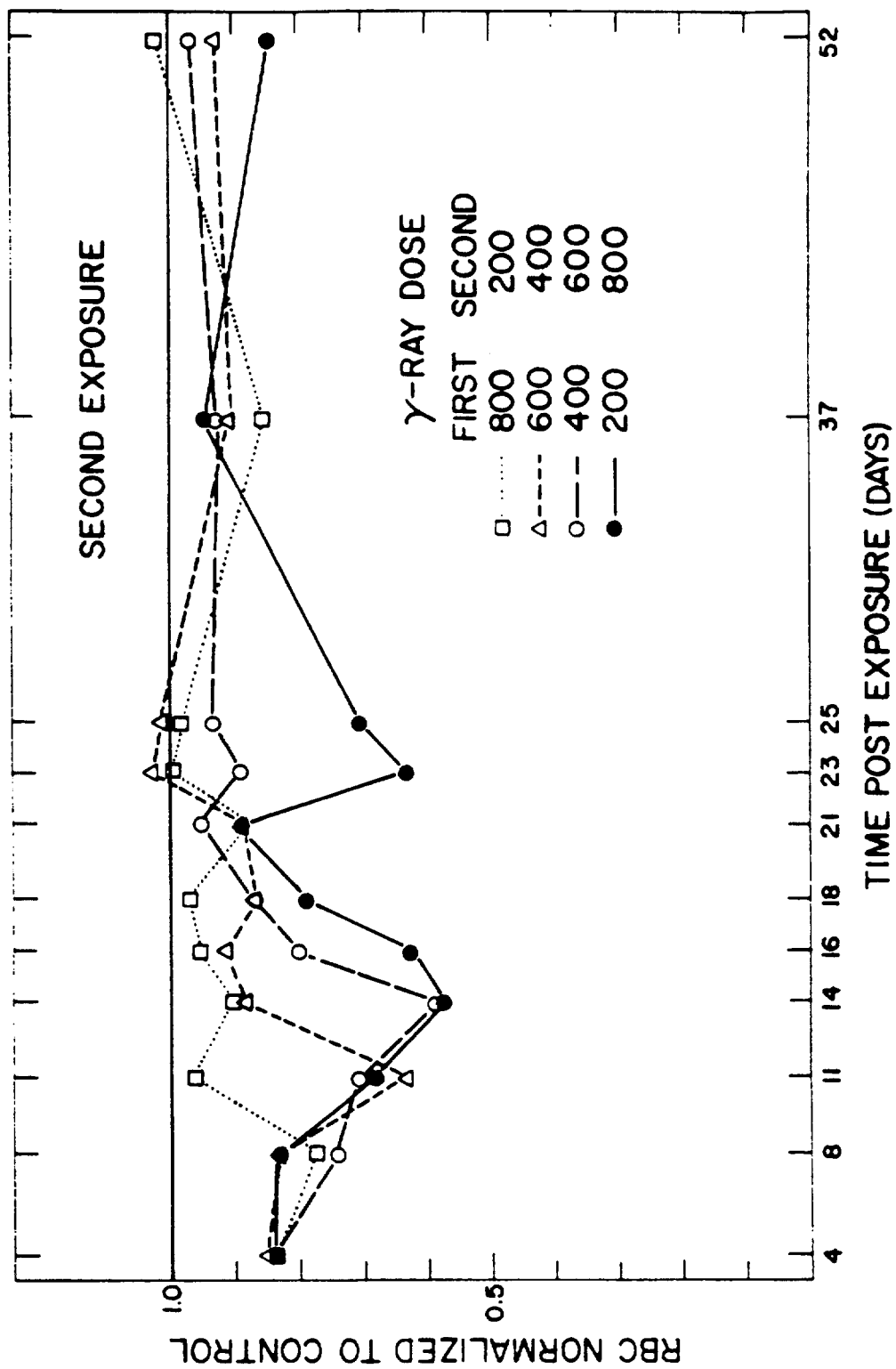


Fig. 2. Red blood cell count (normalized to control) following second, single acute gamma-ray exposure 90 days after first acute dose.

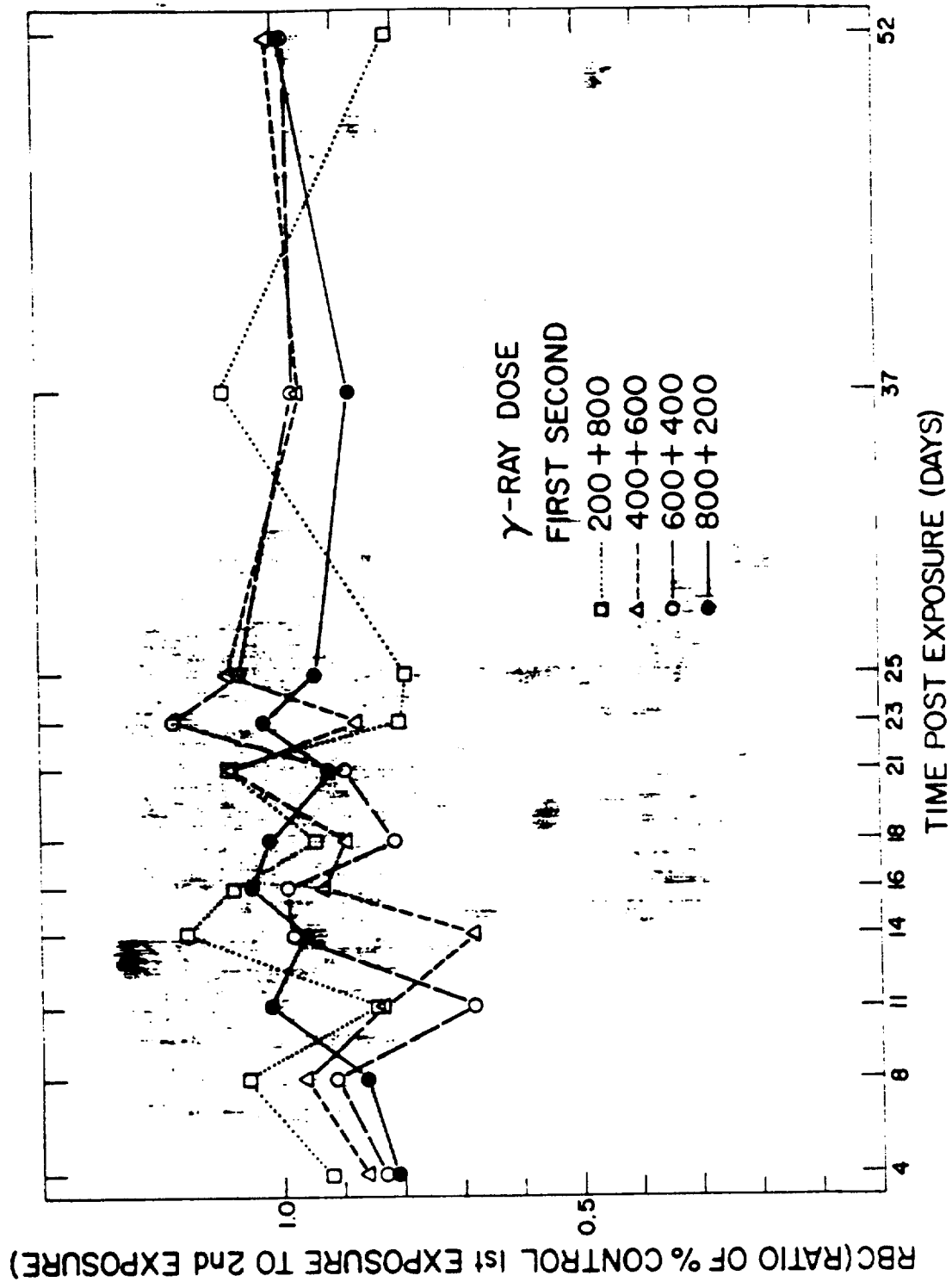


Fig. 3. Graphic plot of the ratios of "control normalized" RBC values from first exposures to "control normalized" RBC values from second exposures.



#### REFERENCE

- (1) M. Tubiana, C. M. LaLanne, and J. Surmont, In: Diagnosis and Treatment of Acute Radiation Injury, World Health Organization, Geneva (1961), pp. 237-263.

# PHENCYCLIDINE HYDROCHLORIDE AS A GENERAL ANESTHETIC FOR LABORATORY PRIMATES (J. C. Hensley)

## INTRODUCTION

A suitable general anesthetic with a wide margin of safety for laboratory primates has been of considerable interest for many years. A study on the use of phencyclidine hydrochloride\* in *Macaca speciosa* and *Macaca mulatta* was, therefore, undertaken.

## METHODS AND RESULTS

Serylan, under the name of "Sernyl," was received in 10-cc vials (25 mg/cc). The intramuscular route was chosen because of more rapid absorption and consequent rapid induction of anesthesia compared to subcutaneous routes. Initial administration of 2.5 mg/kg resulted in loss of cognizance of surroundings, incoordination, and convulsive seizures with rigidity of extremities. No respiratory arrest was noted, however, and the animals returned to relative normalcy within 4 to 6 hours.

### Single-Dose Administration

Two hundred and twelve injections were made in *M. speciosa* and 61 in *M. mulatta* (1 mg/kg), resulting in light surgical anesthesia. This usage facilitates handling of primates for physical examination, chest radiography for tuberculosis detection, intradermal testing, minor surgical procedure, light wound repair, and extraction of large canine (first premolar) teeth from the males of the species. Procaine hydrochloride was frequently employed as a topical anesthesia, and atropine sulfate was used in animals known to exude large amounts of saliva.

After a single dose at 1 mg/kg, loss of interest in surroundings, depression, and incoordination were noted with complete helplessness between 12 to 15 minutes, lasting for a period of 30 to 45 minutes. A reversal of effect then occurred,

---

\*Serylan<sup>R</sup>, Protocol No. V395-23 from Parke, Davis and Company, Detroit, Michigan.

usually complete to the state of loss of surroundings in 1 hour to 1-1/4 hours. This effect may be prolonged to 2 hours or more in *M. speciosa*. Recovery was generally complete within 2-1/2 to 3 hours in both species. After repeated injections, tolerance to the drug developed in *M. mulatta* but was not noted in *M. speciosa*. A single injection of the drug in *M. speciosa* prevented thrashing about in the post anesthesia recovery period. *M. mulatta* evidenced minor delirium, quite unlike post barbiturate recovery which can result in injury to the animal. No incidence of respiratory arrest or cardiac arrhythmia was noted in either species during 275 anesthetics.

#### Multiple- or Repeated-Dose Administration

It was necessary to administer Sernyl over periods of 4 to 5 hours to several *M. speciosa* to maintain light surgical anesthesia, and atropine sulfate was administered to prevent excessive salivation. No side effects were noted, but a drop in rectal temperature did develop (Fig. 1). After an initial 1-mg/kg dose was administered intramuscularly, it was found that 0.33 mg/kg supplemented at half-hour intervals was sufficient to maintain proper anesthesia for 4- to 5-hour periods. Recovery after the last 0.33-mg/kg dose was within 2 hours of administration. Depression accompanied recovery for a period of 4 to 6 hours after administration of the final dose. For the average animal, atropine sulfate (1/300 gr.) was given at 2-hour intervals throughout the anesthesia period. It is possible that atropine sulfate at these levels potentiates the anesthetic action of Serylan. Table 1 shows respiratory and cardiac rates for a single animal subjected to multiple anesthesia at 3 different times 2 weeks apart. The regularity of respiratory rates is striking. The pharmacological basis for cardiac irregularity is unknown.

#### DISCUSSION

For routine handling and minor surgical procedures on either *M. mulatta* or *M. speciosa*, phencyclidine hydrochloride is excellent in the range of 1 mg/kg. Although drug tolerance seems to develop in *M. mulatta*, it has not been evidenced in *M. speciosa* even after as many as 15 single doses at this level. Subjects anesthetized with multiple doses for as many as 12 prolonged experimental periods have shown no

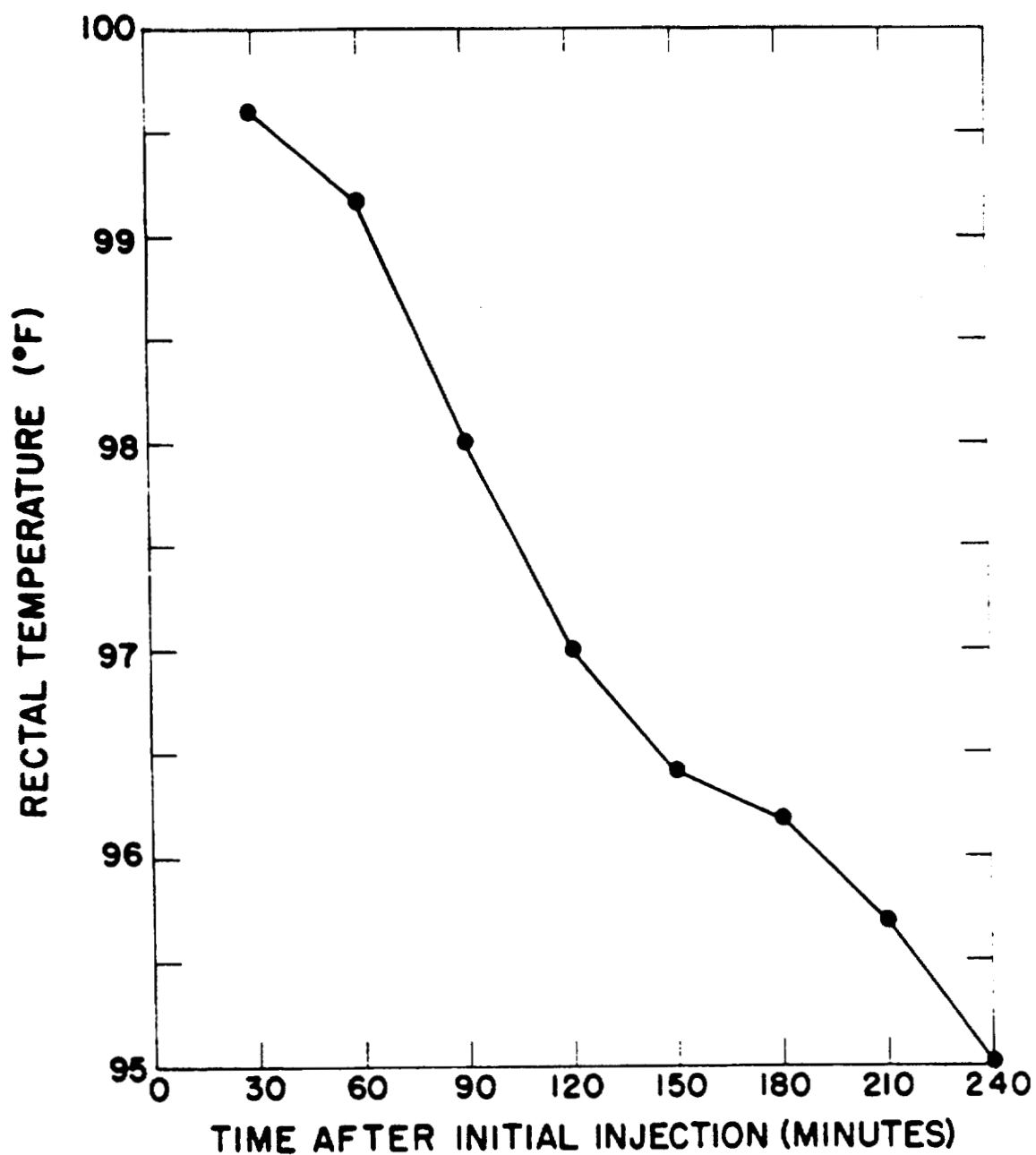


Fig. 1. Typical rectal temperature change in a *M. speciosa* male to which phencyclidine hydrochloride was administered initially at 1 mg/kg and 0.33 mg/kg each half-hour thereafter.

TABLE 1. TYPICAL POST INJECTION RESPIRATORY AND CARDIAC RATES OF AN ANIMAL SUBJECTED TO MULTIPLE DOSES OF SERYLAN AT THREE DIFFERENT TIMES

Post Injection 30-Minute Period	Respiratory Rate (per minute)			Cardiac Rate (per minute)		
	I	II	III	I	II	III
1	48	48	36	240	240	228
2	36	36	36	204	168	228
3	36	48	36	180	192	228
4	36	36	36	180	180	228
5	36	36	36	192	180	228
6	36	48	36	168	192	276*
7	36		36	204		216
8	36		36	204		204
Time to Recovery after Last Injection				180 minutes	192 minutes	227 minutes

\*Etherization to supplement phencyclidine administration.

tolerance development. Recovery after a 4- to 5-hour anesthesia is uneventful. In 42 animals anesthetized by merely estimating body weights and administering 1 mg/kg, only 1 animal (35 pounds) did not reach the proper anesthetized state, and 1 small male (11 pounds) was perhaps over-anesthetized.

Since side effects from general anesthetics used on primates are often severe, phencyclidine hydrochloride is a welcome adjunct to primate medicine. No laryngeal spasm, cardiac arrest, dyspnea, depression, or hypotension have been encountered with this drug. A disadvantage, not marked because of wide margins of safety, is that there is no known antagonist such as exists for most other anesthetic agents.

**COMPARATIVE EXTRACTION TECHNIQUES FOR MANDIBULAR AND MAXIL-  
LARY CANINE TEETH (CUSPIDS): DENTITIOUS AND GINGIVAL MOR-  
PHOLOGY OF MACACA MULATTA AND MACACA SPECIOSA (R. I. Howes,  
Jr., and J. C. Hensley)**

**INTRODUCTION**

The canine teeth (cuspids) of subhuman primates are used in the wild and captive states for self-protection and aggression. Captive primates use these teeth ("fangs") to a suitable advantage to discourage handling by animal caretakers, the result being deep puncture wounds or lacerations on the most careful handlers. Fight wounds inflicted on cage mates prove difficult to heal or are even lethal.

As part of a continuing study (1,2) on comparative characteristics of *Macaca mulatta* and *Macaca speciosa*, surgical extraction techniques were compared for the canine teeth. Oral morphology and tooth morphological characteristics were compared. A correlative study involving extraction and morphology comparisons of two different human racial groups in New York City relates well to this study, especially with regard to morphological similarities and extraction difficulty.

**METHODS AND RESULTS**

Thirty-six canine teeth from *M. speciosa* and 8 from *M. mulatta* have been extracted. Pre- and post surgical oral examinations were made. Figure 1 shows a typical pair of exposed *M. speciosa* canines which are quite large compared to the other teeth. The caudal edges (distal) are razor-sharp at maturity. An intramuscular injection of phen-cyclidine hydrochloride at 1 mg/kg (3) was used as a general anesthetic, with a maintenance dose of 0.33 mg/kg at half-hour intervals as necessary. Atropine sulfate was used to prevent excessive salivation and adrenosem salicylate (5 mg) pre-operatively to reduce capillary bleeding. A 2 percent procaine hydrochloride solution was used for local infiltration of the surgical site and primary neural blocks. This particular technique decreased the necessity for deep surgical anesthesia.

Post-surgically, Furacin-soluble dressing was used to promote



Fig. 1. Exposed canine teeth of a 3-1/2-year-old *M. speciosa* male. Maximum length has not been obtained, but the teeth are obviously long enough to cause severe injury to personnel or other animals.



healing, and routine antibiotic prophylactic therapy prevented complications due to infection. Where pain was evident, 1/8 grain of morphine sulfate was used.

Pre-operatively, lateral radioautographs of the large canine teeth (Fig. 2) were taken to detect obscure morphological difficulties. Direct lateral views such as this were sufficient for visualization of the tooth shape and its relationship to the maxillary sinus and first premolar teeth.

For extraction of the mandibular canines an inferior alveolar neural block was made with 2 percent procaine hydrochloride, and gingival infiltration completed the local anesthesia. An incision was made along the long axis of the tooth for 1 to 1-1/2 in. toward the mucobuccal fold and the alveolar bone exposed by elevation of the gingival flap by blunt dissection. At this point continuous mechanical aspiration was necessary to prevent aspiration of mucous, saliva, and blood by the animal. The overlying alveolar bone was removed with elevators and with double-action rongeurs. Periodontal ligament and gingival attachments were severed with the elevator. The tooth was then loosened with the dental elevator by forcing it to the open buccal side of the alveolus. On occasion this was sufficient for removal of the tooth. Otherwise, dental forceps or large common pliers were applied to the tooth and the tooth luxated bucco-lingually, then rotated lingually and buccally. When final traction was applied, the tooth was rotated buccally and distally (caudally) as it was extirpated from the socket.

In maxillary canine extraction the anterior-superior alveolar anesthetic block was utilized with local infiltration, and an incision similar to the mandibular extraction was made, the periodontal ligaments severed, and the alveolar bone removed. The elevator was most effective in loosening the tooth when applied at the mesial-lingual area, wedging the tooth down and buccal. When forceps were applied, traction brought the tooth out with movement first rostrally and then caudally, following the tooth curvature. In closure, alveolar osseous residues were carefully removed and the socket compressed latero-mesially. The mucosal flap was replaced and the incision closed with small medium chromic cat gut placed in single interrupted sutures. Furacin-soluble dressing was then applied and allowed to infiltrate into the wound. Hertwig's root sheath was replaced in the alveolar socket prior to closure in young animals.

A 1-year post-surgical photograph (Fig. 3) of an extraction

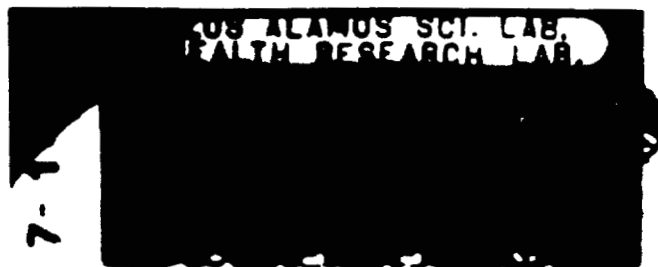


Fig. 2. Radioautograph of the head of a mature *M. speciosa* male, showing the large bulbous root of the superior canine (cuspid) tooth.



Fig. 3. Lateral and anterior-posterior views of the teeth of an animal 1 year post-operatively. Little to no scarring has been noted in operated animals after periods of 1 year or more.

site shows excellent repair with little to no scarring. No post-extractive pathology has been noted thus far.

Pre-eruptive removal was performed in two maxillary extraction cases. First, the deciduous predecessor was removed to gain access to its permanent counterpart which was located slightly to the lingual side and which had absorbed most of the deciduous roots. The difficulty in extraction lay in its close proximity to the roots of the first premolar and from the fact that the wide cervix was lingual and posterior to this root; extensive buccal luxation had to be avoided to prevent injury to the premolar roots. The tooth was carefully removed by separating it and gently loosening the lingual and anterior surfaces. The most effective traction was counterclockwise, exerting pressure distally and ventrally, keeping the cervix as lingual as possible.

Table 1 shows measurements of each tooth extraction with speciosa measurements compared with those of rhesus. The measurements of the teeth of the rhesus population fall well within the range of the speciosa measurements. Examination of the teeth themselves showed no evident morphological differences. The one prominent feature is that the rhesus canines projected more to the lateral than the speciosa. This may be due to smaller jaw and face of the M. mulatta.

## DISCUSSION

There are several precautions which the surgeon must recognize when removing the canine teeth of both species:

(a) avoid excess leverage upon adjoining teeth to preserve the roots of the adjoining premolar teeth in both erupted and unerupted canines; (b) preserve the thin alveolar plate separating the root from the maxillary sinus; (c) avoid fracturing the tooth; and (d) avoid fracture of the mandible, particularly in the rhesus.

The optimum time to remove the canines with minimal trauma to both animal and surgeon is after the permanent canines have erupted but before they attain full occlusal height. During this period of development, the root is not fully developed and the periodontal ligament is least developed. As would be expected, extraction of teeth which are so intricately a part of the osseous structure of the mandible and maxillae even at an optimum time is a decidedly traumatic experience. In our experience, extraction of all four

TABLE 1. MEASUREMENTS OF EXTRACTED UPPER AND LOWER CANINES

	Macaca speciosa			Macaca mulatta		
	Upper (16)*		Lower (16)	Upper (4)		Lower (4)
	Ave.	Range	Ave. Range	Ave.	Range	Ave. Range
Crown length (mm)	20.8	23.5-18.8	15.4 16.5-13.5	22.6	23.2-22.5	14.7 15.6-13.7
Root length (mm)	16.3	25.8-8.80	13.4 17.7-9.50	12.1	13.6-11.1	11.8 13.9-10.5
Total length (mm)	35.3	43.0-29.2	28.2 32.7-23.6	31.5	31.8-31.3	26.3 26.9-26.0
Mesial distal diameter (mm)	9.7	11.0-8.20	9.7 11.0-8.50	9.8	11.0-8.70	8.9 9.8-8.20
Buccal-lingual diameter (mm)	7.9	9.0-7.00	5.7 6.7-5.00	7.8	8.2-6.50	5.4 5.9-4.80

\*Numbers in parentheses indicate number of teeth examined.

canine teeth during one surgical episode exposes the animal to trauma and post-operative pain, resulting in depression, general malaise, and loss of weight from inanition. Consequently, two opposing canines are removed at one surgical episode, and after 10 to 14 days for adequate healing of the site post-surgically the two canines on the opposite side are removed. Healing with this technique proves to be uneventful.

Extraction procedures as previously described varied somewhat between species. The canines of the rhesus, for instance, were from a physical exertion standpoint much easier to extract. The teeth were quite easy to loosen, by comparison, and periodontal membranes were not nearly so well secured as in the *M. speciosa*. Final removal of teeth in the rhesus required much greater rotation. Comparative morphology of the teeth of both species is not indicative of a cause for this difference. Radioautographically, the alveolar bone density in *M. speciosa* is greater than that of *M. mulatta*. Ease of expansion of the alveolus to allow for extraction due to decreased density of the bone in the rhesus may adequately explain the relative difficulty of extraction in *M. speciosa*.

In a study involving two human racial populations in New York City which somewhat correlates with this study, it was found that, although teeth are morphologically similar, extraction of the teeth from clinical necessity was much more difficult in the racial group in which bone density is greatly increased. This particular finding is in agreement with radioautographic and clinical findings in this study.

In the rhesus, receding gingiva and tooth attrition are a consistent finding. *M. speciosa*, on the other hand, exhibited extremely healthy gingiva which remained high on the crown of the tooth and tightly adhered. Consequently, no proximal carious lesions would be expected and have not been found in this species. Periodontal pathology of any description is non-existent in the *M. speciosa* examined to date. After a period of 1 year or more since extraction of canines, no adverse effects on oral health have been noted in either species. Normal weight gains and food prehensile activity indicate that there is no useful position in food gathering activity for the canines. No malocclusion has been noted in operated subjects to this date.

Extraction of the canines in these species has been observed to be an advantage to both the animal handlers and other

animals. Although one may be "nipped" by the prehensile incisors or have a finger crushed to some degree by the premolars or molars, the deep slash wound so typical of monkey bites and fighting ceases to be a problem. It has been our observation that the temperament of the animal is markedly changed after extraction. The relatively easy-to-handle *M. speciosa* becomes even more docile, as does the not-so-docile *M. mulatta*.

Continued studies include re-examination of post-operative subjects, temperament change observations, and continued extraction of the canines of remaining male (and some female) subjects of the primate colony. Improved radioautographic methods enable visualization of the considered teeth and provide direction for surgical extraction.

#### REFERENCES

- (1) J. C. Hensley and W. H. Langham, Lab. Animal Care 14, 105 (1964).
- (2) J. C. Hensley, C. F. Bidwell, and A. M. Martinez, Lab. Animal Care (June 1964), abstract.
- (3) J. C. Hensley, this report, p. 85.

MAMMALIAN RADIOBIOLOGY SECTION

PUBLICATIONS AND ABSTRACTS OF MANUSCRIPTS SUBMITTED

DOSE RATE EFFECT ON SURVIVAL OF MICE DURING CONTINUOUS (23-24 hr/day) GAMMA RAY EXPOSURES, J. F. Spalding, T. T. Trujillo, and P. McWilliams. Health Phys. 10, 709 (1964).

Abstracted in Los Alamos Scientific Laboratory Report LA-3132-MS (1964), p. 140.

RADIATION LETHALITY AND CIRCADIAN RHYTHMICITY IN MICE, J. F. Spalding and P. McWilliams. Health Phys. 11, 647 (1965).

Abstracted in Los Alamos Scientific Laboratory Report LA-3132-MS (1964), p. 140. (Originally submitted to Science under the title "On the Question of Cyclic Variations in Radiosensitivity").

DOSE RATE EFFECTS ON LETHALITY OF MICE EXPOSED TO FISSION NEUTRONS, J. F. Spalding, J. A. Sayeg, and O. S. Johnson. In: Biological Effects of Neutron and Proton Irradiations, Vol. II, International Atomic Energy Agency, Vienna (1964), pp. 267-273.

Abstracted in Los Alamos Scientific Laboratory Report LA-3132-MS (1964), p. 139.



**OBSERVATIONS ON LIFESPAN, RADIORESISTANCE, AND PRODUCTIVITY IN OFFSPRING FROM 5 TO 25 GENERATIONS OF X-IRRADIATED MALE MICE**, J. F. Spalding, M. Brooks, and P. McWilliams. *Genetics* 50, 1179 (1964).

Male mice have been exposed to 200 rads of X rays (acute whole-body exposures) for 30 consecutive generations. Comparative studies on productivity of mice from 5, 10, 15, and 20 generations of X-irradiated males have shown a consistent decrement in many litter and breeding characteristics but have also shown that irradiated-line mice produce more litters and have a longer fertile life. Lifespan studies of offspring and grandoffspring from 5 through 15 generations of X-irradiated sires have shown no reduction in survival which can be attributed to irradiated ancestry. A radioresistance decrement in irradiated-line mice after 10 generations of X-irradiated sires has persisted through the 25th generation, and the genetic nature of this decrement is still in question.

**A STUDY ON THE EFFECTIVE RESIDUAL DOSE CONCEPT OF EXPOSURE TO IONIZING RADIATION**, J. F. Spalding, P. McWilliams, J. Basmann, and W. H. Langham. *Radiation Res.* 25, 73 (1965), Abstract No. 193.

A program is being carried out to test mathematical models describing various biological repair and irreparable injury conditions from exposure to gamma rays. The hypothesis at test is that, given the proper exposure conditions, a mammal may be able to absorb amounts of ionizing radiation equivalent to several acute lethal doses and suffer only those effects generalized as chronic. Acute exposures at random time intervals are given to bring residual doses to arbitrarily established maximum permissible levels. Body weights, red blood cell counts, and voluntary activity are some of the biological indices used in these studies. The results of the first in a series of studies to be done will be discussed.

**ACUTE RADIOSENSITIVITY AS A FUNCTION OF AGE IN MICE**, J. F. Spalding, O. S. Johnson, and R. F. Archuleta. Submitted to *Nature*.

Some 2900 RF strain virgin female mice of 14 age groups were

used to establish a functional relationship between age and acute radiosensitivity. Radioresistance increased with age from 3.6 weeks, reaching maximum resistance at 13 to 17 weeks. A steady decline in resistance was observed from 20 weeks of age through the remainder of life.

**REDUCTION IN LIFE EXPECTANCY AS A MEASURE OF RADIATION-INDUCED GENETIC DAMAGE IN MICE, J. F. Spalding and M. R. Brooks.**  
Submitted to Proc. Soc. Exptl. Biol. Med.

Life span studies on first generation male and female breeders and on second generation virgin females from 20 generations of X-irradiated sires were done. The results of this and other studies strongly suggest that factual statements crediting reduction of life span as being a measure of a radiation-induced genetic decrement in viability are premature and inconsistent with experimental evidence at this date.

**CHANGES IN A MOUSE POPULATION RESULTING FROM A SINGLE DOSE OF X-IRRADIATION OF EACH MALE PROGENITOR FOR AS MANY AS 31 GENERATIONS, R. R. J. Chaffee, J. C. Hensley, E. A. Hyatt, and W. H. Langham.** To be published as a supplement of Federation Proceedings, 23rd International Congress of Physiological Sciences (September 1-9, 1965), Tokyo, Japan.

The conditions and dosage of X irradiation and the origin of the control and irradiated mouse lines are described elsewhere (Spalding et al., Genetics 46, 129). The progeny of the irradiation mice were smaller, had less body fat, larger kidneys, and hemoglobin which differed in electrophoretic pattern from that of the controls. The amino acid composition of the hemoglobin was unchanged. To date no significant differences have been found in oxidative enzyme systems of heart, liver, fat tissue, and kidney of the two groups of mice. Further enzymatic studies are currently underway.

## CHAPTER 4

### BIOPHYSICS SECTION

ERYTHROCYTE VOLUME DISTRIBUTIONS DURING RECOVERY FROM BONE MARROW ARREST (M. A. Van Dilla, N. J. Basmann, J. M. Hardin, and J. F. Spalding)

#### INTRODUCTION

Some of the problems in electronic cell sizing and their solution have been discussed previously (1). We now apply the method to an experiment in the kinetics of erythropoiesis, in which bone marrow cell proliferation is suppressed for about 2 weeks by continuous irradiation. The changes in the volume distribution of the circulating red cells after release from the radiation exposure were studied and yielded information on the validity of the electronic sizing method and also on bone marrow response.

#### METHODS AND RESULTS

Twenty RF strain female mice were exposed to whole-body gamma irradiation at 5 rads/hr for 13.3 days for a total dose of 1600 rads. Previous experience has shown that this treatment causes bone marrow arrest, probably within the first few days of exposure. Blood samples were taken from 4 or 5 irradiated mice and 2 control mice at 2- to 4-day intervals during the 4-month recovery period to observe the replenishment of circulating erythrocytes. Red cell count and volume distribution were measured electronically. The experimental distributions were fit with an iterative least-squares code.

A skewed normal distribution (2) was found to fit the unimodal distributions better than a symmetrical normal curve. In cases such that the observed data were bimodal, the sum of two normal distributions was used because the extra two parameters required for the skewed functions made convergence difficult.

Figure 1 shows typical results; prior to the 13th day the volume distributions were similar to the controls but of smaller area (i.e., count) and mean (i.e., mean cell volume). The second population of large cells appeared between the 9th and 13th days after the end of exposure and increased in mean volume to a maximum on the 15th day. This population was identified as reticulocytes on microscopic examination of dry films made from these blood samples.

Figure 2 summarizes the results of the computer fits to all the experimental data. The parameters plotted are area, mean, and fractional standard deviation of the fitted functions all normalized to the control values so that they are dimensionless quantities, normally unity. Thus, they represent red cell count, mean cell volume (for each population when two are present), and variation in size of the red cells. The red cell count dropped to about half-normal at 10 days after the end of exposure and then slowly returned to near-normal. Mean cell volume was slightly (2 percent) below normal initially, falling steadily for about 10 days to 7 to 8 percent below normal, then rising rapidly to 30 percent above normal as the reticulocytes appeared; thereafter there was a slow decline to normal. The width of the distribution showed changes similar to the mean. The reticulocytes were 60 to 70 percent larger than normal red cells at first, and the mean volume of this abnormal population declined until it could no longer be resolved at about 30 days after the end of exposure. The mean cell volume of the normal population declined slightly, and then returned to normal (and overshot somewhat) as the reticulocytes appeared.

## DISCUSSION

These results suggest the following conclusions:

(a) The volume distributions measured with a long aperture ( $30\ \mu$  in diameter and  $225\ \mu$  long) seem to reflect accurately the actual red cell volume distributions existing in the blood. Normally, a single population is present and this is

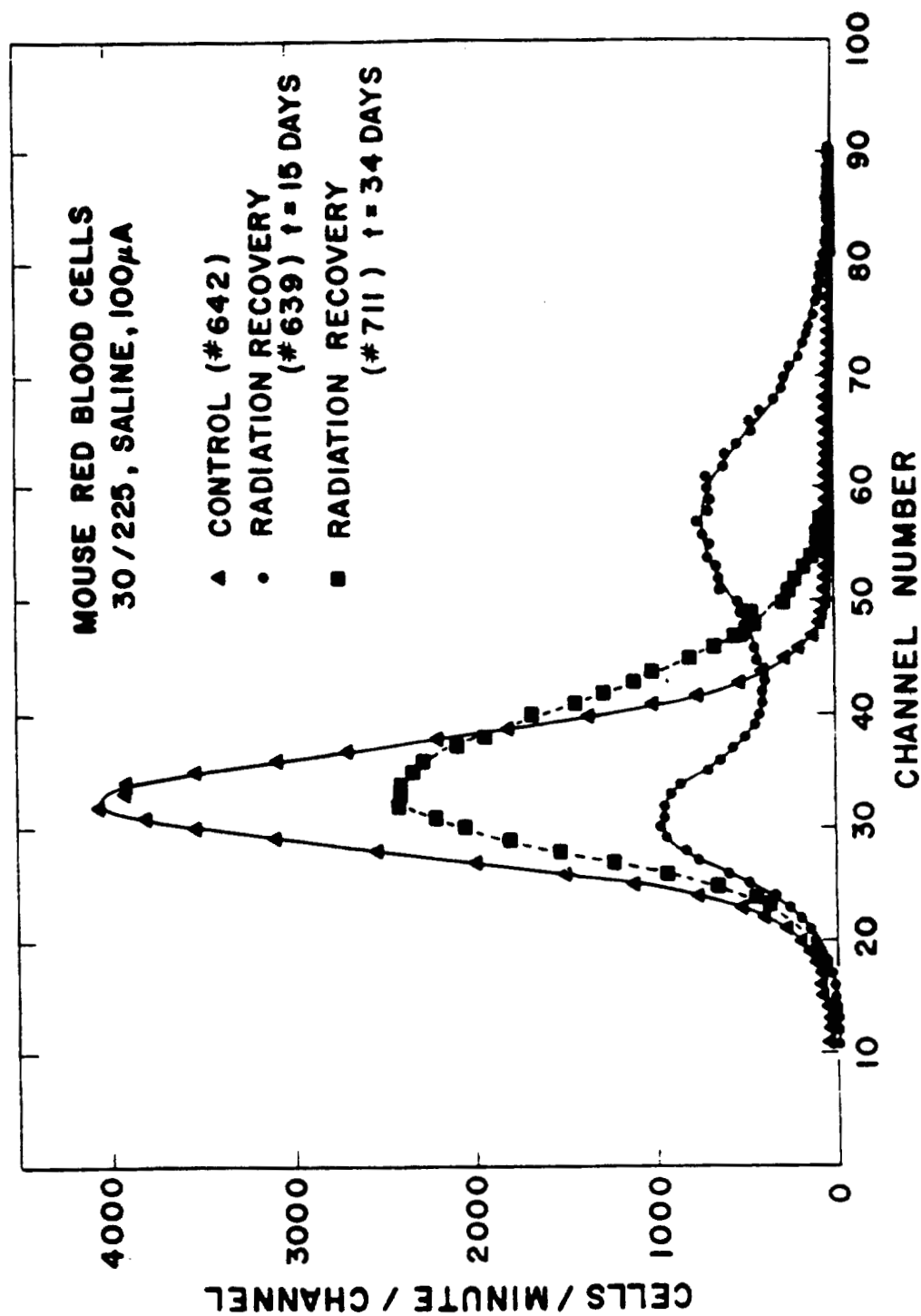


Fig. 1. Mouse red cell volume distribution 15 and 34 days post irradiation compared with control; dilution factor and volume of cell suspension measured are constant so that the areas under the curves are proportional to red cell count.

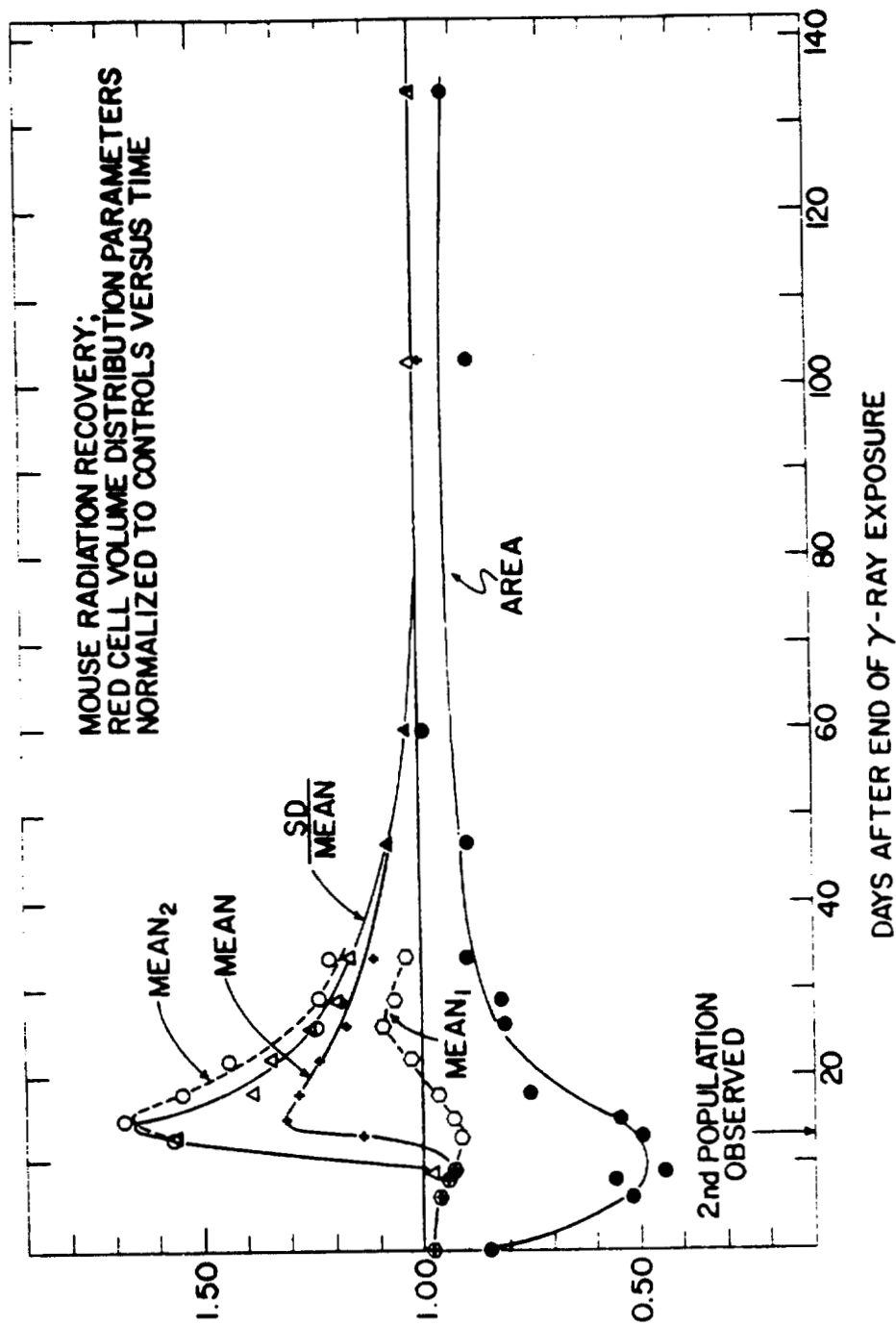


Fig. 2. Variation of computer-derived red cell volume distribution parameters with time after end of gamma-ray exposure, normalized to control values. Curve labels have the following meaning: area is red cell count; mean<sub>1</sub> is mean cell volume of normal population; mean<sub>2</sub> is mean cell volume of macrocytic reticulocytes; mean is mean cell volume of total population; and SD is standard deviation.

also the result given by the electronic sizing procedure. When a second population of larger cells is present (as proved by microscopic examination), this population is clearly observed in the measured volume distributions. In addition, the number of reticulocytes obtained from slide counts agrees with that from electronic sizing.

(b) The volume distribution of normal mouse red cells is well described by a skewed normal function with only a slight asymmetry to the large volume side. The skewness parameter ( $\alpha_3$  in Ref. 2) is in the range of 0.1 to 0.3.

(c) The macrocytic reticulocytes seem to be the same as previously reported by Brecher and Stohlman (3) and Seno et al. (4) as a result of other stimuli such as phenylhydrazine and bleeding. Apparently the severe need for circulating red cells results in the skipping of a terminal cell division, leading to macrocytosis followed by replacement by cells of more normal size.

(d) If it is assumed that red cell production was reduced by the radiation exposure, then mean age of the circulating erythrocytes gradually increased until appearance of the reticulocytes. Since mean volume decreased simultaneously, it follows that red cell volume decreases with age (it has been previously established that red cell density increases with age).

#### REFERENCES

- (1) M. A. Van Dilla, N. J. Basmann, and M. J. Fulwyler, Los Alamos Scientific Laboratory Report LA-3132-MS (1964), p. 182.
- (2) F. E. Croxton and D. J. Cowden, Applied General Statistics, Prentice Hall, Englewood Cliffs, New Jersey (1955), p. 619.
- (3) L. O. Jacobson and M. Doyle, eds., Erythropoiesis, Grune and Stratton, Inc., New York (1962), pp. 216-221.
- (4) S. Seno, M. Miyahara, H. Asakuru, O. Ochi, K. Matsuska, and T. Toyama, Blood 24, 582 (1964).

# FLOW OF PARTICLES THROUGH A COULTER APERTURE: HYDRODYNAMIC CONSIDERATIONS (F. H. Harlow\* and M. A. Van Dilla)

## INTRODUCTION

When very uniform polystyrene spheres flow through a Coulter aperture of such dimensions that their transit time approximates the rise time of the pulse amplifier, a distorted bimodal pulse-height distribution results (1). The detailed shape of this distribution is a function of particle transit time. It appears that this type of distribution can be at least partly accounted for by the pattern of hydrodynamic flow through the aperture and the rise time characteristic of the amplifier. Theoretical analysis of the transit time distribution imposed by the boundary layer and fluid core in the region of unestablished flow in a short pipe (i.e., aperture) leads to a bimodal distribution which approximates what is observed experimentally.

## METHODS AND RESULTS

The theoretical treatment which follows contains simplifications to make the mathematics tractable; only an outline will be given in the interests of conserving space. The general plan is: (a) calculation of the distribution of transit times; and (b) calculation of the pulse-height distribution resulting from modification of the transit time distribution by the response of the amplifier.

Assuming that fluid flow through the aperture is laminar and if  $t$  equals transit time and  $u(r,z)$  equals fluid velocity at any point in the aperture, then

$$t = \int_0^L \frac{dz}{u(r,z)}, \quad (\text{Eq. 1})$$

where the geometry is shown in Fig. 1. If the incoming particle distribution is uniform and  $N$  particles enter during an

---

\*LASL Theoretical Division.



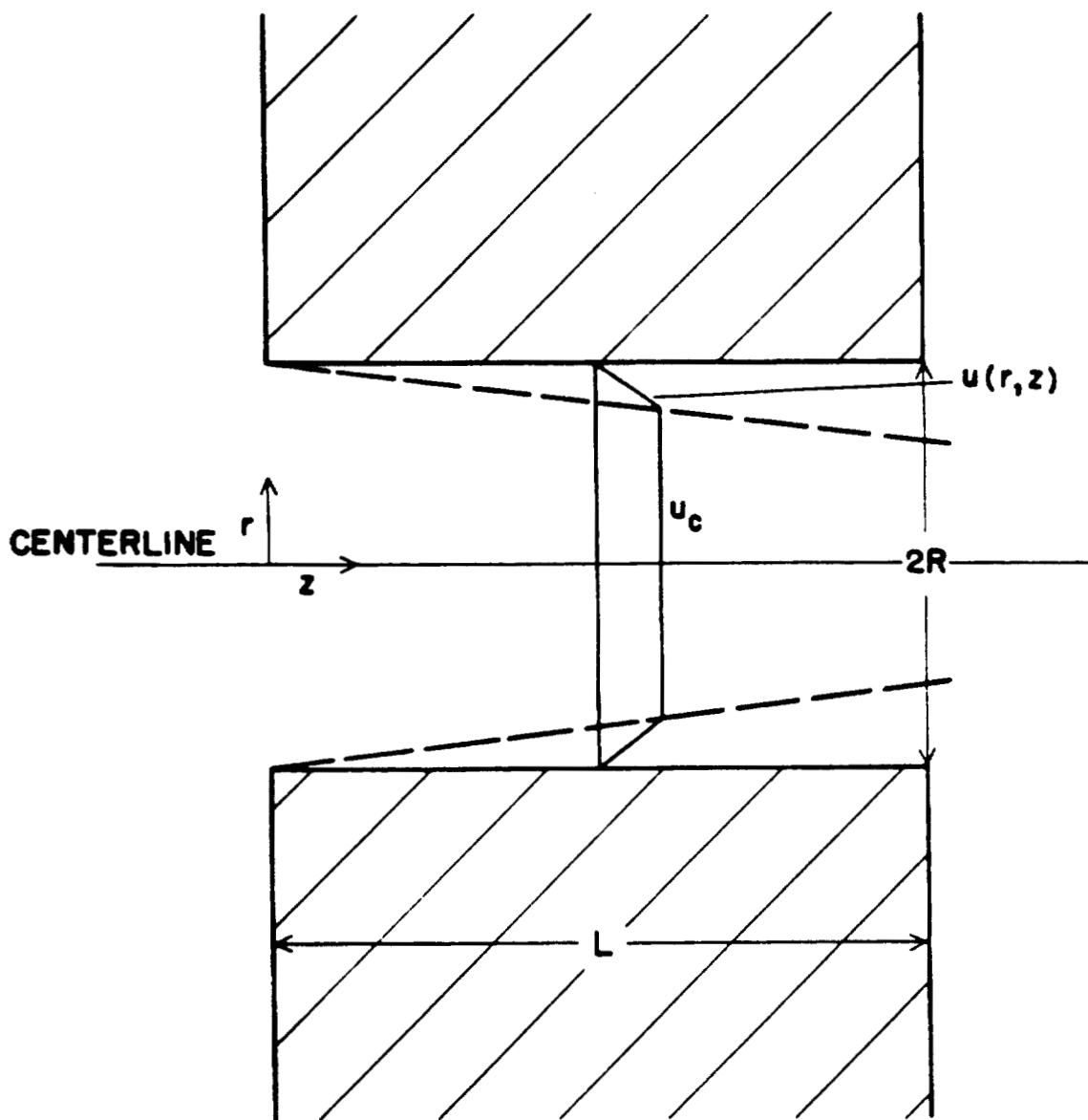


Fig. 1. Aperture cross section showing coordinate system and velocity profile.

experiment, then the number of particles traversing between  $r$  and  $r + dr$  is

$$N(r) dr = N \frac{2\pi r dr}{\pi R^2} = \frac{2 Nr}{R^2} dr.$$

The difference in transit time across the radius interval  $dr$  is

$$dt = - \int_0^L \left[ \frac{dz}{u^2(r,z)} \frac{\delta u(r,z)}{\delta r} \right] dr.$$

But

$$\left[ N(t) dt = N(r) dr \right] = \frac{2 Nr}{R^2 \int_0^L \left[ \frac{1}{u^2(r,z)} \frac{\delta u(r,z)}{\delta r} dz \right]} dt, \quad (\text{Eq. 2})$$

where  $N(t)$  is the transit time distribution function desired. Assume the pulse amplifier response to a step function input is

$$P(t) = P_0 (1 - e^{-t/\tau}), \quad (\text{Eq. 3})$$

where  $\tau$  is the amplifier rise time. Then

$$N(P) dP = N(t) dt, \quad (\text{Eq. 4})$$

where  $N(P)$  is the desired pulse-height distribution function in parametric form. The next part of the problem, then, is to find workable expression for the velocity,  $u(r,z)$ .

The case of importance is the aperture of length equal to diameter of  $30 \mu$ , which has been shown to give a highly distorted bimodal distribution for uniform spheres. For this aperture the boundary layer (2) does not extend to the center line (i.e., the flow is unestablished), and we make the approximation that the velocity is proportional to distance from the wall out to the transition interface (3) and constant to the center line:

$$u(r,z) = u_c = \text{constant (central region)}$$

$$u(r,z) = (R - r)(u_c \sqrt{\frac{u_c}{\pi \nu z}}) \text{ (boundary layer),}$$

where  $u_c$  = center line velocity and  $\nu$  = viscosity. Substituting in Eq. (1), neglecting the term in  $(R - r)^2$ , and then using Eq. (2) results in the following transit time distribution:

$$\frac{\alpha N L}{u_c} \frac{1}{t^2}, \text{ for } t > t_{\min} = \frac{L}{u_c}$$

$$N(t) = \text{constant} \times \delta(t - t_{\min}), \text{ for } t = t_{\min}$$

$$0, \text{ for } t < t_{\min}$$

where constant =  $N(1 - \alpha)$ ,  $\alpha = \frac{4\sqrt{\pi}}{3} \sqrt{\frac{L}{R} \frac{1}{Re}}$ ,  $Re$  = Reynolds' number =  $\frac{u_c R}{\nu}$ , and  $\delta$  = delta function.

The final step is the modification of this transit time distribution by the response of the amplifier. To do this we combine the expressions for  $N(t)$  with Eqs. (3) and (4). For  $t > t_{\min}$ , the result is

$$\frac{P_0}{N} N(P) = \frac{\alpha L}{u_c \tau} \frac{1}{(1 - \lambda) \ln^2 (1 - \lambda)}$$

$$\lambda = P/P_0,$$

and for  $t = t_{\min}$ , the result is

$$\frac{P_0}{N} N(P) = \frac{1 - \alpha}{0.2} = 3.63,$$

where a delta function width of 0.2 has been assumed and  $L = 2R = 3 \times 10^{-3}$  cm,  $u_c = 10^3$  cm/sec, and  $\nu = 10^{-2}$  stoke (which are typical aperture conditions). A plot of this result (Fig. 2) shows the general features of the resultant pulse-height distribution: (a) bimodal shape; (b) peak at minimum pulse-height due to particles traversing aperture in minimum time (central region of flow); and (c) peak at maximum pulse-height due to particles traversing aperture more slowly (boundary layer).

In practice, both peaks will be broadened and blurred into smooth curves by such effects as amplifier noise, turbulence, and possible radial component of particle velocity. But it does seem that this rough approach shows how uniform particles can produce a spurious, bimodal pulse-height distribution with varying areas in each peak as hydrodynamic parameters change.

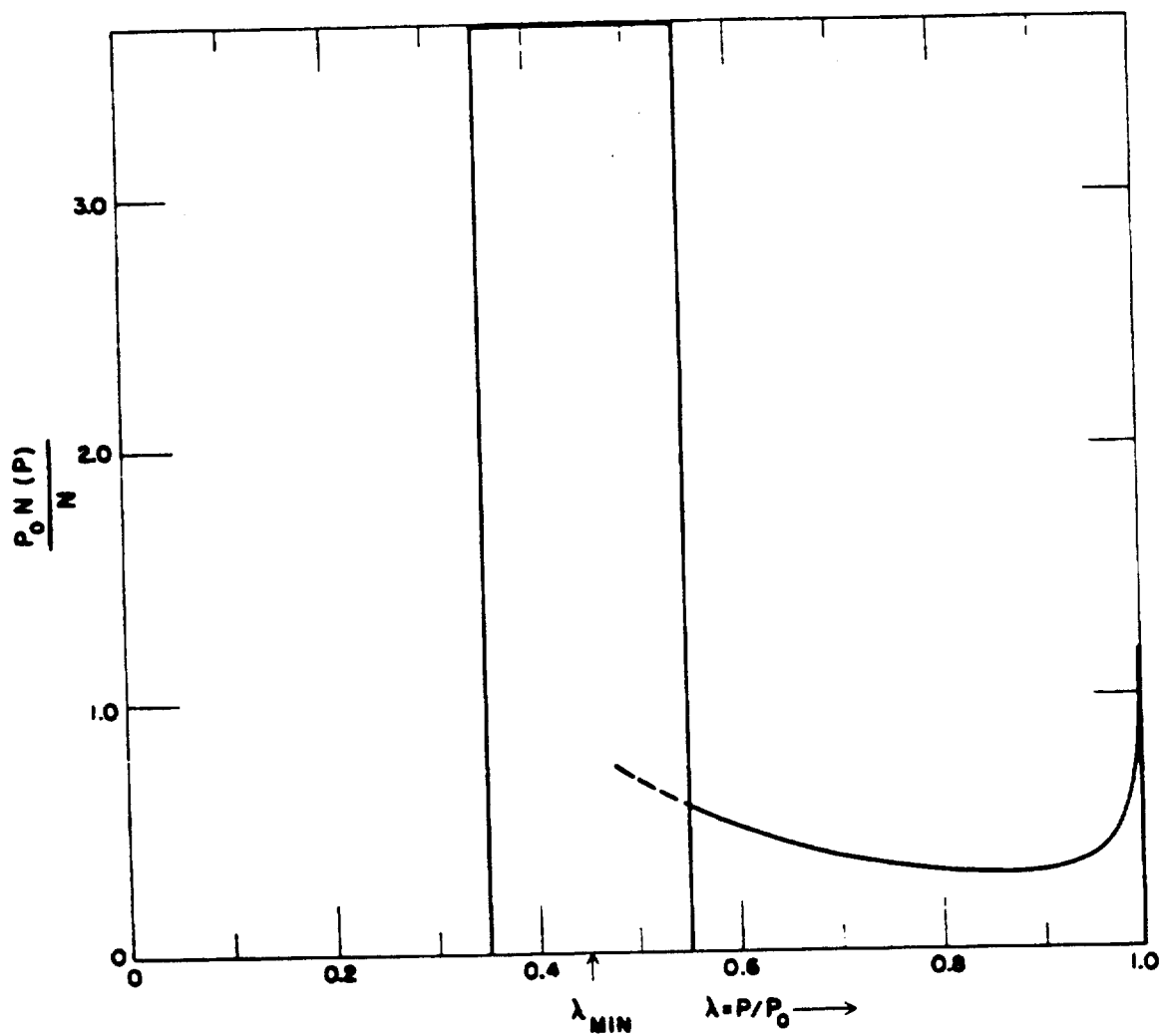


Fig. 2. Theoretical pulse-height distribution for an aperture of length equal to diameter of  $30 \mu$  traversed by uniform particles.

## REFERENCES

- (1) M. A. Van Dilla, N. J. Basmann, and M. J. Fulwyler, Los Alamos Scientific Laboratory Report LA-3132-MS (1964), p. 190.
- (2) J. K. Vennard, Elementary Fluid Mechanics, Wiley and Sons, New York (1961), pp. 244-247.
- (3) V. L. Streeter, ed., Handbook of Fluid Dynamics, McGraw-Hill, New York (1961), Section 9, p. 11.

## AN ELECTRONIC PARTICLE SEPARATOR WITH POTENTIAL BIOLOGICAL APPLICATION (M. J. Fulwyler)

### INTRODUCTION

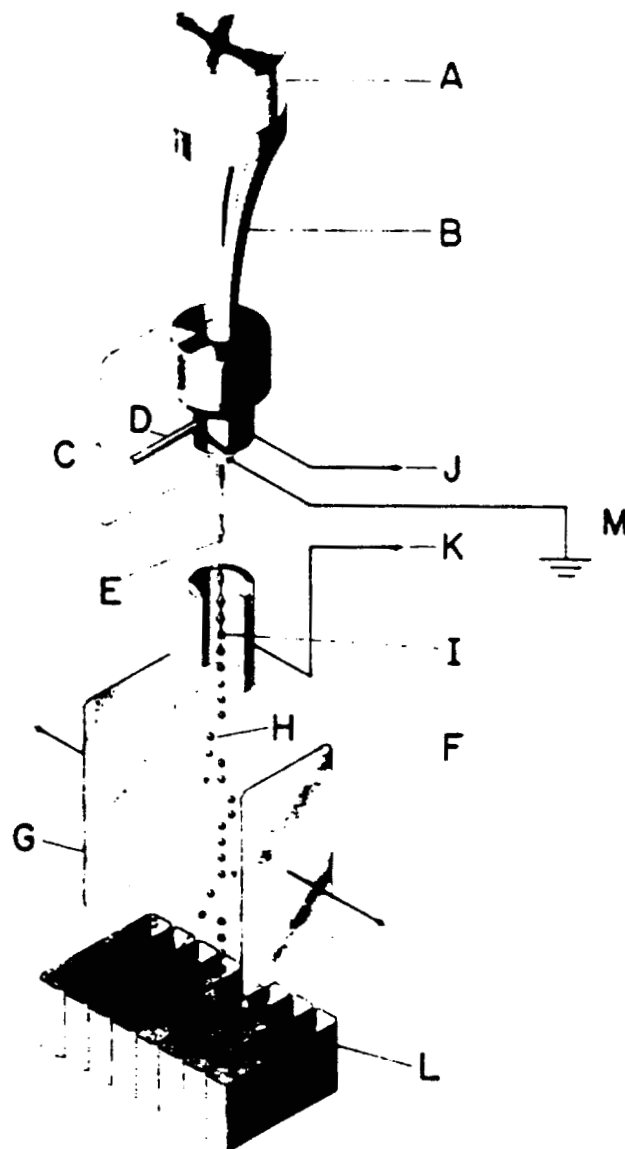
The particle separator is a device which, in principle, is capable of separating microscopic particles according to an electronically measurable characteristic such as volume, optical density, or fluorescence. Separation is accomplished as follows. The particle, in liquid suspension, passes by a sensor which measures the characteristic of interest. The suspension is forced through a nozzle and emerges as a jet which is broken into droplets, thereby isolating the suspended particles. The droplets containing the particles of interest are charged and then deflected by an electrostatic field into a collection vessel.

### METHOD

Shown in Fig. 1 is a device which is being developed to separate particles according to their volume. A cell suspension (under 4 atmospheres pressure) enters the droplet generator (C) via a tube (D) and emerges as a high-velocity fluid jet (E) [diameter 36  $\mu$ , velocity 15 m/sec]. A piezoelectric crystal (A), driven at a frequency of 72,000 c/sec, produces vibrations which pass down the Lucite rod (B) into the liquid within the droplet generator. The catenoidal shape of the rod amplifies the magnitude of the vibrations within the liquid, and the velocity fluctuations of the emerging liquid cause the jet to break into 72,000 very uniform droplets each second.

Droplets are charged as they pull away from the charged liquid column by applying a voltage at (K) relative to (M), which is in contact with the emerging stream. As the droplet separates, it carries away a charge proportional to the instantaneous charge on the column of liquid. In this way one or more droplets may be charged. The charged droplets are deflected (H) on entering the electrostatic field (7,000 volts/cm) between the deflection plates (G). A series of collection vessels (L) receives the deflected droplets.

The sequence of events leading to separation is as follows. Cell volume is sensed as the cell passes through a Coulter



### CELL SEPARATOR

Fig. 1. Cell separator: (A) piezoelectric crystal; (B) acoustic coupling rod; (C) droplet generator; (D) fluid entry tube; (E) fluid jet; (F) charging collar; (G) electrostatic deflection plates; (H) deflected droplets; (I) droplet separation point; (J) cell volume signal contact; (K) charging collar contact; (L) droplet collection system; and (M) ground contact for emerging jet.



aperture (I) within the droplet generator (C). An electric pulse proportional to cell volume is obtained at (J). The cell then emerges in the jet and, 250  $\mu$ sec later, arrives at the separation point (I) within the charging collar (F). The size of the charging pulse needed to deflect droplets into the proper vessel is electronically determined from the cell volume pulse. Approximately 240  $\mu$ sec later the charging pulse is applied to the charging collar (K); the cell is caught in a forming droplet which is charged and then deflected by the electrostatic field into the appropriate collection vessel. The method of forming, charging, and deflecting droplets is a modification of that developed as an ink-writing oscillograph by Richard Sweet (2).

## RESULTS AND DISCUSSION

Figure 2A is the volume spectrum, obtained on a volume spectrometer (3), of polystyrene spheres ranging in diameter from 7 to 14  $\mu$ . The separator was adjusted to remove a volume increment from the mid-portion of the spectrum. Figure 2B shows the volume spectra of the separated spheres (triangular data points) and the residue remaining after separation. It has been shown that the device is capable of simultaneously separating two discrete volume increments, and electronics are being built to enable simultaneous separation of a sample into 6 or more discrete volume increments.

Quantitative separations have been made of human red blood cells and mouse red blood cells from a mixture of the two. Also volume fractions of mouse lymphoma cells growing in suspension culture have been separated. Other applications of the device currently underway include exfoliative and bone marrow cytology. Tests with Chinese hamster ovary cells showed 96 percent viability and normal growth rate after passing through the device.

Development and refinement of the device are proceeding. Separations under sterile conditions are expected in the near future. Investigation is underway of a sensor system able to measure optical characteristics of a particle. With such a system, it may be possible to measure simultaneously two (or more) characteristics of a cell and to make separation dependent on the relation of these two characteristics.

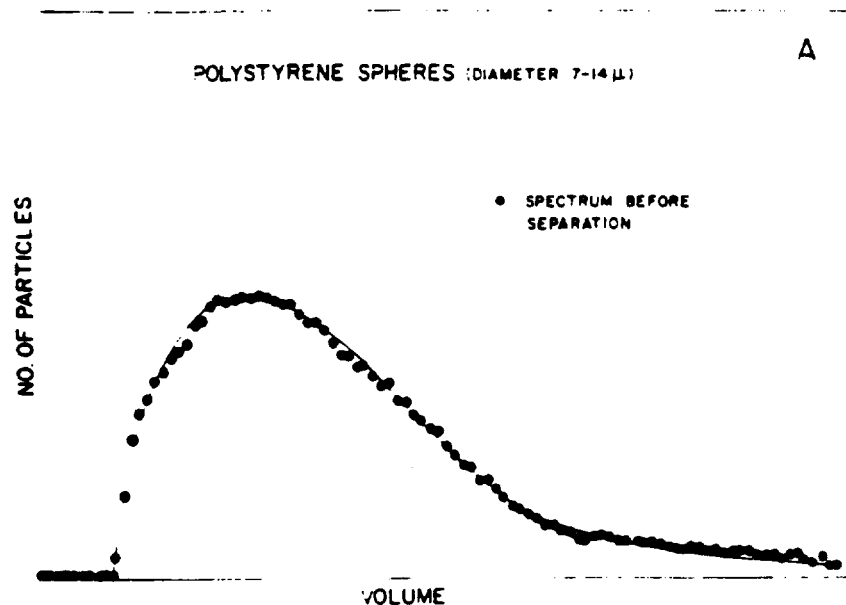


Fig. 2A. Volume spectrum of polystyrene spheres ranging in diameter from 7 to 14  $\mu$ .

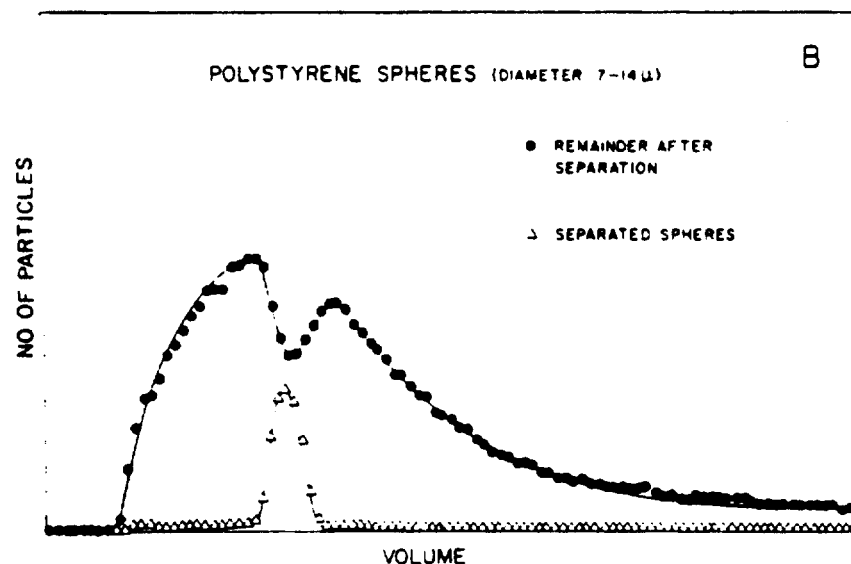


Fig. 2B. Volume spectrum of separated spheres (triangles) and the volume spectrum of the residue after separation (solid points).

### REFERENCES

- (1) W. H. Coulter, U. S. Patent No. 2,656,508 (1953); W. H. Coulter, Proceedings of the National Electronics Conference 12 (1956), p. 1034.
- (2) R. G. Sweet, Stanford University Technical Report 1722-1. Available from Defense Document Center, Washington, D. C., Report SU-SEL-64-004 (1964).
- (3) M. A. Van Dilla, N. J. Basmann, and M. J. Fulwyler, Los Alamos Scientific Laboratory Report LA-3132-MS (1964), p. 182.

# IN VIVO MEASUREMENT OF PLUTONIUM-239 LUNG BURDENS IN HUMANS (P. N. Dean and J. H. Larkins)

## INTRODUCTION

Evaluation of the lung burden of plutonium in chronically exposed plutonium operators is needed for proper industrial medical control of this material. Urine and fecal assays for plutonium are unreliable and are primarily a measure of the systemic burden. Conventional whole-body counting techniques cannot be used for plutonium assay because of the soft X-ray characteristic radiation of this material. The present endeavor of this Laboratory is to develop a gas-filled proportional counter to measure these X rays. This type of counter was chosen to utilize its good resolution, low background, and easily varied shape.

## METHOD

A large-volume proportional counter has been constructed with a surface area of  $1000 \text{ cm}^2$ , thickness of 13 cm, and total volume of 12 liters. The counter utilizes a built-in anti-coincidence shield to reduce the counter background, due primarily to cosmic rays. Figure 1 shows a cross sectional view of the counter. There are three wire grids. The upper row of wires forms the anticoincidence array, the second layer provides a ground plane, and the lower layer forms the collecting grid for the main counter. The window is a 1.6-mm thick layer of Lucite plated with  $75 \mu\text{g}/\text{cm}^2$  of aluminum. This type of window was selected because of its rigidity and its absorption of most of the potassium-40 beta rays.

## RESULTS AND DISCUSSION

It is intended to operate this counter with a gas filling of xenon-methane to obtain a counter efficiency of greater than 90 percent. Presently the counter is being checked out with a gas mixture of argon-methane. Figure 2 is the spectrum of a 5-ml sample of plutonium-239 as measured with this gas filling. Figure 3 is the spectrum of plutonium-239 plated on a 3-mm thick sheet of Lucite. The energy resolution of the 13.6-keV X ray is 14 percent. It may be possible to relate

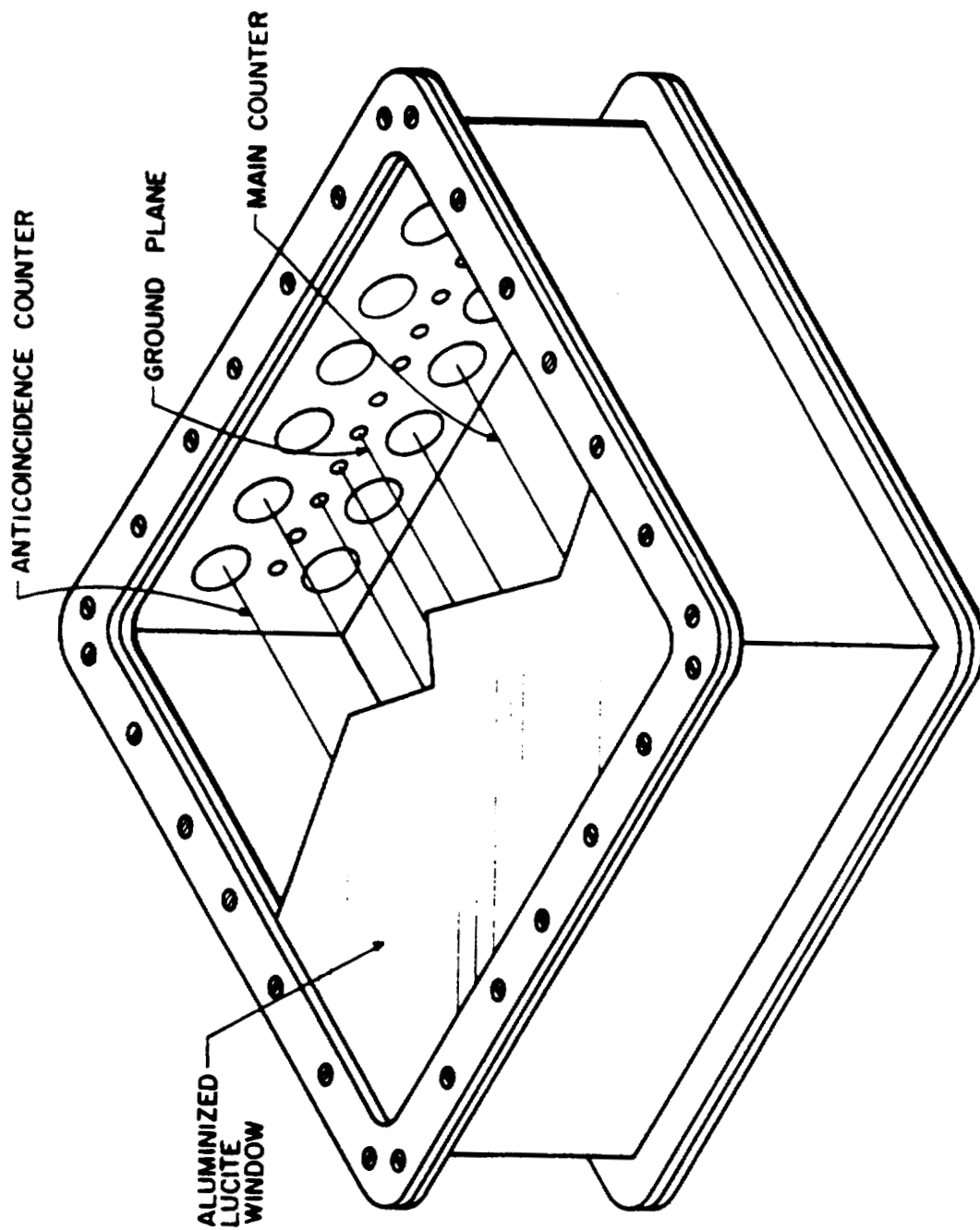


Fig. 1. Cross sectional view of proportional counter. Some of the wires are not shown to increase clarity.

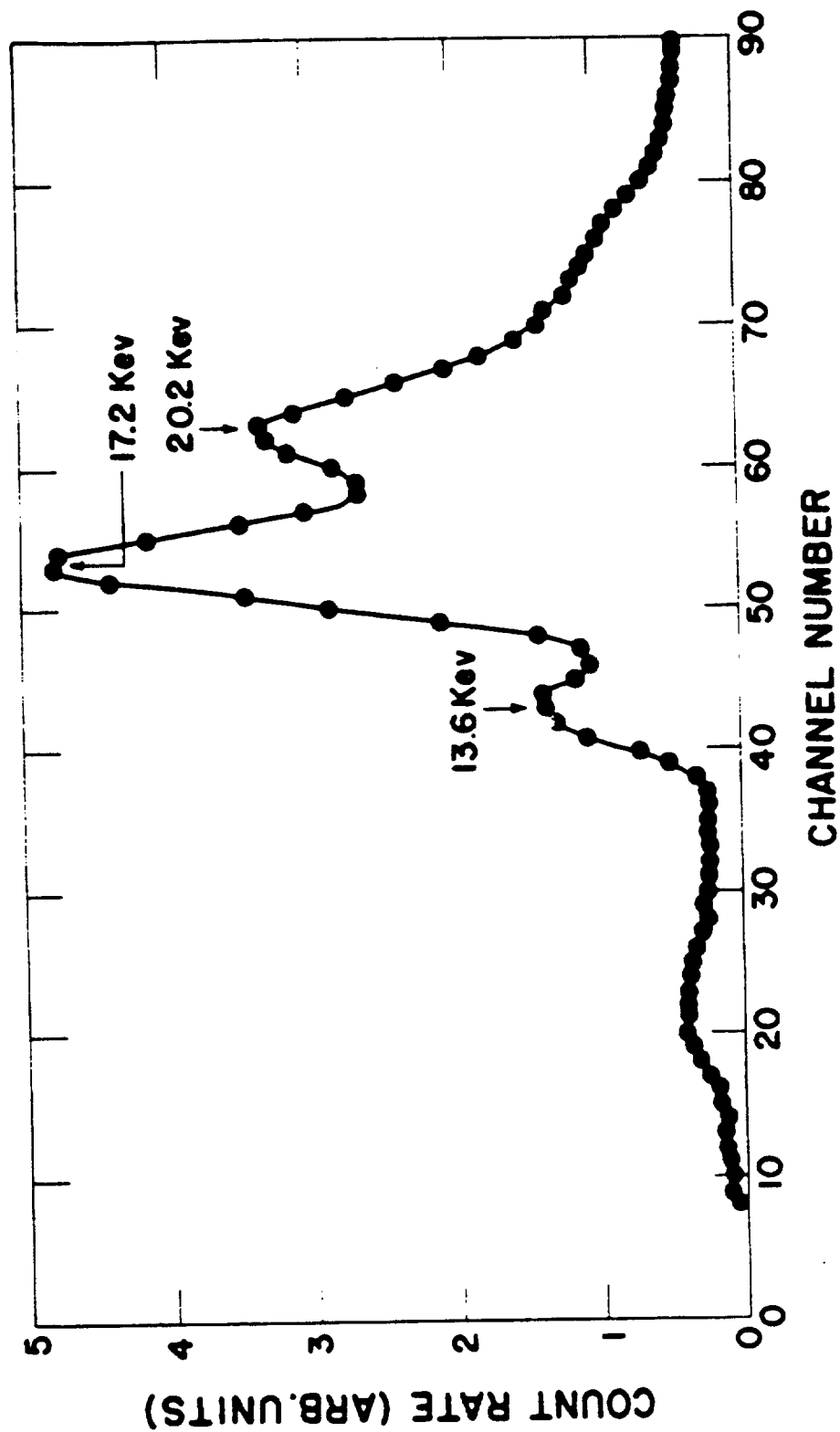


Fig. 2. X-ray spectrum of 5-ml sample of plutonium-239 in aqueous solution as measured with proportional counter.

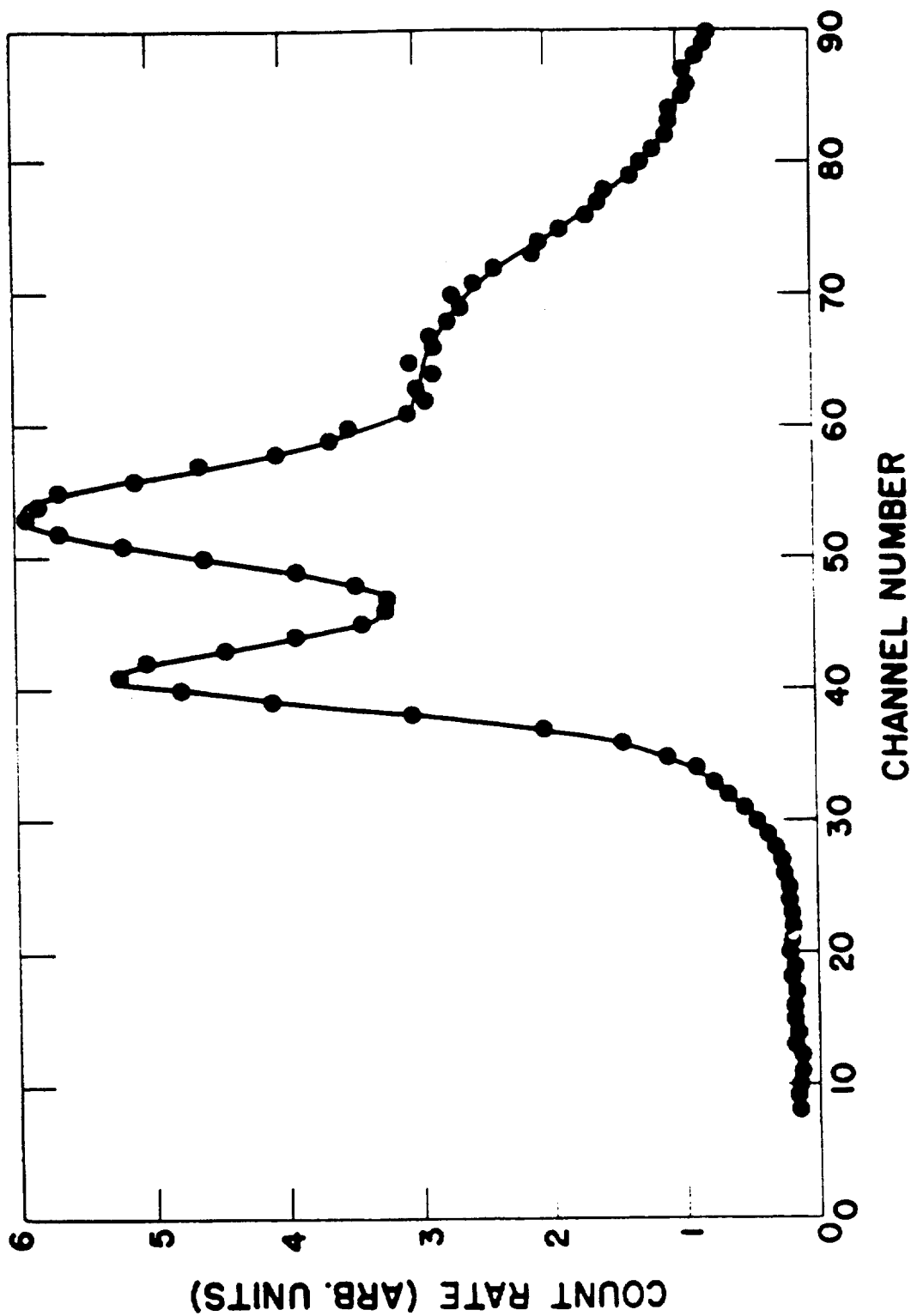


Fig. 3. X-ray spectrum of thin layer of plutonium-239 as measured with proportional counter.

the relative peak heights of the three X rays to depth of deposition of the plutonium in the lungs. This would be a great help in calibration of the counter and will be thoroughly investigated.

This counter is a preliminary model constructed to study the feasibility of in vivo measurement of plutonium-239 lung burdens. If the system proves to be useful, additional counters will be constructed to increase the geometrical efficiency.



## BIOPHYSICS SECTION

### PUBLICATIONS AND ABSTRACTS OF MANUSCRIPTS SUBMITTED

HALF-LIFE OF CESIUM-132, P. N. Dean and C. R. Richmond.  
Health Phys. 10, 764 (1964).

Abstracted in Los Alamos Scientific Laboratory Report LA-3132-MS (1964), p. 207.

DETECTION OF AN INTERSTELLAR FLUX OF GAMMA-RAYS, A. E. Metzger, E. C. Anderson, M. A. Van Dilla, and J. R. Arnold.  
Nature 204(4960), 766-767 (1964).

Gamma-ray spectrometry measurements with a 7-cm cesium iodide crystal during the flights of two Ranger spacecraft at distances of the order of  $10^5$  km from the earth demonstrate the existence of a gamma flux with integrated intensity of about 3 c/cm<sup>2</sup> sec and a differential spectrum which varies roughly as  $E^{-2}$ . The gamma rays do not originate from the earth, the sun, nor from the spacecraft as cosmic-ray secondaries. Absence of a line at 0.5 Mev makes it unlikely that the flux results from nuclear reactions of high-energy particles.

ON THE RETENTION OF CESIUM-137 IN PEOPLE, M. A. Van Dilla.  
Health Phys. 11, 21-22 (1965).

Abstracted in Los Alamos Scientific Laboratory Report LA-3132-MS (1964), p. 206.

EXPERIMENTAL TECHNIQUE FOR HIGH PRECISION CALIBRATION OF WHOLE-BODY COUNTERS: APPLICATION TO A  $4\pi$  LIQUID SCINTILLATOR AND A LARGE SODIUM IODIDE (TI) CRYSTAL SPECTROMETER, P. N. Dean. In: Radioactivity in Man (G. R. Meneely and S. M. Linde, eds.), Charles C. Thomas, Publ., Springfield, Ill. (1965), pp. 94-103.

With the  $4\pi$  liquid scintillator, potassium determinations can be made on random subjects to a precision of  $\pm 2.1$  percent based on the calibration alone. Including statistics, the precision is  $\pm 3.0$  percent for a counting time of 200 sec.

With the crystal spectrometer, potassium determinations can be made on random subjects to a precision of  $\pm 2.7$  percent based on the calibration alone. Including statistics, the precision is  $\pm 3.5$  percent for a counting time of 50 min.

ERYTHROCYTE SIZE DISTRIBUTIONS FOLLOWING RADIATION-INDUCED BONE MARROW ARREST, M. A. Van Dilla, J. M. Hardin, N. J. Basmann, and J. F. Spalding. Radiation Res. 25, 79 (1965). Abstract No. 209.

The principle of cell counting invented by W. H. Coulter has been extended to red cell sizing. The size distribution of erythrocytes in normal people and mice is shown to be unimodal, approximately normal with a standard deviation of close to 15 percent. Using improper aperture conditions, however, spurious bimodal distributions are obtained which can lead to the notion that two volumetrically distinct populations are present in the blood of normal individuals. The reasons for these artifacts are not clear, but they are avoided by proper choice of aperture dimensions, cell transit time, and by using minimum aperture current. In an experiment on bone marrow arrest, mice were exposed to a gamma-ray dose of 5 rads/hr for 14 days, after which they were removed to allow resumption of bone marrow activity. Red cell sizing began at the end of exposure; in the following 2 weeks red cell concentration dropped to 50 percent of normal while mean cell volume and fractional standard deviation dropped from 2 to 7 percent below normal. Then a sudden release of immature red cells into the circulation was observed. A second oversized population of 60 to 70 percent greater volume appeared, reversing the downward trend of red cell concentration and causing the mean cell volume to rise

to 30 percent over normal and the fractional standard deviation to increase to 65 percent over normal. In the following weeks the second population diminished in concentration and size; mean cell volume and fractional standard deviation returned to normal while red cell concentration climbed to within 5 to 10 percent of normal.

**RADIOACTIVE CONTAMINATION OF CONTEMPORARY LEAD**, R. I. Weller, E. C. Anderson, and J. L. Barker. Nature 206(4990), 1211-1212 (1965).

A study of the gamma-ray activity of 8 samples of commercial lead showed that 3 of them were equivalent to the best "aged" lead for low-level shielding. The contaminant in the other 5 was identified as lead-210 plus daughters at concentrations up to 38 nc/kg. The results indicate that selected commercial lead can be used where ultimate shielding quality is required.

**RADIATION BIOLOGY AND SPACE ENVIRONMENTAL PARAMETERS IN MANNED SPACECRAFT DESIGN AND OPERATIONS**, W. H. Langham, P. M. Brooks, and D. Grahn, eds. Aerospace Med. 36(2), Section II (1965), 55 p.

The purpose of this report is to derive, insofar as possible, criteria for consideration of man's response to space radiation exposure so that radiation risks may be taken into account, during spacecraft design and operational planning phases, along with the other inherent hazards of manned space flight. The only basis for derivation of such criteria is the vast amount of data on effects of so-called conventional radiation exposures (involving low and intermediate energy electromagnetic and particulate radiations) on animals and occasionally man. Unfortunately, exposures in space will not be conventional either with regard to exposure conditions or nature, energy, and spectral distribution of the radiations. It seems necessary, therefore, to discuss first some of the general and specific aspects of the space radiation environment and some of the exposure conditions that may be contemplated.

AUTOMATIC DATA ACQUISITION, REDUCTION AND ANALYSIS, P. N. Dean and C. R. Richmond. To be published in the Proceedings of the IAEA Symposium on Radioisotope Sample Measurement Techniques in Medicine and Biology, Vienna, Austria (May 24-28, 1965).

High-speed electronic computers process and analyze data at a remarkably fast rate. For example, a least squares curve-fit analysis of a single exponential function (two parameters) comprised of 227 data points required 14 seconds compilation time and 13 seconds for data read-in and actual problem execution. It is easy to see that cost per run is very inexpensive even if we are concerned with computer costs of 500 dollars per hour. At this particular rate, the cost would be less than 5 dollars. We must also consider that the output is in a neat, legible standard format for perusal and subsequent storage. Obviously data must be handled prior to computer analysis, but this time can be considered as usual technician work time.

Another consideration is that of rechecking data analyses. Least squares analyses done on usual desk-type calculators can be very time-consuming, and commonly the problem is rechecked before the answers are considered valid. This is not true of computer analyses. Also, errors of omission, translocation, and transcription can be very troublesome when one collects large amounts of counting data -- even if the percent incidence is small. These rarely occur with automated systems and can be reduced still further by using parity checks during tape or card punching.

We also want to point out that the RTW programs are not linked to a particular detection instrument. Rather, by changing the data card format the basic program applies to virtually any type of counter. The IQ program is normally used in conjunction with spectra obtained from multichannel analyzers. It has recently been adapted for analysis of base ratios of oligonucleotides. The ultraviolet absorption spectra of mixtures of thymine and cytosine derivatives are treated as pulse-height spectra and the analysis carried out as described.

The application of automation techniques to four gamma-ray assay devices has been described. The relative merits of three methods of transferring data from counters to computer-compatible forms have been presented along with the practical application of two of them. Computer methods of data reduction and analysis have been discussed, with particular

attention to metabolic studies. All of the above -- data acquisition, reduction and analysis -- have proven to be indispensable to programmatic research of the Biomedical Research Group of the Los Alamos Scientific Laboratory.

SOME BIOLOGICAL ASPECTS OF RADIOACTIVE MICROSPHERES, W. H. Langham, C. R. Richmond, J. C. Hensley, P. N. Dean, and M. A. Van Dilla. Los Alamos Scientific Laboratory Report LA-3365-MS (in press).

The effectiveness of particle size control as a means of alleviating the potential radioactive particle inhalation hazards inherent in space use of nuclear power systems will depend on a variety of factors, among which are biological effects produced by radioactive particles too large to enter the respiratory tract. If insoluble, such particles will constitute discrete radiation sources. Discrete sources deposited on the skin surface may produce significant lesions and, if swallowed, may result in irradiation of the gastrointestinal mucosa during passage. If soluble, the radioactive materials present may be absorbed into the body or enter the ecological cycle, resulting in an internal source of radiation exposure. This report covers some preliminary observations believed pertinent to assessing the biological effects of discrete radiation sources, particularly fissioned uranium-235 carbide microspheres in the size range of about 100 to a few hundred microns.

COMPUTER REDUCTION OF METABOLIC DATA OBTAINED FROM SCINTILLATION COUNTERS, P. N. Dean. Los Alamos Scientific Laboratory Report LA-3298 (in press).

This report describes in detail the RTW series of computer programs written to analyze metabolic data. The programs calculate elapsed time between radionuclide administration and time of measurement, correct all data for changes in counting efficiency relative to measurements made on standards at zero time and for physical decay, if desired, and express the observed counting information as effective or biological retention at time of measurement.

**ELECTRONIC SEPARATION OF BIOLOGICAL CELLS BY VOLUME, M. J. Fulwyler. Science (in press).**

A device has been developed which is capable of separating biological cells (suspended in a conducting medium) according to volume. Cell volume is measured in a Coulter aperture, and the cells are subsequently isolated in droplets of the medium which are charged according to the sensed volume. The charged droplets then enter an electrostatic field and are deflected into a collection vessel. Mixtures of mouse and human erythrocytes and a large volume component of mouse lymphoma cells were separated successfully. In tests with Chinese hamster ovary cells, essentially all survived separation and grew at their normal rate.

## CHAPTER 5

### CELLULAR RADIOBIOLOGY SECTION

TIME OF SYNTHESIS OF RNA AND PROTEIN SPECIES ESSENTIAL TO DIVISION IN FOUR CELL LINES (R. A. Tobey, D. F. Petersen, and E. C. Anderson)

#### INTRODUCTION

For mitosis and cell division to occur in suspension cultures of Chinese hamster ovary (CHO) cells, RNA and protein synthesis must continue up to 1.87 hours and 0.60 hour, respectively, prior to division. To establish whether these time measurements pertained exclusively to CHO cells or, in fact, described the timing of synthesis of RNA and protein essential to cell division in other cell lines as well, the rate of cell division was determined in synchronized suspension cultures of L, HeLa, and hamster C-13 cells to which inhibitors of nucleic acid or protein synthesis were added at varying times after release from thymidine blockade. Comparisons were made among the cell lines of the latest times in the life cycle at which inhibitors could be added without subsequent division of the cell. In addition, correlations were made between these biochemical markers and the morphological beginnings of prophase.

#### METHODS

Actinomycin (2  $\mu\text{g}/\text{ml}$ ) or puromycin (50  $\mu\text{g}/\text{ml}$ ) was added to suspension cultures of cells [synchronized with 10 mM thymidine (1)] at varying times preceding the division wave to

inhibit the synthesis of either RNA or protein. The rates of cell division in the synchronized cultures were determined at hourly intervals with an electronic particle counter (2), and mitotic indices were determined by the method described elsewhere (3).

## RESULTS AND DISCUSSION

If there is a time in the life cycle preceding division at which all of the macromolecules essential for division have been synthesized, then cells past this point will divide even in the presence of inhibitors; cells at earlier stages of the life cycle will be prevented from dividing, since the inhibitor will prevent the synthesis of the entire complement of macromolecules essential for division. The time interval between addition of inhibitors (actinomycin or puromycin) and cessation of cell division then provides an estimate of the time in the life cycle preceding division up to which RNA or protein synthesis is required for cell division (i.e., only cells past effects of inhibitors continue to divide).

Table 1 summarizes the results obtained for four different cell lines. The time of action of actinomycin (end of essential RNA synthesis marker) is very similar among the four lines studied, although the generation times of HeLa and L cells are approximately twice as long as those of the hamster cell lines. The end of essential protein synthesis marker (obtained from puromycin experiments) shows a greater variation among the four cell lines. When this marker is compared to the duration of M [calculated from randomly growing suspension cultures by the formula  $N_m = e^{0.693 T_m/T_g - 1}$ , in which  $N_m$  is the mitotic index,  $T_m$  the duration of the mitotic period in hours, and  $T_g$  the generation time in hours (3)], one obtains fairly good agreement, suggesting that the last essential proteins are made shortly before the beginning of the mitotic period. Determination of the mitotic index in synchronized cultures showed that shortly after addition of puromycin the mitotic index dropped to zero, indicating that the drug did indeed prevent the synthesis of proteins required for formation of mitotic figures. Those cells which had reached prophase when the drug was added continued through mitosis and eventually divided.

In addition to the markers for end of essential RNA and protein synthesis, the interval between completion of synthesis of RNA and protein is another parameter of interest that can



TABLE 1. EFFECT OF ACTINOMYCIN (2  $\mu\text{g}/\text{ml}$ ) AND PUROMYCIN (50  $\mu\text{g}/\text{ml}$ ) ON THE DIVISION OF SYNCHRONIZED SUSPENSION CULTURES OF FOUR CELL LINES

Cell Line	Source	Time between Addition of Actinomycin and Cessation of Division (hours)	Time between Addition of Puromycin and Cessation of Division (hours)	Duration of Mitotic Period (hours)
CHO	Chinese hamster	1.70	0.55	0.71
C-13	Syrian hamster	1.83	1.06	0.56
HeLa <sup>*</sup>	Human	1.42	0.85	0.80
L	Mouse	1.61	1.21	1.16

<sup>\*</sup> Later shown to be infected with PPLO.

be derived from these data. The time difference between the two markers may represent the interval required for m-RNA transport from nucleus to ribosome plus assembly time of the complete protein; the difference ranges from 1.1 hours for CHO cells to 0.4 hour for L cells.

In future studies with synchronized cells, attempts will be made to characterize the proteins specified by m-RNA species synthesized during the pre-mitotic portion of the life cycle.

#### REFERENCES

- (1) D. F. Petersen and E. C. Anderson, Nature 203, 642 (1964).
- (2) H. Kubitschek, Nature 182, 234 (1958).
- (3) T. T. Puck, P. C. Sanders, and D. F. Petersen, Biophys. J. 4, 441 (1964).

**RNA SYNTHESIS IN CULTURED MAMMALIAN CELLS DURING THYMIDINE INHIBITION OF DNA SYNTHESIS AND DURING SYNCHRONOUS GROWTH FOLLOWING RELEASE (A. G. Saponara and M. D. Enger)**

**INTRODUCTION**

The addition of 10 mM thymidine to an exponentially growing culture of Chinese hamster ovary (CHO) cells causes an abrupt cessation of DNA synthesis. If the thymidine is removed after 0.7 of a generation time DNA synthesis resumes, and after an additional 0.55 of a generation time a synchronous division of cells is seen. A detailed examination suggests that during thymidine block cells are prevented from entering that portion of their cyclic growth phase during which DNA is made (S phase) but that cells which are distributed elsewhere in this growth cycle ( $G_1$ , M, and  $G_2$ ) proceed at a normal rate toward the point of block (1).

Preliminary data on the incorporation of  $^3\text{H}$ -uridine into RNA suggested that RNA synthesis decreased very abruptly to 5 percent of normal following the addition of a blocking concentration of thymidine. Sucrose-gradient zone-sedimentation analysis of the RNA made under these conditions showed that all species were affected to the same extent. A more extensive analysis of this apparent effect on RNA synthesis was considered of interest for a number of reasons. A compulsory prerequisite to an investigation of the synthetic capabilities of a synchronized culture is evidence that the synchronization procedure does not perturb the cell with respect to its macromolecular constitution. It is apparent that a continued deposition of the culture at this point of block in the absence of concomitant RNA synthesis would lead to a population with a two fold variance of RNA concentration. Furthermore, the ability of a cell to traverse three-quarters of its normal growth cycle in the apparent absence of RNA synthesis would be an occurrence of great theoretical interest. Thus, it was decided to investigate further the synthesis of RNA during thymidine block. The results of these studies and of preliminary studies on RNA synthesis in synchronized cultures of CHO cells are reported here.

**METHODS AND RESULTS**

A portion of a culture of CHO cells growing exponentially in

serum-supplemented Ham's F-10 medium was pulsed with either  $^3\text{H}$ -uridine for 1 hour or with  $^{32}\text{P}$ -phosphate for 30 minutes. Cells were harvested and analyzed for acid-soluble pool, RNA, DNA, and protein by a modified Schmidt-Thannhauser procedure. During random growth all of these substances showed a rate of accumulation, measured by absorbance at 260  $\mu$ , and a rate of incorporation of isotope which had the same doubling time as the cell population. Upon the addition of 10 mM thymidine, DNA accumulation stopped immediately (Fig. 1); However, RNA mass continued to increase at a steadily declining rate for 9 hours, after which time it remained constant. In contrast to this continued synthesis of RNA is the abrupt cessation of  $^3\text{H}$ -uridine incorporation following the introduction of thymidine (Fig. 2). Figure 3 shows that the reason for this anomaly is that  $^3\text{H}$ -uridine no longer enters the cell in the presence of thymidine. More recent experiments have shown that thymidine also prevents the entry of cytidine and adenosine. The rate at which cells will accumulate at the block point can be easily calculated. The theoretical curve plotted on Fig. 4 depicts the manner in which RNA could accumulate if cells which are in S at the time of thymidine introduction stop making RNA immediately and those which are distributed elsewhere continue to synthesize RNA only until they have accumulated at the S boundary. The calculation assumes that capacities for the synthesis of stable RNA are constant throughout this portion of the growth curve. Comparison of this curve with the experimental data shows that the time required for the total cessation of RNA accumulation is almost precisely the time required for the non-S segment of the population to accumulate at the S boundary.

Figure 4 also shows that  $^{32}\text{P}$ -phosphate incorporation into RNA is not inhibited by thymidine as are uridine, cytidine, and adenosine. The fact that  $^{32}\text{P}$  incorporation does not follow its theoretical curve is a graphic demonstration of RNA turnover. Experiments are currently in progress to elucidate the nature of these unstable RNA's which continue to turn over in late thymidine block. It is interesting to note that a major fraction of the thymidine-blocked population will remain viable for at least a week (2). The rapidly turning-over fraction of RNA may be instrumental in maintaining the cells in a viable state. No extensive studies have as yet been made on protein synthesis in this thymidine-blocked state. Preliminary data suggest that protein accumulation proceeds for at least as long as does RNA accumulation and probably longer.

The course of events following release from thymidine block

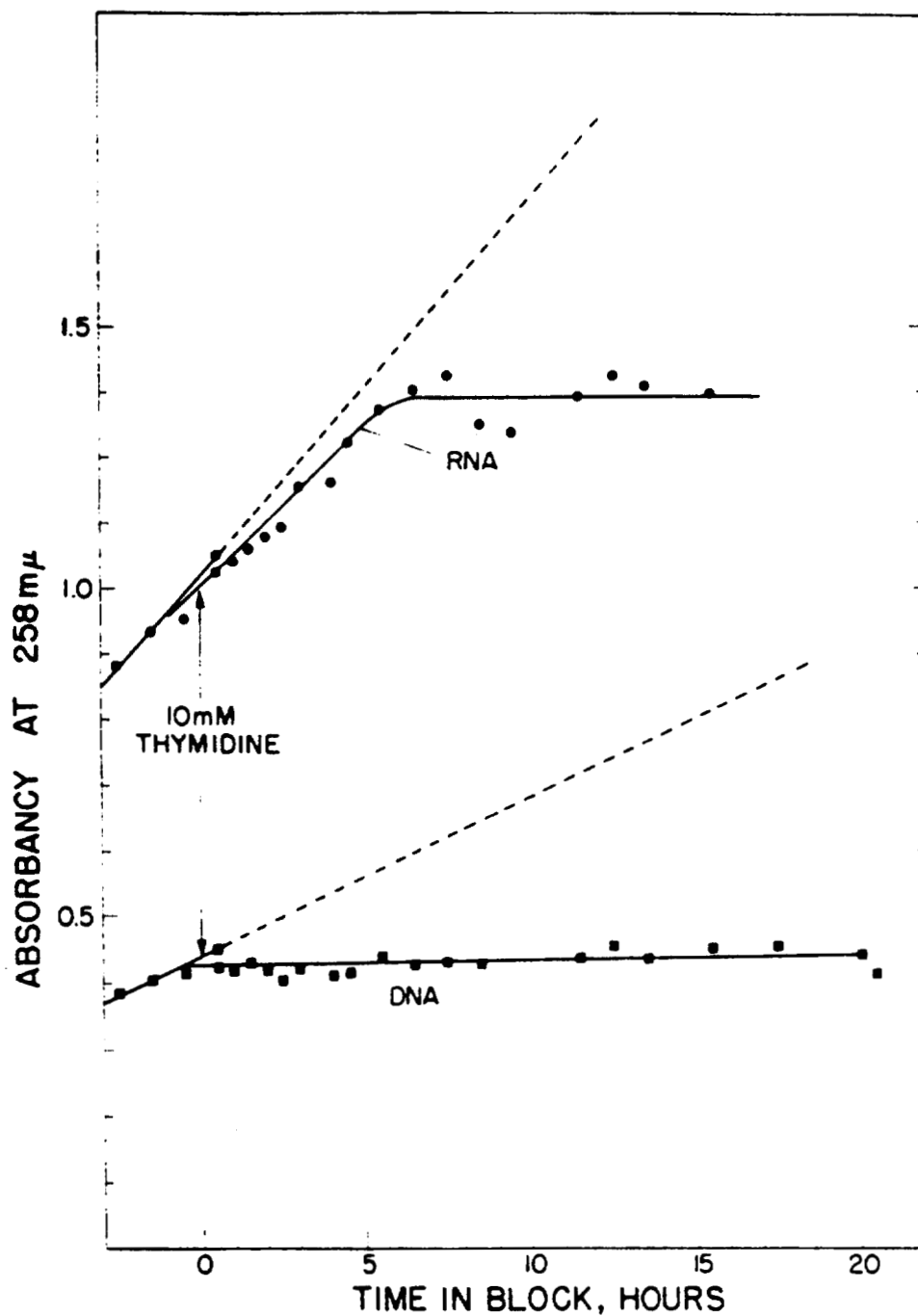


Fig. 1. Comparison of the accumulation of RNA and DNA after the addition of 10 mM thymidine. The decrease in RNA after 17 hours in block is an artifact caused by the destruction of some cells due to frothing as the volume of the suspension becomes too low.

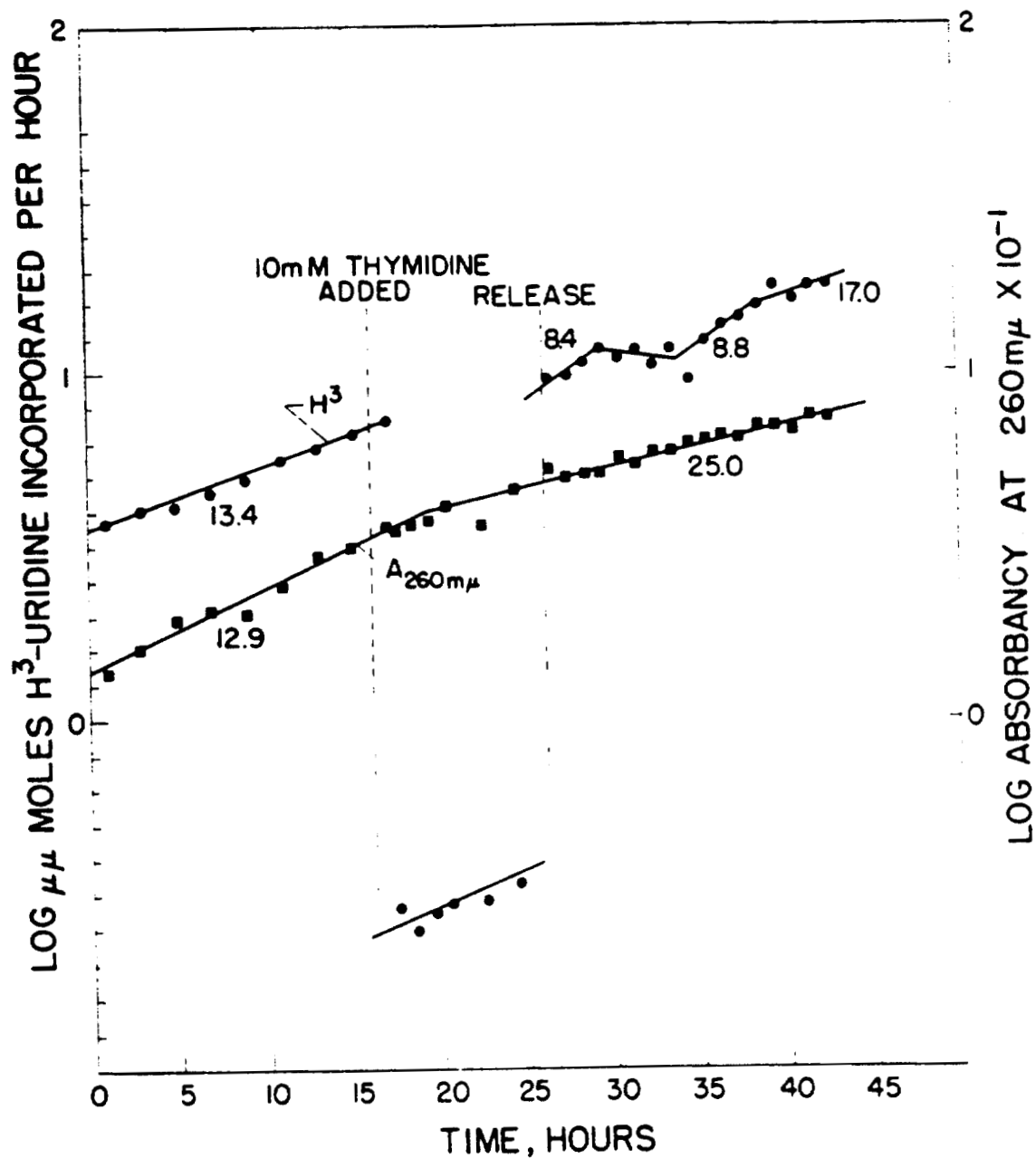


Fig. 2. Accumulation of RNA mass and <sup>3</sup>H-uridine label during random growth, thymidine block, and release.

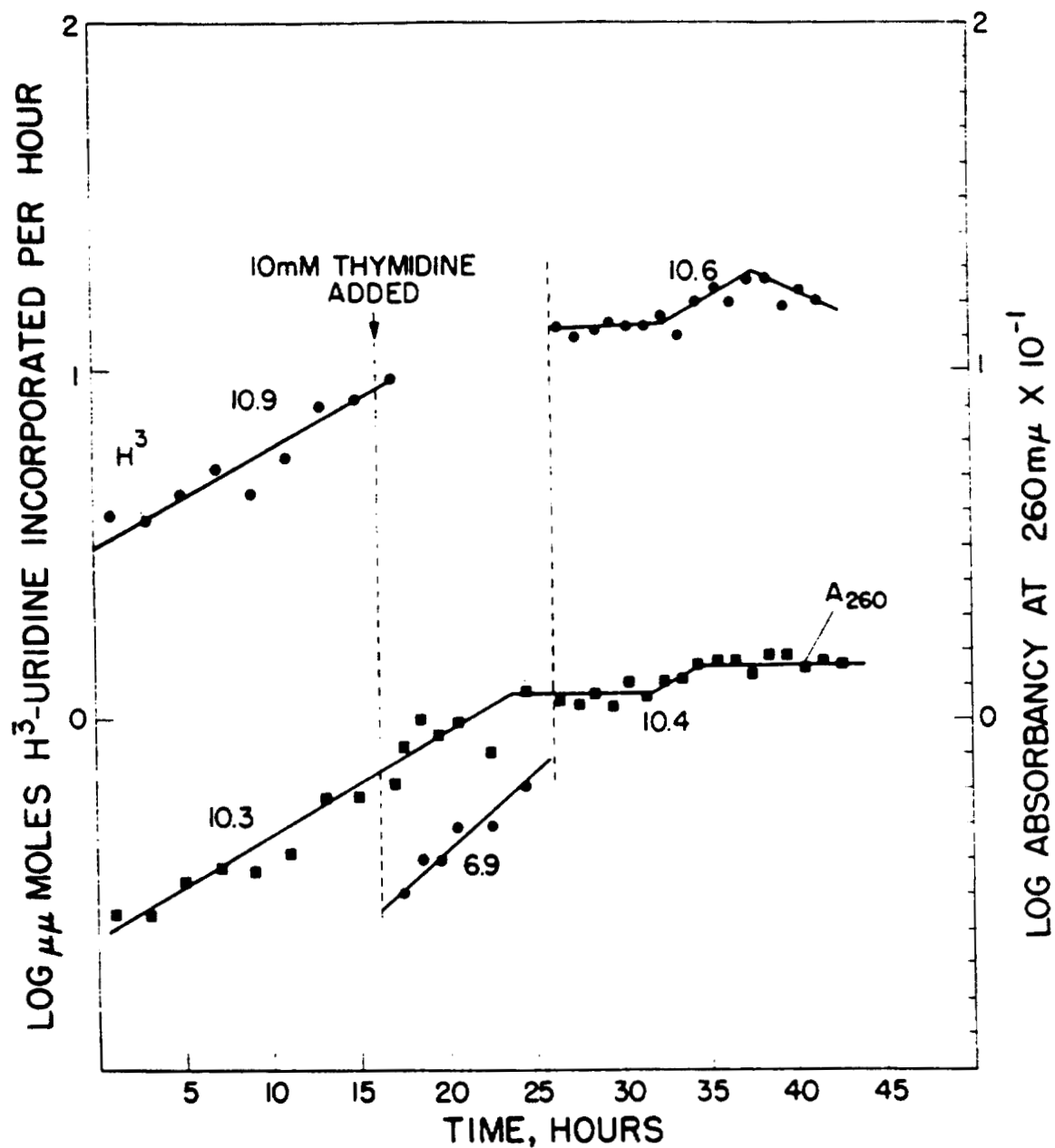


Fig. 3. Accumulation of acid-soluble mass and rate of  $^3\text{H}$ -uridine incorporation during random growth, thymidine block, and release.

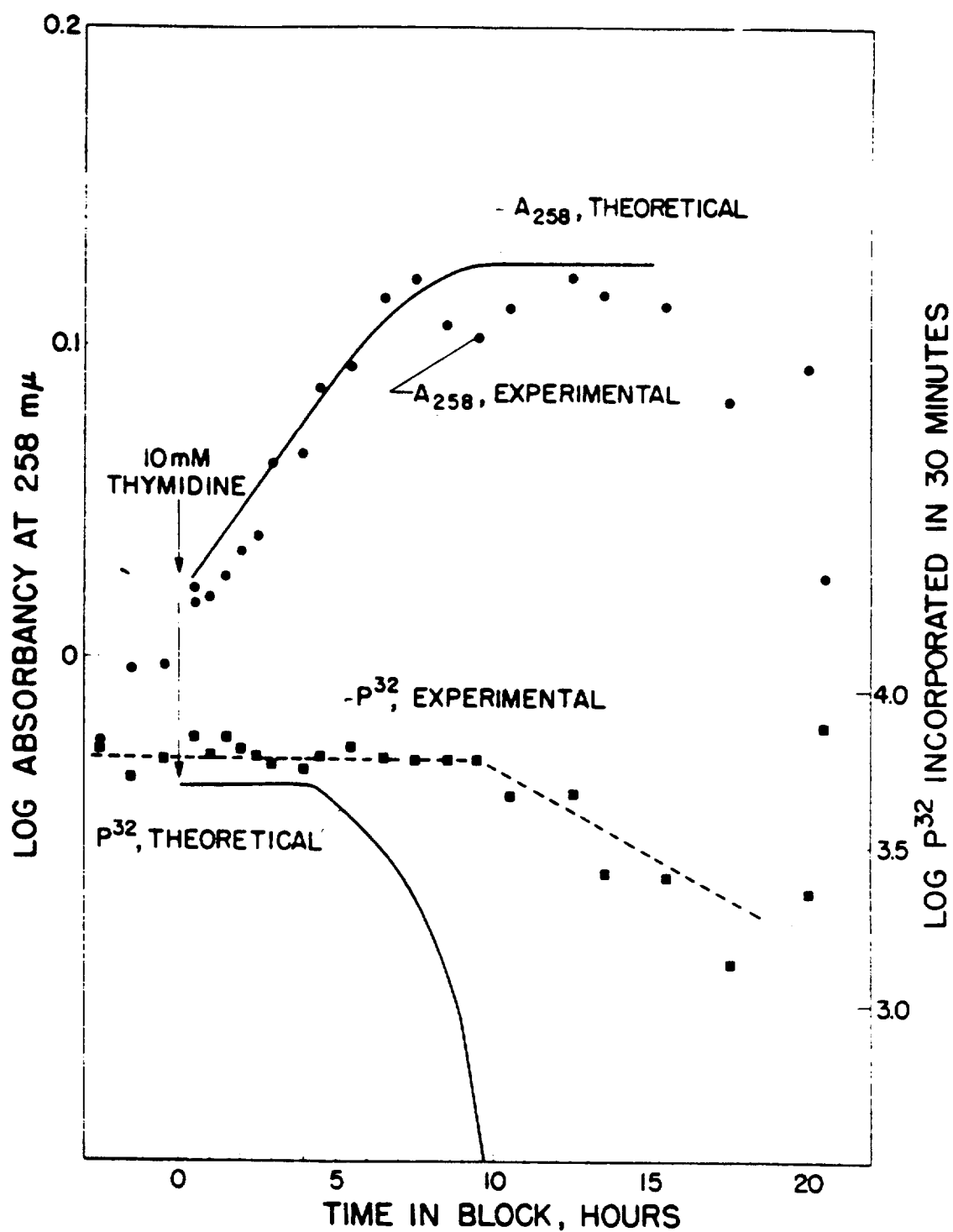


Fig. 4. Accumulation of RNA and rate of incorporation of  $^{32}\text{P}$ -phosphate into RNA during extended thymidine block.



is depicted in Fig. 5. The synchrony in this particular experiment is not as good as others we have obtained by this method. Occasional lapses in the quality of synchrony obtained could possibly result from erratic changes in generation times of the cultures, resulting in a block time of insufficient duration. The rate of incorporation of label into RNA shows the decrease centered around the mitotic period, which has been reported for a variety of other synchronized cell populations.

At various times after release, chosen to include as large a fraction of the population as possible in S, G<sub>1</sub>, or G<sub>2</sub>, cells have been pulse-labeled with <sup>3</sup>H-uridine, and RNA samples obtained by a phenol-SDS-bentonite extraction procedure have been analyzed by sucrose-gradient zone centrifugation. It was found that 40-50S RNA, which is largely pre-ribosomal RNA (3), is synthesized 1.3 times as rapidly during G<sub>2</sub> as during G<sub>1</sub> or S when the synthesis is expressed as rate of <sup>3</sup>H incorporated relative to the mass of RNA present at the end of exposure to label. These data indicate that ribosomal RNA is not synthesized at a constant rate per cell. It is possible, however, that the rate of r-RNA increases as the cells cross S (that is, the rate may be template-limited). Further experiments will be performed to determine the dependence of RNA synthesis rate on life cycle phase.

#### REFERENCES

- (1) D. F. Petersen and E. C. Anderson, *Nature* 203, 642 (1964).
- (2) R. A. Tobey, personal communication.
- (3) K. Scherrer, H. Latham, and J. E. Darnell, *Proc. Natl. Acad. Sci. U. S.* 49, 240 (1963).

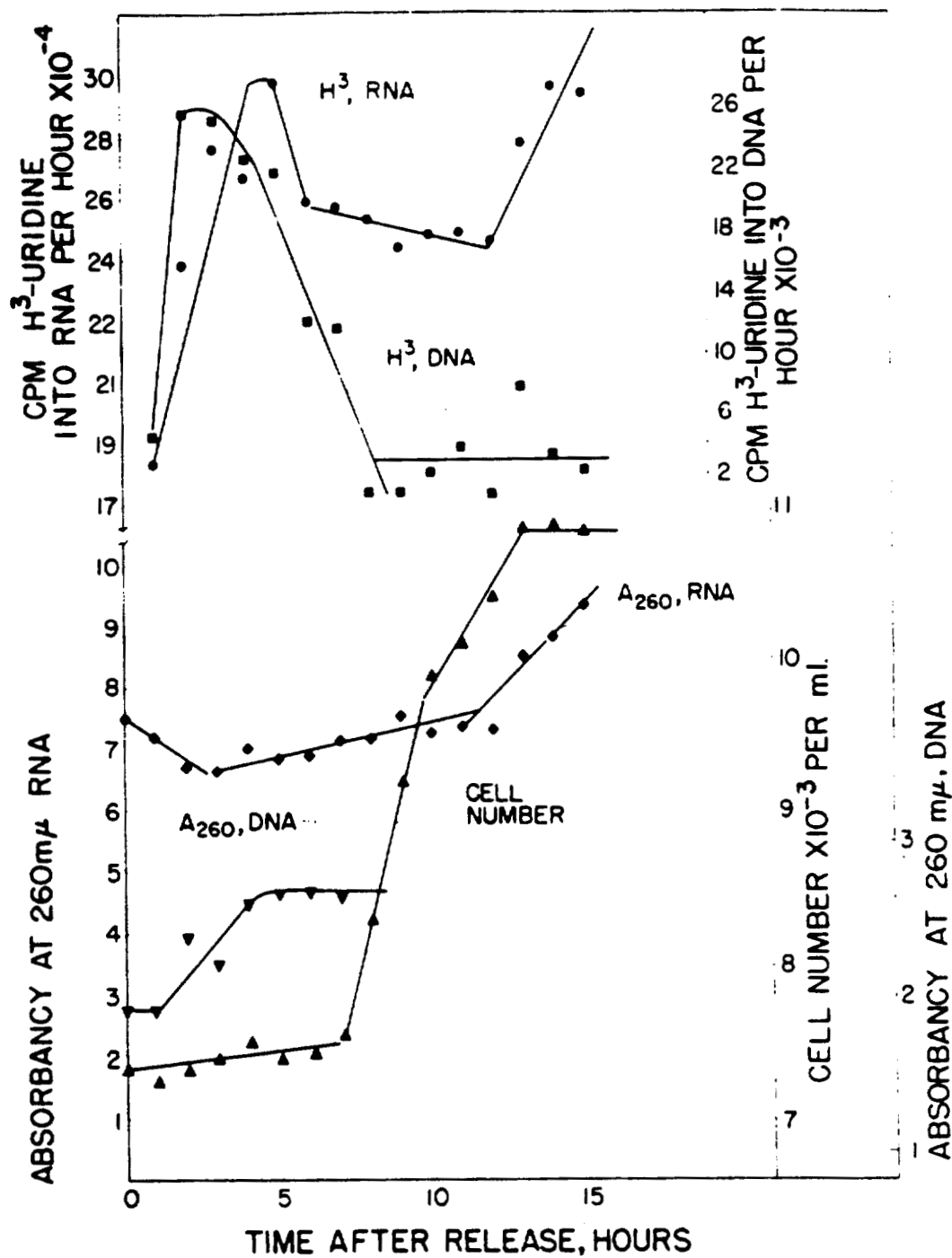


Fig. 5. Rates of incorporation of  $^3\text{H}$ -uridine into RNA and DNA and accumulation of RNA and DNA during synchronous growth.

# THE ENERGY METABOLISM OF CULTURED MAMMALIAN CELLS. I. THE INCORPORATION OF ORTHOPHOSPHATE (C. T. Gregg)

## INTRODUCTION

Although cultured cells represent the simplest type of intact mammalian organism, their energy metabolism has been little studied. Since this process consists largely of the synthesis and utilization of "high energy" phosphate bonds, the metabolism of inorganic phosphate by Chinese hamster ovary (CHO) cells is being investigated, both in randomly growing cells and in cells induced into synchronous growth by the thymidine block technique (1).

The cumulative incorporation of phosphorus-32 into acid-soluble phosphate (intracellular inorganic phosphate and nucleotide mono-, di-, and triphosphates) and into lipid phosphate, DNA, RNA, and phosphoprotein was studied, as well as the incorporation of radioactivity into the various fractions, when either randomly or synchronously growing cells were exposed to labeled phosphate for periods from 5 to 80 minutes. The content of organic and inorganic phosphate in the various fractions from CHO cells was also determined.

## METHODS

Cells were incubated in the presence of phosphorus-32. Aliquots of the cell suspension were withdrawn at various times, chilled, washed to remove labeled medium, and quickly frozen. The several phosphate-containing fractions were subsequently extracted from the cells by a modified Schmidt-Thannhauser method (2). Total incorporation was determined on an aliquot of whole cells hydrolyzed with magnesium nitrate and hydrochloric acid. Recoveries of radioactivity were, in general, above 90 percent.

## RESULTS

### Phosphorus Distribution in Chinese Hamster Ovary Cells

Table 1 shows the amount of phosphorus found in each class

**TABLE 1. DISTRIBUTION OF ORGANIC AND INORGANIC PHOSPHATE  
AMONG THE VARIOUS PHOSPHATE-CONTAINING FRACTIONS  
OF CHINESE HAMSTER OVARY CELLS**

Fraction	Percent of Total	
	Organic Phosphate	Inorganic Phosphate
Acid-soluble	24.3	52.2
Lipid phosphate	25.7	0.0
Ribonucleic acid	40.0	20.5
Deoxyribonucleic acid	10.8	25.7
Phosphoprotein	0.8	1.6

of compounds in CHO cells. The percentages indicated were obtained on the basis of analysis for both inorganic and total phosphorus and on the recovery of labeled phosphorus in each fraction from cells grown for several generations in radioactive medium.

#### Time-Course Studies

In Fig. 1 is presented a time-course of incorporation of phosphorus-32 into RNA, lipid phosphate, and DNA by a synchronously growing culture. The pre-mitotic period is marked by rapid incorporation of label into both RNA and lipid phosphate. At the onset of the mitotic wave (the duration of which is indicated by "M," above the time axis), the rate of incorporation into both fractions slows, abruptly in the case of RNA and somewhat less dramatically for the lipid phosphate fraction. DNA is initially rapidly labeled. There is a subsequent slow (and possibly not significant) loss of activity in this fraction until the appearance, about the middle of the mitotic period, of cells which have become asynchronous. This leads to a gradually increasing incorporation of label into DNA. In this experiment the cells were essentially in completely random growth by the end of the mitotic wave, or shortly thereafter.

The results shown in Fig. 1 are distinctly different from those obtained in similar studies on randomly growing cells in which each fraction incorporates activity exponentially with time. The kinetics of labeling of the acid-soluble fraction likewise differs in the two types of cultures. In both randomly growing and synchronously growing cells, the acid-soluble fraction accounts for 75 to 85 percent of the total activity incorporated 1 hour after addition of phosphorus-32. In randomly growing cells the activity of this fraction falls smoothly, reaching about 35 percent of the total incorporated activity after one generation time. In the synchronously growing cells, however, the activity of this fraction falls slowly until early in the G<sub>2</sub> phase of growth, then drops more steeply during that period in which the activities of the RNA and lipid phosphate fractions are rising. At the beginning of the mitotic period the activity of the acid-soluble fraction shifts again to a slower rate of decline.

It is important to note that, as indicated in Table 1, all fractions (except the lipid phosphate fraction) contain appreciable P<sub>i</sub> which may contribute substantially to the observed

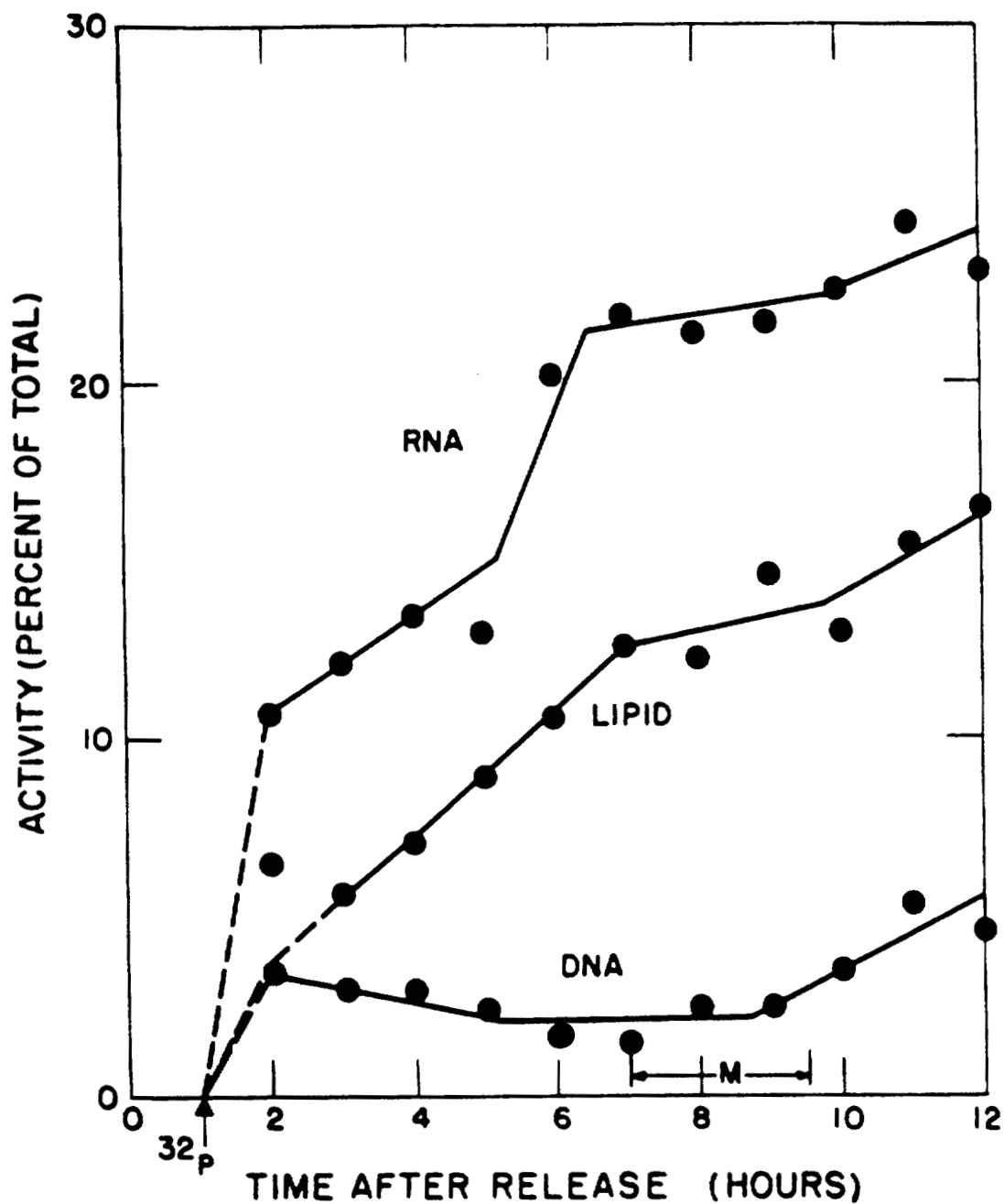


Fig. 1. Time-course of incorporation of phosphorus-32 into RNA, DNA, and lipid phosphate by synchronously growing CHO cells (phosphorus-32 added as indicated, 1 hour after release from thymidine block).

activity. In the randomly growing cultures, for example, the acid-soluble fraction is approximately 80 percent  $P_i$  1 hour after addition of phosphorus-32. After one generation time in the labeled medium, the acid-soluble fraction is only 34 percent orthophosphate. Comparable data on the synchronously growing cells are not yet available.

### Pulse Experiments

Two types of pulse experiments have been carried out. In the first, phosphorus-32 was administered to aliquots of synchronously growing cells for seven 30-minute periods spaced around the cell cycle. The rates of incorporation at the various points were consistent with the experiment described above. The most striking observation was the fact that, following a 30-minute pulse, all of the activity incorporated by the CHO cells was accounted for as acid-soluble phosphate and lipid phosphate. Within experimental error, no activity was incorporated into RNA, DNA, or phosphoprotein at any point in the cycle. The amount of activity contributed to the total by the lipid phosphate fraction ranged from a high of 38 percent, observed shortly after release, to a low of 5 percent, observed after the cells had reverted to random growth. Thus the imposition of synchronous growth by the thymidine block technique led to a 6 fold increase in the proportion of label incorporated per cell into phospholipid. Since perhaps 90 percent of the total incorporation into the acid-soluble fraction after 30 minutes represents  $P_i$ , it is clear that, just following release, total incorporation of radioactivity from the intracellular orthophosphate pool into the lipid phosphate fraction may take place at a rate comparable to that of the incorporation into the nucleotide phosphates of the acid-soluble fraction.

In the second kind of pulse experiment, randomly growing cells were exposed to phosphorus-32 and aliquots taken at 5, 10, 20, 40, and 80 minutes after addition of the labeled compound. Under the conditions of these experiments the cells incorporated label at a linear rate throughout the 80-minute period. Incorporation into the acid-soluble fraction was also linear for at least 40 minutes. The acid-soluble fraction accounted for 80 to 90 percent of the total activity incorporated throughout the experimental period. In dramatic contrast to the results obtained with the synchronously growing cell population, the incorporation into lipid phosphate never amounted to more than 3 percent of the total activity and was

1 percent or less after 20 minutes of incubation. Incorporation into RNA accounted for the bulk of incorporation other than the acid-soluble fraction. The RNA and acid-soluble fractions accounted for 96 to 98 percent of the total activity incorporated. An identical experiment was carried out on synchronously growing cells with pulses being applied in the middle of  $G_2$ , M, and  $G_1$ ; the results of this experiment are not yet available.

## DISCUSSION

It is clear that the transition from random to synchronous growth leads to a profound alteration of the phosphate metabolism of CHO cells. The monotonic incorporation of  $P_i$  into the various fractions, seen in randomly growing cells, is replaced, in the synchronously growing cells, by sharply discontinuous accumulation into the phosphate constituents. The proportion of the total incorporated activity found in the lipid phosphate fraction as the synchronously growing cells are released from thymidine block is 6 times higher than is found in randomly growing cells. Likewise, RNA phosphate accounts for a much larger proportion of the total activity in synchronously growing cells than in cells in random growth.

Work currently in progress concerns the preparation of RNA, DNA, and acid-soluble organic phosphate free from contaminating  $P_i$  and a study of the kinetics of labeling of the individual components of the organic portion of the acid-soluble fraction. Other aspects of the energy metabolism of CHO cells are discussed elsewhere in this report (3,4).

## REFERENCES

- (1) D. F. Petersen and E. C. Anderson, *Nature* 203, 642 (1964).
- (2) G. Schmidt and S. J. Thannhauser, *J. Biol. Chem.* 161, 293 (1945).
- (3) C. T. Gregg, this report, p. 148.
- (4) W. D. Currie and C. T. Gregg, this report, p. 153.



**THE ENERGY METABOLISM OF CULTURED MAMMALIAN CELLS. II.  
NATURE OF THE PHOSPHOLIPID FRACTION (C. T. Gregg)**

**INTRODUCTION**

Upon release from thymidine block, Chinese hamster ovary (CHO) cells rapidly incorporate orthophosphate into lipid phosphate prior to the beginning of the mitotic wave, as discussed in the preceding report. Phospholipid labeling also accounts for an important fraction of the radioactivity incorporated by randomly growing cells exposed briefly to labeled orthophosphate. In this report the nature of the phospholipid fraction of CHO cells is discussed.

**METHODS**

The phospholipid extracts (1) were concentrated by evaporation of the solvent under a stream of nitrogen. Aliquots were taken for scintillation counting and total phosphate analysis. Small volumes of the extracts were separated into their constituents by thin layer chromatography on silica gel G. The most frequently used solvent was chloroform, methanol, water, ammonium hydroxide (20:16:1:1, v/v). Spots were located by autoradiography, by exposure to iodine vapor or various specific spray reagents, or by charring with dichromate sulfuric acid. Identification of the components of the mixed extract was made by specific staining reactions for various phospholipid moieties (2) and by cochromatography of the labeled compounds extracted from CHO cells with authentic phospholipid standards.

**RESULTS**

Autoradiographs made from thin layer chromatograms of the labeled phospholipid extracted from CHO cells showed 7 clearly separated major components. These were eluted and rechromatographed in the same solvent to determine the degree of cross contamination. Rechromatography showed only 7 constituents, of which 3 account for the bulk of the incorporation of radioactivity into this fraction.

The slowest running component, compound A ( $R_f$  0.059), gave a

positive reaction with ammoniacal  $\text{AgNO}_3$ , indicating the presence of inositol or glycerol. The radioactive spot corresponding to A was eluted and rechromatographed with authentic monophosphatidyl inositol. The radioactivity of compound A coincided with the location of the standard monophosphatidyl inositol on the chromatogram. On the basis of these findings, it is tentatively concluded that compound A is monophosphatidyl inositol; the presence of small amounts of di- and triphosphoinositides cannot be ruled out.

Compound B ( $R_f$  0.183) gave a positive reaction with ninhydrin, indicating the presence of either serine or ethanolamine. Compound B cochromatographs with authentic phosphatidyl serine.

Compound C ( $R_f$  0.308) is similarly identified, provisionally, as lysophosphatidyl choline on the basis of a positive reaction with Dragendorff's reagent, indicating the presence of choline as phosphatidyl choline, lysophosphatidyl choline, or sphingomyelin. Compound C cochromatographs with purified lysophosphatidyl choline but not with sphingomyelin or phosphatidyl choline.

Compound D ( $R_f$  0.425) also reacts with Dragendorff's reagent. It cochromatographs with a phosphatidyl choline standard.

Compound E ( $R_f$  0.525) likewise reacts with ninhydrin and cochromatographs with purified phosphatidyl ethanolamine.

Compound F ( $R_f$  0.684) remains unidentified. It may be a lysophosphatidic acid.

Compound G ( $R_f$  0.825) is tentatively identified as phosphatidic acid on the basis of its  $R_f$  value.

Further evidence for the identity of the various fractions awaits thin layer chromatography of the acid hydrolysis products.

The labeling of the phosphate moiety of the major phospholipids in synchronously dividing cells was also investigated. In a preliminary experiment with synchronously dividing cells, the time-course of labeling of fractions A, B, C, and D was followed (Fig. 1). Following an initial period when all four fractions have about the same total activity, fraction D exhibits an abrupt increase in activity just prior to mitosis. The activity of this fraction then remains at the higher level. Fraction C behaves similarly except that the rise in

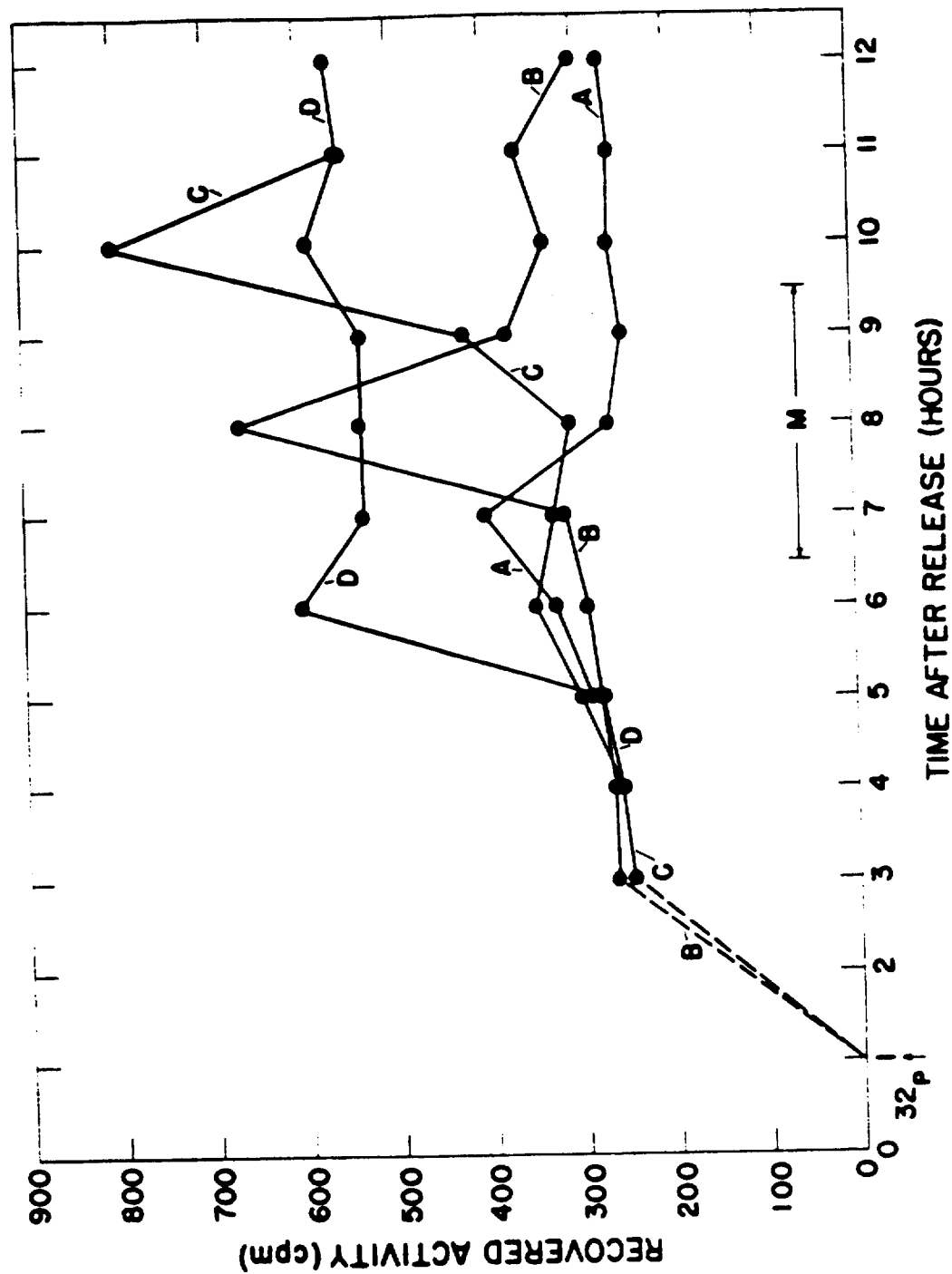


Fig. 1. Time-course of labeling of the major phospholipid constituents by synchronously dividing CHO cells. The region indicated by M corresponds to period of cell division in this experiment. Labeled orthophosphate is added at 1 hour after release from the thymidine block.

activity occurs late in the mitotic period. This result suggests a sudden rise in the activity of phospholipase A (which converts phosphatides to lysophosphatides) beginning about the middle of the mitotic wave. Compounds A and B remain at essentially constant activity following the initial period of rapid labeling, although both compounds show transitory peaks of activity which appear too well defined to be artifacts, especially in the case of compound B.

### DISCUSSION

Phospholipids are largely associated with biological membranes, particularly those of the endoplasmic reticulum and mitochondria. In addition to a structural role, they have been implicated by various investigators in the process of amino acid transport, ion transport, and protein synthesis. The phosphate moiety of these compounds is rapidly labeled by both randomly growing and synchronously dividing CHO cells.

From the preliminary data reported here some inferences can be drawn concerning the biosynthesis of these molecules, although more detailed studies will clearly be required to permit definite conclusions. That phospholipase A activity increases sharply during the mitotic period seems clear. Whether the increase in lysophosphatidyl choline which results actually occurs in the intact cells or results from the activation of the enzyme during extraction remains to be seen. Phosphatidyl choline (compound D) may serve as a precursor of phosphatidyl serine (compound A) in these cells via the process of base exchange, but the reverse reaction does not seem to be significant. Likewise, phosphatidyl choline clearly does not arise from phosphatidyl ethanolamine via methylation; the incorporation of activity into the latter (compound E) is far too low, but the converse reaction (the demethylation of phosphatidyl choline) may take place.

In the next phase of this investigation larger amounts of the various phospholipid constituents will be isolated. This will permit carrying out acid hydrolysis to complete the identification of these compounds and also the determination of the proportions of each compound in the total lipid phosphate fraction.

Further studies of the time-course of labeling of the various

compounds by both randomly and synchronously growing cells, as well as of the biosynthesis of the non-phosphate moieties, are in progress.

#### REFERENCES

- (1) C. T. Gregg, this report, p. 142.
- (2) W. D. Skidmore and C. Enteman, J. Lipid Research 3, 471 (1962).

**THE ENERGY METABOLISM OF CULTURED MAMMALIAN CELLS. III.  
RESPIRATORY PROPERTIES OF CHINESE HAMSTER OVARY CELLS (W. D.  
Currie and C. T. Gregg)**

**INTRODUCTION**

The rate of respiration during each phase of the cell cycle in cultured mammalian cells was investigated. Measurements of respiratory activity have been made on Chinese hamster ovary (CHO) cells induced into synchronous growth by thymidine block (1). The effects of inhibitors of respiration and oxidative phosphorylation on respiratory activity and on cell division were also investigated.

**METHODS**

Cell growth (1), isolation (2), and the measurement of respiration (3) of washed cells from a randomly growing culture were carried out as described earlier. Measurements of respiration in randomly and synchronously growing populations, carried out while cells were in suspension culture, were made by inserting a sterile Clark oxygen electrode into a specially constructed spinner flask and continuously monitoring the oxygen consumption within the closed vessel. The output of the electrode was amplified by an extensively modified version of the transistorized amplifier described by Severinghaus and Bradley (4). Titration of the respiratory activity of CHO cells was performed with microliter quantities of solutions of the various inhibitors. Effects on cell division in randomly and synchronously growing cultures were followed by electronic cell counting (5).

**RESULTS AND DISCUSSION**

Following release from the thymidine block, respiration proceeded rapidly prior to mitosis but declined sharply or stopped completely during cell division. Rapid incorporation of orthophosphate into acid-soluble and lipid phosphate (6) accompanies the rise in respiratory activity; the rate of incorporation into these fractions likewise fell during cell division. These results were in marked contrast to those obtained with randomly growing cells in which the

rates of oxygen utilization and phosphorus uptake per cell remained essentially constant. It was found that the endogenous respiration of cells from a randomly growing culture was completely inhibited by low concentrations of oligomycin, rotenone, Amytal, antimycin A, and cyanide. Studies on randomly and synchronously growing cells indicated that these inhibitors are also capable of slowing or completely inhibiting cell division. Fifty and 100 percent inhibition of respiration occurred at very low inhibitor concentrations (Table 1), comparable to values obtained with mammalian mitochondria. Completion of extensive titration studies on CHO cells with respiratory inhibitors confirmed and extended the results and conclusions of the previous report (2). A more extensive account of the inhibition of respiration by oligomycin is presented elsewhere (7).

Figure 1 shows the results of a representative experiment in which the effect of rotenone at three concentrations was tested on cell division in a culture of synchronously growing CHO cells. The respiratory inhibitor was added, as indicated, at release of the cells from thymidine block. Higher concentrations of rotenone delayed cell division for a longer period, and at appropriate concentrations completely inhibited mitosis. This suggests that other pathways of adenosine triphosphate formation require a longer time to supply the necessary quantity of energy to the cell when terminal electron transport is inhibited. Alternatively, detoxification of the inhibitors may play a role in this phenomenon. Similar results were obtained with oligomycin and antimycin A in randomly growing and synchronously dividing cultures. The uncouplers, 2,4-dinitrophenol and m-chlorocyanocarbonylphenylhydrazine, were also capable of slowing or stopping cell division.

Thus, the importance of respiration to cell growth and division has been demonstrated. Our preliminary data indicate that a continuous supply of energy is required throughout the life cycle. The "reservoir" theory (8), which states that the energy necessary for cell division is generated well before the mitotic period, is inconsistent with our observations, which instead support the more recent findings of Epel (9). Experiments involving addition of respiratory inhibitors to CHO cells during each phase of the cell cycle are underway and should further clarify the significance of respiration to cell division.

TABLE 1. INHIBITION OF THE ENDOGENOUS RESPIRATION OF CHO  
CELLS BY VARIOUS RESPIRATORY INHIBITORS

Inhibitor	Effective Concentration ( <u>M</u> )	
	50 Percent Inhibition	100 Percent Inhibition
Rotenone	$6.1 \times 10^{-9}$	$1.2 \times 10^{-8}$
Antimycin A	$1.3 \times 10^{-8}$	$2.7 \times 10^{-8}$
Oligomycin	$1.1 \times 10^{-7}$	$2.3 \times 10^{-7}$
Sodium cyanide	$2.5 \times 10^{-5}$	$1.0 \times 10^{-4}$
Amytal	$7.0 \times 10^{-4}$	$1.4 \times 10^{-3}$
Iodoacetate	$1.6 \times 10^{-3}$	$3.2 \times 10^{-3}$
Sodium fluoride	$9.3 \times 10^{-2}$	$1.8 \times 10^{-1}$



# EFFECT OF ROTENONE ON CELL DIVISION IN SYNCHRONOUSLY GROWING CHO CELLS

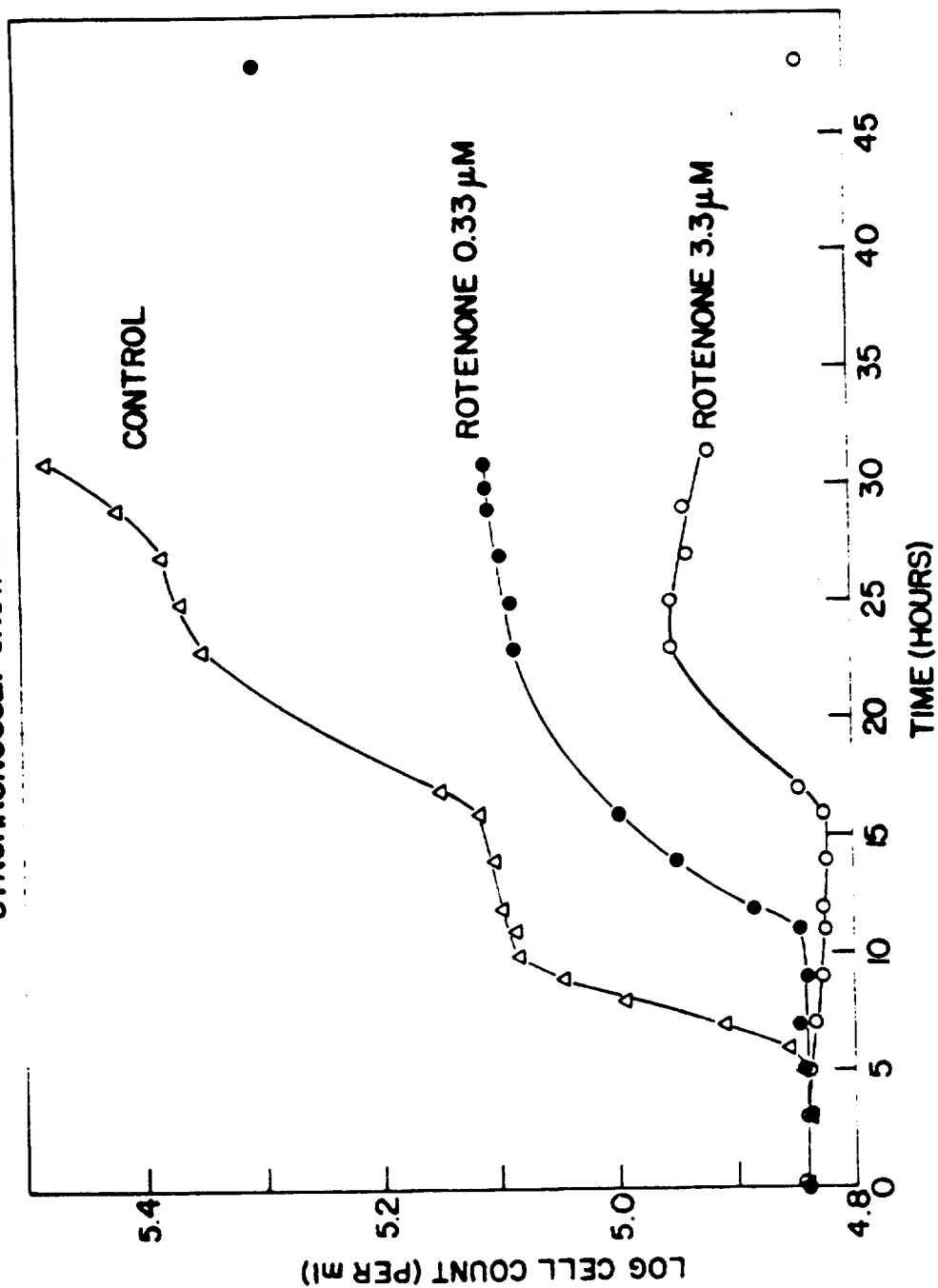


Fig. 1. Effect of increasing concentrations of rotenone on synchronously growing CHO cells.

#### REFERENCES

- (1) D. F. Petersen and E. C. Anderson, *Nature* 203, 642 (1964).
- (2) C. T. Gregg, Los Alamos Scientific Laboratory Report LA-3132-MS (1964), p. 224.
- (3) C. T. Gregg, *Biochim. Biophys. Acta* 74, 573 (1963).
- (4) J. W. Severinghaus and A. F. Bradley, *J. Appl. Physiol.* 13, 515 (1958).
- (5) E. C. Anderson and D. F. Petersen, *Exp. Cell Res.* 36, 423 (1964).
- (6) C. T. Gregg, this report, p. 142.
- (7) W. D. Currie and C. T. Gregg, submitted to *Biochem. Biophys. Res. Commun.*
- (8) M. M. Swann, *Cancer Res.* 17, 727 (1957).
- (9) D. Epel, *J. Cell Biol.* 17, 315 (1963).

# ISOLATION OF NUCLEI FROM CHINESE HAMSTER OVARY AND MOUSE LYMPHOMA L-5178Y CELLS IN TISSUE CULTURE (E. A. Hyatt)

## INTRODUCTION

In order to study the enzymatic activities of the nuclei of tissue culture cells, it has been necessary to devise techniques for isolating nuclei as free of cytoplasmic contamination as possible. The methods as presently employed are described below. They appear to be adequate for qualitative characterization of some, though perhaps not all, of the nuclear enzymes of immediate interest. Further refinements may be necessary before quantitative estimation of enzymatic activity can be made.

## METHODS AND RESULTS

The method described by Hymer and Kuff (1) was employed initially in attempting to isolate nuclei from Chinese hamster ovary (CHO) cells. In this method nuclei are prepared from liver or kidney cells by simply washing nuclei released by homogenization of the tissue with 0.25 M sucrose containing 0.001 M  $MgCl_2$  and 0.5 percent Triton X-100. This detergent effectively solubilizes the cytoplasmic elements present without disrupting the nuclear membrane.

CHO cells could not be disrupted by homogenization without disrupting nuclei as well. Treatment of homogenates with Triton X-100 failed to produce clean nuclei or nuclear suspensions free of cytoplasmic debris. After several modifications of the procedure, very clean nuclei were obtained from these cells (Fig. 1). Cells were removed from a 1-liter culture (approximately 400,000 cells/ml) by centrifugation for 5 minutes at 1500 RPM and washed once in an equal volume of cold 0.25 M sucrose containing 0.001 M  $MgCl_2$ . The cells were resuspended in 20 ml of 0.2 M phosphate buffer at pH 7.0 containing 0.1 percent Triton X-100. Suspension in the dilute phosphate buffer causes the cells to swell and increases their fragility to such an extent that rapid freezing (ethanol, Dry Ice) followed by thawing in a water bath or at room temperature releases the nuclei from the cells. When this is done in the presence of Triton X-100, the cytoplasmic components do not adhere to the nuclei. The phosphate buffer step appears at present to be essential when



Fig. 1. Nuclei from CHO cells, isolated as described in the text (magnification 650 X).

nuclei from CHO cells are required; however, it is undesirable in that it is probable that some soluble nuclear components are lost. In order to minimize this loss, the time of exposure to buffer is kept as short as possible; immediately after the frozen preparation has thawed, 250 ml of cold 0.25 M sucrose, 0.001 M  $MgCl_2$ , are added, and the nuclei are sedimented by centrifugation for 4 minutes at 1500 RPM, resuspended in a small volume of 0.25 M sucrose, 0.001 M  $MgCl_2$ , for storage in Dry Ice. These nuclei are free of debris, but a further purification step may prove necessary.

In contrast to CHO cells, mouse lymphoma cells are easily disrupted by simply washing them once in 0.25 M sucrose, 0.001 M  $MgCl_2$ , and resuspending them in the same medium containing 0.1 percent Triton X-100 (Fig. 2).

The efficiency of recovery of nuclei using these techniques was about 25 percent.

As suggested by Hymer and Kuff (1), this method might be adapted to isolation of mitotic figures from dividing cells. Cultures of mouse lymphoma cells were treated with colcemide (0.25  $\mu g/ml$ ) for 7 hours and then exposed to 0.1 percent Triton X-100 in 0.25 M sucrose, 0.001 M  $MgCl_2$ . The

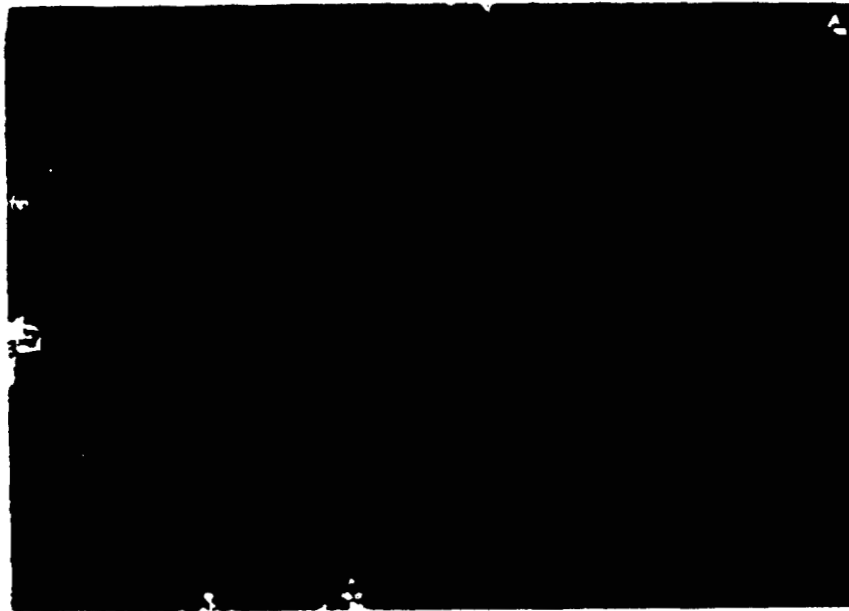


Fig. 2. Mouse lymphoma cell nuclei, isolated as described in the text (magnification 650 X).



Fig. 3. Colcemide-blocked mouse lymphoma cells, treated as described in the text (magnification 520 X).

resulting preparation, shown in Fig. 3, contained a large number of free mitotic figures which are apparently stable in the presence of this detergent. Separation of nuclei from mitotic figures has not been achieved.

## DISCUSSION

While descriptive data on the enzymatic activities of nuclei from these tissue culture cells are of general biochemical interest, quantitative data on changes in activity during the course of the division cycle of such cells, if they occur, would be of particular biological interest. This kind of information can only be obtained from clean nuclei, from which soluble enzymes have not been removed during isolation. In addition, the nuclei must be isolated from synchronized cell cultures. At present the mouse lymphoma cells have not been grown in synchronized culture or these would be the cells of choice for study of enzymatic changes during the life cycle, since nuclei can be isolated without exposure to dilute buffers.

Reliable methods for electronic counting of nuclei and estimating the degree of contamination of nuclear preparations with debris are being developed. Effects of variation in the isolation procedures on nuclear volume are being examined in order to establish conditions which cause the least alteration in this parameter.

## REFERENCE

- (1) W. G. Hymer and E. L. Kuff, J. Histochem. Cytochem. 12, 359 (1964).

# SYNTHESIS OF NUCLEIC ACIDS BY NUCLEI FROM CHINESE HAMSTER OVARY AND MOUSE LYMPHOMA (L-5178Y) CELLS (E. A. Hyatt)

## INTRODUCTION

The primary objective of this study is to determine specific activities of RNA polymerase, DNA polymerase, and ATP polymerase in nuclei from synchronously growing tissue culture cells. These enzymes, involved in polymerization of nucleic acid precursors, are of particular interest since these would appear, at least superficially, to be those most likely to vary in activity during the life cycle of the cell. Preliminary studies indicate that all three of these enzymes are present in nuclei isolated as described elsewhere in this report (1).

## METHODS

Nuclei were assayed for RNA polymerase and ATP polymerase by incubation for varying time intervals at 37°C with the appropriate labeled substrate. The standard assay reaction mixture consisted of the following: 40  $\mu$ moles Tris (pH 7.8), 0.5  $\mu$ mole  $MnCl_2$ , 6  $\mu$ moles mercaptoethanol, 0.3  $\mu$ mole  $^3H$ -GTP, 0.1  $\mu$ mole each of CTP, UTP, and ATP (RNA polymerase), or 0.3  $\mu$ mole  $^{14}C$ -8-ATP (ATP polymerase), in a final volume of 0.6 ml. The assay mixture for DNA polymerase was the same with 1.0  $\mu$ mole  $MgCl_2$  replacing  $MnCl_2$  and, as substrates, 0.002  $\mu$ mole  $^{14}C$ -TTP, 0.05  $\mu$ mole each of dATP, dCTP, and dGTP.

At the end of the incubation period, acid-insoluble material was precipitated by addition of cold TCA (final concentration 10 percent). Precipitates were extracted twice with 5 percent TCA for 40 minutes, and washed once with 5 percent TCA and once with methanol. Precipitates were solubilized in 0.3 ml hydroxide of Hyamine and transferred to 10 ml toluene containing 5 g/liter PPO and 0.3 g/liter dimethyl-POPOP. The amount of labeled precursor incorporated into acid-insoluble material was determined by counting in a Packard liquid scintillation spectrometer.

## RESULTS AND DISCUSSION

Nuclei from either Chinese hamster ovary or mouse lymphoma cells contain activities which strongly suggest the presence of enzymes polymerizing ribo- and deoxyribonucleoside triphosphates, as well as adenosine triphosphate. Optimal conditions for the three polymerizations have not been rigorously established.

The data in Table 1 describe the most pertinent characteristics of the RNA polymerase activity (that is, that incorporation of  $^3\text{H}$ -GTP requires the presence of all four nucleoside triphosphates and is increased by added DNA). Heated DNA (boiling water bath 2 minutes, fast-cooled) is somewhat less effective as a primer. Inhibition by actinomycin D is also characteristic of DNA-dependent RNA synthesis.

DNA polymerase activity, as judged by incorporation of thymidine triphosphate into acid-insoluble material in the presence of dCTP, dATP, and dGTP, is present in both mouse lymphoma and hamster ovary nuclei. The data in Table 2 show that this activity is very low but is stimulated by addition of DNA; again, heated DNA is less effective. The low enzymatic activity probably does not reflect the actual *in vivo* activity, since this enzyme is easily removed during nuclear isolation procedures. In order to assure that changes in enzymatic activity during the cell life cycle will be detected if they occur, the nuclear isolation procedure must ensure that enzymes are not lost. This is presently a problem of major concern. A non-aqueous isolation procedure (2) may become necessary as the work progresses in order to obtain quantitative data.

ATP polymerase, an enzyme which polymerizes ATP and is primed by poly-A, is present in both kinds of nuclei at high specific activity (Table 2). The function of this enzyme in the cell is at present entirely unknown. As the apparent wide distribution of this enzyme in biological systems becomes increasingly well recognized, it seems likely that its role in cellular nucleic acid and/or protein metabolism will be discovered.

Since all three of the enzymatic activities described above are found in nuclei as presently prepared, it should be possible with adequate technical modifications to establish the metabolic relationship of these enzymes to each other in the cell nucleus and during the life cycle of synchronously dividing cells.



TABLE 1. RNA POLYMERASE ACTIVITY IN ISOLATED NUCLEI

Additions or Omissions	Substrate	Nmoles Incorporated (per mg protein/30 minutes)
<u>Mouse Lymphoma Nuclei</u>		
Complete	<sup>3</sup> H-GTP	0.92
+ 50 µg DNA	<sup>3</sup> H-GTP	2.10
+ 50 µg heated DNA	<sup>3</sup> H-GTP	1.83
- CTP	<sup>3</sup> H-GTP	0.00
<u>Chinese Hamster Ovary Nuclei</u>		
Complete	<sup>3</sup> H-GTP	0.12
+ 50 µg DNA	<sup>3</sup> H-GTP	0.46
+ DNA, - CTP	<sup>3</sup> H-GTP	0.05
+ DNA + 10 µg actino- mycin	<sup>3</sup> H-GTP	0.00

TABLE 2. DNA POLYMERASE AND ATP POLYMERASE IN ISOLATED MOUSE  
LYMPHOMA NUCLEI

Additions	Substrate	Nmoles Incorporated (per mg protein/30 minutes)
<u>DNA Polymerase</u>		
Complete	<sup>14</sup> C-dTTP	0.01
+ 50 µg DNA	<sup>14</sup> C-dTTP	0.09
+ 50 µg heated DNA	<sup>14</sup> C-dTTP	0.06
<u>ATP Polymerase</u>		
Complete	<sup>14</sup> C-8-ATP	27.0
+ 50 µg poly-A	<sup>14</sup> C-8-ATP	142.5

#### REFERENCES

- (1) E. A. Hyatt, this report, p. 158.
- (2) G. Siebert, in Biochemisches Taschenbuch, 2nd ed., Vol. II (H. M. Raue, ed.), Springer-Verlag, Berlin (1964). p. 541.

**CONCENTRATIONS OF METALLIC ELEMENTS AT VARIOUS TIMES IN THE  
LIFE CYCLE OF CULTURED MAMMALIAN CELLS (R. R. J. Chaffee,  
D. F. Petersen, and C. F. Metz\*)**

**INTRODUCTION**

It is well known that certain metal ions are either integral parts of cellular enzymes or act as cofactors or activators of certain enzymes (1-3). The intake of such elements is believed to be controlled by requirements within the cell (4). A knowledge of changes in the concentration of these elements during the cell cycle should contribute to a better understanding of intracellular activities preceding cell division.

**METHODS AND MATERIALS**

Iron, zinc, molybdenum, phosphorus, copper, cobalt, manganese, magnesium, calcium, potassium, and sodium were assayed by the methods of Vallee (3) using emission spectrography (Perkin-Elmer, Egbert-mount spectrophotometer). The method allows for the simultaneous qualitative and quantitative analysis of most of the biologically important elements for concentrations, in some instances, as low as  $1 \times 10^{-8}$  to  $1 \times 10^{-9}$  g/g of sample.

**Method of Preparation of Cell Samples for Spectrographic Analysis**

Four hundred to 500 ml of a synchronously growing culture of Chinese hamster ovary (CHO) cells containing 190,000 to 350,000 cells/ml were assayed at various time intervals with respect to the cell cycle. The results are given in  $\mu\text{g}$  of the element per total number of cells assayed.

The cells from the culture were spun down at  $600 \times g$  for 5 minutes. The supernatant was carefully withdrawn with a Pasteur pipette attached to a suction flask. All glassware coming in contact with the cells from this point on was previously soaked for 6 hours in 10 percent nitric acid in sulfuric acid and rinsed thoroughly afterwards in distilled water and then 6 more times in ion exchange water (specific conductivity of  $1 \times 10^{-8}$  mho). The cells were washed with 8.5 percent sucrose which had been passed twice through a

---

\*LASL Group CMB-1.

Dowex-50 cation exchange resin (5) and gently resuspended in 12 ml of sucrose solution by alternate filling and expulsion of the suspension through an ion-free 10-ml polyethylene pipette with an attached rubber bulb. This was done until the cells were thoroughly separated from one another. The resuspension and spinning down were done twice.

The cells were then transferred to 10-ml clean platinum crucibles using 6 ml of distilled water (two 3-ml washes of the centrifuge tube into the crucible). The cleaning of the crucibles was done by first treating them with fused sodium bisulfite, then washing them thoroughly with distilled water, then soaking them in dilute hydrochloric acid, and finally washing them 6 times in ion exchange distilled water. The crucibles were placed in a quartz container, and the cell suspensions were evaporated to dryness in a dust-free room. The covered dust-free quartz container was then placed in an oven at 590°C for 18 to 24 hours, which was sufficient to reduce the material to ash. After cooling the container to room temperature, the lid was removed in the dust-free room and the crucibles were transferred to a metal-free plastic carrier for transporting the samples.

## RESULTS

The results are not yet adequate to conclude that there are fluctuations around the life cycle in levels of any of the metals, but some changes are indicated. The results of a typical run are shown in Table 1.

## REFERENCES

- (1) A. L. Lehninger, Phys. Rev. 30, 393 (1950).
- (2) R. J. P. Williams, Biol. Rev. 28, 381 (1953).
- (3) B. L. Vallee, Advances in Protein Chemistry X, 317 (1955).
- (4) H. Dawson, A Text Book of General Physiology, Third ed., Chapter X, Little, Brown and Company, Boston (1964).
- (5) R. E. theirs and B. L. Vallee, J. Biol. Chem. 226, 911 (1957).

TABLE 1. METAL CONTENT\* OF CHINESE HAMSTER OVARY CELLS AT G<sub>1</sub>, S, AND G<sub>2</sub> STAGES  
AND IN RANDOM CULTURE

Element	Random	G <sub>1</sub>	S	G <sub>2</sub>
Sodium	$6.33 \times 10^{-7}$	$9.38 \times 10^{-7}$	$8.43 \times 10^{-7}$	$9.25 \times 10^{-7}$
Magnesium	$5.55 \times 10^{-7}$	$7.03 \times 10^{-7}$	$5.56 \times 10^{-7}$	$5.00 \times 10^{-7}$
Calcium	$5.15 \times 10^{-8}$	$1.47 \times 10^{-7}$	$1.32 \times 10^{-7}$	$1.28 \times 10^{-7}$
Potassium	$7.88 \times 10^{-6}$	$5.35 \times 10^{-6}$	$3.54 \times 10^{-6}$	$5.30 \times 10^{-6}$
Copper	$2.38 \times 10^{-9}$	$7.35 \times 10^{-9}$	$6.58 \times 10^{-9}$	$1.28 \times 10^{-8}$
Manganese	$3.47 \times 10^{-10}$	$8.35 \times 10^{-10}$	$1.15 \times 10^{-9}$	$8.29 \times 10^{-10}$
Iron	$1.58 \times 10^{-8}$	$3.00 \times 10^{-8}$	$3.50 \times 10^{-8}$	$3.73 \times 10^{-8}$
Cobalt		---		
Phosphorus	$7.52 \times 10^{-6}$	$8.50 \times 10^{-6}$	$8.63 \times 10^{-6}$	$6.75 \times 10^{-6}$
Zinc	$2.57 \times 10^{-6}$	$3.34 \times 10^{-8}$	$3.70 \times 10^{-8}$	$3.04 \times 10^{-8}$
Molybdenum	$7.42 \times 10^{-10}$	$2.67 \times 10^{-9}$	$4.73 \times 10^{-9}$	$2.08 \times 10^{-9}$

\* In  $\mu\text{g}/\text{cell}$ .

# MECHANISM OF INFECTION OF ESCHERICHIA COLI BY PHAGE $\lambda$ -DEOXY-RIBONUCLEIC ACID (B. J. Barnhart)

## INTRODUCTION

Exposure of *Escherichia coli* K12 to DNA isolated from phage  $\lambda$  results in infection of the cells and the subsequent release of mature phage particles (1). The infection of *E. coli* by  $\lambda$ -DNA has a temperature-sensitive, rate-limiting step which renders the infecting material DNase-insensitive (2).

## METHODS

*Escherichia coli* K12 strain C600 (3) was used as recipient for infection with  $\lambda$ -DNA, which was prepared from the mutant  $i^{\lambda}C72$  (4) by phenol extraction at 4°C. After infection of the recipient cells with phage of type  $i^{434}hyc^{+}$  (5), helper phage, the cells were capable of taking up infectious  $i^{\lambda}C72$ -DNA. Infections due to the DNA were scored by assaying the infected cells on indicator bacteria lysogenic for phage of the same genotype as the helper phage. The latter were thus incapable of forming phage plaques on the mat of lysogenic indicator cells. Plaques appearing on these cells could then be scored as resulting from phage of genotype  $i^{\lambda}C72$ , that of the infectious DNA.

## RESULTS AND DISCUSSION

The work now in progress indicates that at least one step in the infection process is sensitive to two uncouplers of oxidative phosphorylation, 2,4-dinitrophenol and cyanocarbonyl-phenyl hydrazine. These results show that infection is coupled to cellular metabolism, a relationship one might expect for the infection of a cell by a molecule many times its length. The penetration of a cell by such a large molecule favors a mechanism involving infection in an end-to-end manner. This possibility is being investigated by following the time sequence of penetration of widely separated genetic markers on the infecting  $\lambda$ -DNA. The role of helper phage in the infection process will be considered in subsequent experiments.

#### REFERENCES

- (1) A. D. Kaiser, J. Mol. Biol. 4, 275 (1962).
- (2) B. J. Barnhart, submitted to J. Bacteriol.
- (3) R. K. Appleyard, Genetics 39, 440 (1954).
- (4) R. Thomas, J. Mol. Biol. 8, 247 (1964).
- (5) A. D. Kaiser and F. Jacob, Virology 4, 509 (1957).

CELLULAR RADIOBIOLOGY SECTION

PUBLICATIONS AND ABSTRACTS OF MANUSCRIPTS SUBMITTED

CULTURE AND SLIDE PREPARATION OF LEUKOCYTES FROM BLOOD OF MACACA, P. C. Sanders and G. L. Humason. Stain Techn. 39, 209-213 (1964).

Abstracted in Los Alamos Scientific Laboratory Report LA-3132-MS (1964), p. 232.

LIFE CYCLE ANALYSIS OF MAMMALIAN CELLS. II. CELLS FROM THE CHINESE HAMSTER OVARY GROWN IN SUSPENSION CULTURE, T. T. Puck, P. C. Sanders, and D. F. Petersen. Biophys. J. 4, 441-450 (1964).

Abstracted in Los Alamos Scientific Laboratory Report LA-3132-MS (1964), p. 230.

A DIGITIZED COMPARATOR FOR KARYOTYPE ANALYSIS, P. M. LaBauve, R. J. LaBauve, and D. F. Petersen. J. Heredity LVI, 46-52 (1965).

Abstracted in Los Alamos Scientific Laboratory Report LA-3132-MS (1964), p. 230.

QUANTITY PRODUCTION OF SYNCHRONIZED MAMMALIAN CELLS IN SUSPENSION CULTURE, D. F. Petersen and E. C. Anderson. Nature 203(4945), 642-643 (1964).

Abstracted in Los Alamos Scientific Laboratory Report LA-3132-MS (1964), p. 231.



**SYNCHRONIZED MAMMALIAN CELLS: AN EXPERIMENTAL TEST OF A MODEL FOR SYNCHRONY DECAY**, E. C. Anderson and D. F. Petersen. *Exp. Cell Res.* 36, 423-426 (1964).

Abstracted in Los Alamos Scientific Laboratory Report LA-3132-MS (1964), p. 231.

**RNA SYNTHESIS IN SYNCHRONOUSLY-DIVIDING CHINESE HAMSTER OVARY CELLS**, A. G. Saponara, M. D. Enger, and W. H. Langham. *Federation Proc.* 24(2), 664, Part I (1965), Abstract No. 2952.

The rates of incorporation of  $H^3$ -uridine into the RNA of Chinese hamster ovary cells growing synchronously in cell culture were determined. Results are expressed as amount of radioactivity in particular species of RNA relative to mass of unlabeled ribosomal RNA after a 15-minute incorporation period. It was found that label was incorporated into 4S RNA at the same rate during  $G_1$  and  $G_2$  and at twice this rate during S. Rapidly labeled RNA obtained by phenol extraction at  $60^\circ C$  and having sedimentation coefficients greater than 30S was slightly more labeled during  $G_2$  than during S or  $G_1$ . An RNA species found associated with ribosomes isolated in  $5 \times 10^{-3} M Mg^{++}$  labeled at the same rate during  $G_2$  and  $G_1$  but at twice this rate in S. This RNA, which had a sedimentation coefficient of 12S-15S, did not decrease in specific activity when cells were incubated in cold medium for 4 hours after a 15-minute pulse.

**TIMING OF SYNTHESIS OF m-RNA AND PROTEIN ESSENTIAL FOR CELL DIVISION**, R. A. Tobey, D. F. Petersen, and E. C. Anderson. *Federation Proc.* 24(2), 678, Part I (1965), Abstract No. 3033.

Actinomycin D, puromycin, and Mengovirus were added to synchronized Chinese hamster ovary cells in suspension cultures [Petersen and Anderson, *Nature* 203, 642 (1964)] at pre-selected times during  $G_2$  and M. The point of action of each of the inhibitors was shown to be close to entry into prophase by the determination of (1) time of cessation of cell division derived from total cell counts and (2) time of inhibition of mitosis based on mitotic index. The quantitative temporal relationships demonstrate that synthesis of m-RNA and protein essential for mitosis is completed within  $\pm$  30 minutes of the  $G_2/M$  boundary.

**MENGOVIRUS REPLICATION. III. VIRUS REPRODUCTION IN CHINESE HAMSTER OVARY CELLS.** R. A. Tobey and E. W. Campbell. Virology (in press).

Following infection of Chinese hamster ovary cells with Mengovirus there is an initial rapid reduction in the rates of synthesis of RNA and protein, followed by an increase in both synthetic rates at the time of virus maturation. The time required for release of virus is approximately 6 times as long in hamster cells as in L cells, and the yield of infective virus from hamster cells is only 20 percent of that from L cells.

**MENGOVIRUS REPLICATION. IV. INHIBITION OF CHINESE HAMSTER OVARY CELL DIVISION AS A RESULT OF INFECTION WITH MENGOVIRUS,** R. A. Tobey, D. F. Petersen, and E. C. Anderson. Virology (in press).

Chinese hamster ovary cells in suspension culture, synchronized by thymidine blockade and release, were infected with Mengovirus at varying time intervals up to and including mitosis. Cell counts were determined with an electronic particle counter. The time-course of virus production and virus yield per cell are similar in synchronized and randomly growing CHO cells. Virus added to premitotic cells precludes both cell division and formation of mitotic figures, whereas cells in mitosis at the time of virus addition continue to divide. Results indicate that Mengovirus infection results in the inhibition of the synthesis of macromolecules necessary for cell division and are consistent with previous observations that virus infection results in inhibition of cell RNA and protein synthesis. Measurements of the time lag between virus addition and termination of cell division further suggest that the synthesis of all macromolecules essential for cell division is not completed until  $0.66 \pm 0.13$  hour before division.

**INHIBITION OF THE RESPIRATION OF CULTURED MAMMALIAN CELLS BY OLIGOMYCIN,** W. D. Currie and C. T. Gregg. Biochem. Biophys. Res. Commun. (in press).

Complete inhibition of the respiration of intact cells (HeLa S-3, L-929, Stoker's C13, Fischer's L-5178Y, and Chinese hamster ovary) by oligomycin is reported for the first time.

The concentrations required to inhibit completely are as much as 4 fold lower than generally employed. Moreover, the response of the cultured cells to oligomycin yields a titration curve distinctly different from that obtained with intact mitochondria.

NEUTRON ACTIVATION OF SULFUR IN HAIR; APPLICATION IN A NUCLEAR ACCIDENT DOSIMETRY STUDY, D. F. Petersen and W. H. Langham. Health Phys. (in press).

Incident fast neutron doses sustained by personnel involved in the Wood River Junction, United Nuclear Corporation criticality accident of July 24, 1964, have been estimated from induced phosphorus-32 activity in hair sulfur. Fast neutron doses to the head and pubis of the fatally injured victim were 1200 and 4800 rads, respectively, corresponding to total gamma plus neutron dose estimates of ~11,000 and 48,000 rads. Identification of phosphorus-32 in hair samples from two individuals who entered the area later confirmed the notion that the system either remained critical or that a second excursion occurred. Comparison with the Los Alamos fatality of 1958 indicates that, although doses to the pelvis differed by a factor of 40 and the average total body dose may have differed by about a factor of 3, doses to the head may have been essentially the same (~10,000 rads). Similarities in clinical course and survival of the two cases may reflect the approximately equivalent doses to the upper torso and head. These observations suggest that debilitation from massive radiation exposure may be more dependent on dose to the head and thorax than on average total body dose.

INCORPORATION OF [ $^3\text{H}$ ]URIDINE AND [ $\text{Me-}^{14}\text{C}$ ]METHIONINE INTO CHINESE HAMSTER CELL RNA, A. G. Saponara and M. D. Enger. Submitted to Biochim. Biophys. Acta.

Mammalian cells form ribosomal RNA via 35S and 50S precursors. Incorporation of label from [ $^3\text{H}$ ]uridine and [ $\text{Me-}^{14}\text{C}$ ]methionine into precursors and ribosomal RNA (r-RNA) of Chinese hamster ovary cells growing in suspension culture was followed in order to determine the stage in r-RNA formation at which methylation occurs. Of the high-polymeric RNA's, 50S precursor was found to incorporate [ $^3\text{H}$ ]uridine most rapidly but incorporated no detectable label from [ $\text{Me-}^{14}\text{C}$ ]methionine under conditions which allowed substantial

methylation of 35S precursor and ribosomal species. This observation suggests that methylation occurs after the first ribosomal precursor (50S) has formed and has been converted to the next pre-ribosomal species. Consistent with the absence of methylation of the 50S r-RNA precursor, we have observed a lag in the incorporation of [<sup>3</sup>H]uridine relative to <sup>14</sup>C (from [Me-<sup>14</sup>C]methionine) into r-RNA.

TEMPERATURE EFFECTS ON MITOTIC RATE AND CELL VOLUME OF CELLS FROM HIBERNATORS VS CELLS FROM NON-HIBERNATING SPECIES AND OF POLYOMA-TRANSFORMED CELLS VS NON-TRANSFORMED CONTROLS. R. R. J. Chaffee, E. C. Anderson, and D. F. Petersen. Submitted to American Zoologist.

Mean cell volume (CV) of Chinese hamster ovary (CHO) cells, determined by integration of cell spectra from Coulter counting, increases slightly but significantly with decreasing temperature (T). After 4 days of growth at 27 C, with a generation time (T<sub>G</sub>) of 15 hr, the CV was 1.2 times that of cells at 37 C (T<sub>G</sub> 17 hr). This size increase occurs in the first 2 days. Failure of CV to increase more when T<sub>G</sub> is greatly lengthened indicates that the temperature coefficient of CV growth resembles that of division, both being suppressed by lowered T (when division is blocked by thymidine or colcemide, CV increases unrestrictedly). The "activation energy" of reactions leading to division was 16 kcal/mole for the linear portion of the Arrhenius plot between 29 and 34 C. There is a flat maximum at 36 to 38 C and an abrupt increase in slope below 29 C. The plot is similar to data reported by Rao and Engelberg [Science 148, 1092 (1965)] for HeLa, but both the maximum and linear portions are much broader, apparently reflecting a greater low T tolerance in CHO. To see if cells from a hibernating animal, Syrian hamster fibroblasts (Cl3), divide faster at low T's than do cells from non-hibernating species (CHO, HeLa, and L929 cells) T studies on these are in progress. Virus-induced changes in temperature coefficient of mitosis of polyoma-transformed Cl3 cells are being studied.

SIALIC ACID OF MAMMALIAN CELL LINES. P. M. Kraemer. Submitted to J. Cell. Comp. Physiol.

Approximately two-thirds of the total sialic acid (S. A.) per cell of a number of cell lines (L-929, L-5178Y, HeLa, Cl3,

P183, and CHO) was located at the cell surface but was inaccessible to the action of trypsin, pronase, lysozyme,  $\beta$ -glucuronidase, or hyaluronidase. The mean surface density of S. A. ranged from  $5.4 \times 10^5$  molecules/ $\mu^2$  surface area for the L-5178Y cell to  $16.1 \times 10^5$  molecules/ $\mu^2$  surface area for the P183 cell. The P183 cell line, which is a polyoma virus-transformed derivative of Stoker's C13 line, consistently contained more S. A. per cell than the latter under a variety of growth conditions, although the two lines did not differ in mean cell volume. When mean cell volume of C13, P183, or CHO cells was experimentally manipulated by thymidine or colcemide blockade, S. A. content per cell followed size changes closely. No evidence could be found for a shift in total S. A. per unit cell volume accompanying the period of maximum mitotic activity of partially synchronized CHO suspension cultures. Comparisons between cells grown on glass and the same cells grown in suspension, or between cells grown to different densities on glass, indicated no differences in the characteristic S. A. content per cell.

**POLYRIBOADENYLATE SYNTHESIS BY NUCLEI FROM DEVELOPING SEA URCHIN EMBRYOS, E. A. Hyatt. Submitted to J. Biol. Chem.**

The characteristics of an ATP polymerase which occurs in nuclei isolated from developing sea urchin embryos are described. CTP, UTP, and GTP inhibit incorporation of ATP-8- $^{14}\text{C}$  but are not polymerized to any significant extent. The enzyme can polymerize dATP-8- $^{14}\text{C}$  approximately one-tenth as efficiently as it polymerizes ATP. The incorporation of ATP-8- $^{14}\text{C}$  into acid-insoluble material is inhibited by DNA. Some preparations of polyriboadenylic acid (California Biochemical Research Corporation, lot No. 35090), yeast RNA, or small amounts of sea urchin RNA act as primers. It is likely that only low molecular-weight poly-A or RNA with a free 3'-hydroxyl end serves as primer for this enzyme.

**RAPID ESTIMATION OF FAST NEUTRON DOSES FOLLOWING RADIATION EXPOSURE IN CRITICALITY ACCIDENTS. THE  $^{32}\text{S}(\text{n},\text{p})^{32}\text{P}$  REACTION IN BODY HAIR, D. F. Petersen. In: Proceedings of the IAEA/WHO Symposium on Personnel Dosimetry for Accidental High-Level Exposure to External and Internal Radiation, Vienna, Austria (March 8-12, 1965). To be published.**

Unique chemical composition, fixed anatomical location, and

ready availability combine to make human hair a useful material for rapid estimation of fast neutron doses sustained by personnel involved in accidental nuclear critical excursions. The sulfur content of human hair is remarkably constant regardless of sex, color, or distribution; values of  $0.048 \pm 0.005$  gram sulfur per gram hair indicate that 5 percent can be used as a standard figure for the abundance of sulfur in preliminary dose estimates without resorting to individual sulfur analyses. In the absence of easily removable external contamination, hair contains less than 0.025 percent phosphorus; since the activation cross sections of phosphorus and sulfur are similar, the virtual absence of phosphorus permits the use of hair as a biological sulfur threshold detector for measuring the flux of neutrons with energies in excess of 2.5 Mev by the  $^{32}\text{S}(n,p)^{32}\text{P}$  reaction. Techniques for rapid isolation of radiochemically pure phosphorus-32 have been developed with a view toward providing clinically useful estimates of the fast neutron exposure of criticality accident victims. In the absence of gross fission product contamination, preliminary estimates can be made within 2 hours; the more extensive procedure for eliminating fission products requires approximately 6 hours for a preliminary estimate. Experiments employing the well-defined fission spectrum of an unshielded critical assembly have consistently provided estimates of neutron dose within  $\pm 10$  percent of referee dosimetry. Moreover, the fixed anatomical location of hair samples makes it possible to deduce orientation and asymmetry of exposure from a comparison of the relative specific activities of samples from different regions of the body.

Experience with three nuclear critical excursions resulting in fatalities has demonstrated that in each case exposures were markedly asymmetrical. Thus, phosphorus-32 measurements on hair provide valuable complementary information for comparison with average total body neutron exposure estimates based on blood sodium-24 measurements. Fission yield estimates based on deduced geometries in each case were in good agreement with independent determinations of total fissions by more conventional analytical procedures. For rapid approximations of fast neutron dose, phosphorus-32 activity in disintegrations per minute per gram of hair at  $T = 0$  from any counting system of known efficiency is simply multiplied by 0.49 to obtain "sulfur-level" neutron dose in rads.

## CHAPTER 6

### MOLECULAR RADIOBIOLOGY SECTION

ENZYMATIC SYNTHESIS OF POLYDEOXYRIBONUCLEOTIDES 5'-TERMINATED WITH CHEMICALLY SYNTHESIZED OLIGODEOXYRIBONUCLEOTIDES (F. N. Hayes and V. E. Mitchell)

#### INTRODUCTION

Information transfer reactions fundamental to biology can be studied in the test tube with enzymes of high purity and substrates of precisely defined chemistry. Two classes of substrate exist for such reactions: templates and monomers. It is the purpose of this project to synthesize DNA templates which are competent with DNA polymerase and RNA polymerase and which are characterized as to sequence and size.

Chemically synthesized (1) oligo-2'-deoxyribo-5'-nucleotide initiators are being lengthened from their 3'-hydroxyl end by addition of from 50 to 300 2'-deoxy-5'-adenylate units. The enzyme which accomplishes this is Bollum's terminal deoxy-ribonucleotidyl transferase [(2) hereafter, addase].

#### METHODS AND RESULTS

All addase reactions contained 7 mM MgCl<sub>2</sub> and 1 mM 2-mercaptoethanol and were buffered at pH 6.9 with 0.05 M potassium phosphate. Yeast inorganic pyrophosphatase shown to be free of nuclease activity was used in reactions greater than 1 mM in 2'-deoxyadenosine 5'-triphosphate (p3a) to repress pyrophosphate inhibition of the addase reaction. All reactions were

run at  $35 \pm 0.5^\circ$ . The ingredients were mixed at  $4^\circ$  in the following way: addase, majority of buffer, 2-mercaptoethanol and  $\text{MgCl}_2$  were premixed, initiator was added, and finally p3a was put in. Hypochromicity kinetics were followed by removing 50  $\mu\text{l}$  from a 1-mM p3a reaction and adding it to 1 ml of water for each  $A_{260}$  measurement. A representative hypochromicity curve is shown in Fig. 1 for reaction IV.

Protein removal was accomplished either by 1-minute heating of the reaction mixture at  $90^\circ$  to denature the protein followed by centrifugation, or by evaporation to dryness of the high molecular weight column-chromatographic fraction followed by dissolution of the polynucleotide leaving behind the denatured protein.

Polynucleotide was isolated either by the Bollum procedure of repeated precipitation from 0.5 M NaCl solution with two volumes of 95 percent ethanol (2), or by direct gel-filtration chromatography of the reaction mixture. At first Sephadex G-100 was used, but Bio-Gel P-60 with improved column life eventually became the preferred packing. Eluents employed were water or 0.005 M Tris (pH 7.0). No orthophosphate was eluted in the polynucleotide peak. A representative ultraviolet monitored elution profile from G-100 is shown in Fig. 2 for reaction X. Using an average  $\epsilon(P)$  of  $9 \times 10^3$  for these polymers at 260  $m\mu$  and pH 7.0, theoretical yields in  $A_{260}$  units were calculated by multiplying this value by the  $\mu\text{moles}$  of p3a put into each reaction. The average  $A_{250}/A_{260}$  and  $A_{280}/A_{260}$  ratios and wavelength for  $A_{\text{max}}$  at pH 7.0 for the polymers were 0.86, 0.32, and 257  $m\mu$ .

Specific reaction details are supplied in Table 1. Addase units were assigned according to the procedure of Ratliff and Trujillo (3). Special details on the reactions follow.

#### Reaction I

In spite of the initial availability of very little addase, this reaction was highly interesting both as a first try and as a source of some polymer which might be degraded to oligomers of 2'-deoxy-5'-adenylic acid. A preliminary DNase I treatment of 75  $A_{260}$  units polymer was run for 15 hours with 0.5 mg enzyme and 5 mM  $\text{MgCl}_2$  in 0.05 M Tris (pH 7.9) and 0.2 M NaCl. The enzyme was denatured by heating and then centrifuged. The supernatant was applied to a short DEAE-cellulose column and washed on with 0.005 M triethylammonium



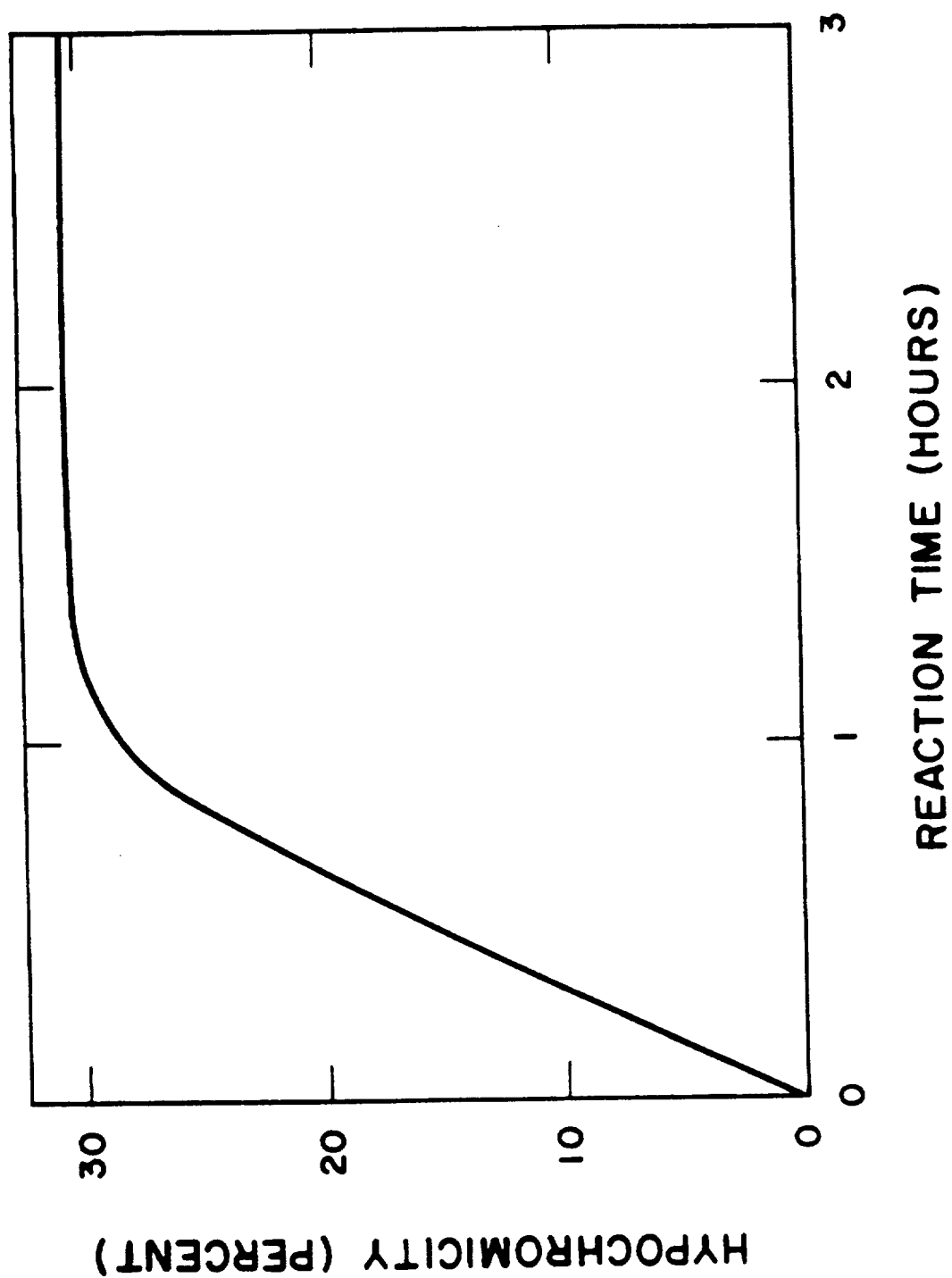


Fig. 1. Hypochromicity kinetics for reaction IV.

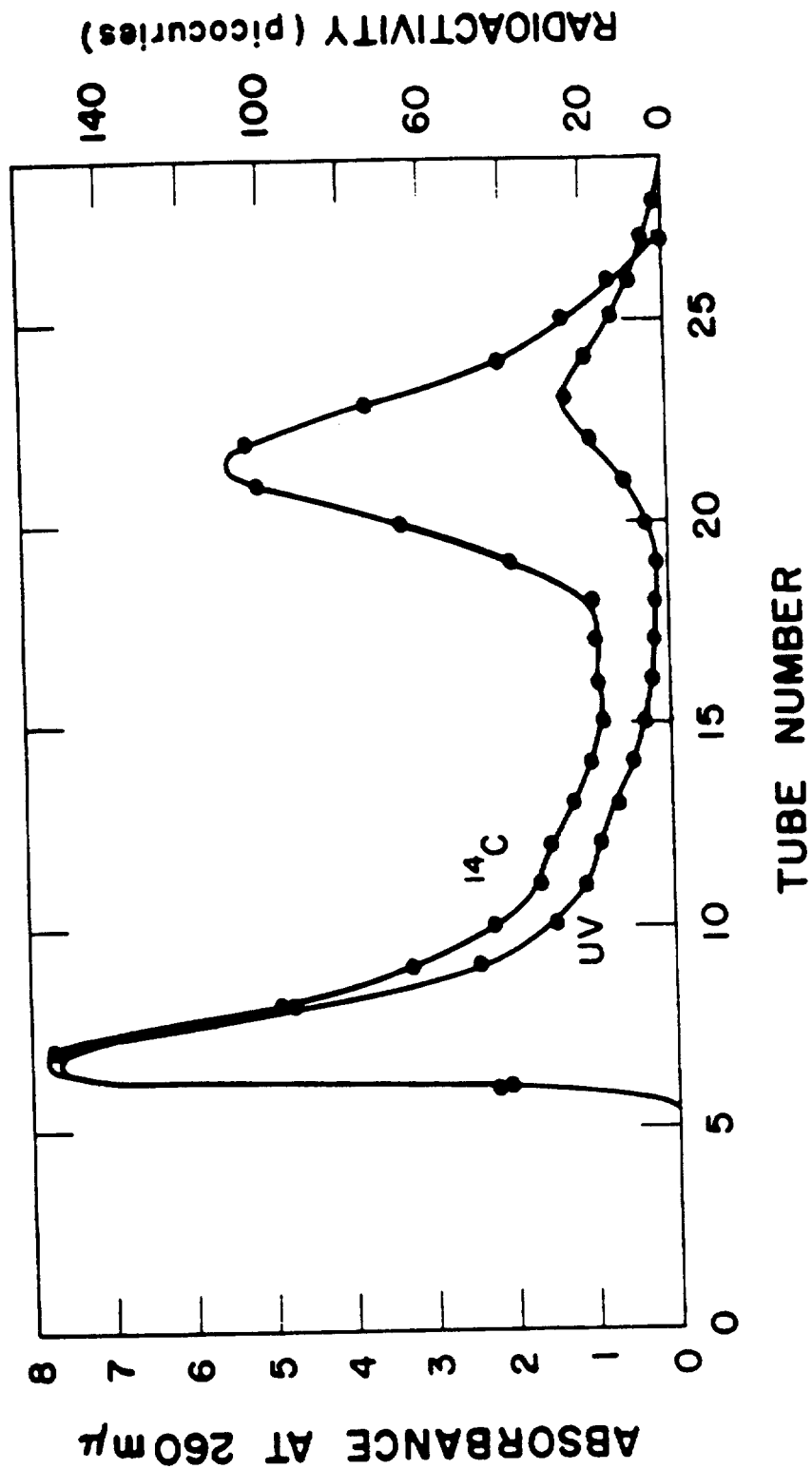


Fig. 2. Sephadex G-100 elution profiles for reaction X (2.0-cm diameter x 30-cm column operated with water as the ascending eluent, 0.5 ml/min).

TABLE 1. ADDASE REACTION DETAILS

Reaction Number	Initiator (p3a/initiator)	Mole Ratio (p3a/initiator)	p3a Conc. (mM)	Addase Conc. (units/ $\mu$ mole p3a)	Volume (ml)	Reaction Time (hr)	Yield (percent based on p3a)	Hypochromicity (percent)
I	(pt) <sub>6</sub>	300	2.0	10	20	15	25 <sup>a</sup>	21
II	(pa) <sub>4</sub>	270	1.9	120	40	17	58 <sup>a</sup>	e
III	(pt) <sub>6</sub> - <sup>14</sup> C <sub>6</sub>	47	0.5	170	6	2	53 <sup>b</sup>	20
IV	(pt) <sub>6</sub>	290	1.5	440	5	3	73 <sup>b</sup>	31
V	(pt) <sub>13</sub>	190	1.5	250	10	4.5	58 <sup>b</sup>	29
VI	(pc) <sub>6</sub>	190	1.5	250	10	4.5	31 <sup>b,c</sup>	33
VII	(pt) <sub>13</sub>	100	1.5	380	13	3	74 <sup>b</sup>	e
VIII	(pt) <sub>3</sub> - <sup>14</sup> C <sub>3</sub>	55	2.0	400	1	0.0	20 <sup>b</sup>	0.0
IX	(pt) <sub>3</sub> - <sup>14</sup> C <sub>3</sub>	55	2.0	400	1	0.33	90 <sup>b</sup>	18
X	(pt) <sub>3</sub> - <sup>14</sup> C <sub>3</sub>	55	2.0	840	1.25	2	90 <sup>b</sup>	33
XI	(pt) <sub>3</sub> - <sup>14</sup> C <sub>3</sub>	10	0.1	7,120	3.5	4.3	78 <sup>d</sup>	28
XII	pyro-(pt) <sub>2</sub>	100	0.84	2,500	25	5	40 <sup>d</sup>	11
XIII	(pc) <sub>6</sub>	94	0.95	2,700	20	2.5	89 <sup>d</sup>	24
XIV	(pg) <sub>3</sub>	50	1.1	1,050	25	2.7	92 <sup>d</sup>	34

<sup>a</sup>From ethanol precipitation.  
p-60.<sup>c</sup>Not measured.<sup>b</sup>From Sephadex G-100. <sup>c</sup>Part of product lost during work-up.<sup>d</sup>From Bio-Gel

bicarbonate (pH 7.5). The flow-through peak exhibited an  $A_{\max}$  of 267 m $\mu$  and was considered to consist of self-eluted fragments of the (pt)<sub>6</sub> portion of the polymer with very little pa-type material present. The remainder of the partially cleaved polymer was washed from the column with 1.5 M triethylammonium bicarbonate. After removal of the volatile salt by rotary film evaporation, a second DNase I degradation was run under the above conditions but this time in the absence of NaCl. DEAE-Cellulose column-chromatography of the second digest with a linear 0.005-0.5 M (pH 7.5) triethylammonium bicarbonate gradient afforded 31.3 percent dimer, 36.4 percent trimer, 21.7 percent tetramer, 8.4 percent pentamer, and 2.2 percent hexamer (percentages based on recovered material). The trimer was rechromatographed on DEAE-cellulose with a linear 0.005-0.3 M (pH 4.0) lithium chloride gradient. A single symmetrical peak emerged at 0.12 M.

#### Reaction II

The initiator came from the two-step DNase I digestion of the product from reaction I. Sedimentation analysis of the polymer showed a double boundary with  $s_{20,w}$  values of 0.460 and 0.913.

#### Reaction III

The (pt)<sub>6</sub>-<sup>14</sup>C<sub>6</sub> initiator was analyzed by liquid scintillation counting to have 28.6 nc/ $\mu$ mole P. The polymer was shown to have been isotopically diluted to 2.09 nc/ $\mu$ mole P. The total length was then calculated to be  $(6)(28.6/2.09) = 82$  units. Therefore, the product has an average structure (pt)<sub>6</sub>(pa)<sub>76</sub>. The reaction stoichiometry predicted the formation of (pt)<sub>6</sub>(pa)<sub>47</sub> if all the initiator and pa had been utilized.

#### Reaction IV

This polymerization was run to obtain the hypochromicity kinetics of Fig. 1.

## Reactions V and VI

These reactions were designed to give polymers with unique base sequences highly suitable for critical evaluation of various RNA polymerase preparations (4).

## Reaction VII

This product was synthesized for a polymer composition study using ultraviolet absorption spectrophotometry. After exhaustive cleavage to nucleosides, separation of 2'-deoxy-adenosine from thymidine on Sephadex G-25 (5) and ultraviolet analysis, the polymer was shown to have the structure (pt)<sub>13</sub>(pa)<sub>73</sub>. Detailed analysis of the initiator by high resolution DEAE-cellulose column chromatography (6) showed the distribution: 2 percent n = 1, 21 percent n = 12, 44 percent n = 13, 26 percent n = 14, 6 percent n = 15, and 3 percent n = 16.

## Reactions VIII and IX

One milliliter of an addase reaction with labeled initiator was fractionated on Sephadex G-100 at 4° immediately after the reaction mixture was prepared at 4°. Even with no incubation time a 20 percent yield of polymer was obtained whose chain length by isotope dilution analysis was about 30 units. A second milliliter was fractionated after 20 minutes at 35° (reaction IX), giving a 90 percent yield of polymer whose chain length was about 100 units.

## Reaction X

This polymerization was run to obtain molecular size distribution (from Sephadex G-100) of total product absorbance and of initiator radioactivity. Tubes collected from the column run were individually analyzed for both A<sub>260</sub> and <sup>14</sup>C-radioactivity (Fig. 2). Although this reaction effectively utilized the p<sub>3a</sub>, 44 percent of the labeled initiator did not participate.

## Reaction XI

In a preliminary attempt to make a very short polymer, initiator and addase concentrations were kept near optimum but the p3a concentration was lowered to 0.1 mM. This allowed the reaction to be continuously monitored without dilution and, therefore, it was run in the sample cuvette of a UNICAM SP-800 capable of retracing the absorption spectrum at preset elapsed time settings. The temperature during the run averaged 32°. For 2 hours no spectral change occurred but in the following 2 hours the A<sub>260</sub> dropped from 2.35 to 1.69, while the  $\lambda_{\text{max}}$  shifted from 260 m $\mu$  to 258 m $\mu$  and the  $\lambda_{\text{min}}$  shifted from 229 m $\mu$  to 236 m $\mu$ . After work-up, isotopic dilution analysis showed the product to be (pt)<sub>3</sub>(pa)<sub>70</sub>, not the desired (pt)<sub>3</sub>(pa)<sub>10</sub>.

## Reaction XII

Bollum (2) has shown that the minimum size oligomer to function as initiator is trimer. In this reaction the dimer in the form of its p<sub>1</sub>,p<sub>2</sub>-pyrophosphate has been found competent to initiate. The nature of the polymers obtained from this and related pyrophosphates is being studied to see if both 3'-hydroxyl sites are initiating and whether the pyrophosphate bond can be cleaved in the polymer.

## Reactions XIII and XIV

These reactions were run expressly to enlarge on the analytical work done with the polymer from reaction VII.

## DISCUSSION

The enzymatic addition of long chains of poly-2'-deoxy-5'-adenylic acid to the 3'-end of a diverse group of oligo-2'-deoxy-5'-nucleotides has been accomplished. Some previously unreported initiator capabilities have been discovered. Further work is in progress on how to utilize the initiator more completely and thereby be able to obtain a polymer whose structure is in agreement with the reaction stoichiometry.

The polynucleotides are being used as templates with RNA polymerase (4) and calf thymus DNA polymerase.

#### REFERENCES

- (1) D. L. Williams, D. E. Hoard, V. N. Kerr, E. Hansbury, E. H. Lilly, and D. G. Ott, this report, p. 187.
- (2) F. J. Bollum, E. Groeniger, and M. Yoneda, Proc. Natl. Acad. Sci. U. S. 51, 853 (1964).
- (3) R. L. Ratliff and T. T. Trujillo, this report, p. 241.
- (4) D. A. Smith, R. L. Ratliff, and T. T. Trujillo, this report, p. 237.
- (5) G. T. Fritz and F. N. Hayes, this report, p. 225.
- (6) A. Murray, this report, p. 215.

THE CHEMICAL SYNTHESIS OF OLIGODEOXYRIBONUCLEOTIDES (D. L. Williams, D. E. Hoard, V. N. Kerr, E. Hansbury, E. H. Lilly, and D. G. Ott)

INTRODUCTION

The synthesis of oligodeoxyribonucleotides with a variety of known base sequences is continuing (1). These are desired for studies on information transfer reactions fundamental to biology (2). Of major interest are trinucleotides, with terminal 5'-phosphate, which have the minimum size for enzymatic addition of deoxyribonucleotide units at the 3'-hydroxyl end. These are being synthesized by the four routes illustrated in Fig. 1 using the four types of nucleoside and nucleotide reactants (I to IV) shown. Route A or B allows (3-5) synthesis of any one of the 64 trideoxyribonucleotides. Route C is a limited polymerization (6) by which 16 trideoxyribonucleotides may be obtained. Route D is a homopolymerization (7) which can provide the four trideoxyribonucleotides.

METHODS AND RESULTS

Route A: Stepwise Synthesis of Trinucleotides with Introduction of Terminal Phosphate in the Final Stage

O<sup>5'</sup>-(Dimethoxytrityl)thymidine (I) (0.81 mmole) and N,O<sup>3'</sup>-diacetyl-2'-deoxy-5'-adenylic acid (IV) (1.0 mmole) in dry pyridine solution (6 ml) were treated with mesitylenesulfonyl chloride (2 mmoles) for 6 hours at room temperature. Chilled water was added, and the solution was extracted repeatedly with ether to remove unreacted I (estimated recovery 0.35 mmole). Products having the dimethoxytrityl group were then isolated from the aqueous pyridine solution by extraction with chloroform. The chloroform extract was concentrated after addition of pyridine, and the residual material was treated for 4 minutes at 0° with N sodium hydroxide in 33 percent aqueous pyridine to remove O<sup>3'</sup>-acetyl groups (8). Chromatography on DEAE-cellulose (Cl<sup>-</sup>), using 10 percent aqueous methanol buffered at pH 7 with Tris, followed by a linear sodium chloride gradient in the same solvent, gave the desired product, O<sup>5'</sup>-(dimethoxytrityl)thymidylyl-(3':5')-N-acetyl-2'-deoxyadenosine, which was converted to the trialkylammonium salt. The yield of 22 percent is lower than previously



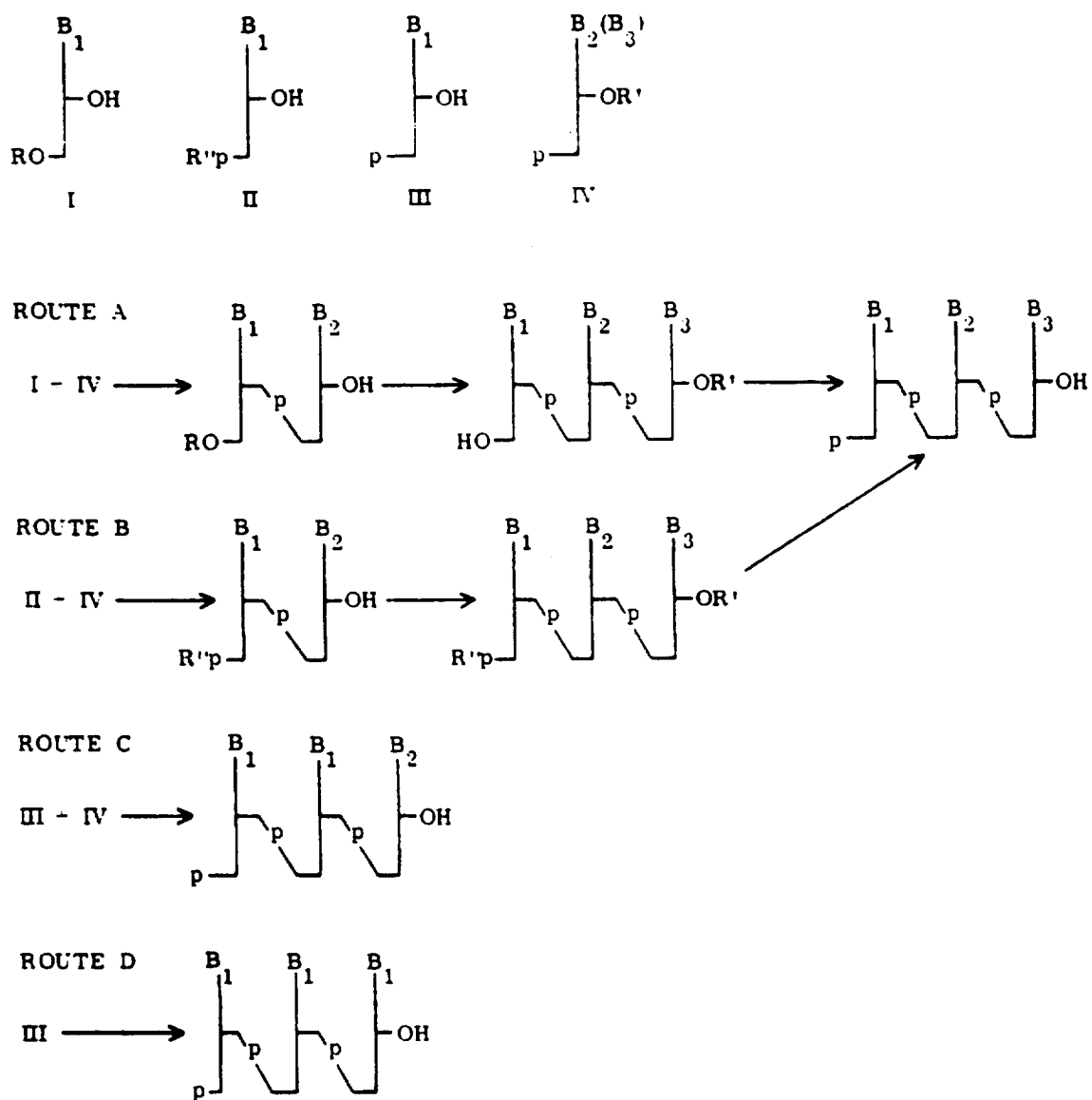


Fig. 1. Oligodeoxyribonucleotide synthetic routes.

obtained for the pyrimidine analogs (1), a result anticipated for these reactions with the bulky purine derivatives (8).

**Route B: Stepwise Synthesis of Trinucleotides Starting from Appropriately Blocked 5'-Mononucleotides**

Progress in this area is described in a separate part of this report (9).

**Route C: Oligonucleotides by Limited Polymerization of a Mononucleotide and a 3'-Blocked Mononucleotide**

**Oligo-5'-thymidylic Acids 3'-Terminated with a 2'-Deoxy-5'-cytidylic Acid Group [(pt)<sub>n</sub>pc].**--A pyridine solution (0.1 ml) containing 48  $\mu$ moles 5'-thymidylic acid (III), 41  $\mu$ moles N,O<sup>3'</sup>-diacetyl-2'-deoxy-5'-cytidylic acid (IV) (0.1  $\mu$ curie carbon-14/ $\mu$ mole), and 0.5 mmole N,N'-dicyclohexylcarbodiimide (DCC) was allowed to react at room temperature for 5.5 days. After pyrophosphate cleavage (10) and ammonolysis to remove acetyl blocking groups, the crude product was fractionated on a DEAE-cellulose column with a linear 0 to 0.7 M (pH 7.5) triethylammonium bicarbonate gradient. The major linear-oligomer peaks were collected, concentrated, rid of the volatile solute, analyzed for esterified phosphorus, and counted for carbon-14 content. Table 1 shows the oligomer length, percent yield based on total starting material, and percent cytidylate-ended component in each peak. From published data (6), some exclusively thymidylate oligomers in each peak were expected. Rechromatography of the mixed trimer peak on DEAE-cellulose with a linear 0.05 to 0.1 M (pH 3.3) lithium chloride gradient gave purified 2'-deoxy-cytidylyl-(5':3')-thymidylyl-(5':3')-5'-thymidylic acid (ptptpc).

**Thymidylyl-(5':3')-2'-deoxy-5'-adenylic Acid (papt).**--An anhydrous pyridine solution (1 ml) containing 0.29 mmole of pyridinium N-benzoyl-2'-deoxy-5'-adenylate (III) (tritium-labeled) and 0.82 mmole of pyridinium O<sup>3'</sup>-acetyl-5'-thymidylate (IV) was treated with 2.3 mmoles of DCC for 6 days at room temperature. After preliminary work-up, the crude mixture of products was treated with acetic anhydride in pyridine to effect cleavage of pyrophosphates and then fractionated by ion exchange chromatography on DEAE-cellulose with a linear gradient of triethylammonium bicarbonate (pH 7.5).

TABLE 1. YIELD DATA FOR OLIGO-5'-THYMIDYLIC ACIDS 3'-  
TERMINATED WITH 2'-DEOXY-5'-CYTIDYLIC ACID

Oligomer Length (units)	Yield (Percent of Starting Material)	Yield of (pt) <sub>n</sub> pc (Percent of Each Peak)
1	46	57
2	11	61
3	10	73
4	4.4	91
5	1.8	98
6	0.7	99

The recovery of  $O^3$ '-acetylthymidylyl-(5':3')-N-benzoyl-2'-deoxy-5'-adenylic acid was 22 percent, assuming an  $\epsilon_{280}$  for the compound of  $24.3 \times 10^3$ . Also isolated was a small amount (ca. 6 percent) of the protected trinucleotide,  $O^3$ '-acetylthymidylyl-(5':3')-N-benzoyl-2'-deoxyadenylyl-(5':3')-N-benzoyl-2'-deoxy-5'-adenylic acid (protected papapt).

**Oligomers of 2'-Deoxy-5'-cytidylic Acid.**--The chemical polymerization of 2'-deoxy-5'-cytidylic acid was essentially according to published procedures (11). A mixture of 0.75 mmole of N-anisoyl-2'-deoxy-5'-cytidylic acid (III) and 0.25 mmole of N, $O^3$ '-diacetyl-2'-deoxy-5'-cytidylic acid (IV) (pyridinium salts) was thoroughly dried by evaporation of anhydrous pyridine. The residual mixture in 1 ml dry pyridine was treated with 5 mmoles of DCC for 5.5 days. Separation of the resulting oligonucleotides on a DEAE-cellulose column (bicarbonate form), after the cleavage of pyrophosphate linkages, gave the proportions of products shown in Table 2. The linear oligonucleotides,  $(pc)_n$ , were further purified by rechromatography of the individual peaks on DEAE-cellulose ( $Cl^-$ ) at acid pH.

#### Route D: Oligonucleotides by Polymerization of Mononucleotides

**Oligomers of 2'-Deoxy-5'-adenylic- $8-^{14}C$  Acid.**--The polymerization of pyridinium N-benzoyl-2'-deoxy-5'-adenylate (III) (124  $\mu$ moles) was carried out according to published procedures (12). After 7 days the reaction was stopped by the addition of water. The product was treated to cleave pyrophosphate linkages, the blocking groups were removed, and the mixture was fractionated on a 2 x 30-cm DEAE-cellulose column with a linear 0.005 to 0.5 M (8 l., pH 7.5) triethylammonium bicarbonate gradient (Fig. 2A). The oligonucleotides, out to heptamer, were isolated. Negligible radioactivity was found in peaks I, III, and IV, as well as in the leading shoulder of peak V. Peak II exhibited the ultraviolet spectrum typical of 2'-deoxy-5'-adenylic acid, as did peak V and all the peaks following. Peak II is probably cyclic monomer. Peaks V, VII, IX, and XI to XV showed single spots on paper chromatography using the solvent 2-propanol, ammonia, water; 65:10:25. Peaks VI, VIII, and X showed two or more spots under the same conditions. Rechromatography of peak VII (Fig. 2B) on DEAE-cellulose (linear gradient of 0 to 0.5 M lithium chloride, 1 l., pH 5.5) gave the dinucleotide,  $\overline{papa}$  (VIIA),  $\epsilon(P)_{258} 12.4 \times 10^3$ . The major

TABLE 2. DISTRIBUTION OF PRODUCTS FROM POLYMERIZATION OF  
2'-DEOXY-5'-CYTIDYLIC ACID

Column Peak	Nucleotide Material (Percent of Total)	Composition of Peak
6	21.2	Unreacted monomer
7	10.4	Cyclic-dimer*
8	16.0	Mainly dimer
9	2.1	Cyclic-trimer
10	11.8	Mainly trimer
11	1.3	Cyclic-tetramer
12	11.4	Mainly tetramer
13	1.1	Cyclic-pentamer
14	7.9	Mainly pentamer
15	0.8	Cyclic-hexamer
16	5.7	Mainly hexamer
17	0.7	Cyclic-heptamer
18	3.9	Mainly heptamer
19	3.2	Mainly octamer
20	1.8	Mainly nonamer
21	0.8	Mainly decamer

\*These are 3',5'-macrocylic phosphate esters.

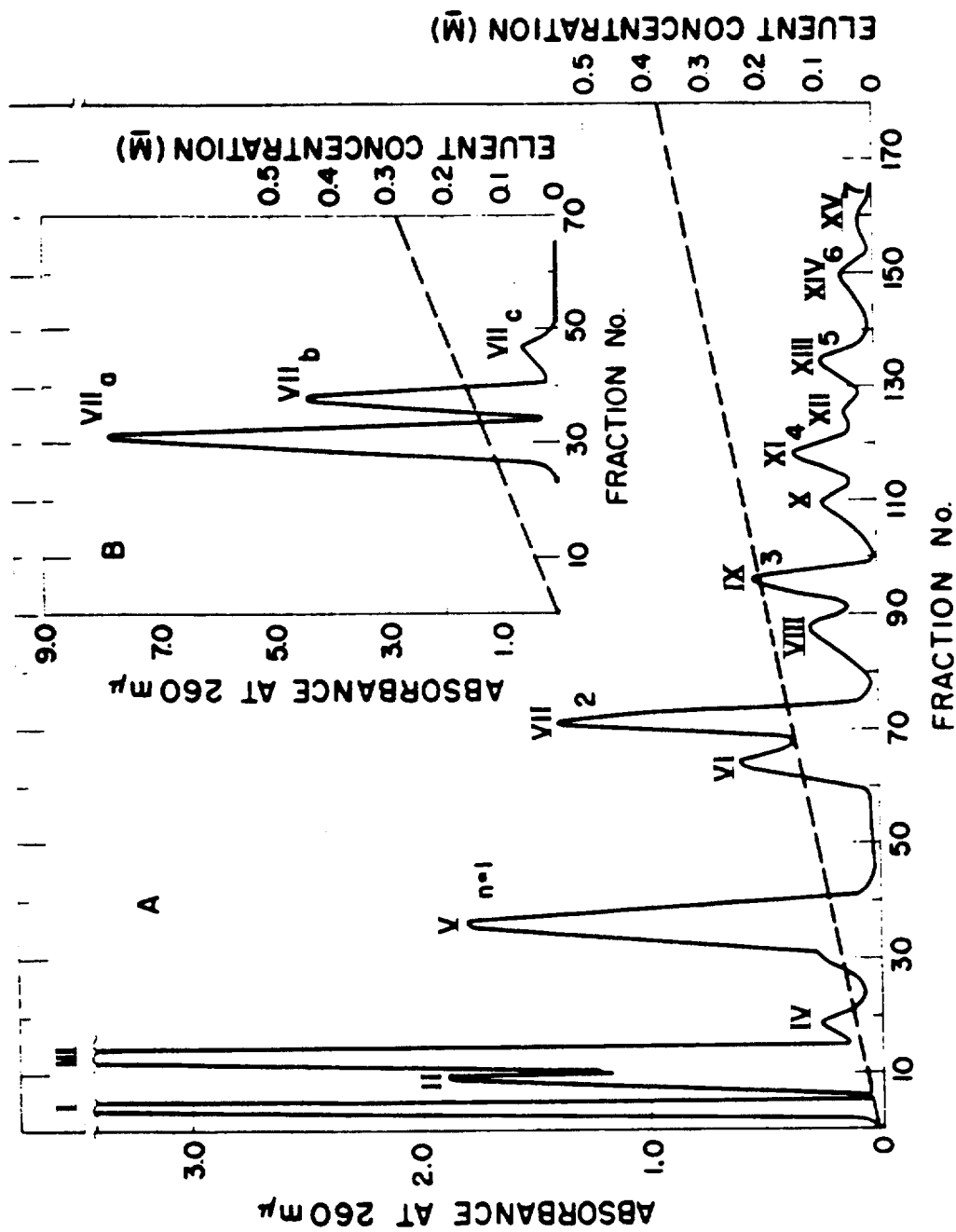


Fig. 2. Column chromatography of polymerization products of 2'-deoxy-5'-adenylic-8-<sup>14</sup>C acid: (A) at pH 7.5, and (B) rechromatography of peak VII (dimer) at pH 5.5.

contaminant, VIIB, was identified as the unsymmetrical pyrophosphate of pa and papa.

Oligomers of 2'-Deoxy-5'-guanylic Acid.--The polymerization of pyridinium N-acetyl-2'-deoxy-5'-guanylate (III) was carried out with DCC in a solution of N,N-dimethylformamide in the presence of anhydrous pyridinium Dowex 50W-X4 according to published procedures (13). After 7 days the reaction was quenched with water, pyrophosphates were removed by acetic anhydride-pyridine treatment, and the resultant fully acetylated products were fractionated on a DEAE-cellulose column with a linear 0 to 0.5 M (4 l., pH 6.8) lithium chloride gradient. Half the total material was present in fractions beyond the pentamer peak where resolution became increasingly poor. The monomer fraction, the largest, represented 20 percent of the starting material. Dimer (10 percent yield), trimer (9 percent yield), and tetramer (4 percent yield) were identified by total-to-terminal phosphorus ratios following phosphomonoesterase treatment. Values of  $\epsilon(P)$  at  $\lambda_{\max}$  255 m $\mu$  were as follows: monomer (N-acetyl),  $17.6 \times 10^3$ ; dimer (fully acetylated),  $15 \times 10^3$ ; and trimer (fully acetylated),  $10.8 \times 10^3$ .

## DISCUSSION

Although Route B should produce any desired oligonucleotide in the fewest number of reaction steps, the yields in the condensations are only around 50 percent with the most satisfactory terminal-phosphate block (2-cyanoethyl). This group is lost to some extent during the reaction, which leads to undesired by-products (14). The acid-labile blocking group, benzhydryl (9), was unexpectedly found to be completely expelled with the more efficient condensing agents. Route C, limited polymerization, although relatively simple to carry out, can provide only a few possible oligonucleotide sequences and also gives mixtures of compounds which are difficult to separate. Route D, in practical application, is restricted to the homo-oligomers. Route A, therefore, appears to be the method of choice. Although more steps are involved, good yields are obtained with essentially no side reactions or scrambling of sequence.

## REFERENCES

- (1) D. L. Williams, V. N. Kerr, and R. E. Hine, Los Alamos Scientific Laboratory Report LA-3132-MS (1964), p. 263.
- (2) F. N. Hayes and V. E. Mitchell, this report, p. 178.
- (3) T. M. Jacob and H. G. Khorana, J. Am. Chem. Soc. 87, 368 (1965).
- (4) G. M. Tener, J. Am. Chem. Soc. 83, 159 (1961).
- (5) F. Cramer, H. P. Baer, H. J. Rhaese, W. Saenger, K. H. Scheit, G. Schneider, and J. Tennigkeit, Tetrahedron Letters 16, 1039 (1963).
- (6) H. G. Khorana and J. P. Vizsolyi, J. Am. Chem. Soc. 83, 675 (1961).
- (7) H. G. Khorana, Some Recent Developments in the Chemistry of Phosphate Esters of Biological Interest, John Wiley and Sons, Inc., New York (1961).
- (8) H. Schaller and H. G. Khorana, J. Am. Chem. Soc. 85, 3828 (1963).
- (9) D. L. Williams, this report, p. 196.
- (10) H. G. Khorana, J. P. Vizsolyi, and R. K. Ralph, J. Am. Chem. Soc. 84, 414 (1962).
- (11) H. G. Khorana, A. F. Turner, and J. P. Vizsolyi, J. Am. Chem. Soc. 83, 686 (1961).
- (12) R. K. Ralph and H. G. Khorana, J. Am. Chem. Soc. 83, 2926 (1961).
- (13) R. K. Ralph, W. J. Conners, H. Schaller, and H. G. Khorana, J. Am. Chem. Soc. 85, 1983 (1963).
- (14) G. Weimann and H. G. Khorana, J. Am. Chem. Soc. 84, 419 (1962).



# CHEMICAL SYNTHESIS OF OLIGODEOXYRIBONUCLEOTIDES: PROTECTIVE GROUPS FOR 5'-PHOSPHATE (D. L. Williams)

## INTRODUCTION

Report of a preliminary investigation by Cramer (1) indicated that the acid-labile benzhydryl group might be a very good blocking group for phosphate and had afforded good yields of 5'-thymidylic acid dinucleotide. A study of benzhydryl and substituted benzhydryl blocking groups for phosphate in step-wise synthesis of oligonucleotides was consequently undertaken.

## METHODS AND RESULTS

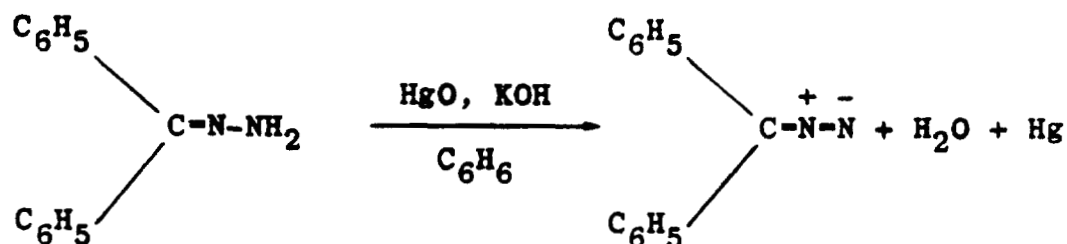
The benzhydryl ester of a nucleotide phosphate is readily obtained by the reaction of diazodiphenylmethane and the nucleotide. Since it was anticipated that mild acidic removal conditions would be an essential factor with purine-containing oligonucleotides, a series of substituted diazodiphenylmethanes was prepared with various electron-donating and electron-withdrawing groups which affect the stability of the benzhydryl phosphate ester bond.

### Substituted Benzophenone Hydrazones

Published procedures (2,3) for the preparation of hydrazones from aromatic ketones afforded mixtures of the desired monohydrazone and the symmetrical dibenzophenone hydrazone (ketazine). Reaction of each ketone with a 5 fold excess of anhydrous hydrazine in refluxing 1-pentanol afforded good yields of the corresponding hydrazone with very little, if any, ketazine formation.

### Diazodiarylmethanes

Oxidation of each hydrazone in benzene solution at 10°C with an excess of yellow mercuric oxide (3) gave the corresponding highly colored (red to purple) diazodiarylmethane, as illustrated by the following equation:



The series of diazodiphenylmethanes prepared by this method are given in Table 1 together with Hammett  $\sigma$  values (4) for the various substituent groups. The  $\sigma$  values are a measure of the ability of the substituent to change the electron density at the reaction center; negative values indicate electron-donating character, whereas a positive value indicates electron-withdrawing ability.

It was expected that reactivity of a diazodiarylmethane in esterifying nucleotide phosphate and ease of removal of the resulting benzhydryl blocking group would parallel the electron-donating character of the substituent group(s). This proved to be the case.

TABLE 1. SUBSTITUTED DIAZODIPHENYLMETHANES

Substituent Group(s)	$\sigma$ Value
4,4'-dimethoxy	- 0.550
4-methoxy	- 0.268
4,4'-dimethyl	- 0.340
4-methyl	- 0.170
none	0.000
4-chloro	+ 0.226
4,4'-dichloro	+ 0.452

## Benzhydryl and Substituted Benzhydryl Esters of 5'-Thymidylic Acid

The reaction of 5'-thymidylic acid, used as a model compound throughout this investigation, with the various diazodiarylmethanes in dimethylformamide at 40° afforded the corresponding benzhydryl 5'-thymidylates in 70 to 95% yields. Since a proton is involved in the reaction mechanism, the reaction was much more rapid with the pyridinium salt of thymidylic acid than with salts of stronger bases such as tributylamine. The resulting esters were purified by evaporation of the solvent, extraction of the residues with ether to remove by-product ketazines, and chromatography on DEAE-cellulose with a triethylammonium bicarbonate gradient.

Acidic hydrolysis studies with the 4-chlorobenzhydryl, benzhydryl, and 4-methoxybenzhydryl esters indicated the 4-chloro ester to be too stable and the 4-methoxy ester to be too labile for the intended use. Consequently, the 4,4'-dichloro and 4,4'-dimethoxy derivatives were not prepared. The benzhydryl ester, which was 50 percent cleaved in 4 hours with dilute acetic acid (pH 2.6) at 26°, was chosen as a model for the following study of dinucleotide formation.

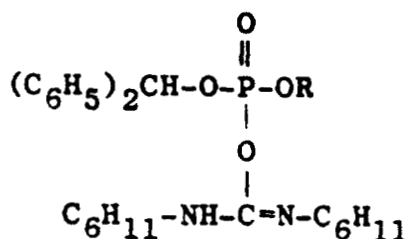
### Reaction of Benzhydryl 5'-Thymidylate with $\underline{O}^{3'}$ -Acetyl-5'-Thymidylic Acid

The reaction of benzhydryl thymidylate (Bhpt) with  $\underline{O}^{3'}$ -acetyl-5'-thymidylic acid (ptAc) and mesitylenesulfonyl chloride in dry pyridine gave an unexpected result. Although 10.4 percent of the Bhpt was recovered unchanged and there was 27 percent of ptpt formed (based on the original Bhpt), there was absolutely no dimer present bearing the benzhydryl phosphate block. A similar reaction, run with 4-chlorobenzhydryl-pt, ptAc, and dicyclohexylcarbodiimide (DCC), gave comparable results.

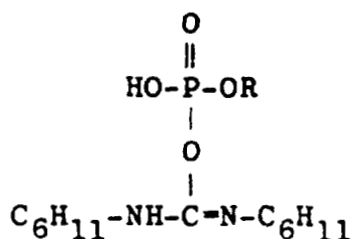
### Reaction of Benzhydryl Thymidylate with Various Carbodiimides

In view of the resulting loss of the phosphate block in the attempted synthesis of a fully protected dinucleotide, various factors were investigated. Bhpt and Bhptpt were unchanged upon standing at room temperature in dry pyridine,

thus eliminating the possibility of a nucleophilic attack on the benzhydryl methyl carbon by pyridine. The results with DCC present suggest that an intermediate, structure A, is formed that is similar to the postulated intermediate formed from unblocked nucleotide and DCC, structure B. Structure A is an unstable phosphate triester and the benzhydryl group could be readily eliminated.



Structure A



Structure B

It was considered possible that sterically hindered carbodiimides might fail to react with Bhpt but still be able to activate ptAc and form a dinucleotide. Hence, Bhpt (0.05 mmole) was treated with several different carbodiimides (0.25 mmole) in dry pyridine (0.5 ml) for 24 hours at room temperature. These reactions were examined by paper chromatography. DCC gave a small amount of pt, a large amount of pyro-pt, and a small amount of residual Bhpt. Diisopropylcarbodiimide gave similar results; the spots, with suitable blanks, were eluted and estimated by ultraviolet absorbance measurements which gave: pt, 6.53 percent; pyro-pt, 32.6 percent; and Bhpt, 60.87 percent. Bis(triphenylmethyl)carbodiimide was practically insoluble and no reaction occurred. Di-p-tolylcarbodiimide gave a very small spot of pyro-pt (1.5 percent), pt was not detectable, and the remainder of Bhpt was unchanged. Di-tert-butylcarbodiimide gave no other products with Bhpt in 24 hours; in fact, the Bhpt was unchanged after 24 days.

Attempted Dinucleotide Formation with Di-tert-butylcarbodiimide (DBC)

Bhpt (0.05 mmole), ptAc (0.1 mmole), and DBC (0.25 mmole)

were dissolved in dry pyridine (0.5 ml) and left for 4 days. Examination by paper chromatography indicated a little pyroptAc and a very small amount of new material at  $R_f$  0.64, which proved to be the protected dimer BhptptAc. Removal of the  $O^{3'}$ -acetyl group with ammonium hydroxide gave a new spot,  $R_f$  0.52, which was completely converted to ptpt,  $R_f$  0.14, by treatment with 80 percent acetic acid. The yield of protected dimer based on Bhpt was 6.3 percent.

### DISCUSSION

In view of the results obtained with the benzhydryl blocking group for phosphate and similar results with benzyl (5) and the base-labile groups 2-cyanoethyl and its derivatives (6,7) and various alkyl ester groups (6,8), it appears that oligonucleotide synthesis with a blocked 5'-terminal phosphate group is not practical with presently known activating agents such as DCC and mesitylenesulfonyl chloride. No further work with this type of reaction is anticipated.

### REFERENCES

- (1) F. Cramer, personal communication.
- (2) A. Schönberg, A. E. K. Fateen, and A. E. M. A. Sammour, J. Am. Chem. Soc. 79, 6020 (1957).
- (3) R. Baltzly, N. B. Mehta, P. B. Russell, R. E. Brooks, E. M. Grivsky, and A. M. Steinberg, J. Org. Chem. 26, 3669 (1961).
- (4) J. Hine, Physical Organic Chemistry, McGraw-Hill Book Company, Inc., New York (1956), p. 144.
- (5) P. T. Gilham and H. G. Khorana, J. Am. Chem. Soc. 80, 6212 (1958).
- (6) D. Soll and H. G. Khorana, J. Am. Chem. Soc. 87, 360 (1965).
- (7) D. L. Williams, V. N. Kerr, and R. E. Hine, Los Alamos Scientific Laboratory Report LA-3132-MS (1964), p. 263.
- (8) F. Cramer, Angew. Chem., Intern. Ed., Vol. I, 331 (1962).

## CHEMICAL STUDIES ON NUCLEOTIDE POLYMERIZATION (A. Murray)

### INTRODUCTION

The synthesis of a library of oligo-5'-thymidylic-2-<sup>14</sup>C acids, for reference use in characterization of new chromatography resins (1) and for highly quantitative use in studying the enzymatic synthesis of polydeoxyribonucleotides, provides an opportunity to determine whether the picryl chloride polymerization mechanism involves the preferential addition of monomer to growing oligonucleotide through addition at the 3'-end, as is generally presumed in the case of dicyclohexylcarbodiimide, DCC (2). or by addition at the 5'-end.

The subject of the present study is (a) the use of isotope to differentiate between these two possible modes of addition of 5'-thymidylic-2-<sup>14</sup>C acid to nonradioactive heptamer; (b) structural analysis of some pyrophosphates formed as by-products; and (c) a comparative evaluation of oligonucleotide stability to DCC and to picryl chloride (PC) under polymerization reaction conditions.

### METHODS AND RESULTS

A mixture of 5'-thymidylic-2-<sup>14</sup>C acid and unlabeled heptamer (0.3 mole percent) was polymerized with PC (1) under very mild conditions (6 hours, room temperature). Following the usual treatment for pyrophosphate cleavage (3), the products were separated cleanly according to charge on a DEAE-cellulose bicarbonate column (pH 7.5) and analyzed with the results presented in Fig. 1. A similar control reaction without added oligomer demonstrated an exponential decrease in yield with  $n$ , as shown by a linear relationship on a semi-log plot, thus validating the extrapolated (dashed) yield line representing only uniformly labeled oligomers  $n = 7 - 11$ . The difference between these values and those for observed yield represents the yield of terminally labeled species. These two values were used with two theoretical models involving labeling separately at the 3'- and 5'-ends to calculate the specific activity of <sup>14</sup>C-pt liberated from the 3'-end by stepwise sequential phosphodiester cleavage of the mixed uniformly and partially labeled isomeric species beyond heptamer. These values are presented in Fig. 2, which defines the limitations inherent in each oligomer for establishing the mode of monomer addition by molecular structure

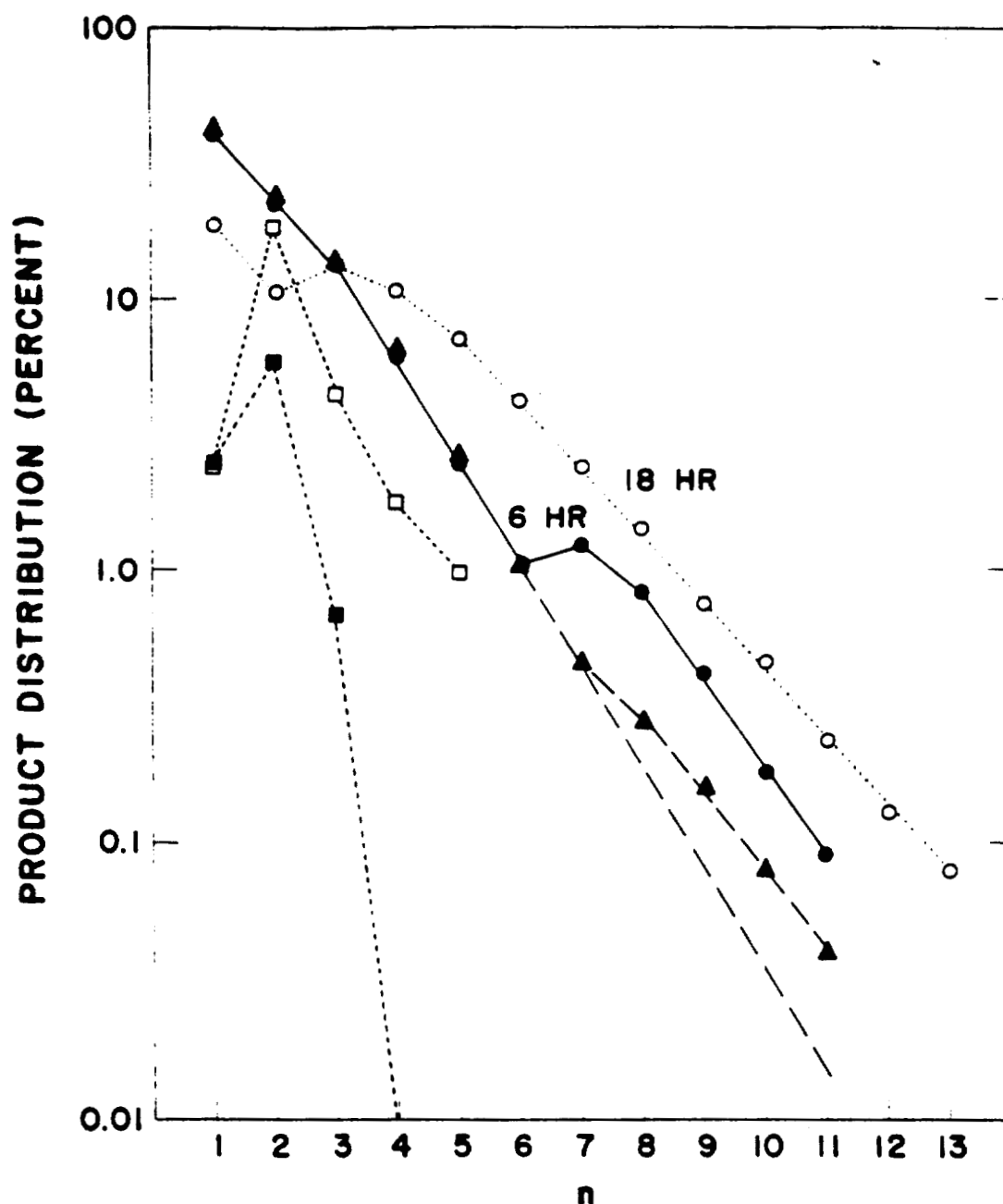


Fig. 1. Distribution of polymerization products formed from  $^{14}\text{C}$ -pt and (pt)7 with picryl chloride (6 hours,  $25^\circ$ ) as isolated by chromatography on DEAE-cellulose bicarbonate at pH 7.5. Linear oligomers: closed circles,  $\text{A}_{267}$ ; closed triangles,  $^{14}\text{C}$ . Cyclic oligomers: closed squares,  $\text{A}_{267}$  and  $^{14}\text{C}$ ; open symbols, control pt only (18 hours).

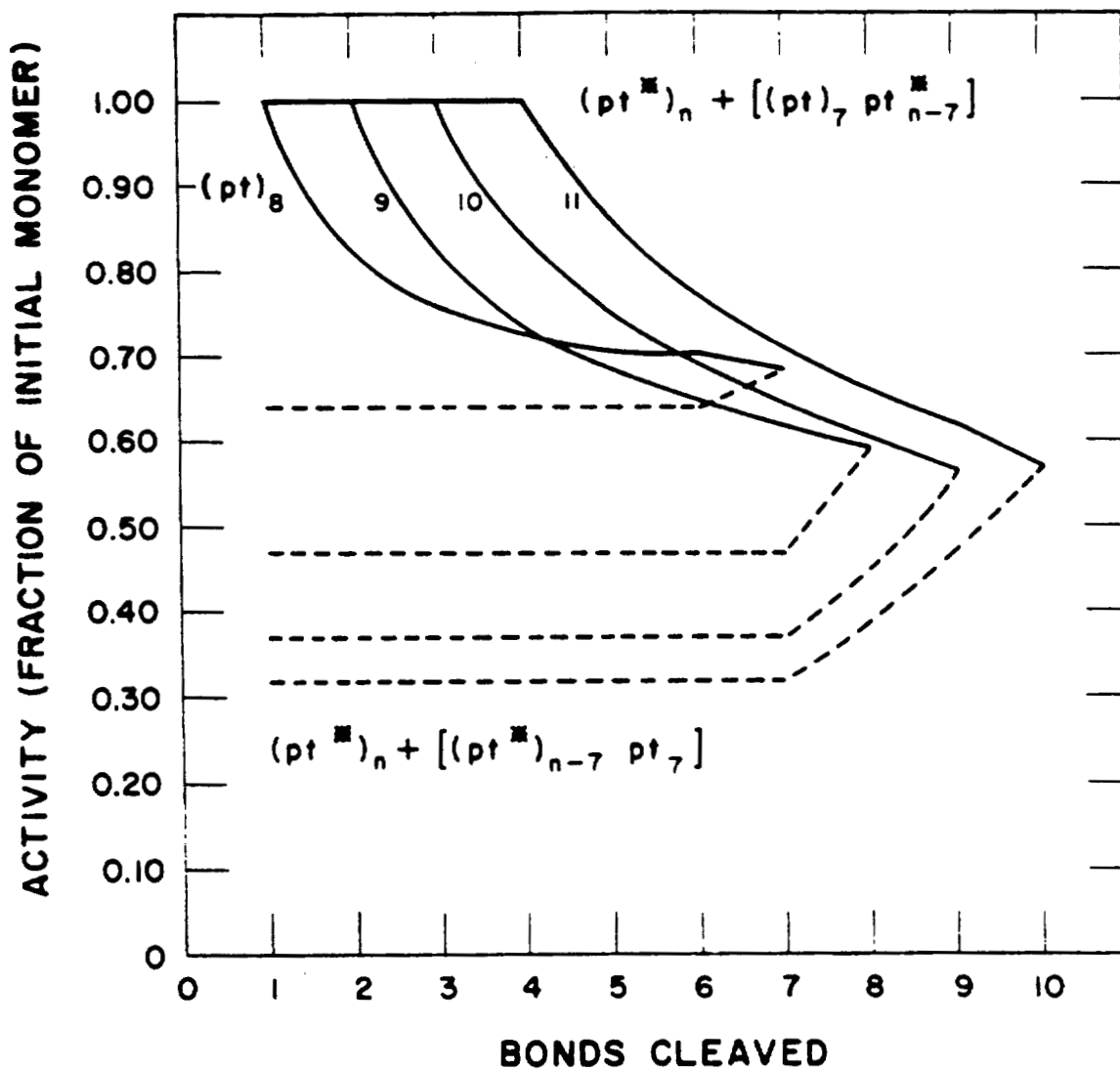


Fig. 2. Calculated specific activity of  $^{14}\text{C}$ -pt liberated stepwise from the 3'-end of isomeric  $^{14}\text{C}$ -oligomers as a function of number of bonds cleaved for two modes of synthesis: — 3'-addition and ---- 5'-addition.



analysis employing the principles of stepwise partial degradation and isotopic dilution.

Two experiments, carried out with Russel's viper venom phosphodiesterase and isolation of the liberated  $^{14}\text{C}$ -pt by column chromatography, yielded specific activities more in agreement with random mode addition than with exclusive addition at either end (Table 1). Figure 3 presents a chromatographic elution profile of these cleavage products which demonstrates that this diesterase contains no endonuclease and, like the more commonly used *Crotalus adamanteus* diesterase, hydrolyzes polynucleotides in a stepwise sequential fashion. It is also apparent from product distribution that continued cleavage of the polynucleotide under attack proceeds more readily than the initiation.

TABLE 1. STRUCTURAL ANALYSIS OF  $^{14}\text{C}$ -pt OLIGOMERS

$^{14}\text{C}$ -(pt) <sub>n</sub>	Bonds Cleaved (average)	Specific Activity (fraction starting value) of pt Liberated by Partial Cleavage with Venom			
		Calculated Addition			Observed
		3'	5'	Random	
9	1.4	1.00	0.47	0.59	0.59
10 + 11	0.9	1.00	0.35	0.56	0.58

Attempts at structural analysis of the other (5') end were made by dephosphorylating  $^{14}\text{C}$ -(pt)<sub>8</sub> with *E. coli* alkaline phosphatase to expose the 5'-terminal nucleoside [giving  $^{14}\text{C}$ -t(pt)<sub>7</sub>], followed by its liberation through complete hydrolysis with venom. These efforts were nullified by mono-esterase contamination present in the diesterase, giving an excessive yield of  $^{14}\text{C}$ -t. This experiment was, however, significant in revealing the presence of a molecular species that resisted repeated dephosphorylation. Investigation

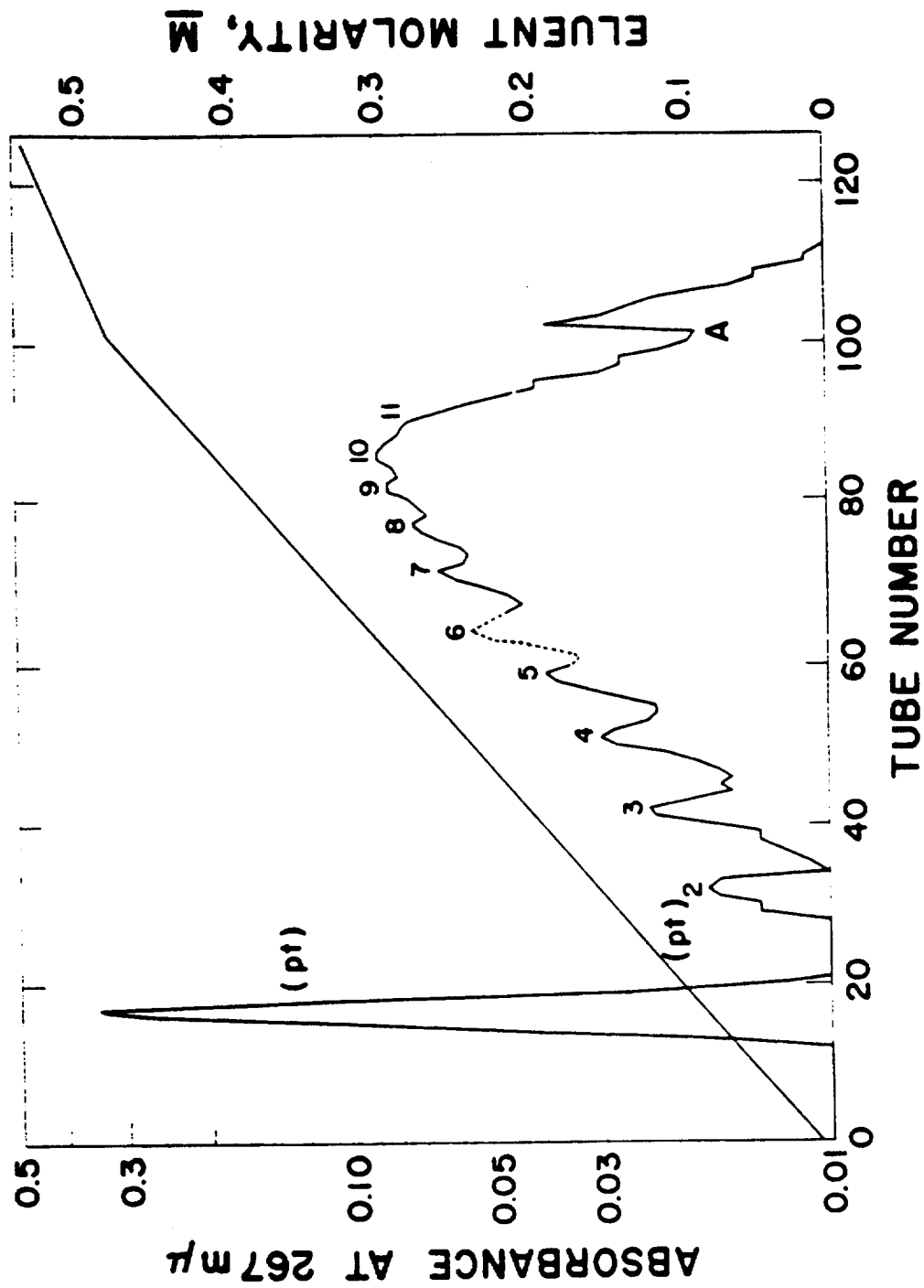


Fig. 3. Elution profile of products released by limited cleavage of  $^{14}\text{C}$ -(pt)10 + 11 by Russell's viper venom phosphodiesterase. Triethylammonium bicarbonate gradient, pH 7.5. Column stopped 3 days at A.

revealed the presence of an unsuspected series of compounds co-eluted with each oligomer in the range  $n = 2$  to at least 8. These compounds were characterized by (a) substantial yields (43 to 62 percent of each "oligomer" peak  $A_{267}$  units); (b) no unique UV or IR spectral properties; (c) specific activities substantially those of the oligomer; (d) no terminal phosphorus (inert to alkaline phosphatase); (e) no 5'-OH (inert to spleen diesterase); (f) presence of 3'-OH (reactive to venom diesterase); (g) no 5'-blocking group that was freed by venom diesterase (collection under vacuum and analysis by gas chromatography with sensitive flame ionization detector); (h) same charge in acid or base; (i) separation from oligomer by rechromatography on DEAE-cellulose chloride with LiCl at pH 4.0; and (j) complete cleavage by resubmission to pyrophosphate cleavage with acetic anhydride-pyridine. Analysis of the degradation products (Table 2) disclosed that the pyrophosphate co-eluted with oligomer  $n$  contained  $n + 1$  monomer units and consisted of a mixture of all possible structures in ratios apparently consistent with the relative abundance of linear oligomer species present in the polymerization mixture (Fig. 1). A discussion of the chromatographic properties of pyrophosphates appears elsewhere in this report.

Parallel experiments under polymerization conditions were carried out (12 days, room temperature) employing PC and DCC with aliquots (3500  $A_{267}$  units) of mixed linear oligomers (pt)5-12 [including  $^{14}\text{C}$ -(pt)6 for identification]. The results following pyrophosphate cleavage and column chromatographic analysis (Table 3) revealed that both condensing agents led to degradation and resynthesis with concurrent shuffling of monomer units. Figure 4 compares elution profiles of aliquot samples, from the DCC run, above and below (pt)4 with the control starting sample.

## DISCUSSION

The unexpected failure of the pyrophosphate removal step after the polymerization of  $^{14}\text{C}$ -pt in the presence of cold (pt)7 and the appearance of  $\text{P}^1, \text{P}^2$ -pyrophosphates among the isomeric-labeled oligonucleotides naturally perturbs any quantitative interpretation of the isotopic dilution measurements. If the radical assumption is made that all initial heptamer was degraded into the monomer pool, its specific activity would be reduced only 2 percent; unreacted  $^{14}\text{C}$ -pt agreed with the calculated starting value. Since the literature indicates the activation of monomer (not oligo) units with resultant 3'-addition is the probable mode of

TABLE 2. DISTRIBUTION OF  $^{14}\text{C}$ -PYROPHOSPHATE DEGRADATION PRODUCTS

Pyro- phosphate Charge	$\mu\text{moles} \left( \frac{A_{267}/\epsilon(P)}{n} \right)$					Assigned Structure	Occurrence Ratio
	pt	(pt) <sub>2</sub>	(pt) <sub>3</sub>	(pt) <sub>4</sub>	(pt) <sub>5</sub>		
4	1.74	2.19	1.85	0	0	$\begin{bmatrix} \text{pt} \\ (\text{pt})_3 \end{bmatrix} \begin{bmatrix} (\text{pt})_2 \\ (\text{pt})_2 \end{bmatrix}$	1.8 to 1
5	0.29	0.90	0.84	0.45	0	$\begin{bmatrix} (\text{pt})_2 \\ (\text{pt})_3 \end{bmatrix} \begin{bmatrix} \text{pt} \\ (\text{pt})_4 \end{bmatrix}$	2.3 to 1

TABLE 3. DISTRIBUTION OF pt OLIGOMERS RESULTING FROM EXPOSURE OF PENTAMER THROUGH DODECAMER TO CONDENSING AGENTS

Reagent	$A_{267}$ Distribution (percent)			Recovery
	(pt) < 5	(pt) 5-12	(pt) > 12	
PC	21.2	75.3	3.5	98
DCC	25.5	64.5	10.0	57
Control	4.0	94.8	1.2	100

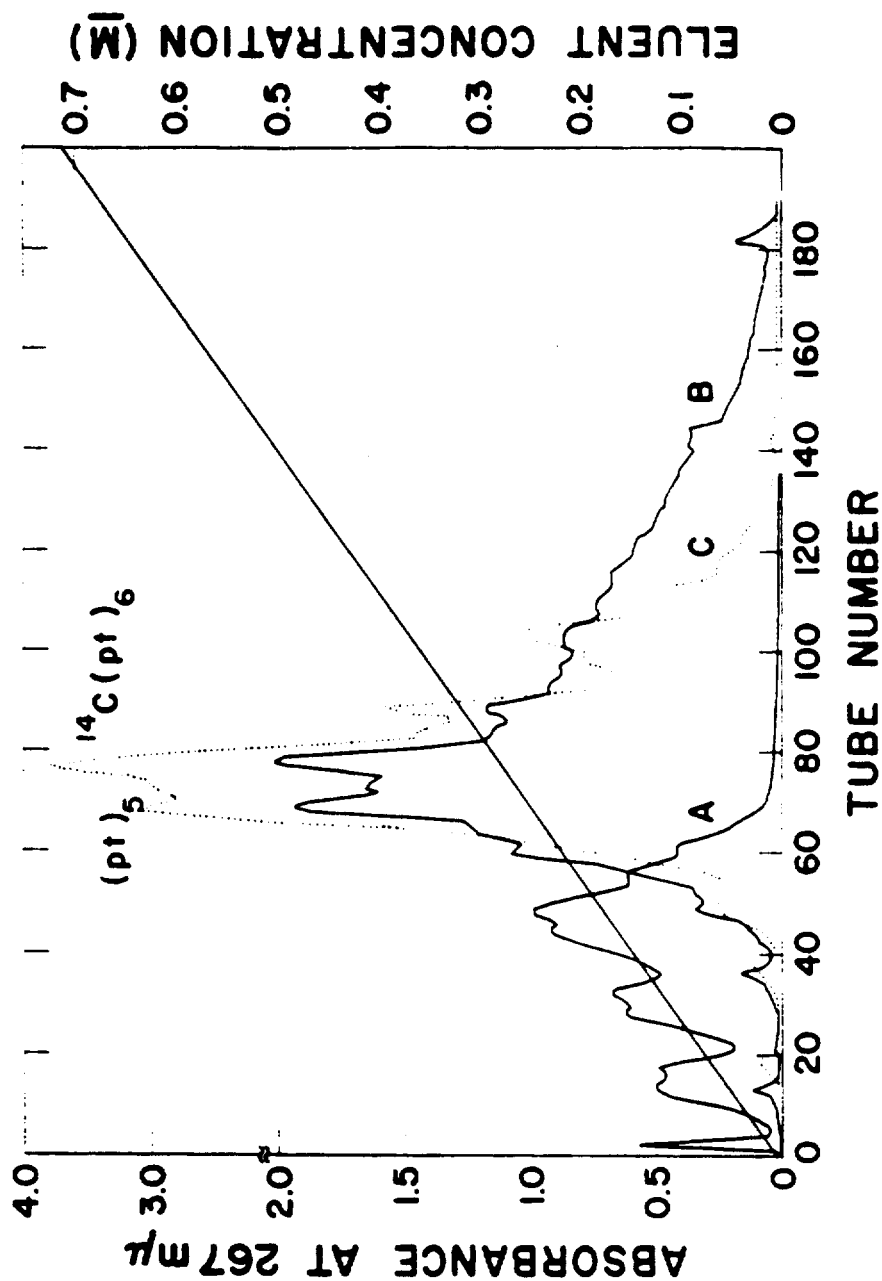


Fig. 4. Chromatographic profiles demonstrating degradation and resynthesis products formed by contact of  $^{14}\text{C}-(\text{pt})_n$  ( $n = 5 - 12$ ) with picryl chloride (12 days, room temperature). DEAE-cellulose column,  $1 \times 14$  cm; triethylammonium bicarbonate gradient, pH 7.5; 7-ml fractions. Curve A, 300 O.D. units,  $n < 5$ ; curve B, 650 O.D. units,  $n > 5$ ; curve C, 650 O.D. units, control.

reaction, it is easier to correlate the measured activity of the 3'-end units with an aberration by dilution rather than enrichment. If it is postulated that initial heptamer may also have contained preformed octamer pyrophosphate (60 percent), which in some manner then largely survived the role of reactive intermediate, the diesterase would have viewed these molecules as two reactive sources of unlabeled pt per molecule. Similarly,  $^{14}\text{C}$ -pyrophosphates formed de novo would provide two sources of  $^{14}\text{C}$ -pt per molecule. A comparison of Fig. 1 with a plot of oligomer specific activity against  $n$  (Fig. 5) indicates that monomer definitely did add to heptamer (2.23 percent initial distribution  $\longrightarrow$  0.43 percent) and suggests the presence of hexameric and especially heptameric species with some degree of nonisotopic origin. The rate of increase in specific activity for the species  $n = 1 - 5$  is too low to be accounted for by hyperchromicity alone and suggests some dilution.

Oligomers for the stability experiments were selected above tetramer so that, while degradation to small species would ultimately result in turnover by resynthesis, a portion would persist as unreactive cyclic isomers. The presence of unsuspected initial pyrophosphates also could account for the observed results. Several observations argue the absence of such contamination: (a) a marked discrepancy between the  $^{14}\text{C}$ - and  $\text{A}_{267}$ -elution profiles (pH 7.5) for tetramer spiked with pyrophosphate-oligonucleotide label; (b) broad center cuts (1/3) from each peak,  $n = 3 - 14$ , contained no component separable by chromatography at pH 4.0. The tetramer and hexamer were not resistant to dephosphorylation, nor were the center cuts (3 to 6 percent) from any peaks; and (c) a different source of oligonucleotides gave similar results with PC (2).

Column separation could be used to evaluate the changes in oligonucleotide-oligopyrophosphate population as a function of polymerization time.

#### REFERENCES

- (1) A. Murray, Los Alamos Scientific Laboratory Report LA-3132-MS (1964), p. 258.
- (2) P. T. Gilham and H. G. Khorana, J. Am. Chem. Soc. 80, 6212 (1958).
- (3) H. G. Khorana, J. P. Vizsolyi, and R. K. Ralph, J. Am. Chem. Soc. 84, 414 (1962).

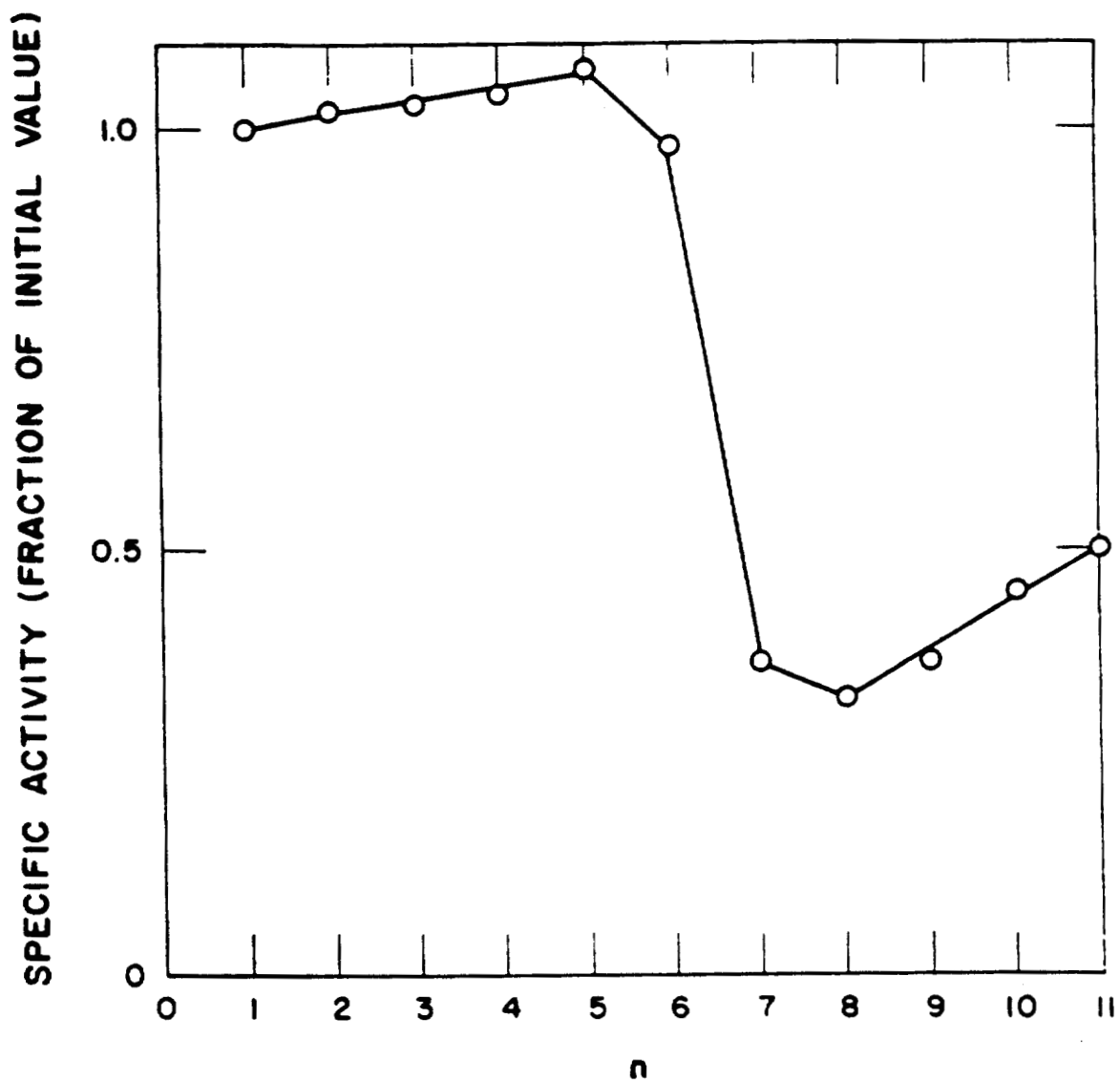


Fig. 5. Specific activity of peaks eluted from DEAE-cellulose at pH 7.5.

# SYNTHESIS OF 2'-DEOXY-5'-NUCLEOTIDE $P^1, P^2$ -PYROPHOSPHATES (A. W. Schwartz and V. N. Kerr)

## INTRODUCTION

Both symmetrical and unsymmetrical nucleotide  $P^1, P^2$ -pyrophosphates are desired as reference compounds in studies of pyrophosphate cleavage and for use as initiators in enzymatic polymerizations.

## METHODS AND RESULTS

According to a published general procedure (1), a mixture of stoichiometric amounts of 5'-thymidylic acid (pt) and thymidylyl-(5':3')-5'-thymidylic acid [(pt)<sub>2</sub>] as pyridinium salts was dissolved in triethylamine and pyridine and N,N'-dicyclohexylcarbodiimide was added in 10 fold excess. After 19 hours, the reaction was quenched with several volumes of water, the dicyclohexyl urea was filtered off, and the filtrate was concentrated. Fractionation was accomplished on a 2 x 30-cm DEAE-cellulose column with a linear 0.005 to 0.5 M (4 l., pH 7.5) triethylammonium bicarbonate gradient. Three peaks were obtained (Fig. 1) with the mid-peak being an obvious composite. Peaks I and III [pyro-(pt) and pyro-(pt)<sub>2</sub>, respectively] were chromatographically homogeneous by paper chromatography, while the first half of peak II (IIa) showed the presence of the mixed pyrophosphate and a trace of (pt)<sub>2</sub> and the latter half (IIb) showed only a single spot of the mixed pyrophosphate (Table 1). No unreacted monomer was found.

To establish the identity of the components in the three peaks, samples were taken from peaks I, IIb, and III. These were individually treated for 4 days with an excess of acetic anhydride and pyridine (2) and were chromatographed on paper. Only pt resulted from peak I, both pt and (pt)<sub>2</sub> resulted from IIb, and only (pt)<sub>2</sub> came from peak III.

The greater reactivity of monomer than dimer can be utilized where only the unsymmetrical pyrophosphate is sought by using an excess of the monomer to completely convert dimer to mixed pyrophosphate. A large-scale reaction mixture was prepared containing a 10 fold excess of pt and run for 1 day. Fractionation of the product was obtained on a 2.2 x 34-cm column



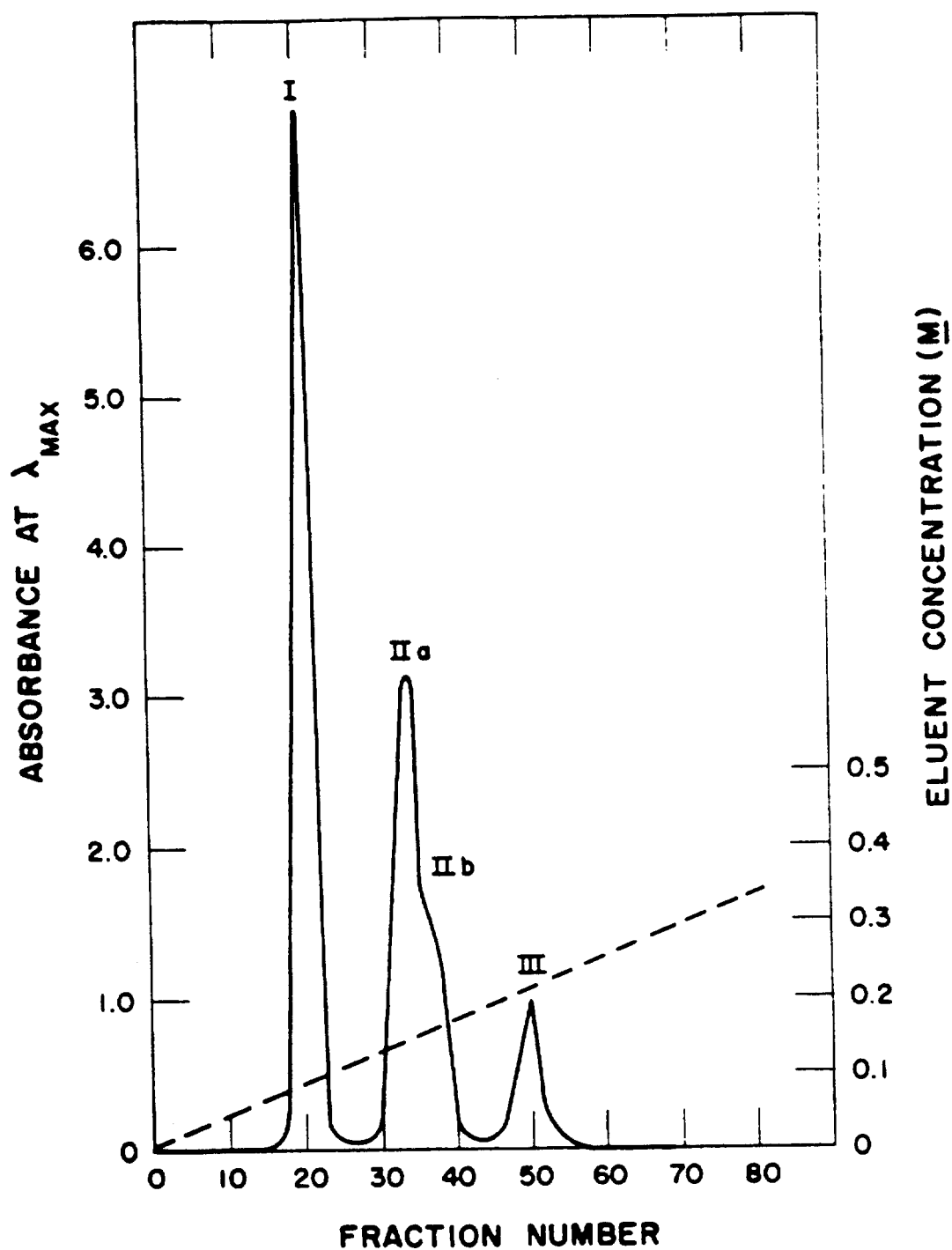


Fig. 1. Column chromatography elution profile for  $P^1, P^2$ -pyrophosphate synthesis from 5'-thymidylic acid monomer and dimer mixture.

TABLE 1. PAPER CHROMATOGRAPHY  $R_f$  VALUES OF PYROPHOSPHATES AND COMPONENTS

Compound	$R_f$ Values*
pyro-(pt)	0.53
pt-pyro-(pt) <sub>2</sub>	0.42
pyro-(pt) <sub>2</sub>	0.36
pt	0.32
(pt) <sub>2</sub>	0.21

\* 2-Propanol, ammonium hydroxide, water; 65:10:25; Whatman No. 31 paper.

of DEAE-cellulose with a linear 0 to 0.5 M (2 l., pH 4.0) lithium chloride gradient. Analysis of the fractions revealed that an excess of 90 percent (neglecting hypochromicity) of the dimer was utilized in the synthesis of the mixed pyrophosphate.

#### DISCUSSION

Symmetrical and mixed  $P^1, P^2$ -pyrophosphates can be obtained from a reaction containing two different nucleotides. This approach will be utilized to synthesize a series of pyrophosphates. The observation that this class of compounds can function to initiate the terminal deoxyribonucleotidyl transferase reaction (3) will be further explored to characterize the macromolecular pyrophosphates thus formed.

#### REFERENCES

- (1) H. G. Khorana and J. P. Vizsolyi, J. Am. Chem. Soc. 81, 4660 (1959).
- (2) H. G. Khorana, J. P. Vizsolyi, and R. K. Ralph, J. Am. Chem. Soc. 84, 414 (1962).
- (3) F. N. Hayes and V. E. Mitchell, this report, p. 178.

## OLIGONUCLEOTIDE CHROMATOGRAPHY (A. Murray)

### INTRODUCTION

The object of this investigation is 4 fold: (a) to develop and employ a standardized analytical chromatography system to (b) characterize new anion exchange media of varying weak-base strength and (c) evaluate the contribution of base strength to the chromatographic binding process in (d) the development of resins with better resolution than the commonly employed DEAE-cellulose for separating oligonucleotides in the size range of decamer and beyond.

### METHODS AND RESULTS

The base strength of 34 previously synthesized new amine-substituted cellulose anion exchange resins (1) has been re-determined by automatic titration for greater reliability. Twenty resins with single inflection curves covered the range  $pK_b$  5.0 to 8.5.

A library of linear oligo-5'-thymidylic acids,  $n = 1 - 23$ , was prepared by DCC polymerization at the 24-mmole scale employing the partial block, unblock, and boost principle (2). Following pyrophosphate cleavage and chromatographic isolation from DEAE-cellulose ( $HCO_3^-$ ), the center (3 to 6 percent) of each peak was pooled and characterized before and after dephosphorylation (bacterial alkaline phosphatase) by column chromatographic properties in a standardized analytical system (fixed conditions of DEAE-cellulose, column size, elution rate, temperature, and linear gradient) with changes of pH and elution ion (Fig. 1). The results of  $\epsilon(P)$  determinations are presented in Fig. 2. Final purification was achieved by re-chromatography, separately, of the pooled odd and even numbered peaks on DEAE-cellulose (pH 7.5, triethylammonium bicarbonate-TEAB). The central one-third of each peak was taken to serve as standard oligodeoxyribonucleotide in the range  $n = 1 - 12$ , while the entire peak was used in the lower yield and more poorly resolved species. The standard test sample for initial screening of resins (1 x 10-cm columns) consisted of an aliquot of a solution containing equal A267 units of the oligomers  $n = 1 - 10$  and one-half amounts of  $n = 11$  and 13; the standard gradient was linear 0 to 0.5 M per 1000 ml.

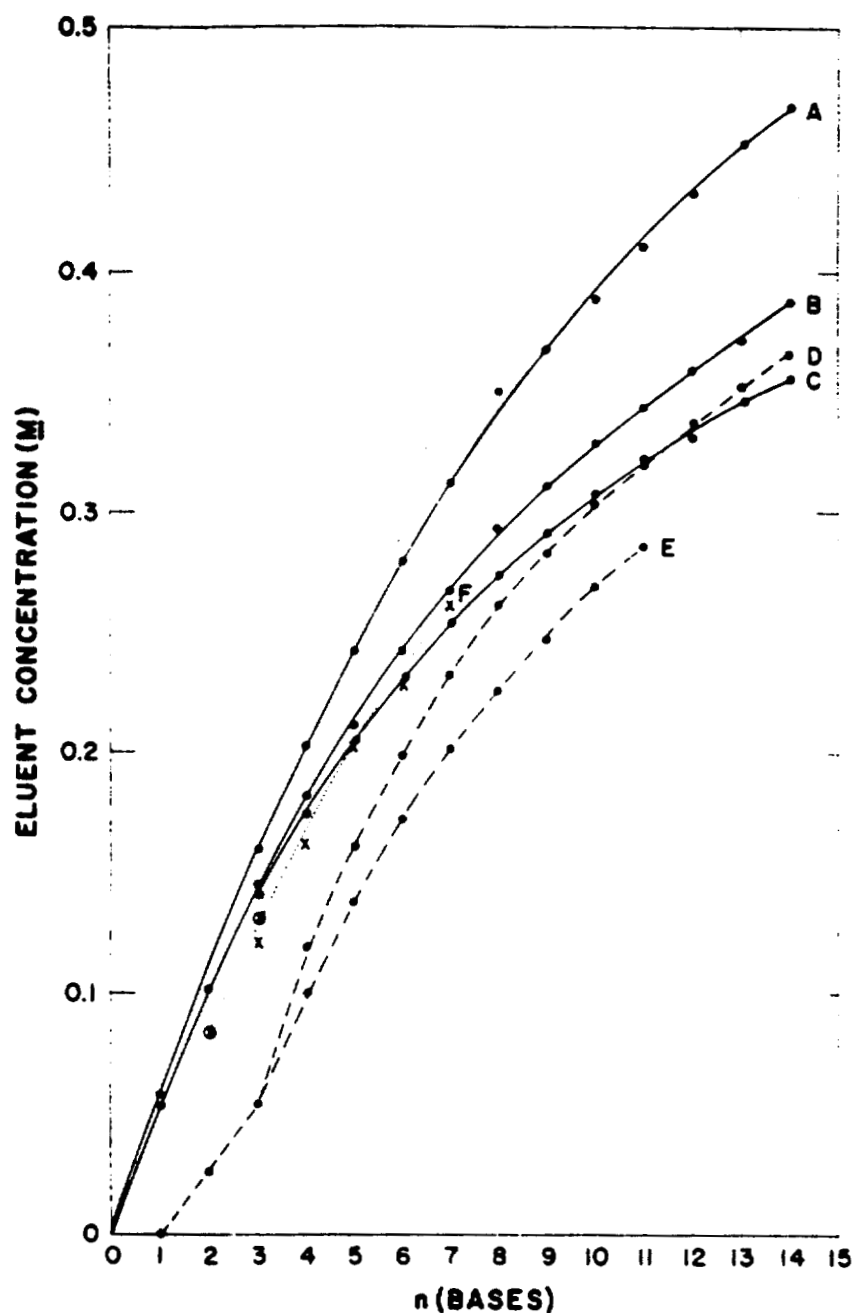


Fig. 1. Chromatographic properties characterizing oligo-5'-thymidylic acids and DEAE-cellulose under standardized conditions (1 x 10-cm column, linear gradient 0 to 0.5 M in 1 l., 1 ml/min). Series (pt)<sub>n</sub>: (A) TEAB, pH 7.5, (B) LiCl, pH 4, (C) LiCl, pH 7.5; t(pt)<sub>n</sub>: (D) LiCl, pH 4, (E) LiCl, pH 7.5; and pyrophosphate: (F) LiCl, pH 4.

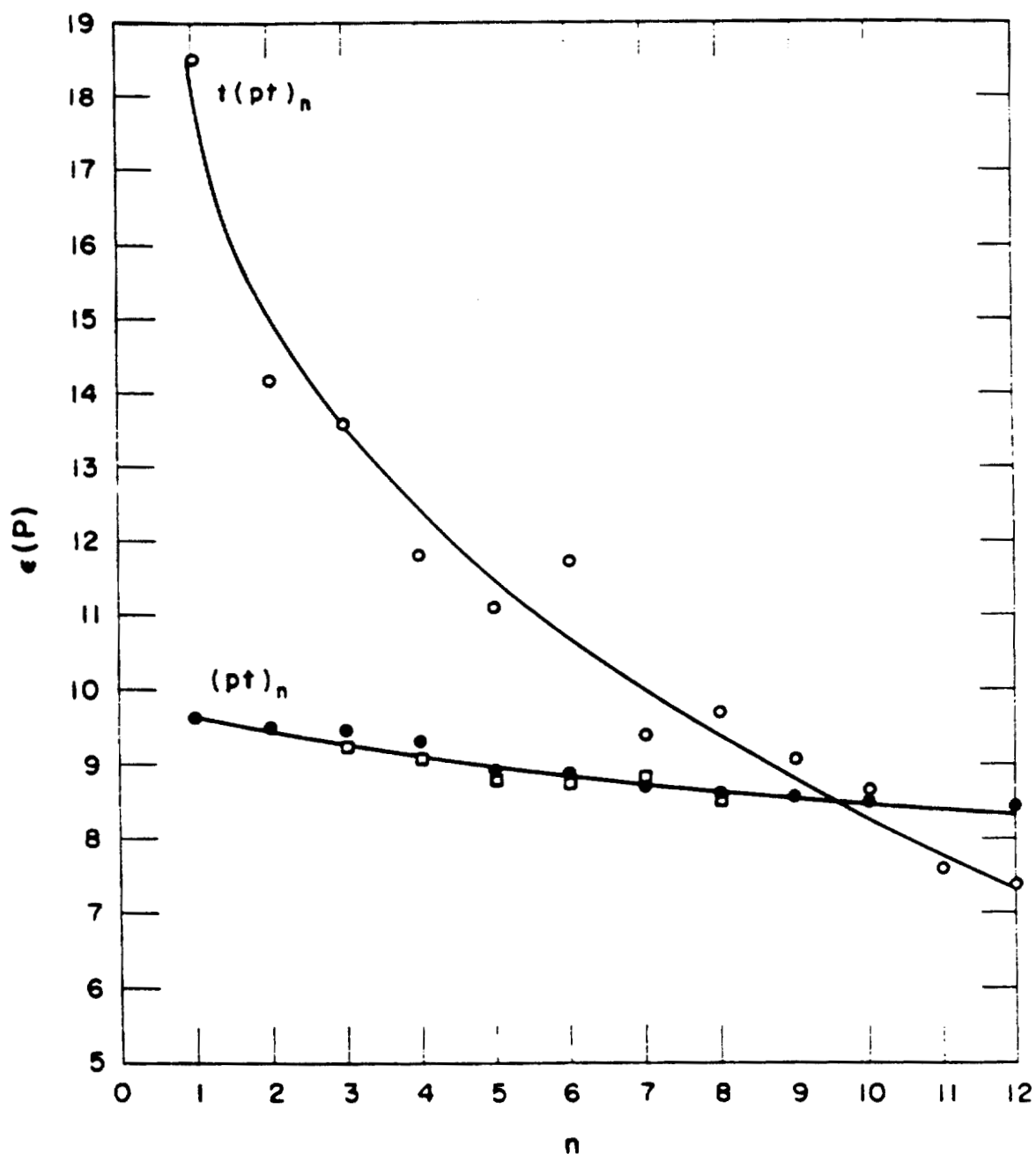


Fig. 2. Specific absorbance of oligo-5'-thymidylic acids and dephosphorylated derivatives (3 to 6 replicate phosphorus analyses).

The TEAB elution profile standardizing the reference DEAE-cellulose (BioRad) showed an essentially unchanged distribution of absorbance units per peak and a progressive degeneration, above dimer, of the base line and resolution as the volume separating peaks decreased to a constant value (Fig. 3). Increasing column length 4 fold resulted in higher, narrower peaks, characterized by 10 percent further spacing, higher elution molarity, and no improvement in base line. Plots of eluent molarity and moles passed through the column, as a function of  $n$ , disclosed that oligomers were released as a linear function of the latter but with a steeper slope in the case of greater number of binding sites (Fig. 4). While molarity is developed linearly with volume, the total mmoles is a second order function of that fundamental parameter characterizing a peak:

$$M = M_0 + V/V_f (M_f - M_0) = M_0 V + V^2/2V_f (M_f - M_0),$$

where  $M$  is the molarity of eluent after volume ( $V$ ) has passed,  $M_0$  and  $M_f$  are initial and final molarities, and  $V_f$  is the final (total) volume.

The (pt)<sub>13</sub> peak revealed the expected two adjacent oligomers when chromatographed alone on DEAE-cellulose (Cl<sup>-</sup>, pH 4.0). Chromatography with a flatter gradient reduced markedly both molarity and total mmoles at elution (Table 1). Similar value changes were observed with the lower oligonucleotides and pyrophosphate derivatives. It was found that washing with 0.130 M TEAB released tetramer pyrophosphate from DEAE after passage of 32.2 mmoles, in agreement with the results of standard gradient elution (0.18 M, 32.3 mmoles).

It is perhaps significant that DEAE-cellulose of approximately the same exchange capacity, but another manufacturer, gave a standard TEAB elution profile characterized by pronounced shift to the left, 15 percent span reduction, extreme degeneration of the base line, and very poor resolution.

A new, relatively stronger base, resin ECP1D-SF1 (pK<sub>b</sub> 5.0), was characterized by a standard TEAB elution profile with very poor resolution and weak binding -- doubtless influenced by its lower exchange capacity, 0.12 meq/g. Monomer was released by 0.49 mmole of loading buffer (0.005 M), and the last oligonucleotide appeared at 0.092 M, 10.8 mmoles. Step elution, on the other hand, with 1000 mI of 0.020 M TEAB gave

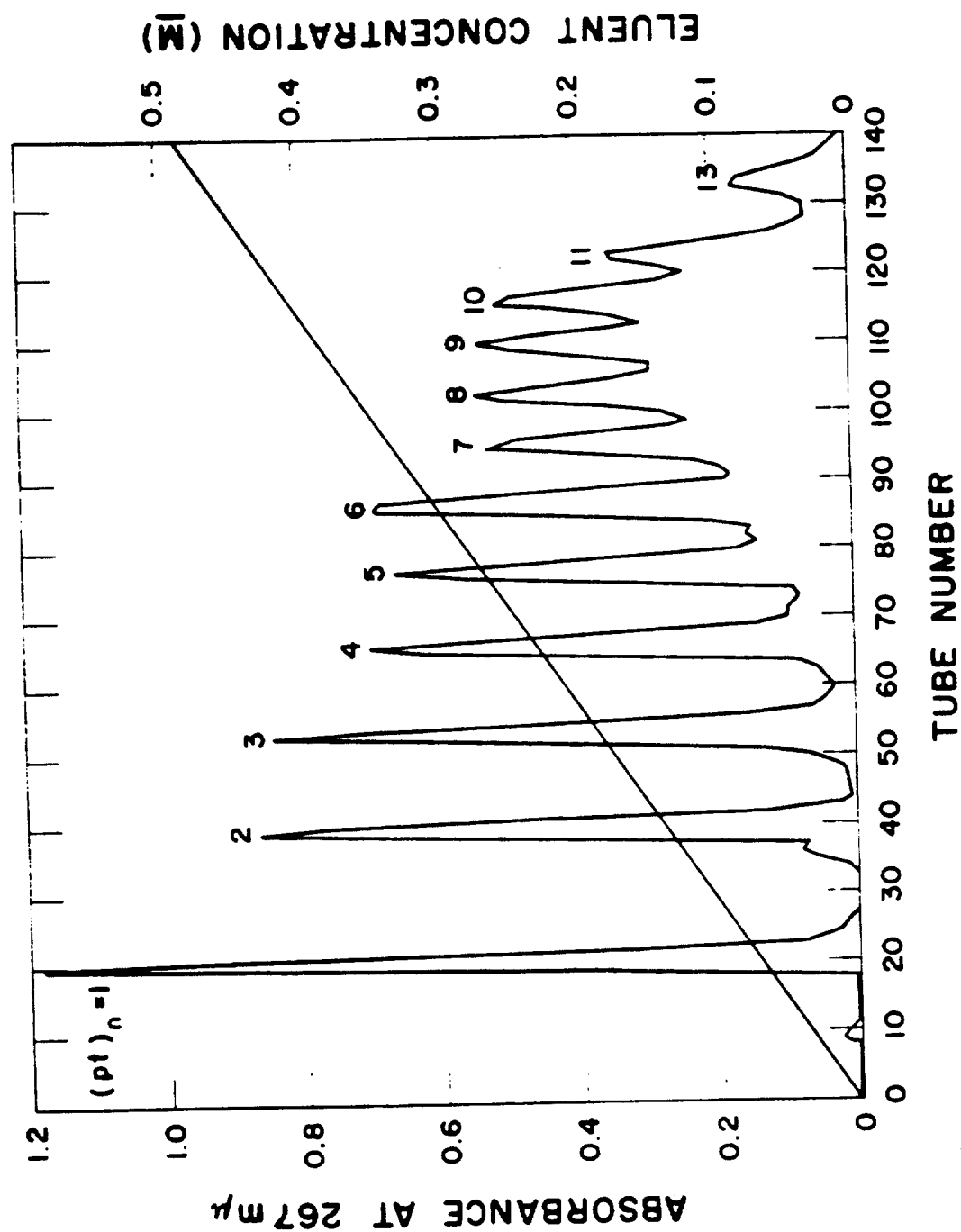


Fig. 3. Chromatographic elution profile of oligo-5'-thymidylic acids with DEAE-cellulose and TEAB (7.1-ml fractions, pH 7.5).



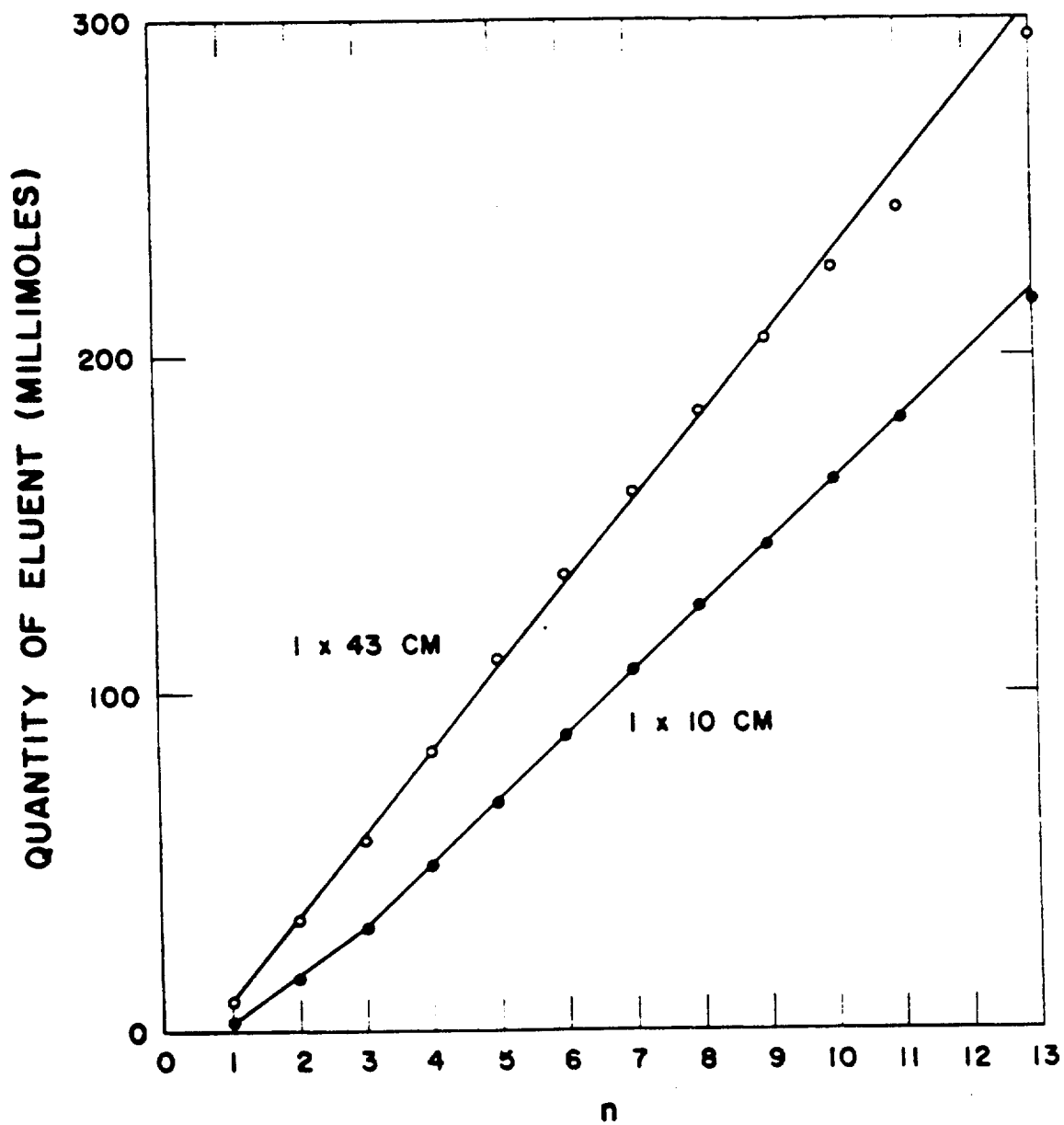


Fig. 4. Elution properties of oligo-5'-thymidylic acids.  $(pt)_n$ , from DEAE-cellulose with TEAB (pH 7.5) as a function of column length.

TABLE 1. VARIATION OF ELUENT MOLARITY AND ELUENT MOLES WITH THE GRADIENT

Linear Gradient LiCl per 1000 ml, pH 4						
0 to 0.5 <u>M</u>				0.3 to 0.5 <u>M</u>		
(pt) <sub>n</sub>	<u>M</u>	mmoles	Distribution (percent)	<u>M</u>	mmoles	Distribution (percent)
12	0.358	128	23	0.339	71	33
13	0.378	143	48	0.350	81	47
14	0.402	162	28	0.371	120	20
10	0.306	94		0.282	56	
10-pyro	0.323	104		0.289	70	

excellent resolution through hexamer, but at an exponential increase in volume and with characteristic tailing. Quantitative analysis of these first 5 peaks, with standardized DEAE-chloride system, showed that separation did follow charge. Loss of resolution attended the higher elution steps, as species tended to concentrate with each new front. Figure 5 shows that the total number of mmoles, characterizing species released by a level eluent, does not follow the linear relationship with  $n$  that is developed by linear gradient elution.

A new, still weaker base, resin ECMOR-SF1 ( $pK_b$  8.5, 1.11 meq/g) was characterized by a TEAB elution profile (0.005 to 0.1 M per 1000 ml) with fair resolution. This time both monomer and dimer were released sequentially by the loading buffer, while the last oligonucleotide appeared at 0.020 M, 4.9 mmoles. This resin is characterized by extreme swelling with ionic strength.

#### DISCUSSION

Contrary to expectation, the degree of column resolution achieved in separating oligo-5'-thymidylic acids on DEAE-cellulose with a linear gradient is not always a function of the elution profile span [see Fig. 1 ( $C > B > A$ ) and Fig. 4 (long > short)]. Rechromatography of pooled alternate members of the series did improve resolution, but the anticipated abrupt return to base line (vacant space) did not occur.

Parameters to be more fully investigated with the standardized resin-oligonucleotide system are varying load, exchange capacity (homo- versus hetero-dilution), gradient (concave upward), pH, and eluting anion. The first order screening of new resins will be continued with the lower oligo- series and TEAB to facilitate sample recovery. With the knowledge gained, changes in eluting ion and pH may then be profitably essayed. The scarcer, higher oligonucleotides are being reserved for the most promising resins. The swelling that accompanies the operation of some resins may be controlled by the use of urea in the eluent.

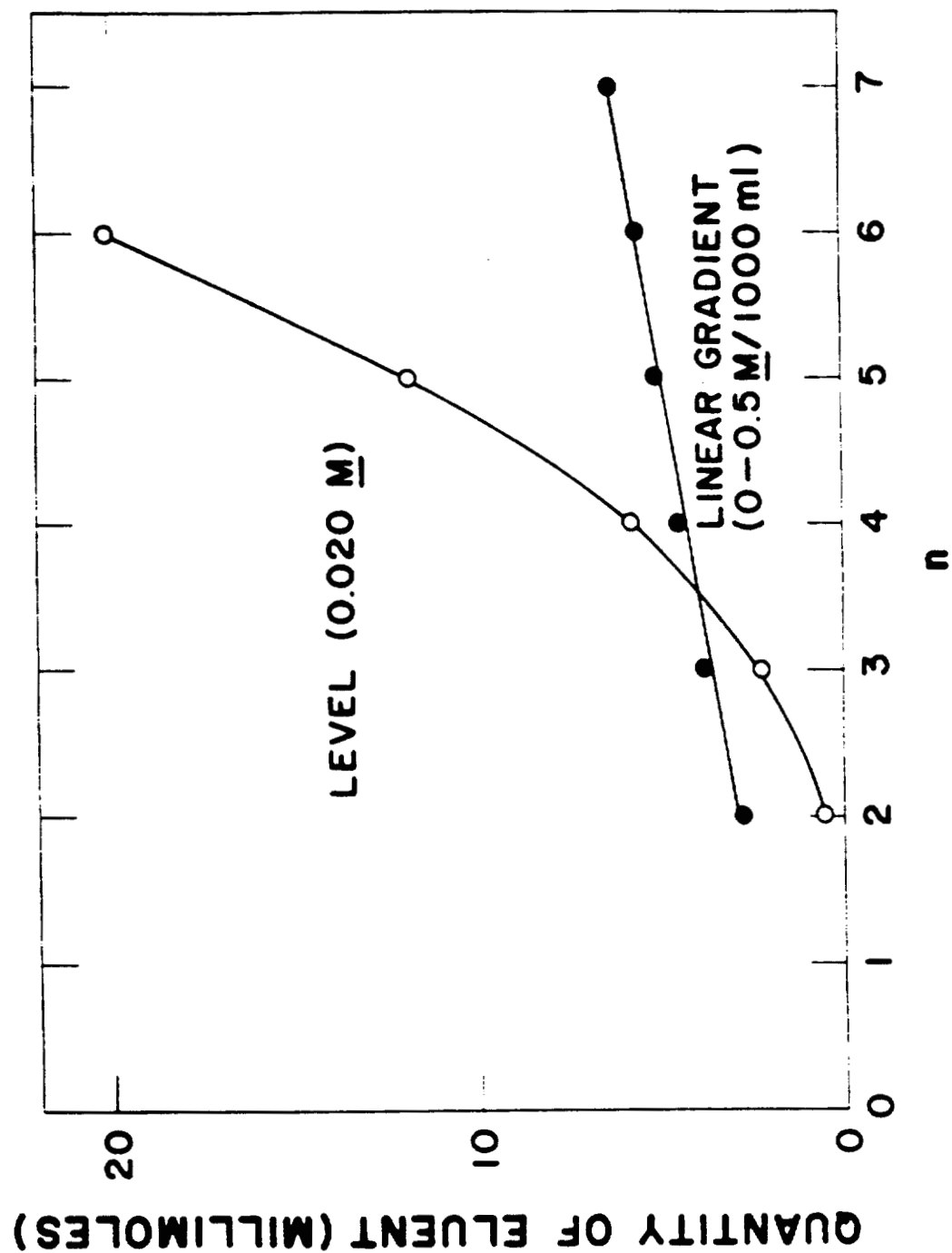


Fig. 5. Elution properties of oligo-5'-thymidylic acids (pt)<sub>n</sub>, from DEAE-cellulose as a function of elution mode.

#### REFERENCES

- (1) A. Murray, V. E. Mitchell, and D. F. Petersen, Los Alamos Scientific Laboratory Report LAMS-2627 (1961), p. 33.
- (2) A. Murray, Los Alamos Scientific Laboratory Report LA-3132-MS (1964), p. 258.

SEPHADEX CHROMATOGRAPHY OF NUCLEIC ACID DERIVATIVES (G. T. Fritz and F. N. Hayes)

INTRODUCTION

Chromatography on gel filtration media is applicable for separation and purification of nucleic acid hydrolysates preliminary to spectrophotometric base analysis. Elution data are being obtained for deoxyribonucleosides and for related compounds likely to be present as impurities.

METHODS AND RESULTS

The compounds were chromatographed on Sephadex G-25 columns at a flow rate of  $0.355 \pm 0.01$  ml min<sup>-1</sup>. Relative  $K_d$  values\* were calculated using a reference value (1) of 1.00 for thymidine when the eluent is 0.005 M triethylammonium bicarbonate (TEAB). Corrections were made for the dead volume of the column and external tubing. Two lots of Sephadex G-25 (one medium and one fine) yielded no observable difference in the relative  $K_d$  values.

Table 1 shows the  $K_d$  values obtained with various eluents. Phosphate buffer at pH 7.0 was chosen to facilitate ultraviolet spectral analysis of the effluent. It was observed that 5'-thymidylic acid (pt), thymidine (t), and thymine (Th) appear as three poorly resolved peaks with equal spacing on an ultraviolet-monitored elution profile using pH 7.0 phosphate buffer as eluent, whereas pt is well separated from t and Th when 0.005 M TEAB is the eluent. Also, it was noted that Zadrazil et al. (2) reported that 5'-uridylic acid (pU) was well separated from uridine (U) and uracil (Ur) in 0.02 M phosphate buffer at pH 7.6. Our values indicate no difference between values obtained with pH 7.0 phosphate buffer and those obtained with pH 7.6 phosphate buffer of the same ionic strength, nor do they show any difference between the series pt, t, and Th and that of pU, U, and Ur. The  $K_d$  of deoxyuridine (u) is indistinguishable from that of U or t.

---

\* $K_d = \frac{V_e - V_o}{V_i}$ , where  $V_e$ ,  $V_o$ , and  $V_i$  are the elution volume, outside volume, and inside volume, respectively.

TABLE 1. RELATIVE  $K_d$  VALUES\* FOR NUCLEIC ACID DERIVATIVES ON SEPHADEX G-25

Compound	Eluent		
	0.02 M Phosphate Buffer at pH 7.0	0.02 M Phosphate Buffer at pH 7.6	0.005 M Phosphate Buffer at pH 7.0 0.005 M TEAB
pu	0.78		0.72
pt	$0.80 \pm 0.01$	$0.82 \pm 0.01$	0.43
u	0.99		1.00
t	1.00	1.00	
U	1.01		1.00
c	$1.07 \pm 0.02$		
Ur	1.18		1.14
Th	$1.20 \pm 0.01$	$1.19 \pm 0.01$	1.18
g	1.76		
a	1.82		

\*Standard deviations are given when more than one determination was made.

\*\*See text for explanation of abbreviations.

The effect of ionic strength was investigated by using 0.005 M phosphate buffer of pH 7.0 as eluent. Although there was an observable difference between it and the 0.02 M buffer, the separation of pU and U was not as great as that of pt and t with TEAB.

Deoxyadenosine (a) and deoxyguanosine (g) have  $K_d$  values similar enough to each other that the two compounds appear in one peak when chromatographed on a column of 1.36 x 100-cm dimensions. A system was set up whereby the effluent was recycled through the column to effect further separation. The result is shown in Fig. 1. A similar separation of deoxycytidine (c) and t should be possible.

#### DISCUSSION

The purine and pyrimidine deoxynucleosides are readily separable as two composite peaks by one pass through Sephadex G-25, and the purine pair can be almost completely resolved from each other by recycling chromatography on the same column. The molecular weights of these compounds are too low and too similar for the gel filtration mechanism to be effective; the results are apparently produced by adsorption effects. Other types of gel filtration media are being investigated for application to nucleic acid degradation products as well as to chemically synthesized derivatives.

#### REFERENCES

- (1) F. N. Hayes, E. Hansbury, and V. E. Mitchell, J. Chromatog. 16, 410 (1964).
- (2) S. Zadrazil, Z. Sormova, and F. Sorm, Coll. Czech. Chem. Commun. 26, 2643 (1961).



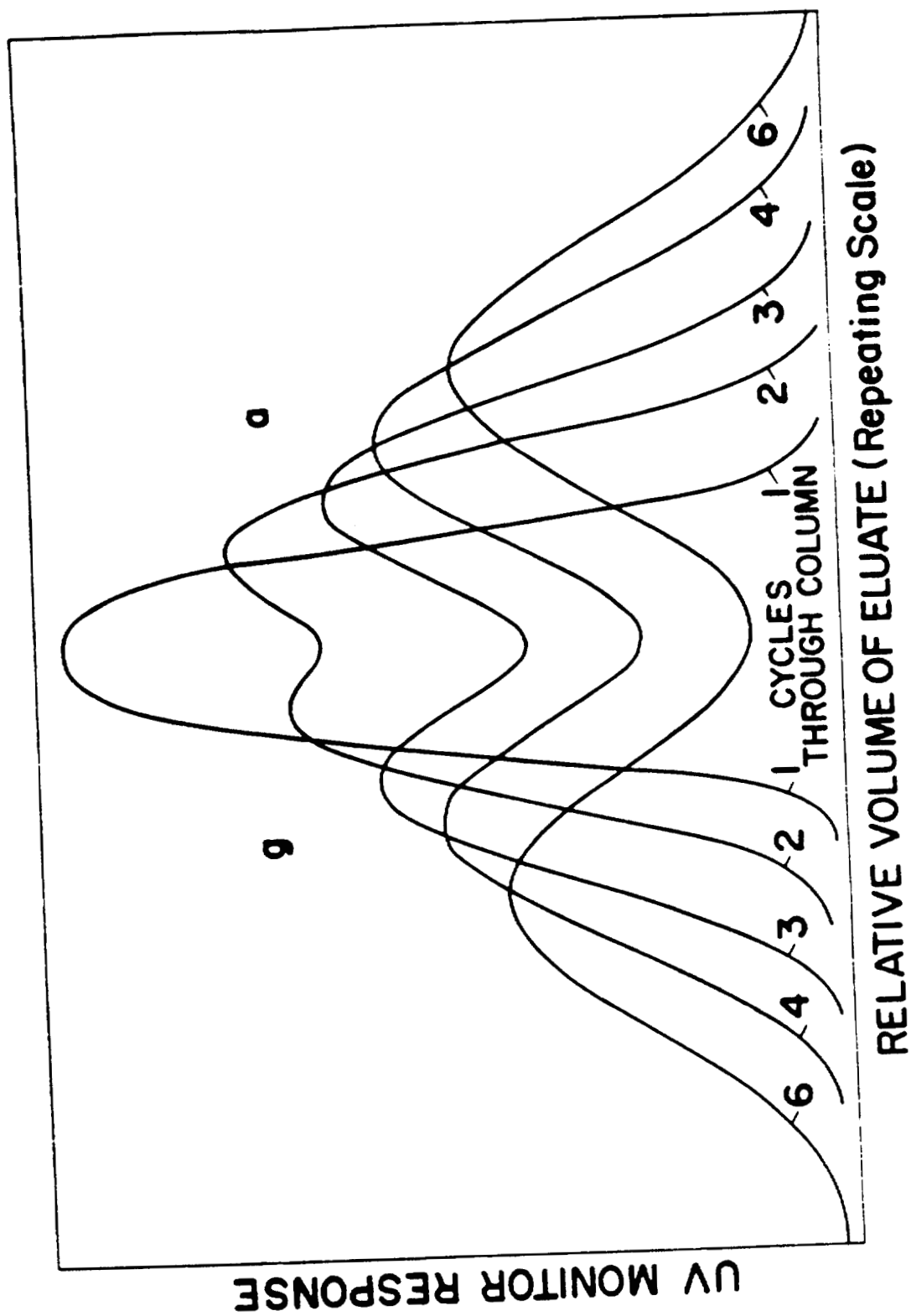


Fig. 1. The effect of recycling on the elution profile of the purine deoxynucleoside peak from Sephadex G-25.

# COMPUTER ANALYSIS OF MULTICOMPONENT ULTRAVIOLET SPECTRA (G. T. Fritz)

## INTRODUCTION

A computer program (1) is being used for the analysis of ultraviolet spectra of multicomponent solutions of nucleic acid derivatives. The object of this study as initially reported (2), the determination of base ratios in naturally-occurring nucleic acids and in oligonucleotides, is being extended to determine base ratios of synthetic polynucleotides. The present report describes the techniques used and the results obtained for a system involving the bases adenine (Ad), guanine (Gu), cytosine (Cy), thymine (Th), and uracil (Ur).

## METHODS

Solutions of the individual bases in the concentration range  $5 \times 10^{-3}$  to  $1 \times 10^{-2}$  M were prepared using Beckman pH 10 buffer as the solvent. The spectra of these solutions were used as the library for the computer analysis. Multicomponent solutions were prepared using appropriate amounts of the reference solutions. Spectra were obtained on a Cary 14 recording spectrophotometer. Absorbance readings were taken every 1.25 m $\mu$ , corresponding to the graduations of the chart paper. The following three schemes were used in the computer analysis by the method of least squares.

### Scheme A

Library consists of spectra of all five possible components. Wavelength range 227.5 to 320 m $\mu$ . Weighting factor 1/Y. Background spectrum subtracted from the solution spectra prior to analysis.

### Scheme B

Library consists only of the spectra of those components known to be present in the solution. Same as scheme A in all other respects.

## Scheme C

Library consists only of the spectra of those components known to be present in the solution. Wavelength range 232.5 to 307.5 mμ. Weighting factor = 1. Background spectrum is treated as a library spectrum.

## RESULTS AND DISCUSSION

Tables 1 and 2 show the results obtained with the three sets of conditions. Using the spectra of all possible components as the library results in some negative values. Computed values are considerably better when the library consists only of the spectra of those components known to be present in the solution. In addition, better results are obtained when the weighting factor equals 1 and when the background spectrum is treated as a library spectrum. As can be seen from Table 1, the standard deviations are in general smaller for scheme C than for scheme A or B. It is instructive to look at the ratios of the two components in the binary solutions (Table 2). Although the errors in the absolute amounts may be larger in scheme C than in scheme B in some cases, the ratios are as good or better in 4 of 6 cases.

Figure 1 is a comparison of the spectrum obtained from a Cary recording (input data) and the best fit found by the computer using scheme B (computed spectrum). Figure 2 is the result of asking the computer to synthesize the binary solution spectrum from the library spectra (computed spectrum) and to compare it to the experimental spectrum (reference spectrum). The discrepancies between the two spectra in Fig. 2 are similar to those between the input spectrum and the computer spectrum in Fig. 1. This fact indicates that the errors incurred are due in large part to unidirectional errors in reading the Cary recording. Several factors may be responsible: (a) slight displacement in origin of recording; (b) slight irregularities in chart paper divisions (sometimes noticeable to the eye); and (c) subjective outlook of operator. Digital output, which is presently being installed, should improve the data with respect to these factors.

More attention will be devoted to obtaining accurate library spectra. The major problem involved in this step is the preparation of reference compounds of known purity and

TABLE 1. COMPUTER ANALYSIS OF MULTICOMPONENT ULTRAVIOLET SPECTRA

Component *	Fraction Taken	Scheme A **		Scheme B		Scheme C	
		Fraction Found	Percent Error	Fraction Found	Percent Error	Fraction Found	Percent Error
Solution A							
Ad	0.6364	0.6468 + 0.0099	1.6	0.6411 + 0.0038	0.7	0.6559 + 0.0037	3.1
Gu	--	-0.0049 + 0.0194					
Cy	--	-0.0101 + 0.0134					
Th	0.3636	0.4100 + 0.0138	12.8	0.3729 + 0.0028	2.6	0.3544 + 0.0055	-2.5
Ur	--	-0.0189 + 0.0176					
Solution B							
Ad	0.5000	0.5084 + 0.0079	1.7	0.5011 + 0.0024	0.2	0.5130 + 0.0022	2.6
Gu	--	-0.0038 + 0.0157					
Cy	--	-0.0162 + 0.0109					
Th	0.5000	0.5443 + 0.0124	8.9	0.5053 + 0.0019	1.1	0.4897 + 0.0032	-2.1
Ur	--	-0.0155 + 0.0152					
Solution C							
Ad	--	-0.0074 + 0.0155					
Gu	0.5714	0.5267 + 0.0300	-7.8	0.5904 + 0.0111	3.3	0.5652 + 0.0023	-1.1
Cy	0.4286	0.4379 + 0.0226	2.2	0.4193 + 0.0115	-2.2	0.4370 + 0.0020	2.0
Th	--	0.0778 + 0.0128					
Ur	--	-0.0148 + 0.0219					
Solution D							
Ad	--	-0.0065 + 0.0154					
Gu	0.5000	0.4583 + 0.0294	-8.3	0.5107 + 0.0091	2.1	0.4929 + 0.0024	-1.4
Cy	0.5000	0.5082 + 0.0224	1.6	0.4950 + 0.0095	-1.0	0.5071 + 0.0022	1.4
Th	--	0.0744 + 0.0122					
Ur	--	-0.0176 + 0.0211					

TABLE 1 (continued)

Component *	Fraction Taken	Scheme A **		Scheme B		Scheme C	
		Fraction Found	Percent Error	Fraction Found	Percent Error	Fraction Found	Percent Error
Solution E							
Ad	0.6670			0.6620 + 0.0067	-0.8	0.6760 + 0.0028	1.3
Ur	0.3330			0.3470 + 0.0046	4.2	0.3310 + 0.0034	-0.6
Solution F							
Ad	0.3890			0.3910 + 0.0098	0.5	0.3990 + 0.0022	2.6
Gu	0.2220			0.1910 + 0.0115	-14.0	0.2310 + 0.0035	4.2
Cy	0.1670			0.1680 + 0.0111	0.6	0.1680 + 0.0032	0.6
Th	0.2220			0.2650 + 0.0063	19.4	0.1990 + 0.0063	-10.4
Solution G							
Ad	0.4550			0.4530 + 0.0120	-0.4	0.4580 + 0.0037	0.7
Gu	0.1820			0.1220 + 0.0217	-33.0	0.1870 + 0.0075	2.7
Cy	0.1360			0.1660 + 0.0160	22.1	0.1460 + 0.0060	7.4
Ur	0.2270			0.2740 + 0.0111	20.7	0.2140 + 0.0061	-5.7
Solution H							
Ad	0.2800			0.2830 + 0.0109	1.1	0.2920 + 0.0020	4.3
Gu	0.3200			0.2750 + 0.0125	-14.1	0.3220 + 0.0033	0.6
Cy	0.2400			0.2480 + 0.0125	3.3	0.2460 + 0.0030	2.5
Th	0.1600			0.2080 + 0.0066	30.0	0.1350 + 0.0059	-15.6
Solution I							
Gu	0.5000			0.4971 + 0.0033	-0.6	0.5030 + 0.0032	0.6
Th	0.5000			0.5104 + 0.0034	2.1	0.5060 + 0.0049	1.2

\*Ad = adenine; Gu = guanine; Cy = cytosine; Th = thymine; and Ur = uracil.

\*\*See text for explanation.

TABLE 2. COMPUTER ANALYSIS OF BINARY SOLUTIONS

Solution *	Ratio Taken	Ratio Found		
		Scheme A **	Scheme B	Scheme C
A	1.75	1.58	1.72	1.85
B	1.00	0.93	0.99	1.05
C	1.33	1.20	1.41	1.29
D	1.00	0.90	1.03	0.97
E	2.00	--	1.91	2.04
I	1.00	--	0.97	0.99

\*See Table 1 for components.

\*\*See text for description.

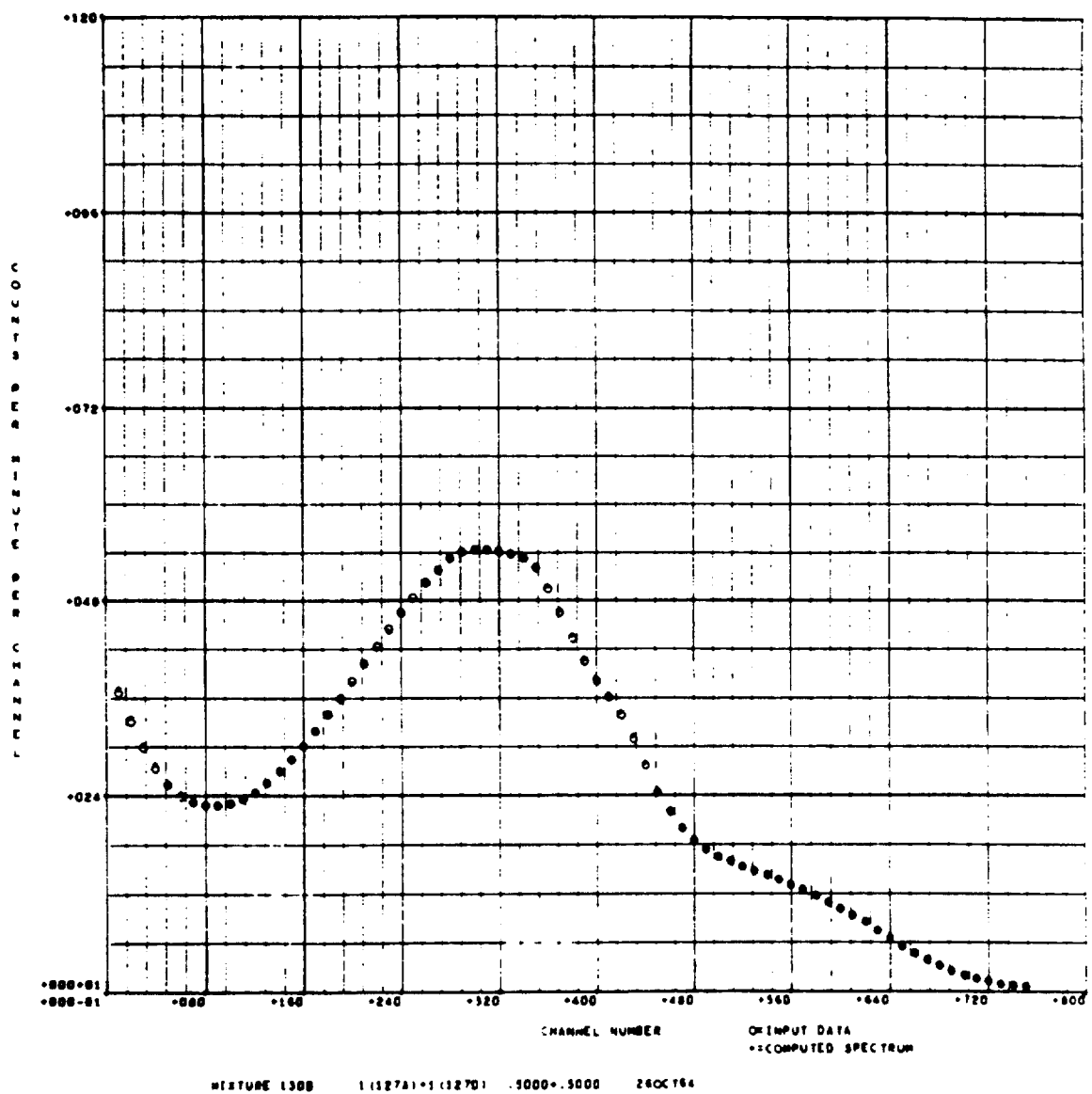


Fig. 1. Experimental spectrum (input data) compared with the best fit found by the computer using scheme B (computed spectrum). Counts/min/channel = absorbance.

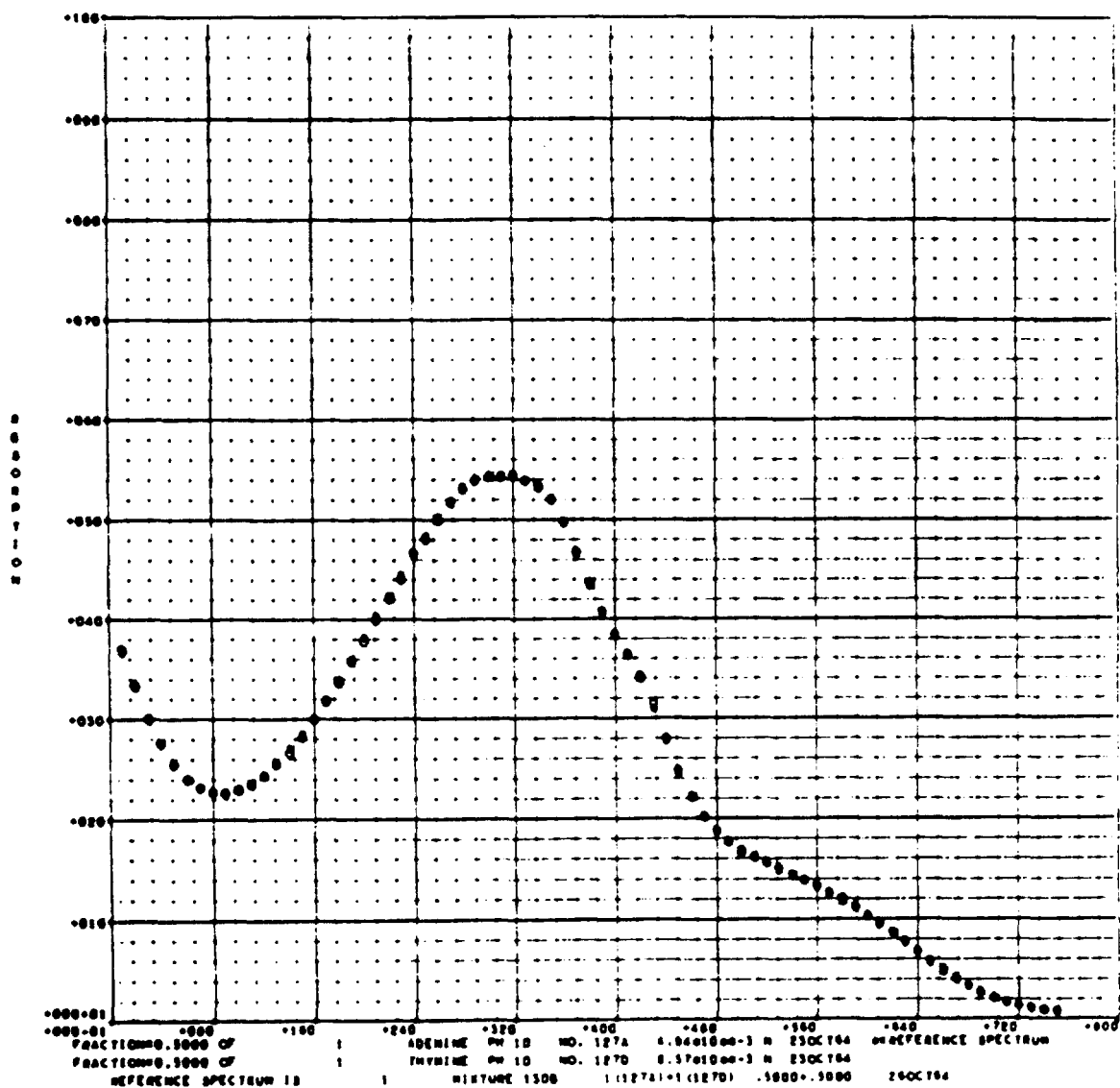


Fig. 2. Experimental spectrum (reference spectrum) compared with the spectrum synthesized by the computer from the library spectra (computed spectrum).



composition. Emphasis will be placed on spectral analysis of nucleosides and nucleotides rather than on bases. It is hoped that the computer analysis will be sufficiently accurate to determine approximately 1 to 5 percent of one nucleoside in a polymer containing 99 to 95 percent of another.

#### REFERENCES

- (1) P. N. Dean, Los Alamos Scientific Laboratory Report LA-3132-MS (1964), p. 180.
- (2) G. T. Fritz, Los Alamos Scientific Laboratory Report LA-3132-MS (1964), p. 249.

STUDIES ON THE RIBONUCLEOTIDE POLYMERASES (D. A. Smith, R. L. Ratliff, and T. T. Trujillo)

INTRODUCTION

A number of ribonucleotide polymerase activities have been observed in vitro. Some anomalous polymerase activities are thought to be catalyzed by the same protein that is responsible for DNA-to-RNA transcription [viz., RNA polymerase (1)]. Our studies on biological information transfer require RNA polymerase as free as possible from interfering enzymatic activities. In attempts to obtain such preparations, it has been found that different purification procedures produce RNA polymerase with different catalytic properties.

METHODS AND RESULTS

Both published (2-4) and new procedures were followed for the purification of RNA polymerase from *Escherichia coli* in order to determine which method yields the best enzyme preparations. During these studies it was observed that the catalytic properties of various polymerase fractions varied greatly. Table 1 illustrates some of these results. Fractions 1, 2, and 3 were part of the same preparation of RNA polymerase. This preparation was obtained using a procedure worked out in this Laboratory. The partially purified enzyme was divided into two portions, one of which was further purified by centrifugation in a glycerol density gradient (fraction 1). The other portion was purified by chromatography on hydroxylapatite (fractions 2 and 3). Fractions 2 and 3 represent enzyme recovered in adjacent tubes. Fraction 4 was obtained by a modification of a published procedure (4).

When assayed by standard procedures, the 4 fractions seemed to have very similar properties. They all had 280 m $\mu$ :260 m $\mu$  absorption ratios of over 1.6. When assayed for RNA polymerase and polyadenylate polymerase (2), fractions 1, 2, and 4 incorporated equal amounts of AMP with both assays. Fraction 3 incorporated 2.5 times as much AMP with the polyadenylate polymerase assay as with the RNA polymerase assay. The most purified fraction, number 4, had about twice the specific activity of the least purified, fraction 2.

TABLE 1. INCORPORATION OF RIBONUCLEOSIDE MONOPHOSPHATES  
USING TERMINAL DEOXYNUCLEOTIDE TRANSFERASE PRODUCTS  
AS PRIMERS

Enzyme Fraction	Ribonucleoside Monophosphate Incorporated (nmoles)				
	(pt) <sub>13</sub> (pa) <sub>200</sub> Primer		(pc) <sub>6</sub> (pa) <sub>200</sub> Primer		
	AMP	UMP	AMP	UMP	UMP*
1	7.6	--	7.1	--	--
2	5.4	38.1	0.0	--	0.1
3	48.8	93.0	0.0	--	0.6
4	45.0	13.4	11.0	15.1	35.0

\* In this experiment only UTP and GTP and 50 nmoles primer as mononucleotide were present. Other experiments were done in the presence of all 4 ribonucleoside triphosphates and 200 nmoles primer.

When polydeoxyribonucleotides prepared with terminal deoxynucleotidyl transferase (5,6) were used as templates (Table 1), the 4 RNA polymerase fractions were found to have widely differing and unexpected catalytic activities. Thus, the ratio of UMP to AMP incorporation was much greater with fraction 2 than fraction 3 when (pt)<sub>13</sub>(pa)<sub>200</sub> was used as a template. With neither fraction is this ratio what would be expected using a template of this composition. When fraction 4 is used, the ratio is even further from that expected. Fractions 1 and 4 stimulate AMP incorporation when (pc)<sub>6</sub>(pa)<sub>200</sub> is the primer, while fractions 2 and 3 do not. One would expect no AMP incorporation in the presence of this primer. In the absence of any primer, no AMP incorporation was observed. Since all 4 ribonucleoside triphosphates were present, it is possible that AMP incorporation was due to the formation of polyuridylylate under the direction of (pc)<sub>6</sub>(pa)<sub>200</sub>, which then served as a template for polyadenylate formation. However, another less pure enzyme preparation obtained later also stimulated AMP incorporation with (pc)<sub>6</sub>(pa)<sub>200</sub> as the primer, with ATP as the only triphosphate present in the reaction mixture. Adenylate incorporation with polydeoxyadenylate as primer has previously been observed (7). Another experiment shows that (pc)<sub>6</sub>(pa)<sub>200</sub> serves as an excellent template for UMP incorporation with fraction 4 but not for fractions 2 and 3. When somewhat different conditions were used and (pt)<sub>13</sub>(pa)<sub>200</sub> was the template, fractions 2 and 3 directed much more UMP incorporation than fraction 4.

#### DISCUSSION

These results show that RNA polymerase purified by density gradient centrifugation had different polymerizing activities than that purified on hydroxylapatite. Furthermore, RNA polymerase recovered in adjacent tubes from hydroxylapatite chromatography apparently had different enzymatic activities. The relative abilities of enzyme fractions to stimulate UMP incorporation into acid-insoluble material varied with the primer used.

One possible explanation of these results is that RNA polymerase is made up of sub-units which may dissociate or rearrange and so alter the catalytic properties of the enzyme (4,8). The secondary structure of the primer may also be important in producing some of the results reported here. These possibilities are among those currently under investigation.

# REFERENCES

- (1) M. Chamberlin and P. Berg, J. Mol. Biol. 8, 708 (1964).
- (2) M. Chamberlin and P. Berg, Proc. Natl. Acad. Sci. U. S. 48, 81 (1962).
- (3) J. J. Furth, J. Hurwitz, and M. Anders, J. Biol. Chem. 237, 2611 (1962).
- (4) E. Fuchs, W. Zillig, P. H. Hofschneider, and A. Preuss, J. Mol. Biol. 10, 546 (1964).
- (5) R. L. Ratliff and T. T. Trujillo, this report, p. 241.
- (6) F. N. Hayes and V. E. Mitchell, this report, p. 178.
- (7) A. Falaschi, J. Adler, and H. G. Khorana, J. Biol. Chem. 238, 3080 (1963).
- (8) S. Lee-Huang and L. F. Cavalieri, Science 148, 1474 (1965).

# PURIFICATION OF POLYDEOXYRIBONUCLEOTIDE POLYMERASES FROM CALF THYMUS (R. L. Ratliff and T. T. Trujillo)

## INTRODUCTION

The polydeoxyribonucleotide polymerases from calf thymus are unique in two respects: first, the terminal deoxyribonucleotidyl transferase or addase can be used to graft 2'-deoxy-5'-adenylic acid units onto initiators of known sequence, thus providing molecules of high molecular weight and known sequence; and second, the DNA polymerase requires single-stranded polydeoxyribonucleotides as primer and once the complementary copy of the primer has been completed the reaction is terminated. Thus, the two enzymes can be utilized to provide double-stranded polydeoxyribonucleotides of known sequence for model studies of the DNA molecule.

## METHODS AND RESULTS

The procedure used for the purification and assay of both enzymes is essentially the same as that described by Bollum et al (1,2), except that frozen calf thymus glands were used as starting material. Enzyme activity is measured as the specific rate of incorporation of radioactive deoxyribonucleotide into acid-insoluble material. The reaction mixture for the assay of addase consisted of 0.3  $\mu$ mole of carbon-14 p<sub>3</sub>a, 3 nmoles of (pt)<sub>6</sub>, 12  $\mu$ moles of potassium phosphate, pH 7.0, 2.4  $\mu$ moles of MgCl<sub>2</sub>, 0.3  $\mu$ mole of 2-mercaptoethanol, and 5 to 50  $\mu$ l of enzyme in a final volume of 0.3 ml. The reaction mixture is incubated at 35°C for 1 hr, and the acid-insoluble material is determined as previously described (3). In the assay of ~~column fractions~~ for addase activity, one-sixth of the above reaction mixture is used and 10  $\mu$ l of enzyme solution is added. One unit of addase is that amount of enzyme required to effect incorporation of 1 nmole carbon-14 p<sub>3</sub>a in 1 hr.

Frozen calf thymus glands were purchased from Pentex Corporation, Kankakee, Illinois. After 2 days of thawing at 10°C. the glands were processed as described by Bollum (2). Since the procedures are almost the same, only the modification will be given.

After the elution of the enzyme from phosphocellulose and

removal of the nucleic acids by passing through DEAE-cellulose ( $\text{Cl}^-$ ), the enzyme solution is dialyzed overnight against 4 volumes of  $10^{-3}$  M 2-mercaptoethanol. The polymerases are again treated with phosphocellulose and fractionated with ammonium sulfate, as previously described, and dialyzed against 50 volumes of 0.2 M ammonium sulfate-0.05 M potassium phosphate, pH 7.5, for 4 hr. The dialyzed solution is chromatographed on hydroxylapatite as described by Bollum. The DNA polymerase, which separated from the addase, and the DNA polymerase-addase mixture are concentrated with ammonium sulfate. The DNA polymerase-addase mixture is dialyzed against 0.05 M phosphate buffer, pH 7.2, and chromatographed on Sephadex G-100 in order to separate the two enzymes. The two enzymes are concentrated with ammonium sulfate at 0.90 saturation. After centrifuging and dissolving in a small volume of phosphate buffer, the enzymes are stored at  $-20^\circ\text{C}$ . If the protein concentration of the addase from the Sephadex column fractions is less than 0.5 mg/ml, the enzyme is concentrated by adsorption on phosphocellulose, using 100 mg/mg protein equilibrated with 0.05 M phosphate buffer, pH 6.9. The enzyme is eluted from the phosphocellulose with 0.3 M of the same buffer. Prior to use of the addase an aliquot is dialyzed against 0.05 M phosphate buffer, pH 6.9.

## DISCUSSION

Although the yield of addase from frozen calf thymus is essentially the same as described by Bollum, the DNA polymerase appeared to be less stable, and greater care must be taken in order to obtain a suitable yield of this enzyme. In addition, the nucleases are not always completely removed during the hydroxylapatite step and usually a second hydroxylapatite step is required. A second passage of the addase through hydroxylapatite results in very little loss; however, the DNA polymerase is often completely lost. We have found that dialysis of the enzyme solution against 0.2 M ammonium sulfate prior to adsorption on hydroxylapatite facilitates the removal of 80 to 90 percent of the nucleases. The hydroxylapatite used in the above experiments was prepared as described by Levin (4) and is far superior to that prepared by admixing with cellulose for the removal of nucleases.

#### REFERENCES

- (1) F. J. Bollum, E. Groeniger, and M. Yoneda, Proc. Nat. Acad. Sci. U. S. 51, 853 (1964).
- (2) M. Yoneda and F. J. Bollum. J. Biol. Chem. (in press).
- (3) R. L. Ratliff and T. T. Trujillo. Los Alamos Scientific Laboratory Report LA-3132-MS (1964). p. 236.
- (4) O. Levin, In: Methods in Enzymology. Vol. V (S. P. Colowick and N. O. Kaplan, eds.). Academic Press, Inc., New York (1962). p. 27.





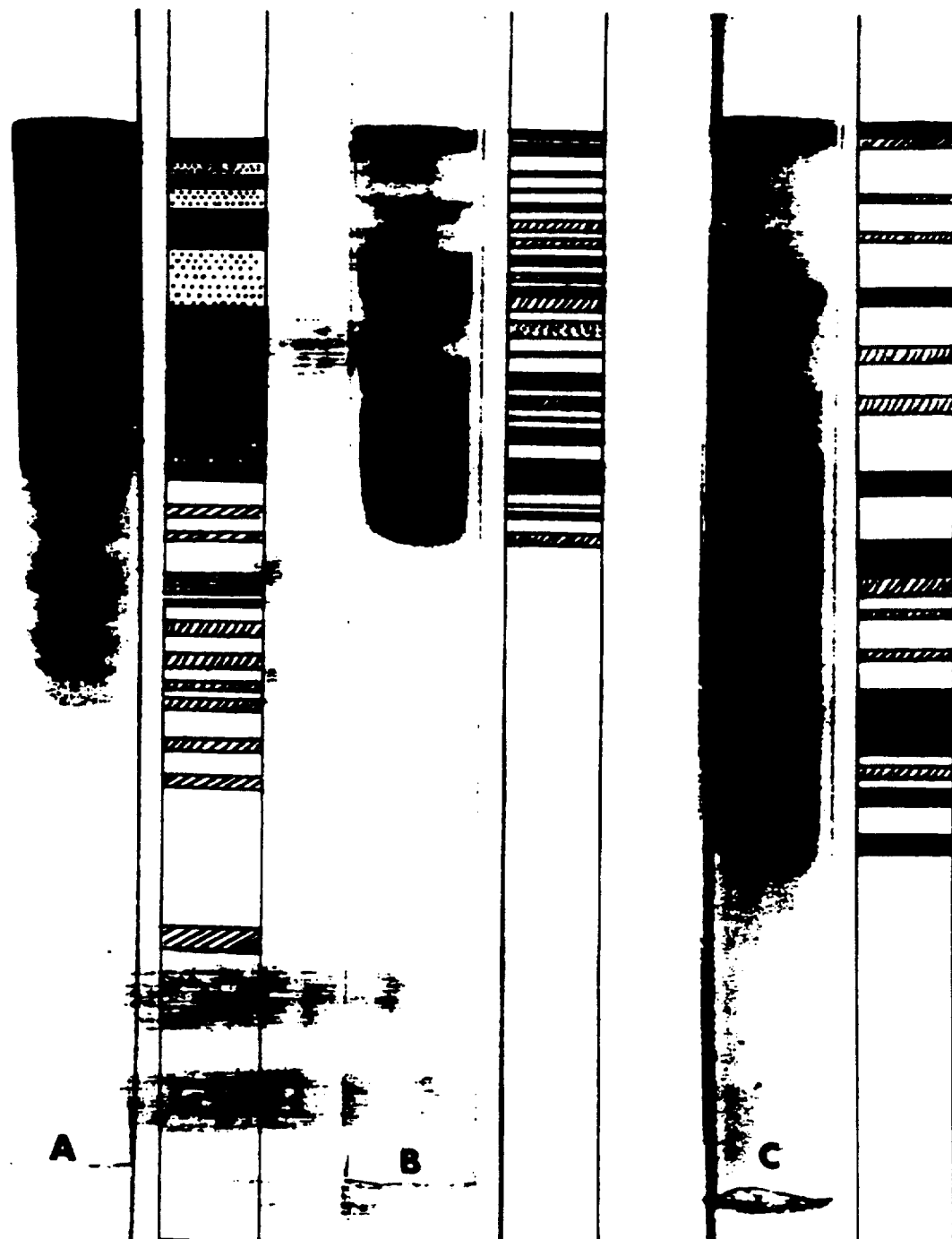


Fig. 1. Electrophoretic separation of the components of whole calf thymus histone: (A) 100  $\mu$ l (300  $\mu$ g). 60 minutes; (B) 15  $\mu$ l (45  $\mu$ g). 60 minutes; and (C) 30  $\mu$ l (90  $\mu$ g). 90 minutes.

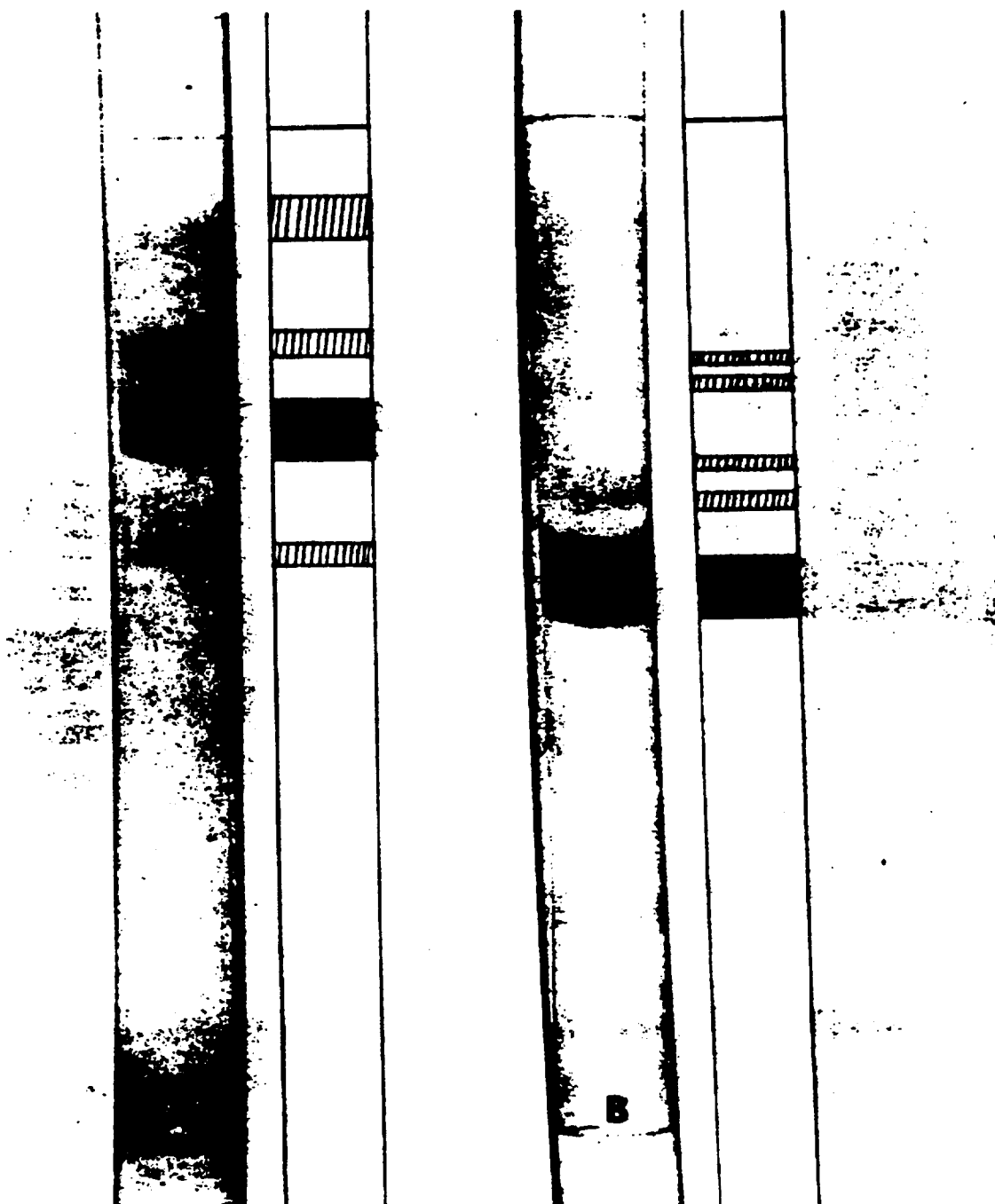


Fig. 2. Electrophoretic separation of the components of (A) trypsin, and (B) ribonuclease; 30  $\mu$ l, 60 minutes.

## DISCUSSION

Somewhat more than 30 single and separate bands may be seen in the 60- and 90-minute gels. Approximately half of these are faintly staining forerunner bands visible only in the 100- $\mu$ l, 60-minute gels. The remainder are well resolved in gels run with lower loads for longer periods. Preliminary evidence, based on extraction-fractionation procedures, suggests that all observed bands may be attributed to specific histone components of the nucleoprotein complex. Further preliminary evidence, presented in a separate inclusion in this report (5), suggests that the many bands observed are real fractions rather than method artifacts.

The polyacrylamide gel electrophoretic technique described herein provides an unprecedented resolution of complex histone preparations. The resolving power of this method, together with its simplicity and sensitivity, recommends it for routine analytical use.

## REFERENCES

- (1) L. Ornstein, Ann. N. Y. Acad. Sci. 121, 321 (1964).
- (2) B. J. Davis, Ann. N. Y. Acad. Sci. 121, 404 (1964).
- (3) H. C. McAllister, Y. C. Wan, and J. L. Irvin, Anal. Biochem. 5, 321 (1963).
- (4) K. Murray, Sixth Intern. Cong. Biochem., Abstract I-141 (1964).
- (5) L. R. Gurley, G. R. Shepherd, and B. J. Noland, this report, p. 248.

HIGH RESOLUTION DISC ELECTROPHORESIS OF HISTONES. II. A  
SURVEY OF HISTONES FROM VARIOUS LABORATORIES (L. R. Gurley,  
G. R. Shepherd, and B. J. Noland)

INTRODUCTION

An improved method of disc electrophoresis has been developed in this Laboratory (1) which offers a high degree of resolution of histones. As an evaluation of this method, unfractionated histones and histone fractions from several laboratories have been subjected to electrophoresis. This report demonstrates that the high degree of resolution of histones is a result of the technique itself and is not inherent in a particular histone preparative procedure or due to complexes of the various histone components. Electrophoresis by this method provides a convenient system for future studies on histone fractionation and on the relation of histones to the cell cycle.

METHODS AND RESULTS

Unfractionated histones extracted from saline-washed calf thymus with 0.2 N HCl were prepared and kindly donated for this study by Dr. L. S. Hnilica, M. D. Anderson Hospital, Houston (2), and by Dr. D. M. P. Phillips, Chester Beatty Research Institute, London (3). Unfractionated histones sequentially extracted from saline-washed thymus with solutions of pH 1.8 H<sub>2</sub>SO<sub>4</sub>, pH 1.0 H<sub>2</sub>SO<sub>4</sub>, and pH 0.6 H<sub>2</sub>SO<sub>4</sub> were prepared in our Laboratory (4). Fractions obtained in each of the sequential extraction steps were kindly donated by Dr. K. Murray, Laboratory of Molecular Biology, Cambridge, England (4). Unfractionated histones prepared from purified nucleoprotein were kindly donated by Dr. J. Logan Irvin, University of North Carolina, Chapel Hill (5). Histone fractions F1, F2a1, F2a2, F2b, and F3, prepared by selective extraction and differential precipitation from saline-washed calf thymus, were kindly donated by Dr. D. M. P. Phillips (6, 7). Histone fractions Ib, IIb, III, and IV, prepared by chromatography on Amberlite IRC-50 ion exchange resin, were kindly donated by Dr. K. Murray (8).

The above preparations were dissolved in sample solvent (4 mg histone per ml), and 5 to 100  $\mu$ l was subjected to electrophoresis for 60 to 90 minutes on polyacrylamide gels by the method described in the accompanying manuscript (1).

The electrophoretic patterns of unfractionated calf thymus histones from four different laboratories were compared (Fig. 1). The four different histone preparations have similar patterns, but one can observe quantitative differences in some fractions. The histones prepared by acid precipitation of DNA from a solution of purified nucleoprotein (gel 4, Fig. 1C) appear to have larger quantities of the faster-moving components and fewer of the slower-moving components than do the three preparations obtained by acid extraction of saline-washed thymus (gels 1, 2, and 3, Fig. 1C). All four preparations contained many forerunner components of low concentration (Fig. 1A).

The electrophoretic patterns of the IRC-50 column fractions Ib, I Ib, III, and IV were examined (Fig. 2). Fraction Ib contained one major and several minor components (gel 2, Fig. 2B). Fraction I Ib contained at least two major and several minor components (gel 3, Fig. 2B). No differences could be observed between fraction III + IV (gel 4, Fig. 1C) and fraction IV (gel 5, Fig. 1C). The positions of the major bands in each of the fractions could be correlated with similar bands in the unfractionated histone pattern (Fig. 3).

The electrophoretic patterns of fractions F1, F2a1, F2a2, F2b, and F3, obtained by selective extraction and differential precipitation, were examined. The forerunner components observed in unfractionated histones (gel 1, Fig. 4A) were found to be concentrated in F1 (gel 2, Fig. 4A). All the fractions were found to be heterogeneous (Fig. 4B), F1, F2a1, and F2b containing one major component, F2a2 containing two major components, and F3 containing three major components (Fig. 4C). The positions of the major bands in each of the fractions could be correlated with similar bands in the unfractionated histone pattern (Fig. 5).

The electrophoretic patterns of histones extracted from saline-washed, pH 3.0 H<sub>2</sub>SO<sub>4</sub>-extracted thymus by sequential extraction with pH 1.8, pH 1.2, and pH 0.6 H<sub>2</sub>SO<sub>4</sub> were examined. The pH 3.0 extract contained no significant amount of histone (gel 1, Figs. 6A, 6B, and 6C). The forerunner components were extracted with pH 1.8 H<sub>2</sub>SO<sub>4</sub> (gel 2, Fig. 6A). It was observed that different histone components were selectively extracted into H<sub>2</sub>SO<sub>4</sub> solutions of various pH (Figs. 6B and 6C).

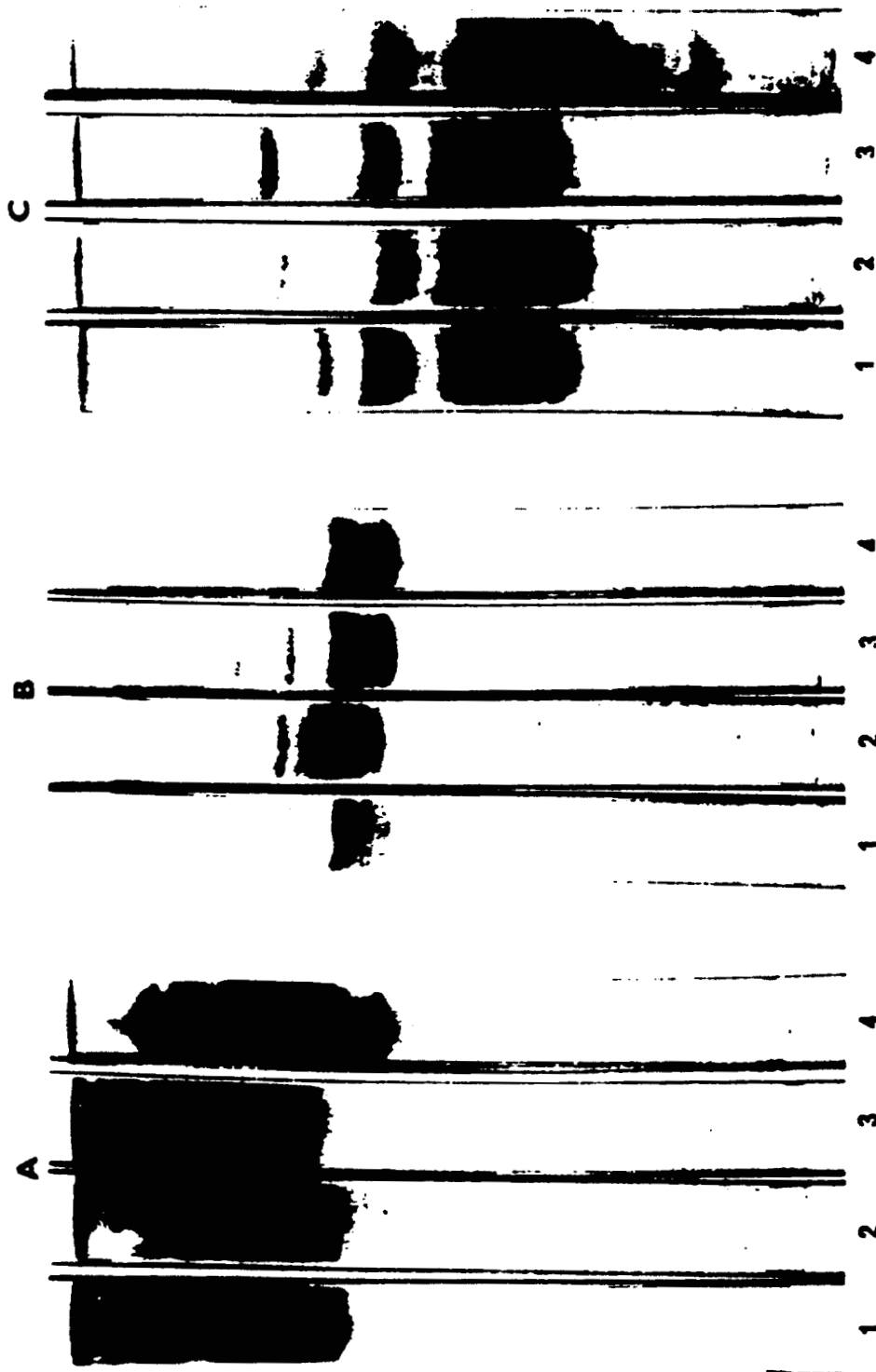


Fig. 1. Unfractionated calf thymus histones. Electrophoresis conditions: (A) 400  $\mu$ g, 60 minutes; (B) 60  $\mu$ g, 60 minutes; and (C) 120  $\mu$ g, 90 minutes. Histones were prepared in the laboratory of the authors (gel 1), Phillips (gel 2), Hnilica (gel 3), and Irvin (gel 4).

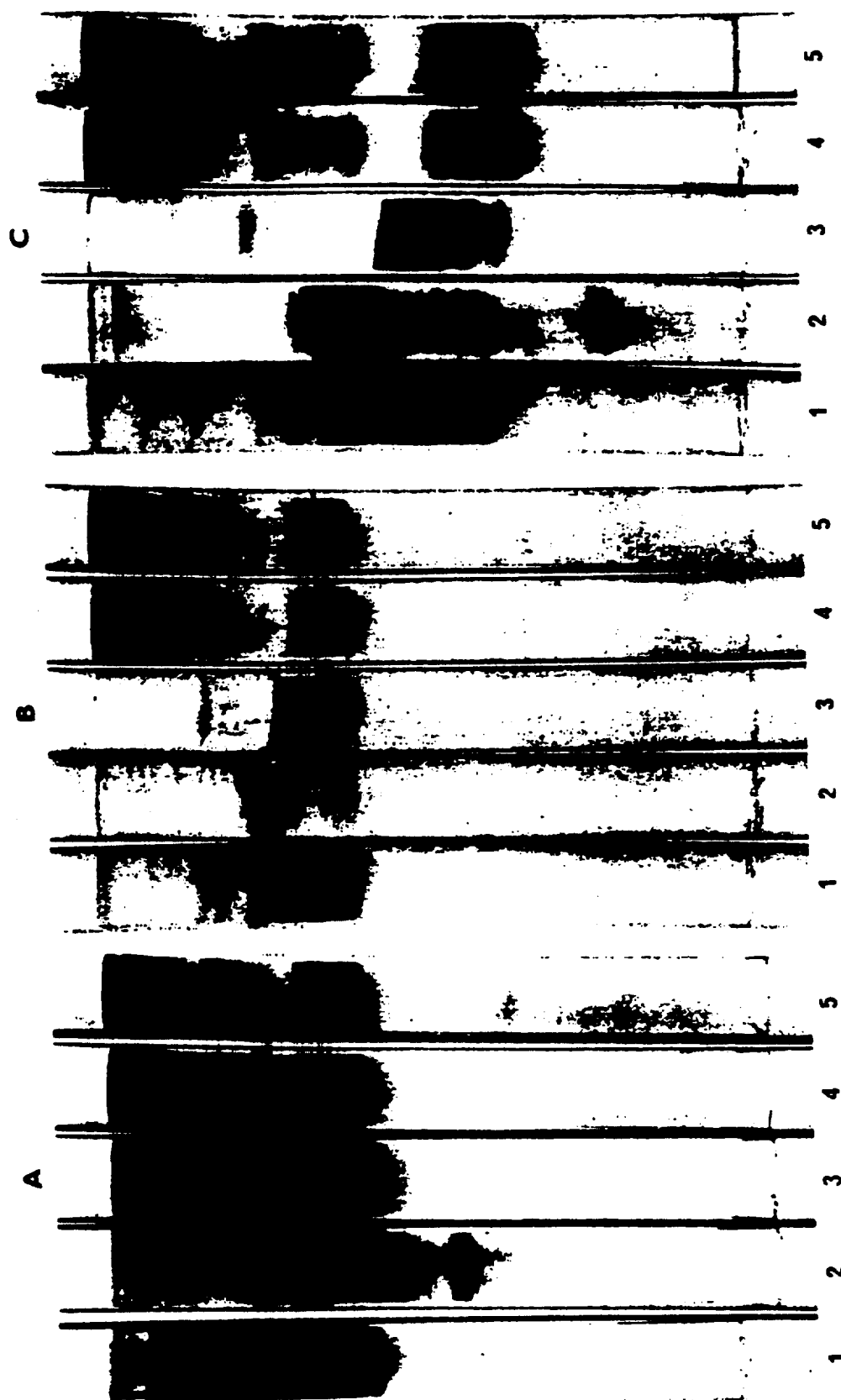


Fig. 2. Amberlite IRC-50 column fractions of calf thymus histones. Electrophoresis conditions: (A) 400  $\mu$ g, 60 minutes; (B) 60  $\mu$ g, 60 minutes; and (C) 120  $\mu$ g, 90 minutes. (Gel 1) unfractionated histones; (gel 2) Ib; (gel 3) IIb; (gel 4) III + IV; and (gel 5) IV.



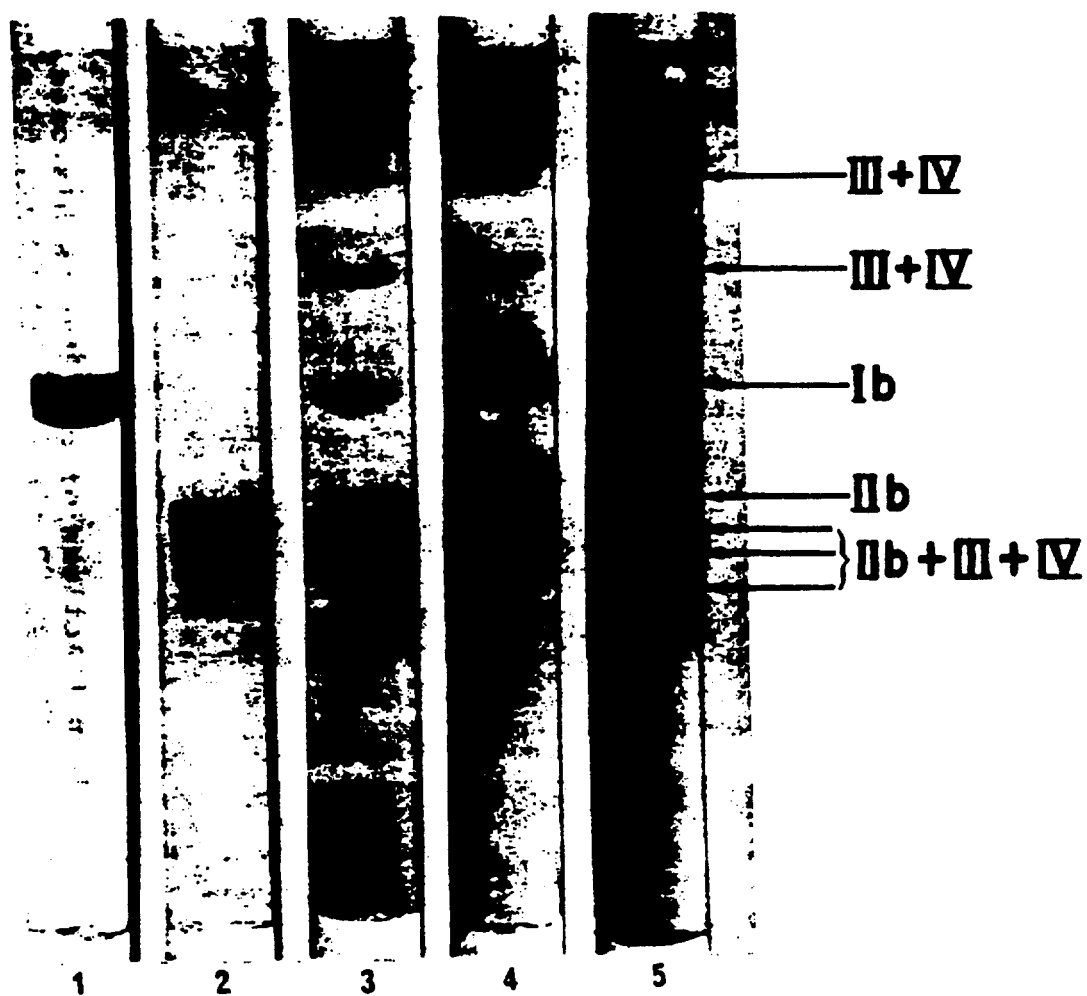


Fig. 3. Amberlite IRC-50 column fractions of calf thymus histones. (Gel 1) Ib, 20  $\mu$ g; (gel 2) IIb, 20  $\mu$ g; (gel 3) III + IV, 20  $\mu$ g; (gel 4) mixture of Ib, IIb, and III + IV, 20  $\mu$ g each fraction; and (gel 5) unfractionated histones, 120  $\mu$ g. All gels run 90 minutes.

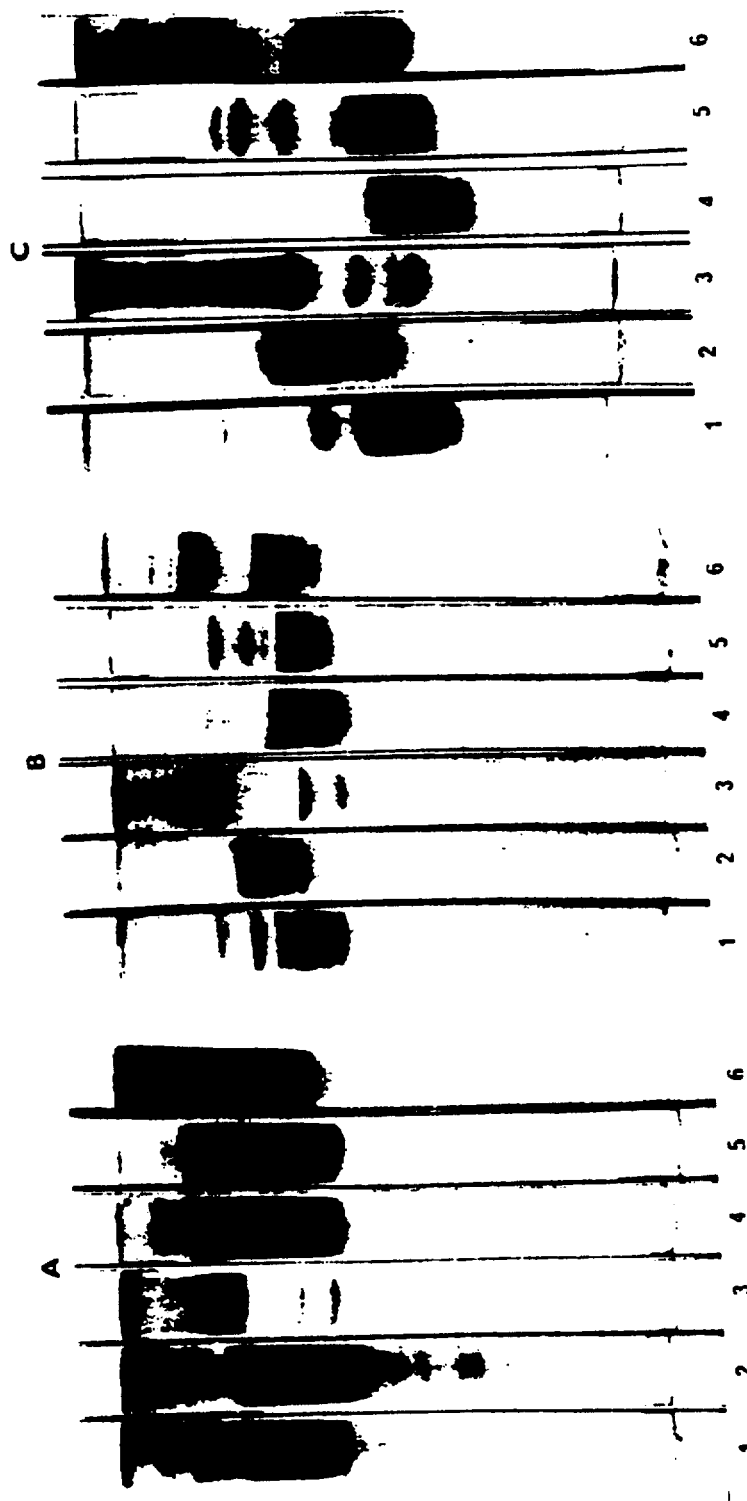


Fig. 4. Extraction fractions of calf thymus histones. Electrophoretic conditions: (A) 400  $\mu$ g, 60 minutes; (B) 60  $\mu$ g, 60 minutes; and (C) 120  $\mu$ g, 90 minutes. (Gel 1) unfractionated histones; (gel 2) F1; (gel 3) F2a2; (gel 5) F2b; and (gel 6) F3.

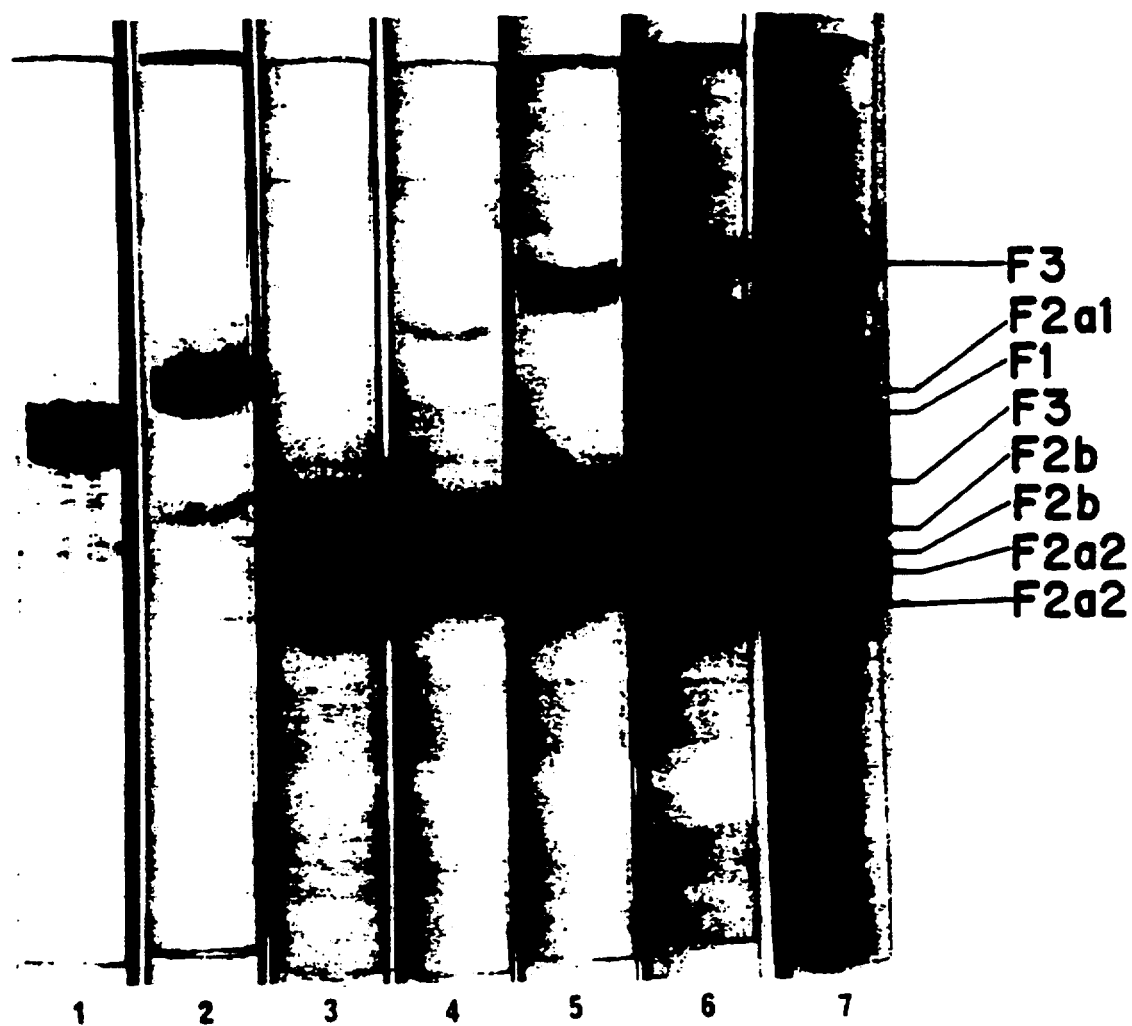


Fig. 5. Extraction fractions of calf thymus histones. (Gel 1) F1, 20  $\mu$ g; (gel 2) F2a1, 20  $\mu$ g; (gel 3) F2a2, 20  $\mu$ g; (gel 4) F2b, 20  $\mu$ g; (gel 5) F3, 20  $\mu$ g; (gel 6) mixture of F1, F2a1, F2a2, F2b, and F3, 20  $\mu$ g each; and (gel 7) unfractionated histone, 120  $\mu$ g. All gels run 90 minutes.

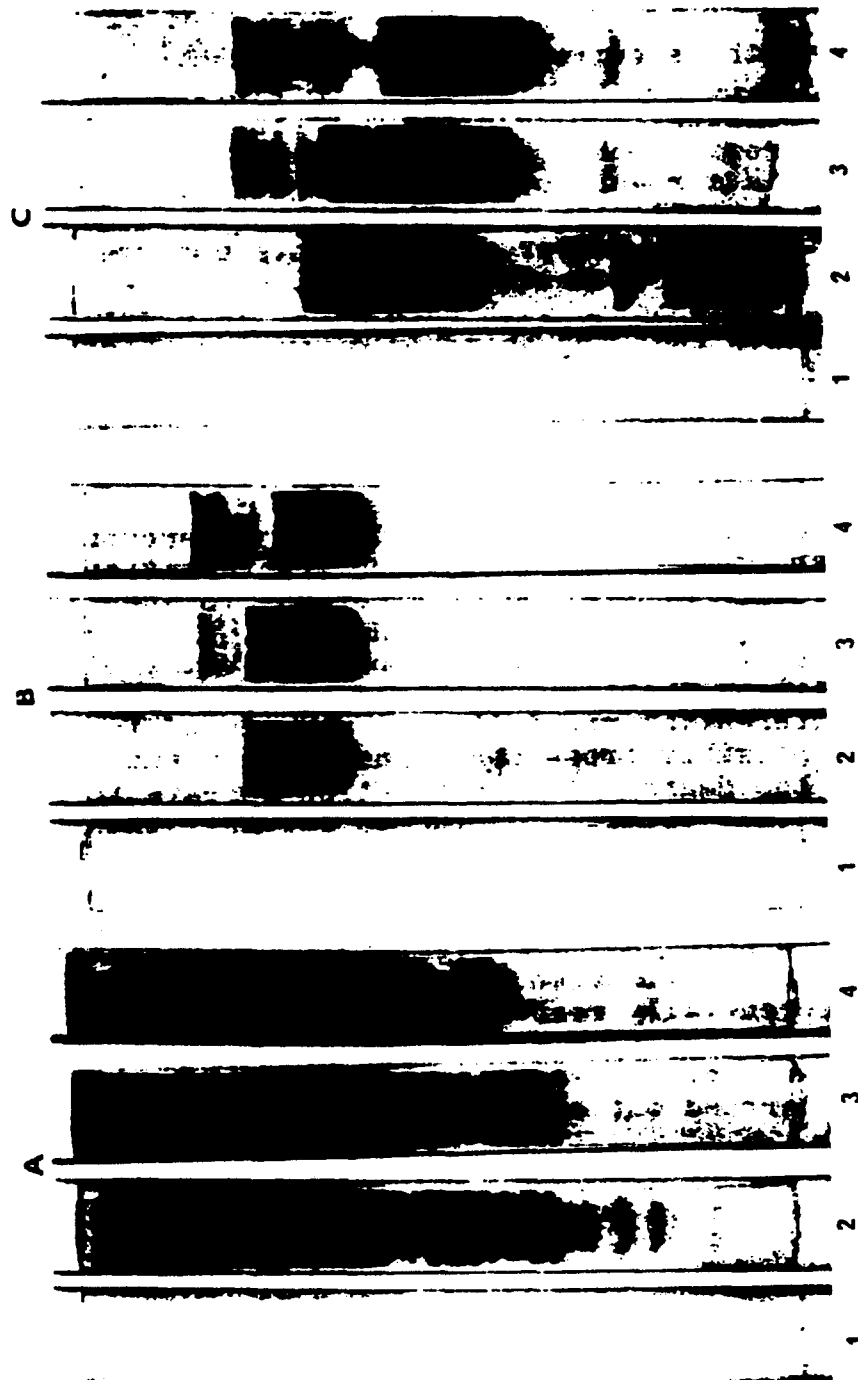


Fig. 6. Sequential extraction of calf thymus histones with  $H_2SO_4$ . Electrophoresis conditions: (A) 400  $\mu g$ , 60 minutes; (B) 60  $\mu g$ , 60 minutes; and (C) 120  $\mu g$ , 90 minutes. (Gel 1) pre-extraction of thymus with pH 3.0  $H_2SO_4$ ; (gel 2) histones extracted with pH 1.8  $H_2SO_4$  after pH 3.0 extraction; (gel 3) histones extracted with pH 1.2  $H_2SO_4$  after pH 1.8 extraction; and (gel 4) histones extracted with pH 0.6  $H_2SO_4$  after pH 1.2 extraction.

## DISCUSSION

The similarities of the electrophoretic patterns of unfractionated histones prepared in different laboratories demonstrate that the complexity of histone patterns obtained by the disc electrophoresis technique presented in the preceding manuscript (1) is a result of the technique itself and is not inherent in a particular preparative procedure. The possibility that the large number of components observed with this electrophoresis technique is due to complexes of the various histone components with each other is greatly decreased by the facts that the patterns of various histone fractions can be found in the pattern of the unfractionated histones and that no bands are present in the unfractionated histone pattern which are not present in the pattern of the histone fractions.

All histone fractions studied were found to be heterogeneous, some much more than others. IRC-50 column fractionation appears to give a clean separation of fractions Ib and IIb, with little or no cross contamination. However, fraction III + IV and fraction IV were indistinguishable and extremely heterogeneous. Histone fractions obtained by selective extraction and differential precipitation were found to be heterogeneous and possibly cross contaminated to a small degree. However, the degree of fractionation appears to be more complete than that obtained on IRC-50 columns, thus indicating the extraction-precipitation fractionation as a more desirable method for obtaining histone fractions.

It is interesting to note that the high mobility forerunner bands, observed in unfractionated histones and concentrated in F1, may be preferentially removed from the nucleoprotein complex between pH 3.0 and pH 1.8 with H<sub>2</sub>SO<sub>4</sub>. Further studies of the pH-dependent dissociation of the nucleoprotein complex are being carried out conjointly with Dr. K. Murray.

## REFERENCES

- (1) G. R. Shepherd, L. R. Gurley, and B. J. Noland, this report, p. 244.
- (2) L. S. Hnilica and H. J. Busch, J. Biol. Chem. 238, 918 (1963).
- (3) P. F. Davison, D. W. F. James, K. V. Shooter, and J. A. V. Butler, Biochim. Biophys. Acta 15, 415 (1954).
- (4) K. Murray, Sixth Intern. Congr. Biochem., Abstract I-141 (1964).
- (5) H. C. McAllister, Y. C. Wan, and J. L. Irvin, Anal. Biochem. 5, 321 (1963).
- (6) E. W. Johns, Biochem. J. 92, 55 (1964).
- (7) D. M. P. Phillips and E. W. Johns, Biochem. J. 94, 127 (1965).
- (8) K. Murray, In: The Nucleohistones (J. Bonner and P. Ts'o, eds.), Holden-Day, Inc., San Francisco (1964), p. 21.

**A PROCEDURE FOR AUTOMATIC AMINO ACID ANALYSIS ON THE NAN-OMOLAR LEVEL (G. R. Shepherd, C. N. Roberts, and R. D. Hiebert\*)**

**INTRODUCTION**

The automated amino acid analysis procedure of Spackman, Stein, and Moore (1,2) has been in use in biochemical laboratories for approximately 6 years. Using this procedure one may routinely quantitate the amino acid composition of 3 mg of an average protein; 0.5- to 1.0- $\mu$ mole quantities of each of 17 common amino acids are required for an accurate determination. Beckman/Spinco has recently introduced a high-sensitivity cuvette modification which allows routine determinations at the 0.1- $\mu$ mole per amino acid level. The majority of efforts in recent years, however, have been expended in accelerating the procedure and decreasing the machine time required for each analysis rather than increasing the sensitivity of the method.

Analyses of peptides eluted from peptide maps, of proteins synthesized in in vitro enzymatic systems, and of protein fractions isolated from analytical zonal electrophoretic support matrices required an analytical sensitivity in the 1- to 10-nanomolar region. Such sensitivity has been achieved, both at Los Alamos (3) and in the Department of Chemistry at La Jolla (4), by combining the Beckman Model 120B automatic amino acid analyzer and the Gilford Model 2000 spectrophotometer system. Such a combination is both bulky and costly and prevents the use of the spectrophotometer for other functions.

**METHODS AND RESULTS**

A Beckman Model 120B analyzer was equipped with the accelerated analysis system using crushed resin and a Beckman high-sensitivity cuvette. Two high-gain ( $\times 10$ ) solid state operational amplifiers (Nexus CLA-12) were installed between the colorimeter photocells and the recorder amplifier in the normal 570-m $\mu$  and 440-m $\mu$  channels (Fig. 1). Each amplifier

---

\*LASL Group P-1, Physics Division.

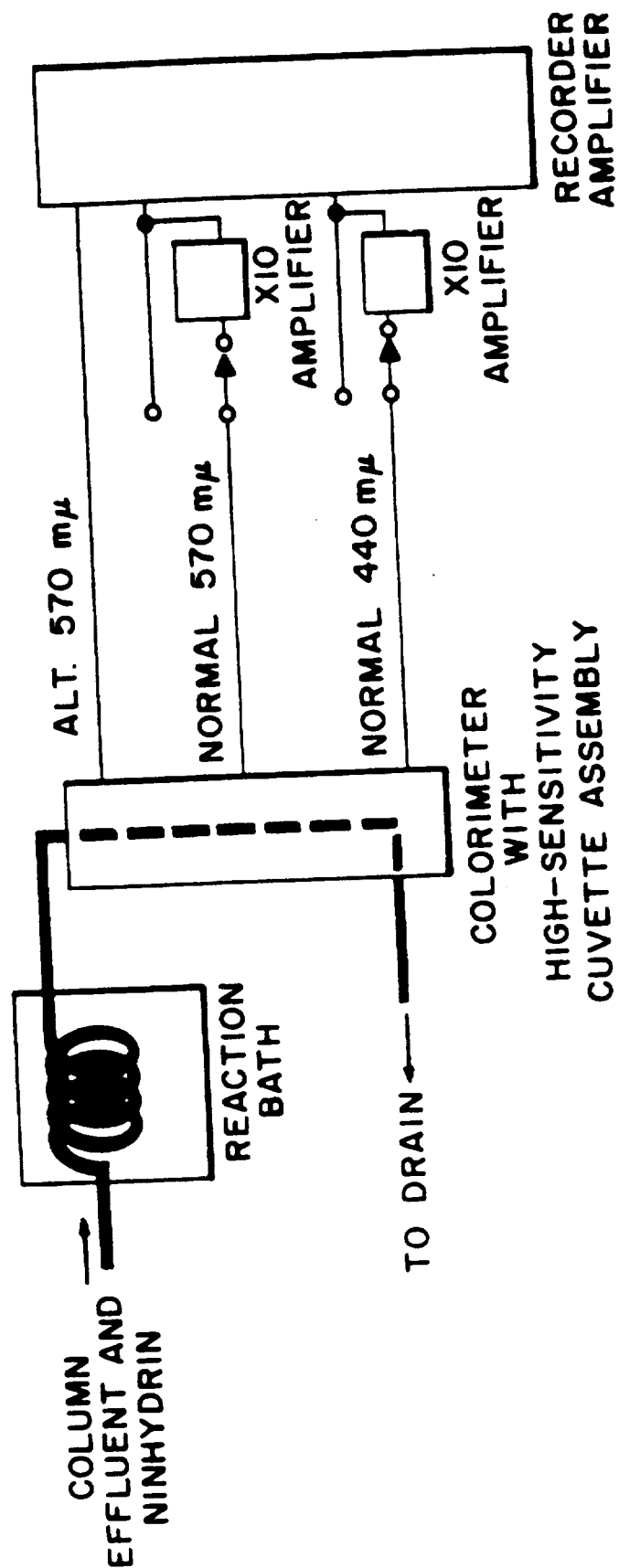


Fig. 1. Block diagram of colorimeter-amplifier circuit.



is equipped with a bypass switch, enabling the operator to select the operating mode of each channel. Thus, input signals from the normal 570-m $\mu$  and 440-m $\mu$  channels may be amplified 10 times or passed directly to the recorder amplifier. The suppressed 570-m $\mu$  channel was allowed to operate in normal fashion.

Base line traces at high sensitivity in the absence of buffer flow fluctuated no more than 0.02 absorbance unit (Fig. 2A). Base line traces at high sensitivity in the presence of buffer flow and the absence of ninhydrin showed slightly greater fluctuations. These were gradual, however, and had periods of 2 hr or more. A minor peak occurred as the second buffer emerged from the column and reactor system and entered the colorimeter, but the base line quickly returned to its previous slope (Fig. 2B). Base line traces at normal flow rates in the presence of ninhydrin exhibited a gradual upward trend. Both amplified traces showed a gradual decrease, followed by an abrupt increase of 0.15 to 0.2 absorbance unit, as the second buffer entered the colorimeter (Fig. 2C). To test the resolution and sensitivity of the system at high sensitivity and low column load a Beckman amino acid standard was diluted with sample-diluter buffer of pH 2.2 to yield a solution containing 5 nanomoles of each of the standard amino acids per ml. A 1-ml sample was applied to a long (50-cm) column, and the run was carried out according to normal procedures. The results are illustrated in Fig. 2D.

Excellent resolution was obtained for all amino acids at this level. Maximum deflection from base line was obtained for aspartic acid (ca. 0.47 absorbance unit), and the minimum deflection was given by proline (ca. 0.06 absorbance unit).

## DISCUSSION

Automatic amino acid analyses in the 1- to 10-nanomolar region may be obtained by the simple expedient of installing high-gain operational preamplifiers between the photocells and the recorder amplifier of a Beckman Model 120B amino acid analyzer. Resolution and sensitivity at this level are excellent during normal operating procedures. Analyses may be carried out using both the 570-m $\mu$  and 440-m $\mu$  channels, and full use may be made of the automated nature of the Model 120B analyzer. Optimal quantitation at this sensitivity could be achieved if observed base line fluctuations were eliminated. An investigation of this phenomenon, and of means to eliminate it, is currently underway.

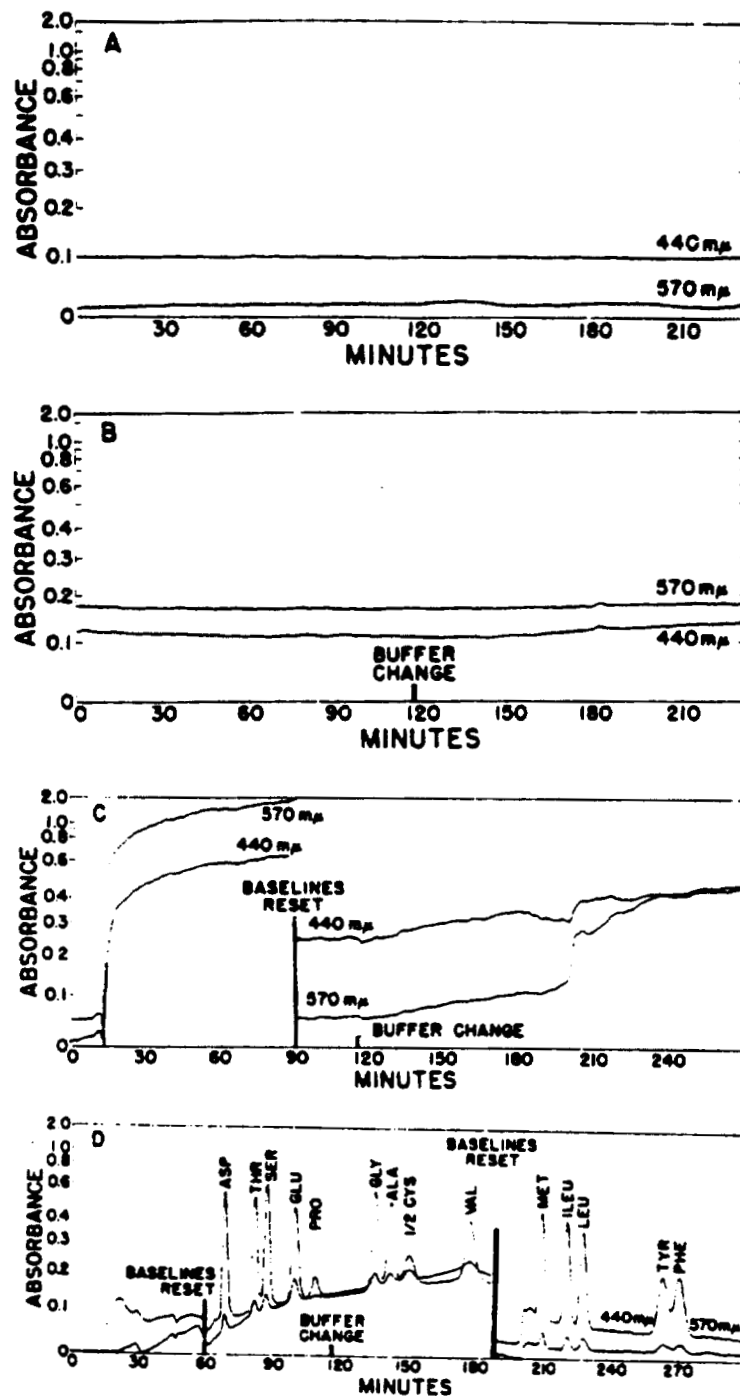


Fig. 2. (A) Electronic base line, high sensitivity, no buffer or ninhydrin flow; (B) buffer base line, no ninhydrin flow; (C) base line with buffer and ninhydrin flow; and (D) amino acid analysis, 5 nanomoles of each amino acid.

#### REFERENCES

- (1) S. Moore, D. H. Spackman, and W. H. Stein, Anal. Chem. 30, 1185 (1958).
- (2) D. H. Spackman, W. H. Stein, and S. Moore, Anal. Chem. 30, 1190 (1958).
- (3) G. R. Shepherd and M. Dekker, unpublished observations.
- (4) K. Dus, M. Dekker, and R. M. Smith, Anal. Biochem. 11, 312 (1965).

## MOLECULAR RADIOBIOLOGY SECTION

### PUBLICATIONS AND ABSTRACTS OF MANUSCRIPTS SUBMITTED

THE REACTION OF 5'-THYMIDYLIC ACID WITH THE CONDENSATION PRODUCT OF PHOSPHORUS PENTOXIDE AND ETHYL ETHER, F. N. Hayes and E. Hansbury. J. Am. Chem. Soc. 86, 4172-4175 (1964).

Abstracted in Los Alamos Scientific Laboratory Report LA-3132-MS (1964), p. 274.

EFFECT OF THE PHOSPHORYLATION STATE OF THYMIDINE DERIVATIVES ON SEPHADEX K<sub>d</sub> VALUES, F. N. Hayes, E. Hansbury, and V. E. Mitchell. J. Chromatog. 16, 410-412 (1964).

Abstracted in Los Alamos Scientific Laboratory Report LA-3132-MS (1964), p. 274.

BODPRO II: ANALYSIS OF T<sub>4</sub>-BACTERIOPHAGE ULTRACENTRIFUGAL BOUNDARIES, G. R. Shepherd, B. J. Noland, and P. N. Dean. Los Alamos Scientific Laboratory Report LA-3098 (August 10, 1964).

A detailed investigation was made of the effects of concentration, rotor speed, and boundary height upon ultracentrifugal sedimentation rates of T<sub>4</sub>-bacteriophage DNA. All experimental data were submitted to a computer program (BODPRO) for computation and analysis. Boundary anomalies such as buckling, reversal, and intermittent rate changes were observed and found to be dependent upon concentration and, to a lesser degree, upon rotor speed. Sedimentation rates were observed to be dependent upon rotor speed at concentrations of 5 to 100  $\mu$ g DNA/ml, though the degree of dependence lessened with increasing concentration. Sedimentation rates at all rotor speeds

were found to be greatly dependent upon concentration, increasing with concentration to the region of 50 to 75  $\mu\text{g}$  DNA/ml and decreasing rapidly beyond this point. Boundaries were observed to form and to migrate as increasingly vertical formations with increasing concentration to a point well beyond the linear response range of the technique.

CONVERSION OF MONO- AND OLIGODEOXYRIBONUCLEOTIDES TO 5'-TRIPHOSPHATES, D. E. Hoard and D. G. Ott. J. Am. Chem. Soc. 87, 1785-1788 (1965).

Reaction of the phosphorimidazolidate formed from a nucleotide and 1,1'-carbonyldiimidazole with inorganic pyrophosphate provides the nucleoside triphosphate in good yield. The method is convenient, generally applicable, and particularly suitable for microscale syntheses from mono- or oligonucleotides.

ARCHPRO: A COMPUTER PROGRAM FOR THE COMPUTATION OF MOLECULAR WEIGHTS BY THE ARCHIBALD METHOD, G. R. Shepherd, P. N. Dean, and B. J. Noland. Los Alamos Scientific Laboratory Report LA-3291 (June 8, 1965).

A computer program (ARCHPRO) has been prepared in FORTRAN for computation of ultracentrifugal data obtained in the determination of molecular weights by the Archibald method.

A FLUORESCENCE ASSAY SUITABLE FOR HISTONE SOLUTIONS, G. R. Shepherd and B. J. Noland. Anal. Biochem. 11, 443-448 (1965).

The dye 8-anilino-1-naphthalenesulfonic acid reacts with whole calf thymus histone to form a fluorescent complex having an excitation maximum at 375 m $\mu$  and an emission maximum at 500 m $\mu$ . The degree of reaction, and hence fluorescence, is enhanced at low pH values. At pH 2, maximum fluorescence is obtained in the region of 1.5  $\mu\text{g}$  dye to 1.0  $\mu\text{g}$  histone. Dye concentrations in excess of 250  $\mu\text{g}/\text{ml}$  result in serious self-extinction. Dye-to-protein ratios considerably lower than 1.5:1 result in incomplete saturation of protein-binding sites, resulting in lowered fluorescence intensity. When the proper ratio is maintained, fluorescence intensity shows a linear relationship to protein

concentration over the range of 1-300  $\mu\text{g}$  histone/ml of sample. The fluorescence assay may be used for quantitation purposes within this range and for qualitative purposes with higher protein concentrations.

LIQUID SCINTILLATORS. XIII. STERIC INHIBITION OF RESONANCE IN LIQUID SCINTILLATORS, R. L. Taber, G. H. Daub, F. N. Hayes, and D. G. Ott. *J. Heterocyclic Chem.* 2, 181-187 (1965).

2'',3'-Dimethyl-p-quaterphenyl (I), 2'',3',5',6''-tetramethyl-p-quaterphenyl (II), 6,7-dihydro-6-methyl-3,9-diphenyl-5H-dibenz[c,e]azepine (III), 5,7-dihydro-3,9-diphenyldibenzo[c,e]thiepin (IV), 5,7-dihydro-3,9-diphenyldibenzo[c,e]-selenepin (V), and 6,6-dicarbethoxy-6,7-dihydro-3,9-diphenyl-5H-dibenzo[a,c]cycloheptene (VI) have been synthesized and screened as potential primary liquid scintillation solutes. The scintillation properties of I, II, III, IV, V, and VI have been compared with 2,7-diphenylfluorene (VII), 9,10-dihydro-2,7-diphenylphenanthrene (VIII), and 5,7-dihydro-3,9-diphenyldibenz[c,e]oxepin (IX). The relative pulse-heights of I, VI, VII, VIII, and IX at 3 mM in toluene gave a linear relationship when plotted against the  $\cos^2$  of the respective estimated angles of torsion about the 1'',4'-bond in the p-quaterphenyl system. The azepine III, thiepin IV, selenepin V, and tetramethyl-p-quaterphenyl II were very poor scintillators in toluene solution.

QUENCH MONITORING AND EFFICIENCY CALIBRATION THROUGH EXTERNAL STANDARDIZATION, F. N. Hayes. *Atomlight* (in press). and In: Advances in Tracer Methodology III. Proceedings of the Ninth Symposium on Advances in Tracer Methodology, held in San Francisco, California (October 22-24, 1964).

Liquid scintillation counting makes use of an intimate mixture of radioactive sample and detecting medium which translates atomic radiation into light flashes. The light intensity of such a flash is proportional to the deposited energy in a burst of radiation, but the constant describing this proportionality may change from sample to sample due to chemical differences in various radioactive preparations. This chemical loss in detection efficiency is known as quenching and needs calibration if one is to get quantitatively meaningful results from liquid scintillation counting. Many ways are available for measuring quenching correction. In

this study one of the methods, external source standardization, has been investigated in detail because it seemed capable of fulfilling the need for a rapid, automatic system which monitors quenching chemistry without direct dependence on the internal level of radioactivity.